# *Research Outputs*

*โครงการ : เทคโนโลยี RNA interference ในการควบคุมโรคติดเชื้อไวรัสของกุ้ง*

โดย

ศาสตราจารย์เกียรติคุณ ดร.สกล พันธุ์ยิ้ม และคณะ

14 พฤษภาคม 2559

สัญญาเลขที่ DPG5680001

# Research Outputs

## โครงการ : เทคโนโลยี RNA interference ในการควบคุมโรคติดเชื้อไวรัสของกุ้ง


| คณะผู้วิจัย | สังกัด |
|---|---|
| 1. นายสกล พันธุ์ยิ้ม, Ph.D. | ภาควิชาชีวเคมี คณะวิทยาศาสตร์ และสถาบันชีววิทยาศาสตร์โมเลกุล มหาวิทยาลัยมหิดล |
| 2. นางสาวพงโสภี อัตศาสตร์, Ph.D. | สถาบันชีววิทยาศาสตร์โมเลกุล มหาวิทยาลัยมหิดล |
| 3. นางสาวเฉลิมพร องศ์วรโสภณ, Ph.D. | สถาบันชีววิทยาศาสตร์โมเลกุล มหาวิทยาลัยมหิดล |
| 4. นายอภินันท์ อุดมกิจ, Ph.D. | สถาบันชีววิทยาศาสตร์โมเลกุล มหาวิทยาลัยมหิดล |
| 5. นายวันชัย อัศวลาภสกุล, Ph.D. | ภาควิชาจุลชีววิทยา คณะวิทยาศาสตร์ จุฬาลงกรณ์มหาวิทยาลัย |
| 6. นางสาวสุพัตรา ตรีรัตน์ตระกูล, Ph.D. | สถาบันชีววิทยาศาสตร์โมเลกุล มหาวิทยาลัยมหิดล |



สนับสนุนโดยสำนักงานกองทุนสนับสนุนการวิจัย

ทุนศาสตราจารย์วิจัยดีเด่น

**ผลงานตีพิมพ์ในวารสารวิชาการนานาชาติ**

1. Protection of yellow head virus infection in shrimp by feeding of bacteria expressing dsRNA. Sanitt P, Attasart P, Panyim S. Journal of Biotechnology. (2014) 179, 26-31.
2. Functional characterization of recombinant gonad-inhibiting hormone (GIH) and implication of antibody neutralization on induction of ovarian maturation in marine shrimp. Treerattrakool S, Boonchoy C, Urtgam S, Panyim S. Aquaculture. (2014) 428-429, 166-173.
3. Molecular cloning and functional characterization of Argonaute-3 gene from *Penaeus monodon*. Phetrungnapha A, Ho T, Udomkit A, Panyim S, Ongvarrasopone C. Fish & Shellfish Immunology. (2013) 35, 874-882.
4. Silencing of PmYPR65 receptor prevents yellow head virus infection in *Penaeus monodon*. Assavalapsakul W, Hoa Khanh Tran Keim, Smith D.R, Panyim S. Virus Research. (2014) 189, 133-135.
5. Molecular characterization of a cDNA encoding red pigment-concentrating hormone in black tiger shrimp *Penaeus monodon* : Implication of its function in molt and osmoregulation. Sathapondecha P, Panyim S, Udomkit A. Comparative Biochemistry and Physiology. (2014) Part A. 175, 124-130.
6. A novel gonad-specific Argonaute 4 serves as a defense against transposons in the black tiger shrimp *Penaeus monodon*. Leebonai W, Sukthaworn S, Panyim S, Udomkit A. Fish and Shellfish Immunoloogy. (2015) 42, 280-288.
7. Correlation between gonad-inhibiting hormone and vitellogenin during ovarian maturation in the domesticated *Penaeus monodon*. Urtgam S, Treerattrakool S, Roytrakul S, Wongtripop S, Prommoon J, Panyim S, Udomkit A. Aquaculture. (2015) 437, 1-9.
8. Molecular cloning and characterization of Mj-mov-10, a putative RNA helicase involved in RNAi of kuruma shrimp. Phetrungnapha A, Kondo H, Hirono I, Panyim S, Ongvarrasopone C. Fish and Shellfish Immunology. (2015) 44, 241-247.
9. Successful yellow head virus infection of *Penaeus monodon* requires clathrin heavy chain. Posiri P, Kondo H, Hirono I, Panyim S, Ongvarrasopone C. Aquaculture. (2015) 435, 480-487.
10. A novel function of bursicon in stimulation of vitellogenin expression in black tiger shrimp, *Penaeus monodon*. Sathapondecha P, Panyim S, Udomkit A. Aquaculture. (2015) 446, 80-87.
11. A formulated double-stranded RNA diet for reducing *Penaeus monodon* densovirus infection in black tiger shrimp. Chimwai C, Tongboonsong P, Namramoon O, Panyim S, Attasart P. Journal of Invertebrate Pathology. (2016) 134, 23.-26.
12. Cholesterol-based cationic liposome increases dsRNA protection of yellow head virus infection in *Penaeus vannamai*. Sanitt P, Apiratikul N, Niyomtham N, Yingyongnarangkul B, Assavalapsakul W, Panyim S. Journal of Biotechnology. (2016) 228, 95-102.
13. Rab5, an early endosomal protein required for yellow head virus infection of *Penaeus monodon*. Posiri P, Panyim S, Ongvarrasopone V. Aquaculture. (2016) 459, 43-53.

# 1. Protection of yellow head virus infection in shrimp by feeding of bacteria expressing dsRNA.

Journal of Biotechnology 179 (2014) 26–31

Contents lists available at ScienceDirect

Journal of Biotechnology

journal homepage: www.elsevier.com/locate/jbiotec

# Protection of yellow head virus infection in shrimp by feeding of bacteria expressing dsRNAs

Poohrawind Sanitt[a], Pongsopee Attasart[a,*], Sakol Panyim[a,b]

[a] Institute of Molecular Biosciences, Mahidol University, Salaya, Nakhon Pathom 73170, Thailand
[b] Department of Biochemistry, Faculty of Science, Mahidol University, Bangkok 10400, Thailand

ARTICLE INFO

*Article history:*
Received 17 December 2013
Received in revised form 21 February 2014
Accepted 7 March 2014
Available online 15 March 2014

*Keywords:*
Yellow head virus
Oral delivery
dsRNA
Rab7
Shrimp

ABSTRACT

Although prevention of shrimp mortality from yellow head virus (YHV) infection via dsRNA injection has been well demonstrated for many years, it has not yet been applied in a farm culture because of its impracticality. Hence, oral administration of dsRNA becomes an alternative and desirable approach. This study is the first to demonstrate that oral feeding of *Escherichia coli* expressing shrimp Rab7 gene (dsRab7) or YHV protease gene (dsYHV) could inhibit YHV replication and lowered shrimp mortality. *E. coli* HT115 expressing dsRab7 or dsYHV or a combination of these dsRNAs were embedded in agar and used to feed vannamei shrimp at early juvenile stage before YHV challenge. After 4 days of continuous feeding of dsRNAs, strong inhibitory effect on shrimp mortality was observed in which dsRab7 gave the highest effect (70% reduction from the control) whereas dsYHV showed a 40% reduction. Our results reveal the potential of anti-YHV strategy via orally delivered dsRNA for application in the shrimp farm industry.



## 1. Introduction

Yellow head virus (YHV) is a major virulent pathogen capable of infecting several penaeid shrimp species (Flegel, 1997). The virus was found in Thailand in 1992 and is named for the yellowish cephalothorax and very sallow overall coloration (Flegel, 1997). YHV is a positive-sense, single-stranded RNA virus with the genome size of 26,622 nucleotides (Sittidilokratna et al., 2008). It causes severe damage in lymphoid and gill leading to high shrimp mortality (Flegel, 2006). YHV outbreaks in penaeid shrimp cause economic loss of millions US dollars in Thailand (Senapin et al., 2010). Therefore, a potent and practical treatment of this disease is needed.

To date, RNA interference is a sequence-specific antiviral mechanism in invertebrate that is triggered by double-stranded RNA (dsRNA) (Robalino et al., 2007). In principle, dsRNA mediated gene suppression in order to block essential viral genes synthesis and/or viral cellular transport was an appropriate strategy to achieve efficient viral inhibition. The Rab-mediated cellular trafficking is a required early step of viral lifecycle prior to its replication in the host cell (Sieczkarski and Whittaker, 2002). Knocking down of Rab may result in traffic disorder leading to virus accumulation in the early endosome and eventually disruption of viral replication. Previous studies have demonstrated that YHV replication is strongly inhibited by injection of dsRNA corresponding to either viral protease gene (dsYHV) (Yodmuang et al., 2006) or shrimp Rab7 gene (dsRab7) (Ongvarrasopone et al., 2008); and that shrimp mortality was effectively suppressed at both the preventive and curative modes (Posiri et al., 2011; Tirasophon et al., 2007; Yodmuang et al., 2006). However, dsRNA administration by injection is not suitable when working in a farm which involves thousands of shrimp. Hence, oral delivery of dsRNA is an alternative and desirable approach. The potential of gene silencing by feeding dsRNA has recently been revealed by several reports. For instance, feeding of dsRab7 being expressed in *Escherichia coli* could significantly reduce Rab7 mRNA expression (Attasart et al., 2013). The level of gonad-inhibiting hormone (GIH) mRNA was decreased when shrimp were fed with artemia enriched with *E. coli* expressing dsRNA-GIH (Treerattrakool et al., 2013). Moreover, ingested dsRNA also showed inhibition of viruses such as white spot syndrome virus (WSSV) (Sarathi et al., 2008) and Laem-Singh Virus (LSNV) in *Penaeus monodon* (Saksmerprome et al., 2013; Thammasorn et al., 2013). However, gill-associated virus (GAV) could be inhibited by dsRNA injection, but not by oral feeding the dsRNA (Sellars et al., 2011).

Here, *E. coli* HT115 expressing dsRNA specific to either shrimp Rab7 gene (dsRab7) or YHV protease gene (dsYHV) or a

* Corresponding authors at: Institute of Molecular Biosciences, Mahidol University, 25/25 Phuttamonthon 4 Road, Salaya, Nakhon Pathom 73170, Thailand. Tel.: +662 441 9003 7x1259; fax: +662 441 9906.
*E-mail addresses:* attasart_aung@hotmail.com, pongsopee.att@mahidol.ac.th (P. Attasart).

http://dx.doi.org/10.1016/j.jbiotec.2014.03.016
0168-1656/

combination of these dsRNAs were embedded in agar and used to feed pacific whiteleg shrimp (*Litopenaeus vannamei*, formerly *Penaeus vannamei*) at early juvenile stage before YHV challenge. This is the first study demonstrating the potency of YHV protection via oral feeding of dsRNA.

## 2. Materials and methods

### 2.1. Shrimp

Post larvae of vannamei shrimp at 15–20 days old were obtained from a farm in Chonburi, Thailand. The shrimp were then reared in sea water at 10 parts per thousand (ppt) salinity (pH 8.0) and fed on commercial tablet food (CP, Thailand) until their body weight were 200–250 mg. The shrimp were fasted and acclimatized one night before starting an experiment.

### 2.2. Virus

The virus stock for all experiments in this study was prepared from hemolymph or gills of infected shrimp. The hemolymph of YHV-infected moribund shrimp (*P. vannamei*) was drawn and immediately mixed with ACD buffer, anticoagulant (85 mM sodium citrate, 62.2 mM citric acid, and 110 mM dextrose, pH 4.9) whereas the gills were ground and resuspended in NTE buffer (0.02 M EDTA, 0.2 M NaCl, 0.2 M Tris/HCl pH 6.5) prior to filter. The solutions were centrifuged at 9000*g* for 10 min at 4 °C. The supernatants, crude viral solutions, were aliquot and kept at −80 °C before use.

### 2.3. Viral infectivity test

The shrimp was placed in transparent plastic container ($10.5 \times 11 \times 7\,cm^3$) with 100 ml of crude YHV diluted in seawater for 4 or 8 h at 25–30 °C. Subsequently, the treated shrimp were transferred into an individual cage and their mortality was recorded everyday afterward. Dead shrimp were sampled for YHV detection by RT-PCR. The optimum lethal dose of YHV was defined as the dilution that gave 70–80% accumulated mortality by day 6–8 post YHV submersion.

### 2.4. RNA extraction and RT-PCR analysis

Total RNA was extracted from gill tissue using Tri Reagent (Molecular Research Center). The extracted RNA (1 or 2 μg for detection of YHV or Rab7, respectively) was then used as a template to generate first-strand cDNA by ImProm-II™ Reverse transcriptase (Promega) and oligo-dT primer (5′TTT TTT TTT TTT TTT TTT3′, Sigma). The PCR reaction was composed of 2 μl of the synthesized cDNA, 1× Thermophilic DNA polymerase buffer, 0.5 mM dNTPs, 2.5 mM $MgCl_2$, and 0.5 U of *Taq* DNA polymerase, 10 nM (each) YHV helicase primers (F: 5′CAA GGA CCA CCT GGT ACC GGT AAG AC3′ and R: 5′GCG GAA ACG ACT GAC GGC TAC ATT CAC3′) (for YHV detection) or 20 nM (each) Rab7 primers (F: 5′ATG GCA TCT CGC AAG AAG ATT 3′ and R: 5′ TTA GCA AGA GCA TGC ATC CTG 3′) (for Rab7 detection) and 10 or 5 nM (each) actin primers (F: 5′GAC TCG TAC GTG GGC GAC GAG G 3′ and R: 5′AGC AGC GGT GGT CAT CTC CTG CTC 3′) for YHV or Rab7 detection, respectively. The primers ratios of YHV or Rab7: actin were 1:1 for YHV detection or 4:1 for Rab7 detection. The PCR condition was carried out at 94 °C for 5 min and 28 cycles of 94 °C for 30 s, 53 °C for 30 s, 72 °C for 30 s. After 28 cycles, the reaction was held at 72 °C for another 7 min. The PCR products were subsequently analyzed by agarose gel electrophoresis.

### 2.5. Sample analysis

Scion image analysis program was used to measure the band intensity of Rab7, YHV or actin amplification product. Then the relative expression level of Rab7 or YHV mRNA was calculated from the band intensity of Rab7 or YHV divided by its internal control (actin). The data was presented as mean ± SD (standard deviation) or SEM (standard error of mean) which was analyzed by GraphPad program.

### 2.6. Double-stranded RNA production in E. coli cells

Three recombinant plasmids, such as pET3a-dsYHV, pET3a-dsGFP, and pET17b-dsRab7, were used to produce dsRNAs (dsYHV, dsGFP and dsRab7, respectively) in this study. The pET3a-dsYHV and pET3a-dsGFP were kindly provided by Dr. Tirasophon (Yodmuang et al., 2006), while pET17b-dsRab7 was kindly provided by Dr. Ongvarrasopone (Ongvarrasopone et al., 2008). Each dsRNA was expressed in *E. coli* HT115 according to the protocol of Ongvarrasopone et al. (2008). The expression of dsRNA was induced by adding 0.4 mM isopropyl-β-D-thiogalactopyranoside (IPTG) in the bacterial culture and the culture was further incubated at 37 °C for 4 h. The bacterial cells were then harvested by centrifugation at 6000 × *g* for 5 min at 4 °C. The cell pellet was then inactivated by resuspending in either 0.5% formaldehyde in 1× phosphate buffer saline (PBS) (137 mM NaCl, 10 mM phosphate and 2.7 mM KCl) pH 7.4 or 75% ethanol in 1× PBS (for feeding dsRab7and dsGFP experiment) and the suspension was left at room temperature for 30 min prior to store at 4 °C overnight before using in food preparation.

### 2.7. Formulated diet preparation

To prepare shrimp formulated diet, the HT115 expressing dsRNA was embedded in an agarose gel. Approximately $3 \times 10^{12}$ CFU of each inactivated bacterial cells were collected by centrifugation and then resuspended in 5 ml of 150 mM NaCl and 5 ml of cooled blended tissue of ark shell (*Anadara granosa*). Thereafter, 10 ml of 2% natural agar (Krungsri Ayudhaya international food industry, Thailand) in 150 mM NaCl (60 °C) was added and the mixture was solidified in petri-dish. The agar with concentration of *E. coli* at $1.5 \times 10^{11}$ CFU/ml was then cut into pieces ($5 \times 5 \times 4\,mm^3$, 100 μl per piece). Each piece contained approximately $1.5 \times 10^{10}$ CFU of *E. coli* cells.

### 2.8. Double-stranded RNA extraction and characterization

To determine the amount and integrity of each dsRNA before and after being embedded in agar, dsRNA was extracted from either a piece of agar containing *E. coli* cells (approximately $1.5 \times 10^{10}$ CFU) or *E. coli* cells ($1 \times 10^9$ CFU) by homogenization in 250 μl of 0.1% SDS in 1× PBS buffer and subsequently boiled for 3 min at 95 °C. The sample was then centrifuged at 12,000*g* for 10 s. Bacterial single-stranded RNA and DNA in the supernatant was destroyed by 1 μg of RNaseA and 3 U of DNase I in 1× RNaseA buffer at 37 °C for 30 min. The treated dsRNA was cleaned up by Tri reagent following the manufacturer's protocol. The dsRNA was finally dissolved in 150 mM NaCl and only 1/50 parts of each dsRNA was loaded and visualized by gel electrophoresis using a standard DNA marker. For dsRNA characterization, 1 μg of either dsYHV or dsRab7 was digested by 0.5 U of RNaseIII (Biolabs) at 25 °C for 10 and 20 min, respectively. The patterns of the digested dsRNAs were then determined by gel electrophoresis with a standard size marker.

### 2.9. Experimental conditions

#### 2.9.1. For Rab7 mRNA suppression

Shrimp (250–300 mg) were divided into groups (nine shrimp for each group) and fed with diet containing dsRNAs (dsRab7 or dsGFP) or agar alone for 9 days, two pieces of formulated diet a day. Subsequently, all shrimp were sacrificed 24 h after feeding and gills were collected for RNA extraction and RT-PCR analysis.

#### 2.9.2. For YHV inhibition

Shrimp (250–300 mg) were divided into two groups and fed with diet containing dsRab7 or agar alone for 6 days, two pieces of formulated diet a day. Twenty-four hours later, the shrimp were soaked with YHV solution ($10^{-2}$) for 4 h and fed with the diet containing dsRab7 or agar for another 3 days prior to determine the YHV inhibition by RT-PCR.

#### 2.9.3. For shrimp mortality prevention

Shrimp (250–300 mg) were divided into groups and fed with diet containing either dsRab7 or dsYHV or combination (dsRab7 and dsYHV) or shrimp commercial food (CP) for 4 days, four pieces of formulated diet a day. Twenty-four hours later, the shrimp were soaked with YHV solution ($4 \times 10^{-4}$) for 8 h. All challenged shrimp were subsequently fed with commercial food for another 6 days and their mortality was monitored every day.

#### 2.9.4. YHV challenge

In this study, shrimp were infected with YHV by soaking. For one plastic box ($10.5 \times 11 \times 7\ cm^3$), ten shrimp were placed in 100 ml of seawater containing YHV solution ($10^{-2}$ or $4 \times 10^{-4}$ dilution from the YHV stock) for 4 or 8 h, respectively. The shrimp were then transferred to an individual cage and continued to be fed on normal shrimp commercial food.

## 3. Results

### 3.1. Characterization and integrity of dsRNAs

In order to ensure that dsYHV and dsRab7 were in the form of double-stranded RNA, both dsRNAs were treated with Ribonuclease III (RNase III) which specifically cleaves dsRNA. The result showed that the synthesized dsYHV and dsRab7 were completely digested after incubating with RNase III (Fig. 1A) indicating that they were double-stranded RNA.

To determine the integrity of dsRNA in shrimp formulated diet, the dsRNAs (dsYHV and dsRab7) were extracted from *E. coli* cells before and after being embedded in agar and subsequently visualized by agarose gel electrophoresis. Both extracted dsRNAs exhibited the same pattern (Fig. 1B) suggesting that dsRNAs in the formulated diets were still intact.

### 3.2. Suppression of Rab7 mRNA by oral administration of dsRab7

To investigate whether oral delivery of dsRNA in the formulated diet could knock down Rab7, shrimp were fed with agar containing $2.7 \times 10^{11}$ CFU of *E. coli* expressing dsRab7 for 9 days. The level of Rab7 mRNA in each fed shrimp was monitored by semi-quantitative RT-PCR. The relative Rab7 mRNA expression normalized by actin was quantified and plotted as a graph. Approximately 7 folds reduction of Rab7 was observed in shrimp that ingested dsRab7 when compared to the control shrimp that fed with agar alone (Fig. 2). This suggested that dsRab7 in the formulated diets could enter into shrimp cells and trigger RNAi that eventually suppressed Rab7 mRNA expression.

### 3.3. Specificity of Rab7 suppression via oral delivery of dsRab7

In order to determine the specificity of Rab7 suppression by orally delivered dsRab7, shrimp were fed with $2.7 \times 10^{11}$ CFU of *E. coli* expressing dsRab7 or unrelated dsGFP for 9 days. The level of Rab7 mRNA in each shrimp was analyzed by semi-quantitative RT-PCR. The relative level of Rab7 mRNA expression of shrimp fed with dsRab7 was lower than that of shrimp fed with dsGFP (Fig. 3). This result demonstrated sequence-specific suppression by feeding dsRab7.

### 3.4. Orally delivered dsRab7 inhibited YHV replication and prevented shrimp mortality

Approximately $1.8 \times 10^{11}$ CFU of *E. coli* HT115 harboring dsRab7 embedded in agar were used to feed shrimp prior to YHV challenge by soaking and then shrimp were fed with another $0.9 \times 10^{11}$ CFU of *E. coli* before analysis. The levels of Rab7 and YHV in each shrimp were analyzed by semi-quantitative RT-PCR. The Rab7 mRNA level

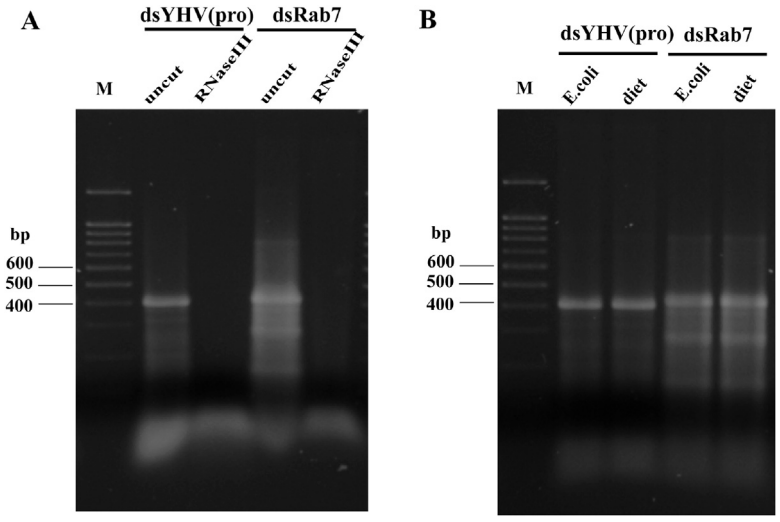


**Fig. 1.** Characterization and integrity of dsRNAs. (A) The dsRNA specific to YHV protease gene or shrimp Rab7 gene was extracted from *E. coli* expressing either dsYHV or dsRab7. Approximately 1 μg of each dsRNA was treated with RNase III and then analyzed by gel electrophoresis alongside its untreated RNA (uncut) and 100 bp DNA marker (M). (B) The dsRNAs (dsYHV and dsRab7) were extracted from $1 \times 10^9$ CFU of *E. coli* cells before (*E. coli*) or after being embedded in the formulated agar (diet) which contained approximately $1.5 \times 10^{10}$ CFU of *E. coli* cells. Only 1/50 parts of extracted dsRNA was loaded in the gel.

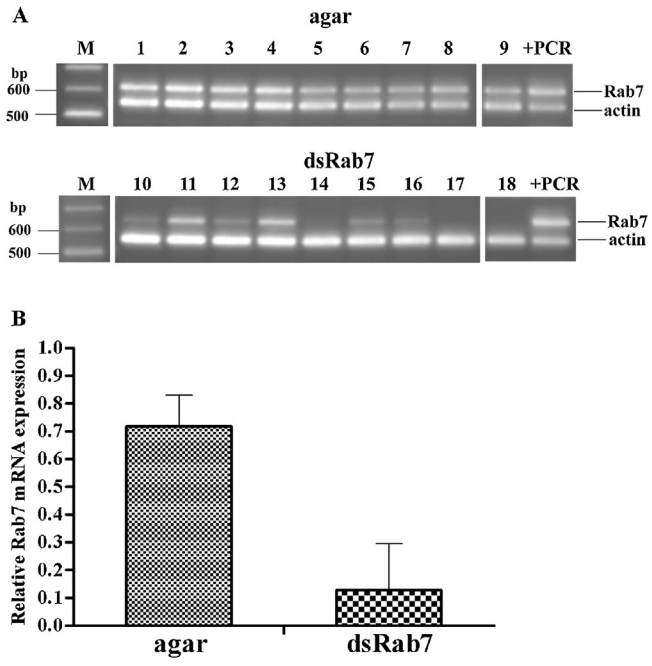


**Fig. 2.** Suppression of Rab7 mRNA by oral administration. Shrimp were fed with $2.7 \times 10^{11}$ CFU of *E. coli* expressing dsRab7 or agar alone for 9 days. Then, the shrimp were sacrificed and total RNA was isolated from gills of individual shrimp for further RT-PCR analysis. Agarose gel electrophoresis of RT-PCR products of Rab7 and actin are shown (A). M is 100 bp DNA ladder plus 1.5 kb. Positive PCR (+PCR) indicates expression level of Rab7 and actin mRNA in normal shrimp. The relative mRNA expression level of Rab7 normalized by actin was presented as mean + SD from $n = 9$ (B).

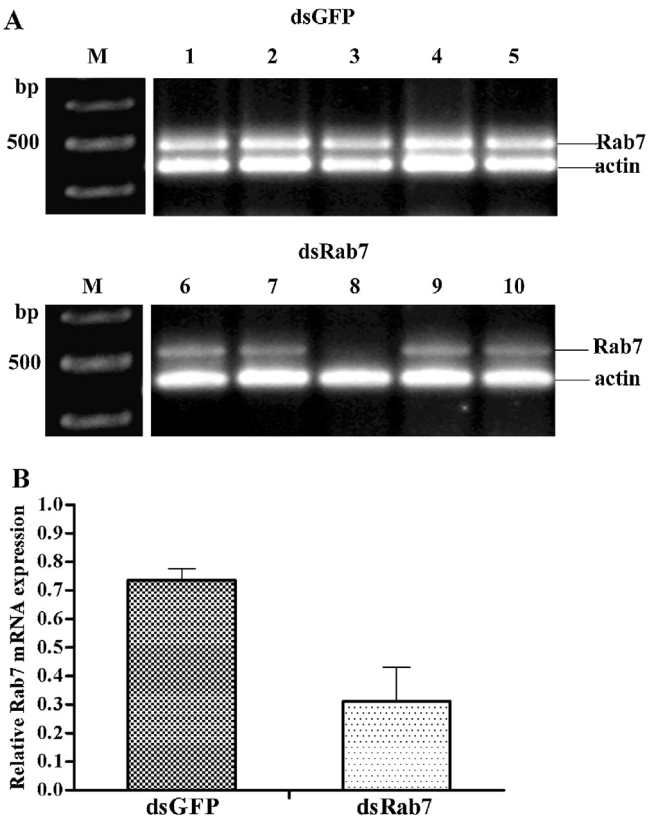


**Fig. 3.** Specificity of Rab7suppression by oral feeding of dsRab7. Shrimp were fed with diet containing $2.7 \times 10^{11}$ CFU of *E. coli* expressing either dsRab7 or dsGFP for 9 days. Thereafter, RT-PCR products of Rab7 and actin mRNA expression of each shrimp were visualized by agarose gel electrophoresis (A). Lane 1–5 and 6–10 present the product from shrimp fed with dsGFP and dsRab7, respectively. The relative mRNA expression level of Rab7 normalized by actin was presented as mean + SD from $n = 5$ (B).

of treated shrimp was significantly lower than the control shrimp that were fed with agar alone (Fig. 4A). Moreover, the levels of YHV as well as shrimp death were decreased in these Rab7 knocked down shrimp when compared to the control (Fig. 4A and B). Another independent experiment was also done by feeding $2.4 \times 10^{11}$ CFU of bacterial cells with dsRab7 for 4 days and then soaking in YHV solution for 8 h. Cumulative percent mortality of treated shrimp was recorded everyday for 6 days post infection. The result showed reduction of shrimp mortality from 75% to 22% (Fig. 4C). These data showed that feeding diet with *E. coli* expressing dsRab7 inhibited YHV replication and thus reduced shrimp mortality.

### 3.5. Feeding dsYHV reduced shrimp mortality upon YHV infection

As previous study demonstrated that not only dsRNA specific to shrimp Rab7 gene (dsRab7) could inhibit YHV but dsRNA specific to YHV protease gene (dsYHV) also gave strong viral inhibition (Yodmuang et al., 2006). Therefore, the inhibitory effect on YHV infection by feeding *E. coli* expressed dsYHV was evaluated. After 4 days of continuous feeding of *E. coli* with dsYHV, shrimp were infected with YHV by soaking for 8 h. The mortality rate of fed shrimp was monitored and compared with the control shrimp that were fed with commercial food. The reduction of cumulative mortality from 75% in the control to 30% in the treated one was revealed (Fig. 5). Nevertheless, all dead shrimp were YHV positive by RT-PCR (data not shown). The result indicated that oral delivery of dsYHV significantly reduced shrimp mortality from YHV infection.

### 3.6. Feeding of combined bacteria expressing dsRab7 and dsYHV exhibited a tendency of improved YHV protection

In order to improve the inhibitory effect on YHV infection, combined bacteria expressing dsRab7 and dsYHV was tested. Shrimp were fed with diets containing *E. coli* expressing either dsRab7 or dsYHV or combination for 4 days before YHV challenge. The result showed that 75% cumulative mortality that observed in the control shrimp (fed with commercial food) was significantly reduced when shrimp were fed with diet containing dsRNAs (dsRab7 or dsYHV or combined dsRNAs) (Fig. 6). The dsRab7 gave the lowest shrimp mortality (22%) and the combined dsRNAs (dsRab7 and dsYHV) showed lower mortality rate (33%) than dsYHV alone (45%). However, all dsRNA fed shrimp did not show significant difference in the YHV inhibitory effect. All dead shrimp were YHV positive by RT-PCR (data not shown).

## 4. Discussion

Although prevention of shrimp mortality from YHV via dsRNA injection has been well demonstrated for many years, it has not been applied in a farm culture yet. The virus could be inhibited by injection of dsRNA specific to shrimp endogenous gene (Rab7) or viral gene (YHV protease) (Ongvarrasopone et al., 2008; Tirasophon et al., 2007; Yodmuang et al., 2006). In this study, we presented oral delivery of dsRNA via shrimp formulated diet. Approximately 80% reduction of Rab7 mRNA was observed after nine days of continuous feeding. This revealed that oral delivery of dsRab7 via shrimp diet could activate RNAi pathway and thus Rab7 mRNA was drastically suppressed. Moreover, the level of Rab7 transcript was not affected by dsGFP suggesting that the suppression of Rab7 was sequence-specific. Our results corresponded to those found by Attasart group (Attasart et al.,

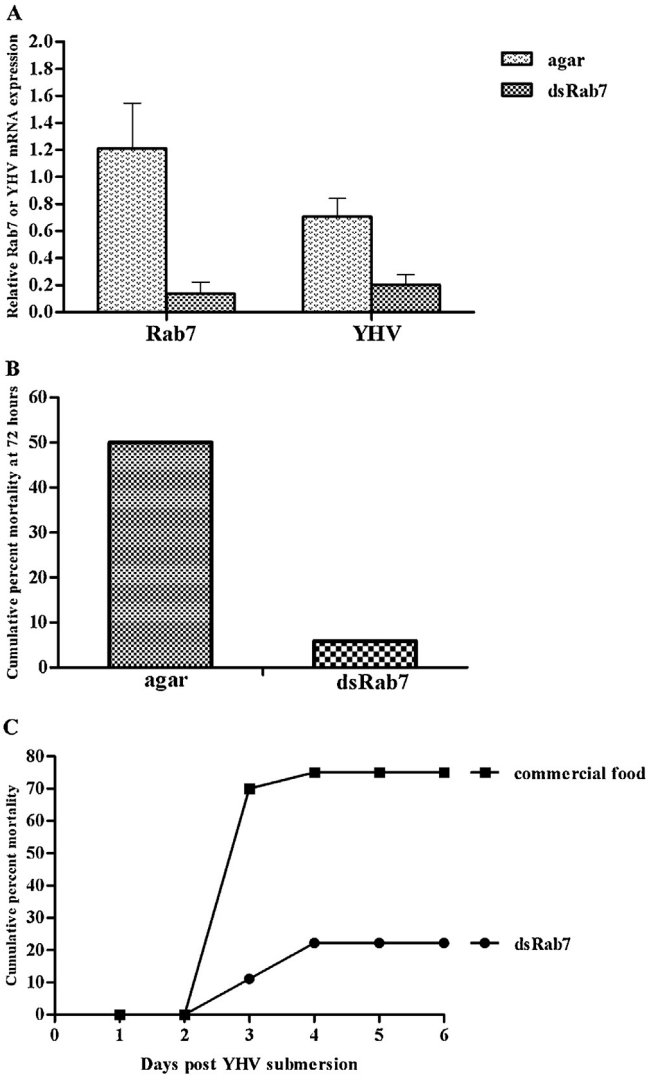


**Fig. 4.** YHV inhibition by feeding bacteria expressing dsRab7. Shrimp were fed with either *E. coli* expressing dsRab7 embedded in agar ($n = 16$) or agar alone ($n = 16$) for 6 days. Subsequently, the shrimp were soaked in YHV solution. The shrimp were then fed with the diet for additional 3 days post YHV challenging. The expression of Rab7 mRNA and viral load in infected shrimp were determined by RT-PCR. The relative mRNA expression of Rab7 or YHV helicase normalized with actin are shown as mean from $n = 16$ (A). Moreover, shrimp mortality was recorded and shown in (B). In another experiment, shrimp were fed with diet containing *E. coli* expressing dsRab7 for 4 day ($2.4 \times 10^{11}$ CFU) before soaking in YHV solution for 8 h. The cumulative percent mortality was recorded everyday and presented from $n = 20$ (C).

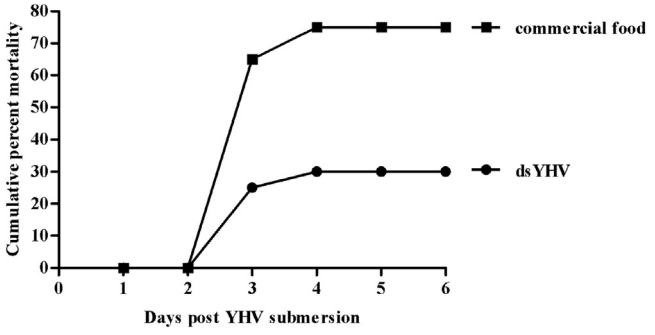


**Fig. 5.** Oral administration of dsYHV prevented shrimp mortality. Shrimp were fed on either diet containing bacteria expressing dsRNA specific to protease gene of YHV (dsYHV) or commercial food for 4 days, $2.4 \times 10^{11}$ CFU of *E. coli* cells in total. The shrimp were subsequently soaked in YHV solution for 8 h. Percent mortality of each group was recorded everyday for 6 days after YHV challenge. Cumulative percent mortality is presented ($n = 20$).

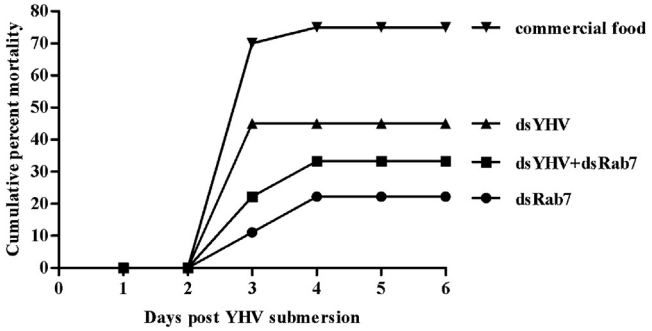


**Fig. 6.** Prevention of shrimp mortality by oral administration of combined bacteria expressing dsYHV and dsRab7. The diet containing either dsRab7 or dsYHV or a combination of dsRNAs (dsRab7 and dsYHV) was used to feed shrimp for 4 days prior to YHV challenge by soaking for 8 h. The cumulative percent mortality was recorded everyday for 6 days. The result is presented from $n = 20$.

2013) that specific RNA silencing in shrimp could be activated via oral feeding *E. coli* expressing dsRNAs. They showed that ingestion of *E. coli* expressing dsRNAs (dsRab7 or dsSTAT) could suppress their particular shrimp genes (Rab7 or STAT) significantly and the suppression was not detected by non-related dsRNA (dsGFP).

Moreover, this is the first demonstration that oral feeding of *E. coli* expressing dsRab7 or dsYHV could prevent shrimp mortality from YHV infection. We found that all orally delivered dsRNAs (dsRab7 or dsYHV or combined dsRab7 + dsYHV) gave strong inhibitory effect on shrimp mortality in which dsRab7 showed the highest effect (70% reduction from the control), 56% for combined dsRNAs and 40% for dsYHV. Although there was no significant difference in their inhibitory effects, it showed a parallel tendency as the study of Posiri et al. (2011) that injection with combined dsRNAs (dsRab7 and dsYHV) could improve shrimp mortality prevention when compared with the effect from dsYHV injection alone. As Rab7 is an important regulator of intracellular trafficking that is required for several viruses such as white spot syndrome virus (WSSV) (Ongvarrasopone et al., 2008), YHV (Ongvarrasopone et al., 2008), Taura syndrome virus (TSV) (Ongvarrasopone et al., 2011) and Laem-Singh virus (LSNV) (Ongvarrasopone et al., 2010), suppression of just Rab7 gene could inhibit the replication of these viruses. Therefore, efficient silencing of shrimp Rab7 gene via orally delivered dsRab7 will provide the opportunity to develop broad spectrum diet that can protect shrimp against a wide range of viruses in the future.

Although high potency of YHV inhibition and shrimp mortality protection were achieved by ingested dsRNA, its efficiency was much lower than those by dsRNA injection. At least 400–800 times higher concentration of fed dsYHV or dsRab7 are required than the injected one to achieve a significant YHV inhibitory effect. It has been shown that to inhibit YHV replication, 25 μg of injected dsYHV was required (Yodmuang et al., 2006); whereas, approximately 10 mg of fed dsYHV was needed in this study. In the case of dsRab7, about 22 mg of fed dsRab7 instead of 25 μg of injected dsRab7 was employed for YHV inhibition (Ongvarrasopone et al., 2008). The low efficiency of oral administration of dsRNA might be explained by dsRNA transportation from gut to target cells. It has been described in *C. elegan* that extracellular dsRNA was taken up into cytosol by an apical intestinal lumen protein, SID2 via endocytosis (McEwan et al., 2012; Winston et al., 2007). SID5 that was endosome-associated protein was then required to release dsRNA into its body cavity or enhance systemic RNAi (Hinas et al., 2012). Thereafter, dsRNA would be selected by a dsRNA-selective channel protein, SID1 to get into intestinal cells or other cell types (Winston et al., 2002) for further RNAi activation. These processes might be required for RNAi mediated gene silencing via orally delivered

dsRNA in shrimp. The dsRNA uptake in shrimp gut might be limited at the internalization step via SID2 resulting in less efficiency of shrimp protection whereas the injected dsRNA could trigger RNAi pathway via only the SID1 protein (McEwan et al., 2012). Additionally, the huge amount of fed dsRNA was required for viral protection probably because of loss or damage of dsRNA in the shrimp gut by enzymatic digestion prior to its internalization into the intestinal cells.

According to the difficulty of culturing *P. monodon* and the good characteristic of *P. vannamei* as it is easier to grow than *P. monodon* (able to grow in a wide range of salinity/temperature; availability of broodstock selection for specific pathogen free/resistant), vannamei shrimp is becoming the most common cultured shrimp in Thailand nowadays. Outbreak of viral diseases is one of the serious problems resulted from culturing vananmei at high density in low salinity water. Hence, we used *P. vannamei* as a shrimp model to demonstrate the potential of YHV protection via oral feeding in this study. The previous results showed that shrimp endogenous gene (Rab7 and STAT) can be suppressed in monodon and vannamei by ingestion of bacteria expressing specific dsRNA (Attasart et al., 2013). In addition, both monodon and vannamei shrimp also showed a similar response to dsRNA mediated YHV inhibition (Assavalapsakul et al., 2009; Yodmuang et al., 2006). Taken together, anti-YHV via feeding dsRNA strategy can work well with *P. monodon* as well.

Our finding demonstrated that dsRNA ingestion could prevent shrimp mortality from YHV infection. However, shrimp at early juvenile stage was used instead of adult shrimp. We expected that a similar result should be obtained if this technique is applied to the shrimp farm industry. Nevertheless, improvement of RNAi-based anti-YHV efficiency via feeding dsRNA is still needed. Further study might include knocking down of shrimp endogenous genes such as YHV receptor, which was already indentified (Assavalapsakul et al., 2006) or genes involved in endocytic pathway such as Rab5 or Rab11, in addition to Rab7.

## Acknowledgements

We thank Assistant Professor Kusol Pootanakit for his grammatical correction, Assistant Professor Chalermporn Ongvarasopone for providing the pET17b-dsRab7 construct and Assistant Professor Witoon Tirasophon for providing the *E. coli* strain HT115, pET3a-dsGFP and the pET3a-dsYHV. Our appreciation is expressed to Mr. Wichai Boonsai and Mr. Prasong Kasetpittaya for their kindness in providing shrimp, Mrs. Orathai Namramoon, Miss Chaweewan Chimwai, Mrs. Suparp Hongthong and Miss Pannee Thongboonsong for their technical assistance. This work is supported by Thailand Research Fund (DPG5680001 to S.P.) and Mahidol University research grant.

## References

Assavalapsakul, W., Smith, D.R., Panyim, S., 2006. Identification and characterization of a *Penaeus monodon* lymphoid cell-expressed receptor for the yellow head virus. J. Virol. 80, 262–269.

Assavalapsakul, W., Chinnirunvong, W., Panyim, S., 2009. Application of YHV-protease dsRNA for protection and therapeutic treatment against yellow head virus infection in *Litopenaeus vannamei*. Dis. Aquat. Organ. 84, 167–171.

Attasart, P., Namramoon, O., Kongphom, U., Chimwai, C., Panyim, S., 2013. Ingestion of bacteria expressing dsRNA triggers specific RNA silencing in shrimp. Virus Res. 171, 252–256.

Flegel, T.W., 1997. Major viral diseases of the black tiger prawn (*Penaeus monodon*) in Thailand. World J. Microbiol. Biotechnol. 13, 433–442.

Flegel, T.W., 2006. Detection of major penaeid shrimp viruses in Asia, a historical perspective with emphasis on Thailand. Aquaculture 258, 1–33.

Hinas, A., Wright, A.J., Hunter, C.P., 2012. SID-5 is an endosome-associated protein required for efficient systemic RNAi in *C. elegans*. Curr. Biol. 22, 1938–1943.

McEwan, D.L., Weisman, A.S., Hunter, C.P., 2012. Uptake of extracellular double-stranded RNA by SID-2. Mol. Cell 47, 746–754.

Ongvarrasopone, C., Chanasakulniyom, M., Sritunyalucksana, K., Panyim, S., 2008. Suppression of PmRab7 by dsRNA inhibits WSSV or YHV infection in shrimp. Mar. Biotechnol. (NY) 10, 374–381.

Ongvarrasopone, C., Chomchay, E., Panyim, S., 2010. Antiviral effect of PmRab7 knock-down on inhibition of Laem-Singh virus replication in black tiger shrimp. Antiviral Res. 88, 116–118.

Ongvarrasopone, C., Saejia, P., Chanasakulniyom, M., Panyim, S., 2011. Inhibition of Taura syndrome virus replication in *Litopenaeus vannamei* through silencing the LvRab7 gene using double-stranded RNA. Arch. Virol. 156, 1117–1123.

Posiri, P., Ongvarrasopone, C., Panyim, S., 2011. Improved preventive and curative effects of YHV infection in *Penaeus monodon* by a combination of two double stranded RNAs. Aquaculture 314, 34–38.

Robalino, J., Bartlett, T.C., Chapman, R.W., Gross, P.S., Browdy, C.L., Warr, G.W., 2007. Double-stranded RNA and antiviral immunity in marine shrimp: inducible host mechanisms and evidence for the evolution of viral counter-responses. Dev. Comp. Immunol. 31, 539–547.

Saksmerprome, V., Thammasorn, T., Jitrakorn, S., Wongtripop, S., Borwornpinyo, S., Withyachumnarnkul, B., 2013. Using double-stranded RNA for the control of Laem-Singh Virus (LSNV) in Thai *P. monodon*. J. Biotechnol. 164, 449–453.

Sarathi, M., Simon, M.C., Venkatesan, C., Hameed, A.S., 2008. Oral administration of bacterially expressed VP28dsRNA to protect *Penaeus monodon* from white spot syndrome virus. Mar. Biotechnol. (NY) 10, 242–249.

Sellars, M.J., Rao, M., Arnold, S.J., Wade, N.M., Cowley, J.A., 2011. *Penaeus monodon* is protected against gill-associated virus by muscle injection but not oral delivery of bacterially expressed dsRNAs. Dis. Aquat. Organ. 95, 19–30.

Senapin, S., Thaowbut, Y., Gangnonngiw, W., Chuchird, N., Sriurairatana, S., Flegel, T.W., 2010. Impact of yellow head virus outbreaks in the whiteleg shrimp, *Penaeus vannamei* (Boone), in Thailand. J Fish Dis. 33, 421–430.

Sieczkarski, S.B., Whittaker, G.R., 2002. Dissecting virus entry via endocytosis. J. Gen. Virol. 83, 1535–1545.

Sittidilokratna, N., Dangtip, S., Cowley, J.A., Walker, P.J., 2008. RNA transcription analysis and completion of the genome sequence of yellow head nidovirus. Virus Res. 136, 157–165.

Thammasorn, T., Somchai, P., Laosutthipong, C., Jitrakorn, S., Wongtripop, S., Thitamadee, S., Withyachumnarnkul, B., Saksmerprome, V., 2013. Therapeutic effect of Artemia enriched with *Escherichia coli* expressing double-stranded RNA in the black tiger shrimp *Penaeus monodon*. Antiviral Res. 100, 202–206.

Tirasophon, W., Yodmuang, S., Chinnirunvong, W., Plongthongkum, N., Panyim, S., 2007. Therapeutic inhibition of yellow head virus multiplication in infected shrimps by YHV-protease dsRNA. Antiviral Res. 74, 150–155.

Treerattrakool, S., Chartthai, C., Phromma-in, N., Panyim, S., Udomkit, A., 2013. Silencing of gonad-inhibiting hormone gene expression in *Penaeus monodon* by feeding with GIH dsRNA-enriched Artemia. Aquaculture 404–405, 116–121.

Winston, W.M., Molodowitch, C., Hunter, C.P., 2002. Systemic RNAi in *C. elegans* requires the putative transmembrane protein SID-1. Science 295, 2456–2459.

Winston, W.M., Sutherlin, M., Wright, A.J., Feinberg, E.H., Hunter, C.P., 2007. Caenorhabditis elegans SID-2 is required for environmental RNA interference. Proc. Nat. Acad. Sci. U.S.A. 104, 10565–10570.

Yodmuang, S., Tirasophon, W., Roshorm, Y., Chinnirunvong, W., Panyim, S., 2006. YHV-protease dsRNA inhibits YHV replication in *Penaeus monodon* and prevents mortality. Biochem. Biophys. Res. Commun. 341, 351–356.

# 2. Functional characterization of recombinant gonad-inhibiting hormone (GIH) and implication of antibody neutralization on induction of ovarian maturation in marine shrimp.

Aquaculture 428–429 (2014) 166–173

Contents lists available at ScienceDirect

Aquaculture

journal homepage: www.elsevier.com/locate/aqua-online

# Functional characterization of recombinant gonad-inhibiting hormone (GIH) and implication of antibody neutralization on induction of ovarian maturation in marine shrimp

Supattra Treerattrakool [a,*], Chanikarn Boonchoy [a], Sittichai Urtgam [a], Sakol Panyim [a,b], Apinunt Udomkit [a]

[a] Institute of Molecular Biosciences, Mahidol University, Salaya Campus, Nakhon Pathom 73170, Thailand
[b] Department of Biochemistry, Faculty of Science, Mahidol University, Rama VI Road, Bangkok 10400, Thailand

ARTICLE INFO

*Article history:*
Received 3 December 2013
Received in revised form 11 March 2014
Accepted 11 March 2014
Available online 20 March 2014

*Keywords:*
Gonad-inhibiting hormone
Vitellogenin
Black tiger shrimp
*Pichia pastoris*
Monoclonal antibody

ABSTRACT

Ovarian maturation in crustacean is controlled by an eyestalk neuropeptide called gonad-inhibiting hormone (GIH) that is presumed to inhibit vitellogenin synthesis. In this study, a recombinant protein of GIH of *Penaeus monodon* (rPem-GIH) was expressed in *Pichia pastoris* expression system and purified to homogeneity by reversed-phase SPE ($C_{18}$). The purified rPem-GIH significantly reduced vitellogenin mRNA level in primary tissue culture derived from previtellogenic ovary of *P. monodon* broodstock by 45.7% compared with the untreated group. This effect was similar to that of partially purified optic lobe extract, and demonstrated that the rPem-GIH possessed gonad-inhibiting activity. A monoclonal antibody specific to Pem-GIH (anti-GIH mAb) was able to neutralize the activity of GIH from the partially purified optic lobe extract to about 58% by in vitro assay in primary tissue culture of the ovary. Peptide mapping revealed that amino acids 16 to 20 (MYNKV) of the mature Pem-GIH may serve as an epitope of anti-GIH mAb. A single injection of anti-GIH mAb into wild previtellogenic *P. monodon* was able to induce ovarian maturation and spawning at a comparable rate to the eyestalk ablation. Our results demonstrate neutralization effect of anti-GIH mAb on vitellogenesis inhibitory action of GIH, and thus provide a potential alternative to induce ovarian maturation in *P. monodon* broodstock.



## 1. Introduction

Traditionally, ovarian maturation in female shrimp can be induced by removal of their eyestalks. The method is invasive, and may be considered cruel to the shrimp. This technique eradicates the X-organ–sinus gland complex; the synthesis and storage sites of a gonad-inhibiting hormone (GIH)/vitellogenesis-inhibiting hormone (VIH) that controls vitellogenesis by inhibiting vitellogenin (*Vg*) synthesis (Wilder et al., 2010). *Vg* is subsequently modified into a yolk protein vitellin (*Vn*), which is then deposited in the oocytes and accumulated during oocyte development (Okumura et al., 2006). Therefore, *Vg* synthesis can be used as an indicator for ovarian maturation.

GIH belongs to a CHH-peptide family that is synthesized in a cluster of neuron perikarya located in the medulla terminalis of the optic ganglia (so-called medulla terminalis ganglionic X-organ; MTGX or XO). These peptide hormones are transported along the axon and stored in the axon terminals forming a neurohemal organ, the sinus gland (SG), of the eyestalk (Böcking et al., 2002; Keller, 1992; Lorenzon, 2005). Most of mature peptides of the CHH family generally comprise between 72 and 83 amino acid residues with the molecular mass of 8 to 9 kDa. These hormones contain six conserved cysteine residues that are aligned in conserved positions and form three intramolecular disulfide bonds (Katayama et al., 2001). Because of the minute amount of these peptides produced in nature, the recombinant technology was employed to obtain the peptides in a large quantity for characterization in both molecular and functional aspects. Comparing to other hormones in the same family, only limited numbers of GIH/VIH have been characterized to date.

Identification and functional characterization of VIH was first reported in *Homarus americanus* (Soyez et al., 1987). The study on VIH expression during the reproduction cycle of female *H. americanus* suggested that VIH may suppress the onset of vitellogenesis as high levels of VIH in the hemolymph were found at immature and previtellogenic stages (De Kleijn et al., 1998). The biological activity of the recombinant VIH of *H. americanus* to inhibit *Vg* mRNA synthesis has also been reported in the ovary of heterologous species, *Marsupenaeus japonicas* (Ohira et al., 2006). In addition, VIH from the crayfish *Procambarus bouvieri* was demonstrated to repress vitellogenin biosynthesis in the cultured *Penaeus vannamei's* ovaries (Aguilar et al., 1992). The cDNA encoding GIH-like peptide is also found in a few other species such as the prawn *Macrobrachium rosenbergii* (Yang and Rao, 2001) and the Norway lobster *Nephrops norvegicus* (Edomi et al., 2002), but their vitellogenesis-inhibiting activity has not yet been characterized.

* Corresponding author. Tel.: +66 2 441 9003x1303, +66 2 441 9003x1273; fax: +66 2 441 9906.
*E-mail addresses:* tsupattra@gmail.com, supattra.tre@mahidol.ac.th (S. Treerattrakool).

http://dx.doi.org/10.1016/j.aquaculture.2014.03.009
0044-8486/

Recently, a cDNA encoding GIH of *Penaeus monodon* (Pem-GIH) was cloned and its biological function was demonstrated by RNA interference technique (Treerattrakool et al., 2008). The dsRNA of GIH was able to knockdown GIH expression and induced ovarian maturation in *P. monodon* (Treerattrakool et al., 2011). A recombinant Pem-GIH (rPem-GIH) cDNA was previously expressed in an *Esherichia coli* expression system as an insoluble form. In order to avoid the problem associated with solubilization and renaturation of the recombinant peptide that is needed to produce biologically active Pem-GIH, the rPem-GIH was instead expressed in an eukaryotic expression system. In this study, a sufficient quantity of the recombinant protein of Pem-GIH (rPem-GIH) was produced in *Pichia pastoris* in the form of secreted protein and was purified to 90% homogeneity prior to verifying its biological function on vitellogenesis-inhibiting activity. Other effective expression system in *E coli* was considered as expression host for large amount of rPem-GIH for antibody production. A specific monoclonal antibody against Pem-GIH (anti-GIH mAb) was produced and tested for its inhibitory effect on the activity of GIH both *ex vivo* and *in vivo*. Further application of anti-GIH mAb to induce ovarian maturation in *P. monodon* broodstock was also implicated.

## 2. Materials and methods

### 2.1. Animals

For optic lobe extraction and primary ovary tissue culture preparation, domesticated previtellogenic female *P. monodon* (100–130 g body weight (b.w.)) at 1–2 years of age were kindly provided by Shrimp Genetic Improvement Center (SGIC), Chaiya District, Surat Thani, Thailand. For induction of ovarian maturation, the wild adult female *P. monodon* (150–250 g b.w.) at previtellogenic stage were caught from Andaman Sea, Southern Thailand. Shrimp from both sources were acclimatized in 30 ppt sea water at the average temperature of 28 °C with a 12 h light:12 h dark photoperiod for 7 days before the experiments.

### 2.2. Construction of the expression plasmid and transformation of *P. pastoris*

To construct GIH expression plasmid in *P. pastoris* system, a DNA fragment encoding the mature *Pem-GIH* was fused in-frame with the α-factor secretion signal of *Saccharomyces cerevisiae* in pPICZαA expression vector without the double Glu-Ala repeat resulting in the recombinant plasmid pαmatGIHEx (Fig. 1A). The transformants were analyzed by restriction enzyme digestion with appropriate enzymes and PCR analysis, and the candidate recombinant clones were confirmed by DNA sequencing. The pαmatGIHEx was linearized by *Dra*I before introduced into *P. pastoris* strain KM71 by electroporation using a Gene Pulser (Bio-Rad, USA) at 1.5 kV, 25 μF and 200 Ω. *Pichia* transformants were selected on YEPD plate (1% (w/v) yeast extract, 2% (w/v) peptone, 2% (w/v) glucose, 2% agar) containing 100 μg/ml Zeocin™ (Invitrogen, USA). The transformants were screened for integration of pαmatGIHEx into the genome by colony PCR amplification with 5′ *AOX1* (5′-GACTGG TTCCAATTGACAAGC-3′) and 3′ *AOX1* (5′-GCAAATGGCATTCTGACATCC-3′) primers. The reaction was initiated by heating at 94 °C for 3 min and amplified with 30 cycles of 94 °C for 30 s, 43 °C for 30 s and 72 °C for 1 min following with 7 min incubation at 72 °C as a final extension (Treerattrakool, 2008). The expected size of the PCR product is 713 bp, and its nucleotide sequence was confirmed by DNA sequencing.

### 2.3. Expression of recombinant Pem-GIH (rPem-GIH) in *P. pastoris*

The rPem-GIH was expressed in *P. pastoris* as previously described for rPem-CHH1 (Treerattrakool et al., 2003). A single colony of *P. pastoris* KM71 recombinant containing pαmatGIHEx was grown in 5 ml of YEPD that contained 100 μg/ml Zeocin™ at 30 °C for 48 h. Then, the cell culture was transferred into 100 ml of fresh BMGY medium (1% yeast extract, 2% peptone, 100 mM potassium phosphate, pH 6.0, 0.67% YNB, 0.4 μg/ml biotin, 1% glycerol) and grown until the culture reached an $OD_{600}$ of 5–6. The cell pellet was then harvested and resuspended in BMMY [1% yeast extract, 2% peptone, 100 mM potassium phosphate, pH 6.0, 0.67% YNB, 0.4 μg/ml biotin, 3% (v/v) methanol] using 1/5 volume of the original culture. Absolute methanol was added to a final concentration of 3% (v/v) to induce the expression for 2 days. The culture supernatant was collected to analyze the secreted rPem-GIH on 16.5% Tricine SDS polyacrylamide gel electrophoresis (SDS-PAGE). The expected size of rPem-GIH is approximately 9 kDa.

### 2.4. Purification of rPem-GIH

After 2 days of induction, the culture supernatant was subjected to partial purification by precipitation with ammonium sulfate at 40–50% saturation. The precipitated proteins were solubilized in 20% acetonitrile before subjected to further purification step by solid-phase extraction (SPE) with Reversed-phase SPE cartridge. The soluble protein was loaded on a Sep-Pak cartridge ($C_{18}$) (Sep-Pak, $C_{18}$: 55–105 μm particle, 125 Å pore size, Waters, USA), and subsequently eluted with 20%, 30%, 40%, 50% and 60% acetonitrile in 0.1% (v/v) trifluoroacetic acid (TFA).

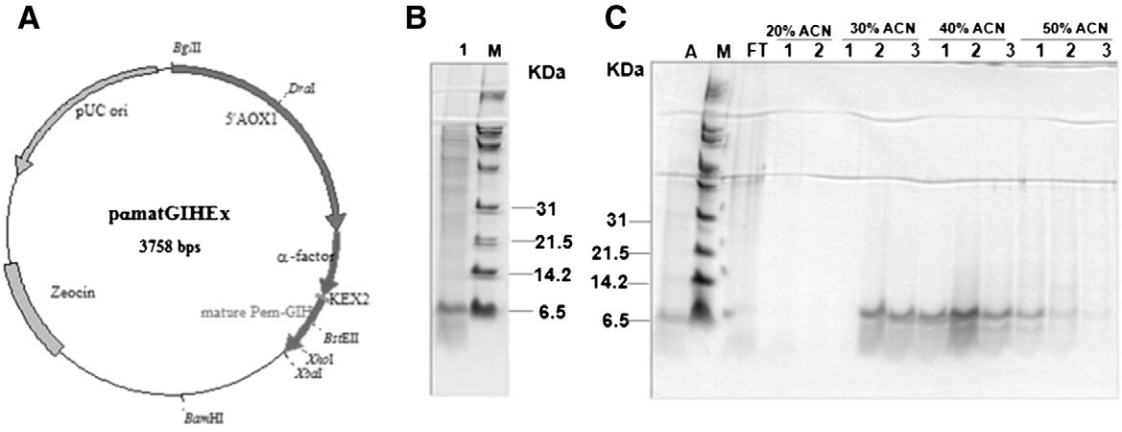


**Fig. 1.** Physical map of pαmatGIHEx and SDS-PAGE analysis of the expression and purification of rPem-GIH from *P. pastoris* transformant. (A) The recombinant pαmatGIHEx plasmid contains the mature peptide of *Pem-GIH* cDNA fused in-frame with the α-factor secretion signal without Glu-Ala repeats. This DNA fragment was inserted into pPICZαA at *Xho* I/*Sal* I compatible site and *Xba* I site downstream of the 5′AOX1 promotor. (B) Coomassie blue-stained tricine SDS-PAGE representing the protein pattern of TCA-precipitated rPem-GIH from *P. pastoris* transformant after induction with 3% (v/v) methanol for 2 days (lane 1). (C) Coomassie blue-stained tricine SDS-PAGE representing the protein pattern of the partially purified rPem-GIH from 40% to 50% ammonium sulfate precipitation (lane A), the flow-through fraction (FT) and reversed-phase SPE ($C_{18}$) purified fractions at 20% (fraction 1–2), 30% (fraction 1–3), 40% (fraction 1–3) and 50% (fraction 1–3) Acetonitrile (ACN) + 0.1% TFA. Lane M shows a broad-range protein marker (Bio-Rad).

The fractions were collected and then evaporated in a Speed-Vac concentrator. The purified protein was dissolved with PBS, pH 7.4 [137.9 mM NaCl, 2.7 mM KCl, 8 mM $Na_2HPO_4 \cdot 2H_2O$, 1.76 mM $KH_2PO_4$] and used for biological activity assay. The purified rPem-GIH was analyzed on 16.5% Tricine SDS-PAGE and determined concentration by Bradford protein assay (BioRad, Hercules, CA).

### 2.5. Extraction and purification of optic lobe extract from adult female *P. monodon*

20 optic lobes of adult female *P. monodon* at previtellogenic stage were isolated and homogenized in 50% acetonitrile containing 0.9% (w/v) NaCl. The crude extract was diluted in 20% acetonitrile, and subsequently loaded on a Sep-Pak cartridge ($C_{18}$) column (Waters, USA). The protein was eluted with 30% and 60% acetonitrile in 0.1% (v/v) TFA. The fractions were collected and evaporated in a Speed-Vac concentrator. The purified protein was dissolved with working medium for primary tissue culture of ovary (see below) and used as a positive control for biological activity assay.

### 2.6. Biological activity assay of rPem-GIH in shrimp primary tissue culture of ovary

The anterior and lateral lobes of the ovary from adult female *P. monodon* at previtellogenic stage were dissected from individual shrimp. The pooled ovary fragments (10 mm. in size/pcs) were washed four times in washing solution I [2× Leibovitz's L-15 medium (GIBCO®), 1% D-Glucose, 0.5% NaCl, 1000 IU/ml penicillin (GIBCO®), 1000 μg/ml streptomycin (GIBCO®) and 4 mg/ml gentamicin sulfate], and then washed twice in washing solution II [2× Leibovitz's L-15 medium (GIBCO®), 1% D-Glucose, 0.5% NaCl, 2000 IU/ml penicillin (GIBCO®), 2000 μg/ml streptomycin (GIBCO®) and 8 mg/ml gentamicin sulfate]. Subsequently, the ovary tissues were minced in a working medium [2× Leibovitz's L-15 (GIBCO®), 1% D glucose, 0.5% NaCl, 100 IU penicillin (GIBCO®), 100 μg/ml streptomycin (GIBCO®), and 40 μg/ml gentamicin sulfate supplemented with 15%(v/v) fetal bovine serum (GIBCO®), 15% (v/v) shrimp meat extract, and 5% (v/v) lactalbumin]. The cell suspension was stirred with a magnetic stirrer in a sterile flask for 15–20 min before transferred to a 50 ml tube and left at room temperature for 5 min. A 1 ml of the primary tissue culture was transferred into a well of 24-well plate and incubated at 26 °C. Propagation of the cells was observed daily under an inverted microscope. After cell propagation for 1–2 days, the primary tissue culture was added with various concentrations of the purified rPem-GIH (1.15 nM, 5.75 nM and 11.5 nM). The negative and positive controls were incubated in the presence of 50 μl of the working medium and partially purified optic lobe, respectively. The treated primary tissue culture of ovary was cultured at 26 °C for 20 h before collected for RNA extraction. The level of *Vg* transcript was detected by RT-PCR with *Vg* specific primers; Vg1-F (5′-CTAAGGCAATTATCACTGCTGCT-3′) and Vg1-R (5′-AAGCTTGGCAAT GTATTCCTTTT-3′) with denaturation at 94 °C for 30 s, annealing at 50 °C for 30 s and extension at 72 °C for 1 min for 34 cycles and followed by a final extension at 72 °C for 7 min. An internal control, *Actin* transcript was amplified with PmActin-F (5′-GACTCGTACGTCGGGCGACG AGG-3′) and PmActin-R (5′-AGCAGCGGTGGTCATCTCCTGCTC-3′) primers in a reaction with 21 cycles of 94 °C for 30 s, 55 °C for 30 s and 72 °C for 1 min. The expected sizes of *Vg* and *Actin* transcripts are 353 and 539 bp, respectively. The intensity of *Vg* and *Actin* bands was quantified by scion image software. Relative *Vg* transcript levels (*Vg*/*Actin* transcripts) were expressed as the percentage of changes relative to non-treated group. The differences between non-treated and tested groups were calculated for significance ($p < 0.05$) using the Kruskal-Wallis test followed by Mann–Whitney *U* test from SPSS 11.5 for Window.

### 2.7. Production and purification of monoclonal antibody

The rPem-GIH expressed from pET3a in *Esherichia coli* BL21 (DE3) pLysS with 0.4 mM Isopropyl-1-thio-β-D-galactoside (IPTG) for 4 h at 37 °C was used for antibody production. The bacterial cells were resuspended in STE buffer [25 mM Tris–HCl (pH 8.0), 150 mM NaCl, 1 mM EDTA] containing 100 μg/ml lysozyme and incubated on ice for 15 min. Subsequently, the cell suspension was sonicated in the presence of 1% triton X-100 and the pellet (inclusion fraction) was washed and resuspended with sterile distilled water. The inclusion fraction of rPem-GIH was subjected to 16.5% Tricine SDS-PAGE and stained with Coomassie blue G-250. The expected rPem-GIH band was excised, and the rPem-GIH was eluted from the gel with 25 mM Tris, 192 mM Glycine and 0.04% (w/v) SDS using a Model 422 Electro-Eluter (BIO-RAD, USA). The eluted rPem-GIH was used as an antigen to produce monoclonal antibody at the Biomedical Technology Research Unit, Faculty of Associated Medical Sciences, Chiangmai University, Thailand.

Monoclonal antibody from positive hybridoma clone (anti-GIH mAb) produced in Hybridoma-SFM medium (Gibco®, USA) was first concentrated with Macrosep® Advance Centrifugal Device (cut-off 30 kDa; Pall, USA) and applied to Acrosep™ Protein A column (Pall, USA). The monoclonal antibody was eluted with 100 mM sodium citrate pH 5 and neutralized by 1 M Tris–HCl (pH 8.8). The purified monoclonal antibody was concentrated with Macrosep® Advance Centrifugal Device (cut-off 3 kDa; Pall, USA). The purified monoclonal antibody was analyzed on 7.5% SDS-PAGE and determined concentration by Bradford protein assay (BioRad, Hercules, CA). The sensitivity and specificity of the monoclonal antibody specific to GIH was determined by dot blot and Western blot analysis, respectively.

### 2.8. Epitope peptide analysis

Eight synthetic peptides were used to evaluate the epitope binding property of anti-GIH mAb. The overlapping peptides from mature *Pem-GIH* were 9–15 amino acids along, with an overlap of five amino acids at the end. All peptides were synthesized at the China Peptide CO., LTD. All peptides were dissolved in DMSO at a concentration of 10 mg/ml. The epitope mapping of Pem-GIH was determined by ELISA and dot blot, respectively. For ELISA, 1 μg of each peptide was coated in Nunc F96 Maxisorp Microwell™ plate (Nunc™ Thermo Scientific, Denmark) and incubated overnight at 4 °C. Then 100 μl of the anti-GIH mAb at the dilution of 1:7500 in 4% non-fat milk was added and incubated at 4 °C for 16 h. The plate was washed three times with PBS supplement with 0.1% Tween® 20 prior to incubation with 1:10,000 dilution of Peroxidase-conjugated anti-mouse IgG (whole molecule) (Sigma, USA) in 4% non-fat milk at 37 °C for 3 h. After the washing step, 0.1 mg/ml of 3,3′,5,5′-Tetramethylbenzidine (Sigma, USA) in substrate buffer (10%(v/v) DMSO, 45 mM Phosphate–Citrate buffer, pH 5 and 0.006%(v/v) hydrogen peroxide) was added and further incubated for 30 min. The reactions were stopped with 2 M sulfuric acid. The color development was measured spectrophotometrically at 450 nm. For dot blot analysis, an aliquot of 2 μl (1, 2.5, 5, 10 μg) of each peptides were spotted on a PVDF membrane (Pall, USA) and placed in diluted anti-GIH mAb (1:7500) in 4% non-fat milk at room temperature for 90 min. The membrane was washed three times with PBS supplement with 0.1% Tween® 20, and then incubated with Peroxidase-conjugate anti-mouse IgG (whole molecule) (Sigma, USA) at dilution of 1:10,000 in 4% non-fat milk at room temperature for 90 min. The immunoreactive spots were developed with Immobilon™ Western chemiluminescent HRP substrate (Millipore, USA).

### 2.9. Neutralization of Pem-GIH activity by anti-GIH mAb in shrimp primary tissue culture of ovary

In order to investigate the effect of antibody neutralization on the activity of Pem-GIH, the partially purified optic lobes at 0.5 eyestalk

equivalent and 100 ng of purified anti-GIH mAb were co-incubated in the primary tissue culture of the ovary. The tissue culture incubated with 0.5 eyestalk equivalent of the partially purified optic lobes alone was used as a positive control. The treated cells were cultured at 26 °C for 20 h, and then collected for RNA extraction. The level of *Vg* transcript was detected by quantitative real-time PCR (qPCR) using KAPA™ SYBR® FAST qPCR Kit (KAPABIOSYSTEMS, USA) with *Vg* specific primers; Vg2-F: 5′-TCCATCTGCAGCACCAATCTTCGC-3′ and Vg2-R: 5′-GCAACAGCCTTCATTCTGATGCCA-3′. An internal control, *EF-1α* transcript was amplified with EF-1α F (5′-GAACTGCTGACCAAGATCGACA GG-3′) and EF-1α R (5′-GAGCATACTGTTGGAAGGTCTCCA-3′) primers. A reaction composing of 1× KAPA SYBR FAST qPCR Master Mix and 200 nM each of forward and reverse primers was carried out in a Mastercycle® ep *realplex* (Eppendorf, USA) following the KAPA™ SYBR® FAST qPCR protocol (KAPABIOSYSTEMS, USA). Relative *Vg* transcript levels (*Vg*/*EF1-α* transcripts) were expressed as the percentage of changes relative to the non-treated group. The differences between non-treated and tested groups were calculated for significance ($p < 0.05$) using the Kruskal–Wallis test followed by Mann–Whitney *U* test from SPSS 11.5 for Window.

### 2.10. Induction of ovarian maturation by GIH mAb injection

Wild *P. monodon* broodstock at previtellogenic stage were cultured in concrete tank filled with 25–30 ppt seawater at the average temperature of 28–30 °C under dark condition. Shrimp were divided into 3 groups, each containing 10–15 shrimp per experiment. The unilaterally-eyestalk ablated shrimp and the normal shrimp were used as a positive and negative control groups, respectively. In the experimental group, shrimp were injected once with 20 μg of purified anti-GIH mAb in PBS (pH 7.4) in the volume of 50 μl through the arthrodial membrane of the second walking leg. Shrimp were fed with fresh food such as live natural polychaetes (blood worms and sand worms) and squid 3–5 times a day throughout the period of the experiment. Developmental stages of the ovary were observed by the appearance of the ovary that could be seen through the dorsal exoskeleton under the torchlight as described previously (Treerattrakool et al., 2011) and recorded daily for 31 days. The experiments were performed at Pichitpol Farm, Bangphra, Chonburi, Thailand.

## 3. Results

### 3.1. Expression and purification of recombinant Pem-GIH

The rPem-GIH protein was expressed as a soluble protein in *P. pastoris* expression system under the control of an alcohol oxidase promoter. The optimal condition for the expression of the rPem-GIH was 3% (v/v) methanol for 2 days. An SDS-PAGE analysis of the culture supernatant of Pem-GIH *P. pastoris* transformants showed a major protein product of about 9 kDa, which corresponds to the expected size of rPem-GIH (Fig. 1B). This protein band was not present in the culture supernatant of *P. pastoris* transformant containing pPICZαA vector alone (data not shown). The amount of the secreted rPem-GIH was approximately 0.5 mg/l of the culture medium. Partial purification by ammonium sulfate precipitation could remove some endogenous proteins from the culture supernatant of *P. pastoris* transformant containing pαmatGIHEx as shown in Fig. 1C (lane A). Subsequent purification by a Sep-Pak cartridge ($C_{18}$) revealed that the expected rPem-GIH was eluted at 30–50% acetronitrile in 0.1% TFA (Fig. 1C). The final yield of rPem-GIH after purification was approximately 30 μg/l of culture medium (equal to 6% of secreted rPem-GIH in the culture medium). Fractions containing the purified rPem-GIH were pooled and further analyzed for GIH activity in ovarian primary tissue culture.

### 3.2. Biological activity assay of rPem-GIH in shrimp primary tissue culture of ovary

The effect of partially purified optic lobes and the purified rPem-GIH on vitellogenin synthesis activity was verified in primary tissue culture of previtellogenic ovary. Inhibition of *Vg* mRNA level was observed when the cells were treated with 1.15–11.5 nM rPem-GIH (Fig. 2B) with a significant reduction of *Vg* mRNA level by 45.7% in 11.5 nM rPem-GIH treated cells compared with that of the non-treated group. This level of inhibition was similar to the effect of partially purified optic lobes at 0.5 ES equivalent (Fig. 2A).

### 3.3. Sensitivity, specificity and epitope mapping of anti-GIH mAb

Only one among three hybridoma clones produced anti-GIH mAb reacting with Pem-GIH in the eyestalk by immunohistology (unpublished data). The anti-GIH mAb belong to IgG1 subclass and κ-type light chain. The yield of the purified anti-GIH mAb from this clone was approximately 45 mg/l. The mAb at dilution of 1:20,000 could detect as low as 50 pg and 250 pg of rPem-GIH as determined by dot blot and Western blot analysis, respectively (data not shown). At the dilution of 1:100,000, the anti-GIH mAb did not cross-react with 30 ng of other structurally-related proteins in the CHH family i.e. rPem-CHH and rPem-MIH (Fig. 3A). Moreover, the anti-GIH mAb at the dilution of 1:20,000 could detect the faint GIH signal in crude optic lobe extract and produce strong GIH signals in the purified rPem-GIH fractions (Fig. 3B). This result showed specificity of the anti-GIH mAb to react with Pem-GIH purified from the optic lobe extract.

The result of epitope mapping on eight partial peptides containing overlapping Pem-GIH sequences by ELISA showed reactivity against only peptide no.2 (Table 1). Dot blot analysis revealed that GIH-mAb could detect a lowest amount of the synthetic peptide epitope at 1 μg as shown in Fig. 4. This result suggested that the peptide no. 2, MGNRDMYNKVERVCE, contains a reactive epitope for anti-GIH mAb.

### 3.4. Neutralization of Pem-GIH activity by anti-GIH mAb in shrimp primary tissue culture of the ovary

In order to determine whether the binding of anti-GIH mAb to GIH can inhibit the activity of the hormone or not, the appropriate amount of anti-GIH mAb was co-incubated with native Pem-GIH peptide from partially purified optic lobes in the primary culture of ovarian cells. The partially purified optic lobes at 0.5 ES equivalent alone could reduce the expression level of *Vg* mRNA by 31% of the control cells. Interestingly, when the partially purified optic lobes at 0.5 ES equivalent and 100 ng of the anti-GIH mAb was co-incubated with the ovarian tissue culture, the expression level of *Vg* mRNA has recovered to about 87.3% of the control cells (Fig. 5). Thus the result demonstrated that the anti-GIH mAb was able to neutralize the biological activity of native Pem-GIH peptide from the eyestalk.

### 3.5. Induction of ovarian maturation by GIH mAb injection

Whether or not the inhibitory effect on the activity of Pem-GIH in shrimp by single injection of anti-GIH mAb would lead to ovarian maturation was examined by following ovarian maturation in anti-GIh mAb injected shrimp for 31 days.

The results in Fig. 6A revealed that eyestalk ablation could induce spawning in approximately 60% of eyestalk ablated shrimp. Interestingly, inhibition of Pem-GIH activity by injection of anti-GIH mAb also induced comparable proportion of spawning shrimp at about 67%, whereas the control shrimp did not show ovarian development. An independent experiment also showed comparable spawning rate in the eyestalk ablated shrimp and the injected shrimp (Fig. 6B). In addition, a large proportion of the control shrimp showed ovary regression at early stages of ovarian development.

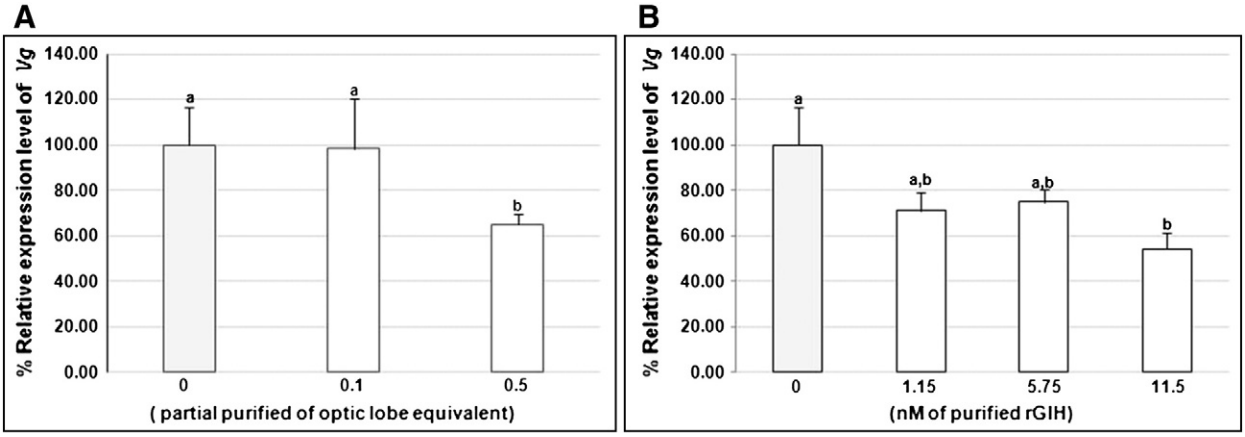


**Fig. 2.** The effect of partial purified optic lobes (A) and rPem-GIH (B) on *Vg* expression in shrimp primary cell culture of the ovary. Relative expression of *Vg* (*Vg*/*β-Actin* mRNA) from each group was expressed as the percentage change (mean ± S.E.M) relative to each non-treated group (control value = 100). (A) Changes in the percentage of relative expression of *Vg* from the ovary primary cell culture incubated either without (n = 7) or with partially purified optic lobes at 0.1 (n = 9) and 0.5 (n = 9) eyestalk equivalent. (B) The relative expression of *Vg* from the ovary primary cell culture incubated either without rPem-GIH (n = 7) or with rGIH at concentrations of 1.15 nM (n = 7), 5.75 nM (n = 9) and 11.5 nM (n = 7). Bars with different letters indicate significant differences ($p < 0.05$).

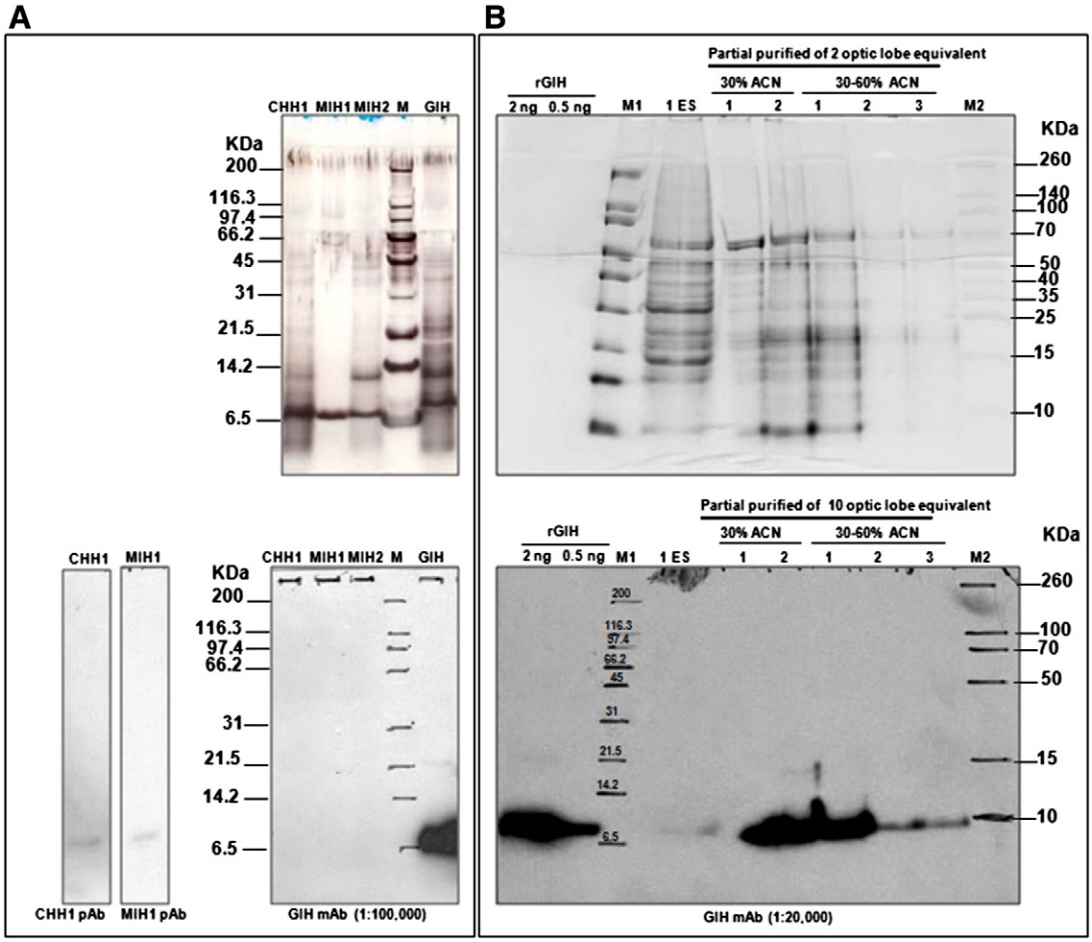


**Fig. 3.** Specificity of anti-GIH mAb (A) specificity against recombinant GIH proteins. The upper panel shows the protein patterns of 30 ng of rPem-CHH 1, rPem-MIH 1, rPem-MIH 2 and rPem-GIH from *P. pastoris* expression system on the tricine SDS-PAGE whereas the lower panel shows the Western blot detection with anti-GIH mAb at dilution of 1:100,000 compared with the positive antibody for rPem-CHH1 and rPem-MIH1 (anti-CHH1 polyclonal antibody at dilution of 1:10,000 and anti-MIH1 polyclonal antibody at dilution of 1:10,000). Lane M1 shows a broad-range molecular weight marker (Bio-RAD). (B) Detection of GIH in *P. monodon's* optic lobes by Western blot analysis with anti-GIH mAb. The upper panel shows the protein patterns on the tricine SDS-PAGE whereas the lower panel shows the Western blot detection by anti-GIH mAb of the corresponding membrane. Lane M1 and M2 show a broad-range molecular weight marker (Bio-RAD) and a spectra™ multicolor broad range protein ladder (Thermo Scientific), respectively. A pooled of extract from 10 optic lobes were partially purified by reversed-phase SPE ($C_{18}$) cartridges. Each fraction of the flow-through (FT) and the reversed-phase SPE ($C_{18}$) purified fractions at 30% (fraction 1–2) and 60% (fraction 1–3) Acetonitrile (ACN) + 0.1% TFA were analyzed and compared to crude optic lobe extract at 1 ES equivalent. The rPem-GIH was loaded and used as a positive control.

**Table 1**
ELISA reactions of anti-GIH mAb with the overlapping synthetic peptide sequences from mature Pem-GIH.

| Peptide sequence | Average ELISA absorbance (450 nm) of GIH mAb ± SD |
|---|---|
| 1. NILDSKCRGAMGNRD | 0.052 ± 0.001 |
| 2. MGNRDMYNKVERVCE | 1.526 ± 0.049 |
| 3. ERVCEDCTNIYRLPQ | 0.055 ± 0.002 |
| 4. YRLPQLDGLCRNRCF | 0.054 ± 0.003 |
| 5. RNRCFNNQWFLMCLH | 0.059 ± 0.003 |
| 6. LMCLHSAKREAELEH | 0.051 ± 0.004 |
| 7. AELEHFRLWISILNA | 0.051 ± 0.001 |
| 8. SILNAGRPW | 0.054 ± 0.001 |

## 4. Discussion

In this study, a gonad-inhibiting hormone of *P. monodon* (Pem-GIH) was produced in the yeast *P. pastoris* expression system and its function on vitellogenin-inhibiting activity was determined in primary tissue culture derived from previtellogenic ovary of *P. monodon*. The rPem-GIH was successfully expressed in *P. pastoris* under the control of *AOX1* promoter and secreted into the culture medium using the α-factor signal sequence without the Glu-Ala repeats from *S. cerevisiae*. This system was used to produce other recombinant eyestalk hormones of *P. monodon* such as Pem-CHH 1–3 and Pem-MIH 1, which were demonstrated to possess biological activities (Treerattrakool et al., 2003; Udomkit et al., 2004; Yodmuang et al., 2004). The partially purified rPem-GIH was subjected to further purification by one step of reversed-phase SPE on the Sep-Pak cartridge ($C_{18}$). The purified rPem-GIH was eluted at the same range of acetronitrile concentration as Pem-CHH 1 that was purified by RP-HPLC (Treerattrakool et al., 2003). Even though the yield of the purified rPem-GIH expressed in this study was lower than that of rHoa-VIH expressed in *E. coli* (Ohira et al., 2006), the rPem-GIH produced in *P. pastoris* could be easily purified by reversed-phase SPE and did not require solubilization and refolding steps that are necessary to obtain biologically active proteins expressed in *E. coli* expression system.

To date, the action of GIH on vitellogenin synthesis in the ovary has been established (Aguilar et al., 1992; Ohira et al., 2006). Apart from the ovary, hepatopancreas has been revealed as another site for vitellogenin synthesis in shrimp (Tseng et al., 2001). However, no evidence about the biological activity of GIH on vitellogenesis in the hepatopancreas has been demonstrated. Therefore, the primary tissue culture from previtellogenic ovary was used to demonstrate the role of rPem-GIH to inhibit of vitellogenin expression. Regardless of the lack of carboxyl-terminus which is important for vitellogenesis-inhibiting activity of VIH of *H. americanus* (Ohira et al., 2006), the rPem-GIH showed

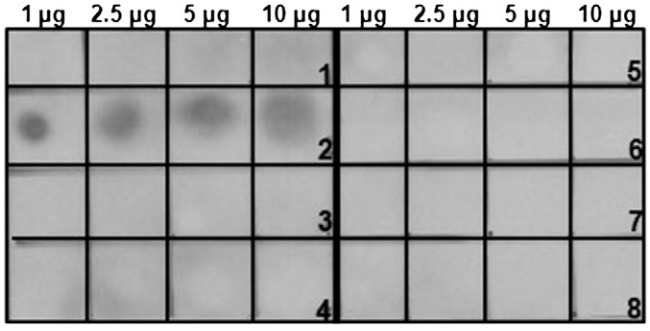


**Fig. 4.** Epitope mapping analysis by dot blot. Eight overlapping synthetic peptides of Pem-GIH are designed as 1–8. Labels 1–8 represent 1, 2.5, 5 and 10 μg of overlapping synthetic peptides of Pem-GIH, respectively. Left panel is the synthetic peptide no. 1–4 and right panel is the synthetic peptide no. 5–8. The dilution of 1:7500 of anti-GIH mAb was used in dot blot analysis to determine the immunoreactive to the overlapping synthetic peptides of Pem-GIH.

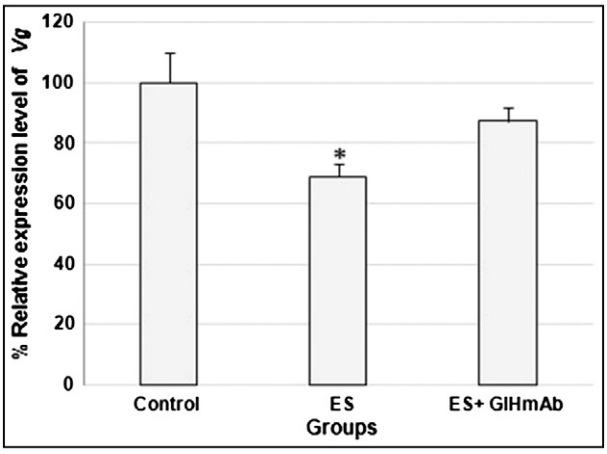


**Fig. 5.** Neutralization assay of Pem-GIH activity by anti-GIH mAb in shrimp primary tissue culture of the ovary. Relative expression of *Vg* (*Vg*/*EF-1α* mRNA) from the primary tissue culture of ovary incubated with the partially purified optic lobes at 0.5 eyestalk equivalent alone (ES) or with partially purified optic lobes at 0.5 eyestalk equivalent and 100 ng of anti-GIH mAb (ES + GIH mAb) was expressed as the percentage change (mean ± S.E.M; n = 6) relative to the non-treated group (control value = 100) (C). An asterisk indicates values significantly different from non-treated group, $p < 0.05$.

the biological activity to inhibit vitellogenin mRNA expression in the primary tissue culture of the ovary similar to the effect of partially purified optic lobes from previtellogenic *P. monodon*. This result supported our previous study by RNA interference technique that Pem-GIH possesses an inhibiting activity on vitellogenin mRNA expression in the ovary from previtellogenic female *P. monodon* broodstock (Treerattrakool et al., 2008). Therefore, we can conclude that the vitellogenesis-inhibiting activity of rPem-GIH, type II subfamily of CHH, is demonstrated in *ex vivo* bioassay. On the other hand, the CHH-family peptides type I from *M. japonicas* (Pej-SPG-I, -II, -III, -V, -VI and -VII) have been characterized as hyperglycemic activity (Nagasawa et al., 1999; Yang et al., 1997) and also as vitellogenesis-inhibiting activity (Khayat et al., 1998; Tsutsui et al., 2013). In addition, the members of CHH-family are multifunctional hormones and often exhibit overlapping biological activity (Webster et al., 2012). Thus, the molecular characteristics of neuropeptide for vitellogenesis-inhibiting activity in penaeid shrimp are still unclear. However, the bioassay system developed in this study could be used for verification of biological function of the hormones involved in ovarian development in other crustaceans.

Additionally, we speculated that the anti-GIH antibody would bind the circulating GIH in the hemolymph or GIH that was stored in the sinus gland, and probably lead to vitellogenesis. Our previous study demonstrated that injection of an antibody against crustacean hyperglycemic hormone (CHH) could inhibit the hormone activity in juvenile *P. monodon* by 30–50% (Treerattrakool et al., 2006). Therefore, the monoclonal antibody against rPem-GIH was produced and used to investigate its effect on the activity of Pem-GIH in ovarian primary tissue cell culture. However, the yield of secreted rPem-GIH from *P. pastoris* was low (approximately 0.5 mg/l), even though the expression conditions e.g. methanol concentration and period of induction had been optimized, comparing to 150 mg/l of rPem-CHH1 (Treerattrakool et al., 2003) and 100 mg/l of rPem-MIH1 (Yodmuang et al., 2004) produced by the same system. Accordingly, *E. coli* expression system was used to produce large amount of rPem-GIH for antibody production instead. Although rPem-GIH was expressed as an insoluble protein in *E. coli*, our previous data showed that the rPem-GIH from *E. coli* partially retained its biological activity (Treerattrakool, 2008). The specificity of anti-GIH mAb was demonstrated by its ability to recognize only rPem-GIH but not other structurally-related proteins in the CHH family. Our result demonstrated that the anti-GIH mAb recognized an epitope that is located between amino acid positions 11 and 25 of the mature Pem-GIH (15 amino acid residues in length) and did not cross-react to the

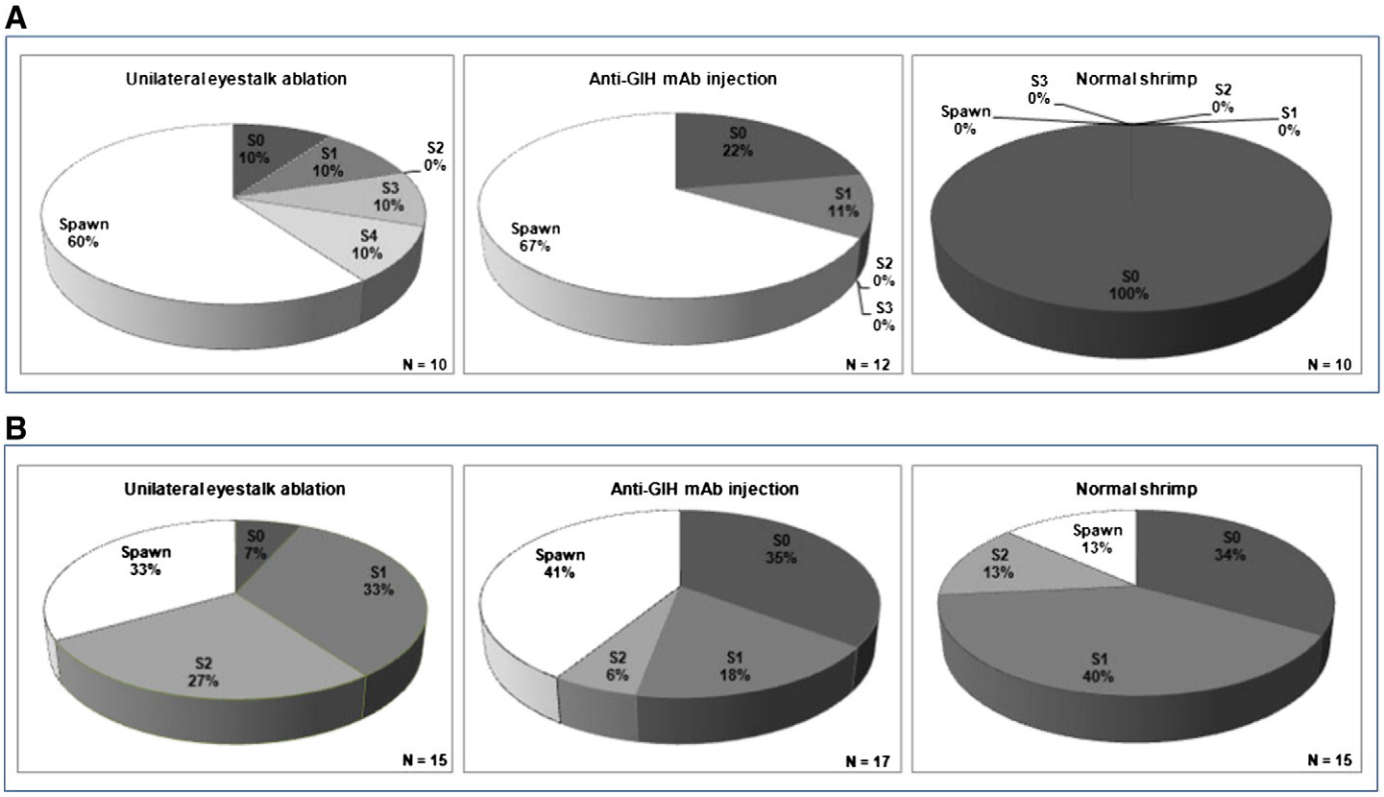


**Fig. 6.** Ovarian maturation and spawning in wild female *P. monodon* after injection of anti-GIH mAb. Ovarian developmental stages were examined under torch light and recorded daily over the 31 days period after either with or without eyestalk ablation and injection of anti-GIH mAb. The sample numbers were 10–12 (A) and 15–17 (B) shrimp in each group. The developmental stages of the ovary were determined according to Tan-Fermin and Pudadera (1989) as follows: the undeveloped ovary (S0) could not be seen under light beam; the previtellogenic ovary (S1) was seen as a thin line; the developing or early vitellogenic ovary (S2) appeared as a linear band through the exoskeleton; the late vitellogenic ovary (S3) could be visualized as a dark band through the exoskeleton with larger expansion at the posterior thorax; the ripe ovary (S4) appeared as a dark band through the exoskeleton with the diamond shape in the first abdominal segment.

other two overlapping peptides that shared amino acids at positions 11–15 and 21–25, suggesting that the residues MYNKV (positions 16–20) may serve as mAb epitope.

Our results demonstrated that the anti-GIH mAb could neutralize the vitellogenesis-inhibiting activity of Pem-GIH and led to an increase in *Vg* expression level in the primary tissue culture of the ovary. We thus next investigate possible application of anti-GIH mAb to induce ovarian development in the shrimp. The results clearly showed that injection of anti-GIH mAb into the broodstock shrimp was able to stimulate spawning at comparable rate to eyestalk-ablation. The ovarian maturation induced by anti-GIH mAb was likely due to the neutralization effect of the mAb on the circulating GIH in the hemolymph, thus reduced the effective concentration of GIH. Previously, we demonstrated the strategy to induce ovarian maturation by GIH-dsRNA (Treerattrakool et al., 2011). However, the GIH-dsRNA would demolish only the newly synthesized GIH mRNA, not the Pem-GIH that was already stored in the sinus gland and ready for being released into the hemolymph (Treerattrakool et al., 2011). The efficiency of ovarian induction could be enhanced by combination of GIH-dsRNA and anti-GIH mAb that would coordinately block the GIH action at both mRNA and protein levels, therefore make it a promising alternative to induce ovarian maturation and spawning.

In conclusion, we have demonstrated the utilization of rPem-GIH to determine the biological function of the hormone that may be useful for further studies such as the study on the relationship between GIH and *Vg* during ovarian development and characterization of GIH receptor for a better understanding of how GIH controls vitellogenesis. Additionally, the developed bioassay system may be used for biological characterization of other proteins involving in ovarian development. Moreover, our study exhibited an effective approach for induction of ovarian maturation in female broodstock of *P. monodon* based on the utilization of the antibody against Pem-GIH that will be useful for shrimp aquaculture. We also proposed that the combination of anti-GIH mAb and GIH-dsRNA to completely block the GIH activity would lead to a higher efficiency of this strategy to enhance ovarian maturation and spawning that could substitute for the brutality of eyestalk ablation technique.

## Acknowledgments

We thank Dr. Pongsopee Attasart and Assistant Professor Witoon Tirasophon for their suggestions on primary tissue culture preparation, Dr. Sittiruk Roytrakul (National Center for Genetic Engineering and Biotechnology (BIOTEC), Thailand) for his suggestion on protein purification, Dr. Saengduen Moonsom and Dr. Promsin Masrinoul for their suggestions on epitope mapping, Prof. Boonsirm Withyachumnarnkul for providing the anti-MIH 1 polyclonal antibody, Mr. Banchong Nissagavanich for his suggestion on reproductive performance in *P. monodon* and Ms. Somjai Wongtripop (Shrimp Genetics Improvement Center, Surat Thani, Thailand) for providing the domesticated *P. monodon* broodstock. We thank Mr. Vichai Boonsai (Pichitpol farm, Chonburi, Thailand) for his kind assist in culturing wild broodstock and recording the ovarian maturation. This work was supported by the Thailand Research Fund (TRG568002 to S.T. and DPG5680001 to S.P.), Cluster and Program Management Office, National Science and Technology Development Agency and Mahidol University research grant.

## References


Aguilar, M.B., Quackenbush, L.S., Hunt, D.T., Shabanowitz, J., Huberman, A., 1992. Identification, purification and initial characterization of the vitellogenesis-inhibiting hormone from the Mexican crayfish *Procambarus Bouvieri* (Ortmann). Comp. Biochem. Physiol. 102B, 491–498.

Böcking, D., Dircksen, H., Keller, R., 2002. The crustacean neuropeptides of the CHH/MIH/GIH family: structures and biological activities. In: Wiese, K. (Ed.), The Crustacean Nervous System. Springer, Heidelberg, pp. 84–97.

De Kleijn, D.P., Janssen, K.P., Waddy, S.L., Hegeman, R., Lai, W.Y., Martens, G.J., Herp, F., 1998. Expression of the crustacean hyperglycaemic hormones and the gonad-inhibiting hormone during the reproductive cycle of the female American lobster *Homarus americanus*. J. Endocrinol. 156, 291–298.

Edomi, P., Azzoni, E., Mettulio, R., Pandolfelli, N., Ferrero, E.A., Giulianini, P.G., 2002. Gonad-inhibiting hormone of the Norway lobster (*Nephrops norvegicus*): cDNA cloning, expression, recombinant protein production, and immunolocalization. Gene 284, 93–102.

Katayama, H., Ohira, T., Nagata, K., Nagasawa, H., 2001. A recombinant molt-inhibiting hormone of the kuruma prawn has a similar secondary structure to a native hormone: determination of disulfide bond arrangement and measurements of circular dichroism spectra. Biosci. Biotechnol. Biochem. 65, 1832–1839.

Keller, R., 1992. Crustacean neuropeptides: structures, functions and comparative aspects. Experientia 48, 439–448.

Khayat, M., Yang, W.J., Aida, K., Nagasawa, H., Tietz, A., Funkenstein, B., Lubzens, E., 1998. Hyperglycaemic hormones inhibit protein and mRNA synthesis in *in vitro*-incubated ovarian fragments of the marine shrimp *Penaeus semisulcatus*. Gen. Comp. Endocrinol. 110, 307–318.

Lorenzon, S., 2005. Review: hyperglycemic stress response in Crustacea. ISJ 2, 132–141.

Nagasawa, H., Yang, W.J., Aida, K., Sonobe, H., 1999. Chemical and biological characterization of neuropeptides in the sinus glands of the kuruma prawn, *Penaeus japonicus*. In: Shimonishi, Y. (Ed.), Peptide Science — Present and Future. Kluwer, Dordrecht, pp. 453–454.

Ohira, T., Okumura, T., Suzuki, M., Yajima, Y., Tsutsui, N., Wilder, M.N., Nagasawa, H., 2006. Production and characterization of recombinant vitellogenesis-inhibiting hormone from the American lobster *Homarus americanus*. Peptides 27, 1251–1258.

Okumura, T., Kim, Y.K., Kawazoe, I., Yamano, K., Tsutsui, N., Aida, K., 2006. Expression of vitellogenin and cortical rod proteins during induced ovarian development by eyestalk ablation in the kuruma prawn, *Marsupenaeus japonicus*. Comp. Biochem. Physiol. A Mol. Integr. Physiol. 143, 246–253.

Soyez, D., Van Deijnen, J.E., Martin, M., 1987. Isolation and characterization of a vitellogenesis-inhibiting factor from the sinus gland of the lobster, *Homarus americanus*. J. Exp. Zool. 244, 479–484.

Tan-Fermin, J.D., Pudadera, R.A., 1989. Ovarian maturation stages of the wild giant tiger prawn Penaeus monodon Fabricius. Aquaculture 77, 229–242.

Treerattrakool, S., 2008. Molecular and Functional Characterization of Gonad-inhibiting Hormone (GIH) from the Shrimp *Penaeus monodon*. (Ph.D. Thesis in Molecular Genetics and Genetic Engineering) Mahidol University, Thailand.

Treerattrakool, S., Udomkit, A., Eurwilaichitr, L., Sonthayanon, B., Panyim, S., 2003. Expression of biologically active crustacean hyperglycemic hormone (CHH) of *Penaeus monodon* in *Pichia pastoris*. Mar. Biotechnol. 5, 373–379.

Treerattrakool, S., Udomkit, A., Pamyim, S., 2006. Anti-CHH antibody causes impaired hyperglycemia in *Penaeus monodon*. J. Biochem. Mol. Biol. 39, 371–376.

Treerattrakool, S., Panyim, S., Chan, S.M., Withyachumnarnkul, B., Udomkit, A., 2008. Molecular characterization of gonad-inhibiting hormone of *Penaeus monodon* and elucidation of its inhibitory role in vitellogenin expression by RNA interference. FEBS J. 275, 970–980.

Treerattrakool, S., Panyim, S., Udomkit, A., 2011. Induction of ovarian maturation and spawning in *Penaeus monodon* broodstock by double-stranded RNA. Mar. Biotechnol. 13, 163–169.

Tseng, D.F., Chen, Y.N., Kou, G.H., Lo, C.F., Kuo, C.M., 2001. Hepatopancreas is the extraovarian site of vitellogenin synthesis in black tiger shrimp, *Penaeus monodon*. Comp. Biochem. Physiol. A 129, 909–917.

Tsutsui, N., Nagakura, N.A., Nagai, C., Ohira, T., Wilder, M., Nagasawa, H., 2013. The *ex vivo* effects of eyestalk peptides on ovarian vitellogenin gene expression in the kuruma prawn *Marsupenaeus japonicus*. Fish. Sci. 79, 33–38.

Udomkit, A., Treerattrakool, S., Panyim, S., 2004. Crustacean hyperglycemic hormones of *Penaeus monodon*: cloning, production of active recombinant hormones and their expression in various shrimp tissues. J. Exp. Mar. Biol. Ecol. 298, 79–91.

Webster, S.G., Keller, R., Dircksen, H., 2012. The CHH-superfamily of multifunctional peptide hormones controlling crustacean metabolism, osmoregulation, moulting, and reproduction. Gen. Comp. Endocrinol. 175, 217–233.

Wilder, M.N., Okumura, T., Tsutsui, N., 2010. Reproductive mechanisms in Crustacea focusing on selected prawn species: vitellogenin structure, processing and synthetic control. ABSM 3, 73–110.

Yang, W.J., Rao, K.R., 2001. Cloning of precursors for two MIH/VIH-related peptides in the prawn, *Macrobrachium rosenbergii*. Biochem. Biophys. Res. Commun. 289, 407–413.

Yang, W.J., Aida, K., Nagasawa, H., 1997. Amino acid sequences and activities of multiple hyperglycemic hormones from the kuruma prawn, *Penaeus japonicus*. Peptides 18, 479–485.

Yodmuang, S., Udomkit, A., Treerattrakool, S., Panyim, S., 2004. Molecular and biological characterization of molt-inhibiting hormone of *Penaeus monodon*. J. Exp. Mar. Biol. Ecol. 312, 101–114.

# 3. Molecular cloning and functional characterization of Argonaute-3 gene from *Penaeus monodon*.

Fish & Shellfish Immunology 35 (2013) 874–882

Contents lists available at SciVerse ScienceDirect

Fish & Shellfish Immunology

journal homepage: www.elsevier.com/locate/fsi

# Molecular cloning and functional characterization of Argonaute-3 gene from *Penaeus monodon*

Amnat Phetrungnapha [a,1], Teerapong Ho [a,1], Apinunt Udomkit [a], Sakol Panyim [a,b], Chalermporn Ongvarrasopone [a,*]

[a] Institute of Molecular Biosciences, Mahidol University, Phutthamonthon 4 Road, Salaya, Nakhon Pathom 73170, Thailand
[b] Department of Biochemistry, Faculty of Science, Mahidol University, Rama VI Road, Phayathai, Bangkok 10400, Thailand

ARTICLE INFO

*Article history:*
Received 15 November 2012
Received in revised form
8 June 2013
Accepted 21 June 2013
Available online 30 June 2013

*Keywords:*
Argonaute
RNAi
Double-stranded RNA
Black tiger shrimp
YHV

ABSTRACT

Argonaute (Ago) proteins play a crucial role in the shrimp RNA interference pathway. In this study, we identified and characterized a novel Ago gene from black tiger shrimp, *Penaeus monodon*. The complete open reading frame of *P. monodon* Ago3 (*PmAgo3*) consisted of 2559 nucleotides encoding a polypeptide of 852 amino acids with a predicted molecular weight of 97 kDa and an isoelectric point of 9.42. Analysis of the deduced amino acid sequence of *PmAgo3* revealed the presence of two signature domains of the proteins in Argonaute family including PAZ and PIWI. Phylogenetic analysis indicated that *PmAgo3* is classified into Ago subfamily and shared the highest amino acid sequence identity (83%) with *Litopenaeus vannamei* Ago2. Monitoring of the *PmAgo3* expression by quantitative real-time PCR revealed that this gene was significantly up-regulated following dsRNA administration, while no significant difference in its expression was observed following yellow head virus (YHV) challenge. In contrast, inhibition of YHV mRNA expression was observed in *PmAgo3*-knockdown shrimp. These data imply that PmAgo3 is involved in the dsRNA-mediated gene silencing mechanism and plays an important role in YHV replication in the black tiger shrimp.



## 1. Introduction

RNA interference (RNAi) is a post-transcriptional gene silencing process mediated by a unique family of RNA-binding proteins named Argonaute (Ago). Ago proteins bind small regulatory RNAs such as siRNA (short-interfering RNA), miRNA (microRNA), and piRNA (Piwi-interacting RNA) to form the RNA-induced silencing complex (RISC), and then direct either target RNA degradation or translational inhibition. All Ago proteins share two main structural features including PAZ (PIWI/Argonaute/Zwile) and PIWI domains [1]. Crystallographic studies of Ago protein structures from both prokaryotes and eukaryotes revealed the presence of a bilobed structure composing of four distinct domains including N, PAZ, MID and PIWI connected through two linkers [2,3]. The N domain is involved in small RNA duplex unwinding during RISC assembly [4]. The PAZ domain exhibits oligonucleotide-binding fold which can recognize the 2-nt overhang at the 3′-end of the small RNA duplex [5,6]. The MID domain forms a binding pocket for anchoring 5′-phosphate of the small RNA [7,8]. The PIWI domain is structurally similar to ribonuclease H (RNase H) enzyme, and consists of the conserved catalytic residues Asp-Asp-His (DDH) motif which is crucial for the endonucleolytic “slicer” activity of the RISC [3,9].

Argonaute proteins are evolutionarily conserved in a wide range of eukaryotes. Based on phylogenetic analysis, Ago proteins can be classified into three categories including Ago subfamily, Piwi subfamily, and worm-specific Argonautes (WAGO) [10]. The Ago subfamily is ubiquitously expressed and is involved in siRNA and miRNA pathways, whereas the Piwi subfamily is a germ-cell specific Ago family involving in piRNA pathway. WAGO is a worm-specific Ago family which was identified in *Caenorhabditis elegans*, and was found to be involved in a variety of cellular processes in worm, such as chromosome segregation, fertility, and endogenous RNAi pathway [11]. The number of Ago genes presented in different species is varied. Some species such as *Schizosaccharomyces cerevisiae* encodes a single Ago protein whereas most species contain multiple Ago proteins. For example, 5, 8, 10, and 27 Ago genes were identified in *Drosophila*, human, *Arabidopsis thaliana*, and *C. elegans*, respectively [1]. In penaeid shrimp, two Ago genes, including *PmAgo1* (*Pem-Ago1*) and *PmAgo2* were identified and

* Corresponding author. Institute of Molecular Biosciences, Mahidol University (Salaya Campus), 25/25 Phutthamonthon 4 Rd., Salaya, Phutthamonthon District, Nakhon Pathom 73170, Thailand. Tel.: +66 2 8003624x1280; fax: +66 2 4419906.
*E-mail address:* chalermporn.ong@mahidol.ac.th (C. Ongvarrasopone).
[1] Both authors have equal contribution.

1050-4648/$ – see front matter © 2013 Elsevier Ltd. All rights reserved.
http://dx.doi.org/10.1016/j.fsi.2013.06.025

characterized in the black tiger shrimp. PmAgo1 was involved in dsRNA-mediated gene silencing, and responded to yellow head virus (YHV) infection [12,13]. PmAgo2 is a germ cell-specific Ago protein with an unknown function (Udomkit et al., unpublished data). In pacific white shrimp, *Litopenaues vannamei*, two Ago genes, including *LvAgo1* and *LvAgo2* were identified and characterized. Chen et al. demonstrated that LvAgo2 interacted with LvDicer2 and LvTRBP1 [14]. Robalino et al. demonstrated that *LvAgo2*, but not *LvAgo1*, responded to double-stranded RNA (dsRNA) [15]. In addition, two Ago genes were also identified and characterized in *Marsupenaeus japonicas* [16,17].

Accumulating evidence demonstrates that RNAi plays an important role in antiviral immunity in penaeid shrimp [18–20]. Nevertheless, the information of the RNAi-based mechanism in penaeid shrimp is still largely elusive. Identification of the RNAi-related proteins is not only important for elucidating their functions but also provides more insights into RNAi-based mechanism and antiviral defense in these economically important species. Here, we identified and characterized a novel Ago gene from *P. monodon*, *PmAgo3*. The expression of *PmAgo3* in response to dsRNA administration and YHV challenge was also investigated. The functional significance of *PmAgo3* on YHV replication was also investigated.

**Table 1**
Primers used in this study.

| Primers | Sequences (5′ → 3′) | Purposes |
|---|---|---|
| PRT-oligo-dT | CCGGAATTCAAGCTTCTAGAGGATCC TTTTTTTTTTTTTTT | Reverse transcription |
| NPAZ-F3 | ATGCCTTGGATATCAGAAGTC | RT-PCR |
| NPAZ-R3 | GTTCAAAGATTTTGTGACCCT | RT-PCR |
| Ago3-F2 | CCAAAGGACAGAGGGTCACA | 3′ RACE |
| PIWI-R3 | CAGGGATTGACACTGATCTTG | 3′ RACE |
| Ago3-F3 | CGTTGACCAGATCATCACTC | 3′ RACE |
| LvAgo2-R | CTACAAGAAGTACATTTTAT | 3′ RACE |
| PmAgo3-F1 | GGTGGAAGGATTTCCCACTT | RT-PCR and qRT-PCR |
| PmAgo3-R1 | CACTGGGGAGTGAGTTGCTT | RT-PCR and qRT-PCR |
| PmAgo1-F | CAAGAATTTGGTCTGACGAT | RT-PCR |
| PmAgo1-R | AGTGTCACCCACACGCTTCAC | RT-PCR |
| PmActin-F | GACTCGTACGTCGGGCGACGA | RT-PCR |
| PmActin-R | AGCAGCGGTGGTCATCACCTG | RT-PCR |
| EF1a-F | GAACTGCTGACCAAGATCGACAGG | qRT-PCR |
| EF1a-R | GAGCATACTGTTGGAAGGTCTCCA | qRT-PCR |
| dsAgo3 *Xba*I_F1 | GCTCTAGATCAGCTCAGGGAAT CAGACT | dsRNA expression plasmid |
| dsAgo3 *Xho*I_F2 | CCGCTCGAGTCAGCTCAGGGAAT CAGACT | dsRNA expression plasmid |
| dsAgo3 *BamH*I_R1 | CGGGATCCGGGAGGCAAAATTC GACCAT | dsRNA expression plasmid |
| dsAgo3 *BamH*I_R2 | CGGGATCCCTCAAATGGATATCT GGCAGC | dsRNA expression plasmid |

## 2. Materials and methods

### 2.1. Shrimp and virus stock

Black tiger shrimp, *P. monodon* (approximately 10 g body weight) were obtained from local shrimp farms in Thailand. They were reared in the laboratory tanks containing artificial sea water (10 ppt) and fed *ad libitum* for a week to gradually acclimatize to the laboratory condition. Apparently healthy shrimps free of yellow head virus (YHV) and white spot syndrome virus (WSSV) were chosen for the experiments. Preparation of YHV stock and determination of the viral titer ($\sim 3 \times 10^9$ virions $ml^{-1}$) were performed as described by Assavalapsakul et al. [21]. YHV stock was diluted $10^5$ fold prior to use.

### 2.2. Total RNA extraction and reverse transcription

Total RNA was extracted from tissues using TRI-REAGENT® or TRI-LS® (Molecular Research Center), according to the manufacturer's protocol. The concentration of RNA was determined by Nanodrop® ND-1000 spectrophotometer (Nanodrop Technologies). The $A_{260}/A_{280}$ ratio of 1.8–2.0 indicated that the RNA samples were relatively pure. One microgram of total RNA was reverse transcribed into cDNA by Impromp-II™ reverse transcriptase (Promega) following the manufacturer's protocol. The PRT-oligo-$dT_{12}$ primer used for reverse transcription is shown in Table 1.

### 2.3. Cloning of the full-length open reading frame (ORF) of PmAgo3

Hemolymph was used as a source of total RNA for *PmAgo3* cloning. Total RNA extraction and reverse transcription were performed as described above. VENT® DNA polymerase (New England Biolabs) was used for all PCR amplifications. The partial fragment of *PmAgo3* was amplified using the primers designed based on *LvAgo2* sequence, NPAZ-F3 and NPAZ-R3 primers, following the condition: denaturation at 95 °C for 3 min, followed by 30 cycles of 95 °C for 30 s, 49 °C for 30 s, and 72 °C for 90 s. The final extension was carried out at 72 °C for 7 min. The PCR product was purified from the gel using QIAquick gel extraction kit (Qiagen) and subsequently added A-tail. The tailed PCR product was cloned into pGEM®-T Easy vector (Promega) and subsequently subjected for sequencing by First Base Co., Ltd. (Malaysia).

To identify the sequences at the 3′-end of *PmAgo3*, 3′ RACE-PCR was performed with Ago3-F2 and PIWI-R3 primers. The second 3′ RACE-PCR was performed with Ago3-F3 and LvAgo2-R primers. Gel purification of the PCR product, A-tailing, cloning, and sequencing were performed as described above. All primers used for cloning are listed in Table 1.

### 2.4. Sequence and phylogenetic analysis

The deduced amino acid sequence of *PmAgo3* was compared with other known Ago sequences available in the GenBank database using Blast program. To perform multiple sequence alignment and phylogenetic analysis, Ago protein sequences from several organisms were retrieved from the GenBank database. Multiple sequence alignment was performed by using ClustalW program. Phylogenetic tree was constructed by using MEGA 5.05 program, based on the Neighbor-joining method [22]. Bootstrap values of 1000 replicates were used for the consensus tree. The Ago protein sequences from various species used for multiple sequence alignment and phylogenetic analysis are listed in Table 2. Molecular weight and isoelectric point were predicted by tools in Expasy website (www.expasy.org). Motifs of proteins were identified by using ScanProsite.

### 2.5. Tissue distribution study

Several tissues including hemolymph, gill, lymphoid organ, hepatopancreas, heart, thoracic ganglia, nerve cord, brain, eyestalks were collected from wild broodstock shrimps. Total RNA extraction and reverse transcription were performed as described above. Expression of *PmAgo3* was determined by RT-PCR with PmAgo3-F1 and PmAgo3-R1 primers, following the condition: denaturation at 94 °C for 5 min, followed by 30 cycles of 94 °C for 30 s, 60 °C for 30 s, and 72 °C for 30 s. The final extension was carried out at 72 °C for 7 min. The internal control gene, *β-actin* was amplified following the condition: denaturation at 94 °C for 5 min, followed by 21 cycles of 94 °C for 30 s, 55 °C for 30 s, and 72 °C for 45 s. The final

**Table 2**
Argonaute proteins used for multiple sequence alignment and phylogenetic analysis.

| Species | Proteins | Abbreviations | Acc. numbers |
|---|---|---|---|
| *Apis mellifera* | Aubergine | ApAub | NP_001159378 |
| *Bombyx mori* | Argonaute-1 | BmAgo1 | NP_001095931 |
| | Argonaute-2 | BmAgo2 | BAD91160 |
| | Argonaute-3 | BmAgo3 | BAF73717 |
| *Bos taurus* | Argonaute-2 | BtAgo2 | NP991363.1 |
| *Caenorhabditis elegans* | ALG1 | CeALG1 | CAR97837 |
| | ALG2 | CeALG2 | CCD73271 |
| | PRG-1 | CePRG1 | CAA98113 |
| | PRG-2 | CePRG2 | CCD62443 |
| | RDE-1 | CeRDE1 | CAB05546 |
| *Drosophila melanogaster* | Argonaute-1 | DmAgo1 | AAF58313 |
| | Argonaute-2 | DmAgo2 | NP_730054 |
| | Argonaute-3 | DmAgo3 | EAA45981 |
| | Aubergine | DmAub | CAA64320 |
| | Piwi | DmPiwi | AAP08705 |
| *Homo sapiens* | Argonaute-1 | HsAgo1 | NP_036331 |
| | Argonaute-2 | HsAgo2 | NP_036286 |
| | Argonaute-3 | HsAgo3 | NP_079128 |
| | Argonaute-4 | HsAgo4 | NP_060099 |
| | Hiwi | HsHiwi | AAC97371 |
| | Hili | HsHili | NP060538.2 |
| *Litopenaeus vannamei* | Argonaute-1 | LvAgo1 | ADK25180 |
| | Argonaute-2 | LvAgo2 | ADK25181 |
| *Marsupenaeus japonicus* | Argonaute-1 | MjAgo1 | ADB44074 |
| | Argonaute-2 | MjAgo2 | BAM37459 |
| *Mus musculus* | Argonaute-2 | MmAgo2 | NP_694818 |
| | Miwi | MmMiwi | BAA93705 |
| | Mili | MmMili | BAA93706 |
| *Neurospora crassa* | QDE-2 | NcQDE2 | AAF43641 |
| *Penaeus monodon* | Argonaute-1 | PmAgo1 | ABG66640 |
| | Argonaute-3 | PmAgo3 | JX845575 |

extension was carried out at 72 °C for 7 min. PCR products were analyzed on 2% agarose gel electrophoresis, stained by ethidium bromide, and visualized under ultraviolet light.

### 2.6. Construction of a hair-pin dsRNA expression plasmid (pET17b-St-PmAgo3)

Recombinant plasmids expressing stem loop *PmAgo3* dsRNA were constructed in pET17b vector (Novagen, USA). A sense-loop PCR fragment (517 bp, located at nucleotide position 747–1263) covering the PAZ domain of *PmAgo3* gene was amplified using specific primers; dsAgo3-*Xba*I_F1 and dsAgo3-*BamH*I_R1, The antisense PCR fragment (394 bp, located at nucleotide position 747–1140) was amplified using primers; dsAgo3-*Xho*I_F2 and *BamH*I_R2. The sense-loop PCR fragment and pET17b vector were digested with *Xba*I and *BamH*I whereas the antisense PCR fragment was digested with *Xho*I and *BamH*I. The PCR products and the linearized vectors were purified using QIAquick gel extraction kit (QIAGEN). Finally, the recombinant plasmid containing an inverted repeat of the stem loop *PmAgo3*, pET17b-st-*PmAgo3* was obtained and used for *in vivo* bacterial expression of dsRNA. The insert fragment of stem loop *PmAgo3* was subjected for automated DNA sequencing (First Base Co., Ltd. (Malaysia)).

### 2.7. Preparation of double-stranded RNAs (dsRNA)

The dsRNA-*PmAgo3* and dsRNA-GFP were produced by using bacterial expression system [23]. Briefly, the plasmids, pET17b-st-*PmAgo3* and pET-3a containing stem-loop GFP insert (pET3a-st-GFP) were transformed into *Escherichia coli* HT115 (DE3). Expression of dsRNA-*PmAgo3* and dsRNA-GFP was induced by an addition of IPTG to the final concentration of 0.4 mM at $A_{600} \sim 0.6$ and proceeded for 4 h at 37 °C with shaking. Extraction and purification of both dsRNAs were performed as previously described by Ongvarrasopone et al. [24]. The concentration of both dsRNAs was determined by agarose gel electrophoresis and Nanodrop® ND-1000 spectrophotometer (Nanodrop Technologies). The quality of dsRNAs was determined by ribonuclease A (RNase A) and ribonuclease III (RNase III) digestion assay.

### 2.8. Expression analysis of PmAgo3

To determine the expression of *PmAgo3* in response to dsRNA or YHV injection, shrimps ($n = 6–8$) were injected with 25 μg of dsRNA-GFP, or challenged with 50 μl of the diluted YHV stock. Injection of dsRNA or YHV was done intramuscularly via the fourth abdominal segment. Hemolymph was collected from individual shrimps at 0, 3, 6, 9, 12, 24, 48 and 72 h-post injection (hpi). Total RNA extraction from hemolymph and reverse transcription were performed as described above. Expression of *PmAgo3* in response to YHV or dsRNA-GFP injection was further determined by quantitative real-time PCR (qRT-PCR). qRT-PCR was performed in a Mastercycler® ep realplex (Eppendorf) using KAPA™ SYBR® FAST qPCR kit (KAPA Biosystems). *PmAgo3* was amplified by PmAgo3-F1 and PmAgo3-R1 primers. The internal control gene, EF1-α was amplified by EF1a-F and EF1a-R primers. The primers used for qRT-PCR are listed in Table 1, qRT-PCR was carried out in triplicates for each sample. A 20-μl qRT-PCR reaction contains 10 μl of 2× SYBR® FAST qPCR master mix, 2 μl of 1:20 diluted cDNA, 1 μl of 10 mM of PmAgo3 primers or 1 mM of EF1-α primers, and 7 μl of DEPC-treated water. qRT-PCR was performed under the following condition: denaturation at 95 °C for 3 min, followed by 40 cycles of 95 °C for 5 s and 60 °C for 30 s. The melting curved analysis was performed after PCR amplification in order to determine the specificity of primers. The cycle threshold (Ct) of *PmAgo3* and EF1-α was determined by the Mastercycler® ep realplex software. Relative expression of *PmAgo3* normalized by EF1-α was calculated by comparative Ct method [25] and expressed as mean ± standard error of mean (SEM). The statistical analysis was performed by using Levene's test of independent sample *t*-test in SPSS program. A *p*-value below 0.05 ($p < 0.05$) was accepted as statistically significance.

### 2.9. Functional assay of PmAgo3

Shrimps (size 10 g, 5–10 shrimp per group) were intramuscularly injected with dsAgo3 or dsGFP (2.5 μg $g^{-1}$ shrimp) for 48 h prior to injection with 50 μl of the 100 fold diluted YHV. Hemolymph was individually collected at 0 and 48 h-post dsAgo3 injection. After YHV challenge, hemolymph was individually collected at 0, 24, 30, 36, and 48 h-post YHV injection. Shrimps injected with 150 mM NaCl alone or dsGFP were used as control groups. Total RNAs of hemolymph were extracted and used for cDNA synthesis. To determine sequence specific knockdown by dsAgo3, expression of *PmAgo3* (using PmAgo3-F1 and PmAgo3-R1 primers) and *PmAgo1* (using PmAgo1-F and PmAgo1-R primers) (Table 1) was used to perform multiplex RT-PCR analysis. PmActin was used as an internal control. In addition, a multiplex RT-PCR analysis of helicase gene of *YHV* and PmActin was also performed [24].

## 3. Results

### 3.1. Cloning and sequence analysis of PmAgo3

Two types of Ago proteins were identified in *P. monodon*, including *PmAgo1* (*Pem-Ago1*) [12,13] and *PmAgo2* (Udomkit et al., unpublished data). Therefore, in this study, our newly identified Ago gene was designated as *PmAgo3*. A 1089-bp fragment of

*PmAgo3* was first amplified by the primers designed based on *LvAgo2* sequence, NPAZ3-F and NPAZ3-R. Blastp against GenBank database revealed that the deduced amino acid sequence of this fragment shared a significant homology with LvAgo2 and *M. japonicus* Ago2 (MjAgo2) (*E*-value = 0.0). Based on the sequence of the amplified fragment, gene specific primers were designed, and 3′ RACE-PCR was performed in order to identify the remaining sequence at the 3′ end of *PmAgo3*. After two rounds of 3′ RACE-PCR, the nucleotide sequences of each fragment were combined to obtain the complete ORF of *PmAgo3*. The *PmAgo3* mRNA sequence was submitted to GenBank under the accession number JX845575.

The ORF of *PmAgo3* was 2559 bp, encoding a polypeptide of 852 amino acids with a molecular weight of 97.02 kDa and isoelectric point of 9.42. Motifs scan by using ScanProsite revealed the presence of two distinctive domains, PAZ and PIWI which are the signature domains of Ago proteins (Fig. 1). The result obtained from Blastp analysis showed that PmAgo3 shared the highest amino acid sequence identity of 83% and 77% with LvAgo2 and MjAgo2, respectively. PmAgo3 shared 40%, 27%, and 26% amino acid sequence identities with human, *Drosophila melanogaster* and *Bombyx mori* Ago2, respectively. In addition, only 41% amino acid sequence identity was observed between PmAgo1 and PmAgo3. To compare the sequence features, the deduced amino acid sequence of *PmAgo3* and some representative Ago proteins were analyzed by using multiple sequence alignment based on the conserved PIWI domain. The alignment revealed several conserved motifs within the PIWI domain. These motifs were predicted to be involved in an anchoring of the 5′-end of the small

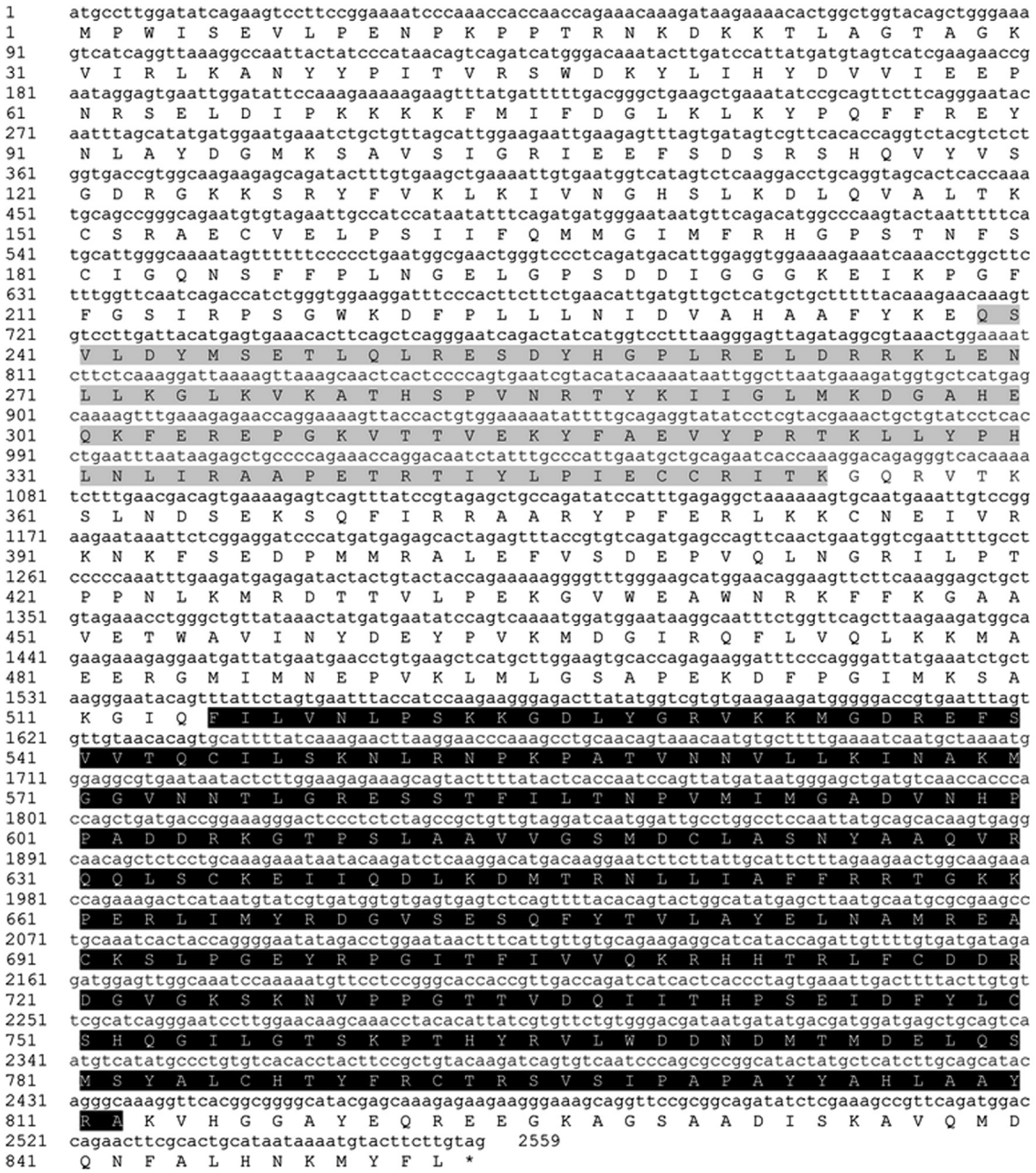


**Fig. 1.** Nucleotide and the deduced amino acid sequences of the complete ORF of *PmAgo3*. The deduced amino acid sequence of *PmAgo3* is shown in a single letter under the respective codon. The PAZ and PIWI domains are highlighted in light gray and black, respectively. The nucleotide sequence is available in the GenBank database under the accession number JX845575.

RNA to target RNA degradation. The conserved catalytic triad composing of DDH motif was also identified (Fig. 2). To study the molecular evolution of PmAgo3, several Ago proteins sequences from vertebrate and invertebrate organisms were retrieved. The Neighbor-joining tree was constructed based on the multiple sequence alignment of the PIWI domain. However, WAGO family was not included into this analysis. The bootstrapped NJ tree separated Ago proteins into two subfamily, including Ago and Piwi subfamilies. PmAgo3 was classified into the Ago subfamily and clustered in the same group with LvAgo2 and MjAgo2. This cluster was on a separated branch that located between invertebrate Ago1 and Ago2 clusters (Fig. 3).

### 3.2. Expression of PmAgo3 in shrimp tissues

RT-PCR was employed to determine *PmAgo3* expression in various tissues of shrimp. The result showed that *PmAgo3* was ubiquitously expressed in all examined tissues, such as hemolymph, ovary, hepatopancreas, lymphoid, gill, heart, nerve, thoracic ganglia, brain, and eyestalk (Fig. 4).

### 3.3. Expression of PmAgo3 in response to dsRNA and YHV injection

To examine the expression of *PmAgo3* in response to dsRNA or YHV injection, shrimps were injected with dsRNA-GFP or challenged with YHV. Expression of *PmAgo3* in response to dsRNA or YHV injection at various time points was determined by qRT-PCR. The results showed that the expression of *PmAgo3* significantly increased following injection of dsRNA-GFP ($p < 0.05$) (Fig. 5(A)). The expression of *PmAgo3* reached the peak at 9 h-post injection and then decreased gradually. On the other hand, in the shrimps challenged with YHV, no significant difference in *PmAgo3* expression was observed at any time point (Fig. 5(B)). To confirm the expression of YHV mRNA in these samples, multiplex RT-PCR

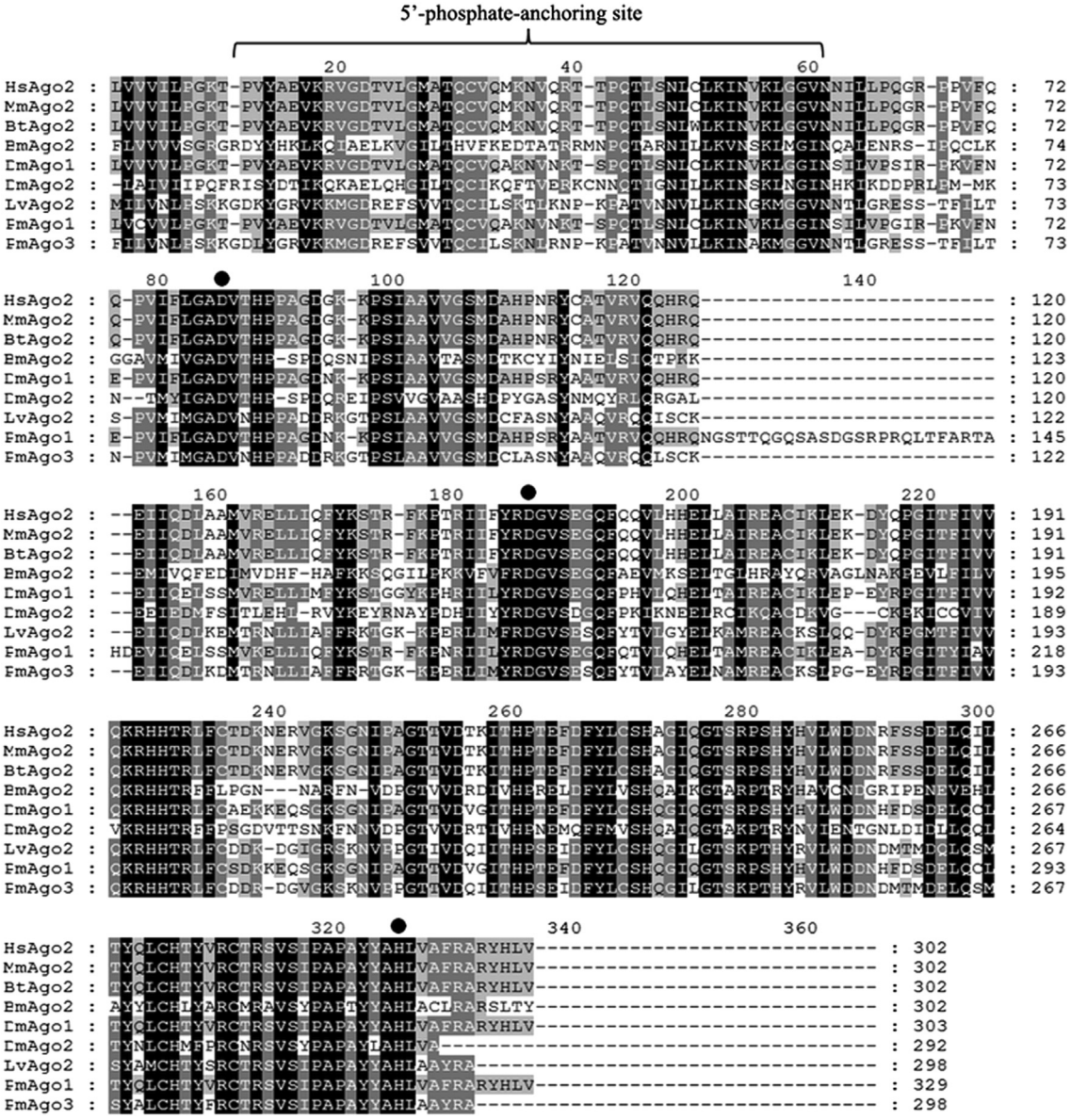


**Fig. 2.** Multiple sequence alignment of the PIWI domains from PmAgo3 and representative Ago proteins by ClustalW. Identical amino acids are highlighted in black, while similar amino acids are highlighted in gray. Abbreviations are listed in Table 2. The position of catalytic residues DDH motif is indicated with solid circle (●).

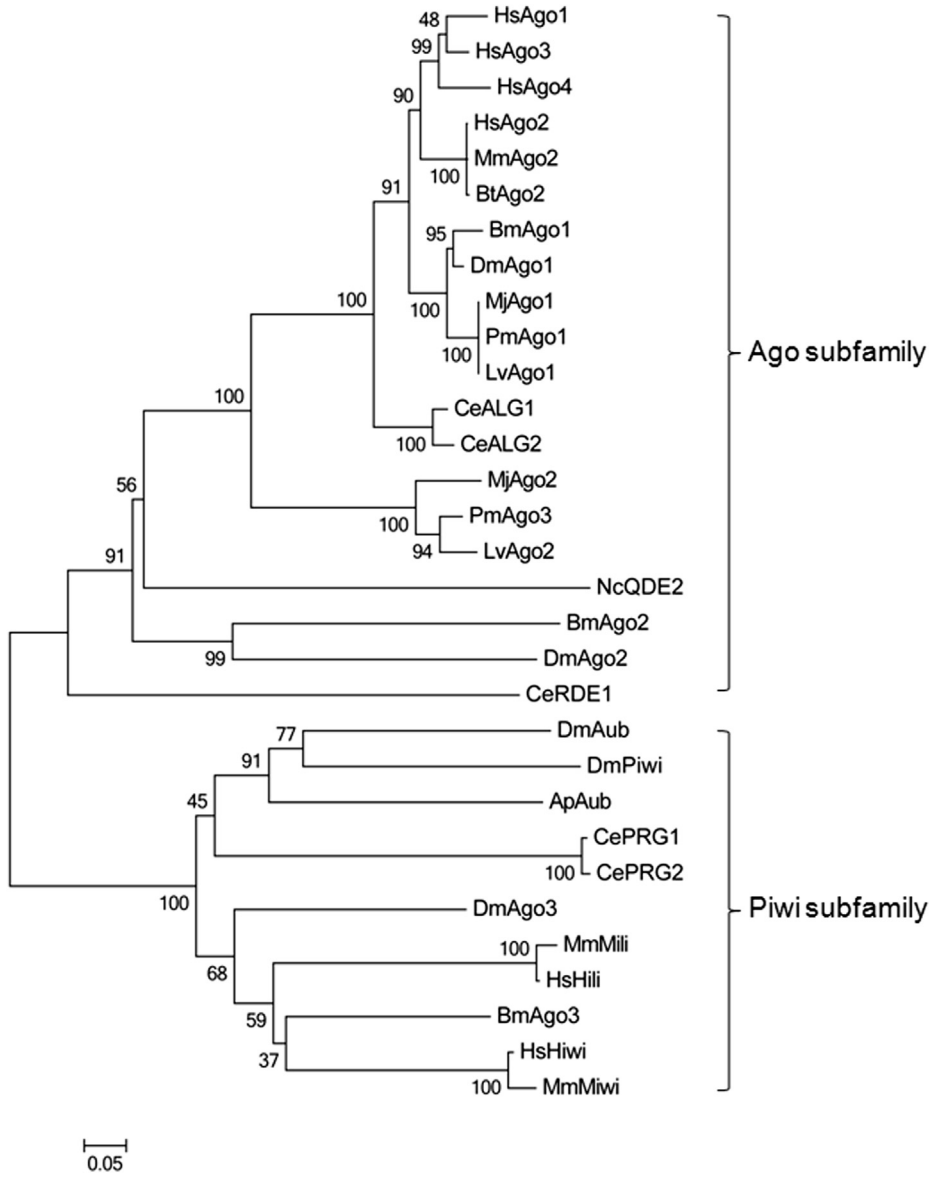


**Fig. 3.** Phylogenetic relationship of Argonaute proteins. Multiple sequence alignment of PIWI domains was performed by ClustalW. The Neighbor-joining tree was constructed by MEGA 5.05 program. Abbreviations are listed in Table 2. Bootstrap values from 1000 replicates are indicated at the nodes.

analysis of *YHV* and *β-actin* demonstrated that expression of YHV can be detected in all samples at 72 h-post YHV challenge (Fig. S1). These data showed that *PmAgo3* expression was stimulated by dsRNA, but not by YHV challenge.

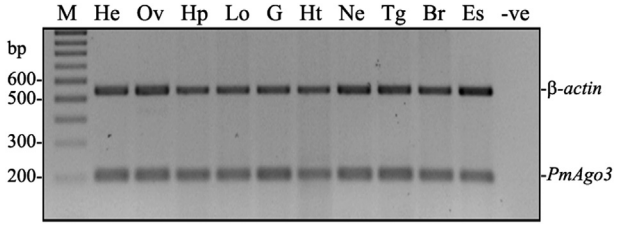


**Fig. 4.** Tissue distribution of *PmAgo3* expression. A representative gel represents RT-PCR products of *PmAgo3* and *β-actin*. M, 100-bp DNA ladder; He, hemolymph; Ov, ovary; Hp, hepatopancreas; Lo, lymphoid organ; G, gill; Ht, heart; Ne, nerve cord; Tg, thoracic ganglia; Br, brain; Es, eyestalks; −ve, negative control.

### 3.4. Knockdown effect of PmAgo3 expression on YHV replication

To study the functional significance of PmAgo3 on YHV replication, shrimps were injected with dsAgo3 48 h prior to YHV challenge. Expression of *PmAgo3* can be completely suppressed after 48 h dsAgo3 injection (Fig. 6) whereas its expression was unchanged in the group that injected with NaCl. Similar to the previous result, expression of *PmAgo3* was slightly increased in dsGFP-injected group. In addition, expression of PmAgo1 was unchanged in dsAgo3-injected group suggesting the sequence specific inhibition of *PmAgo3* expression by dsAgo3 (Fig. S2). To determine the knockdown effect of *PmAgo3* on YHV replication, expression of YHV mRNA was determined from the hemolymph collected from *PmAgo3*-knockdown shrimp individually at 24, 30, 36 and 48 h-post YHV challenge. Interestingly, the expression of YHV mRNA could not be observed after 24, 30, 36 and 48 h-post YHV challenge in *PmAgo3*-knockdown shrimps. On the other hand, the expression of YHV mRNA can be detected at 48 h-post YHV challenge in shrimp

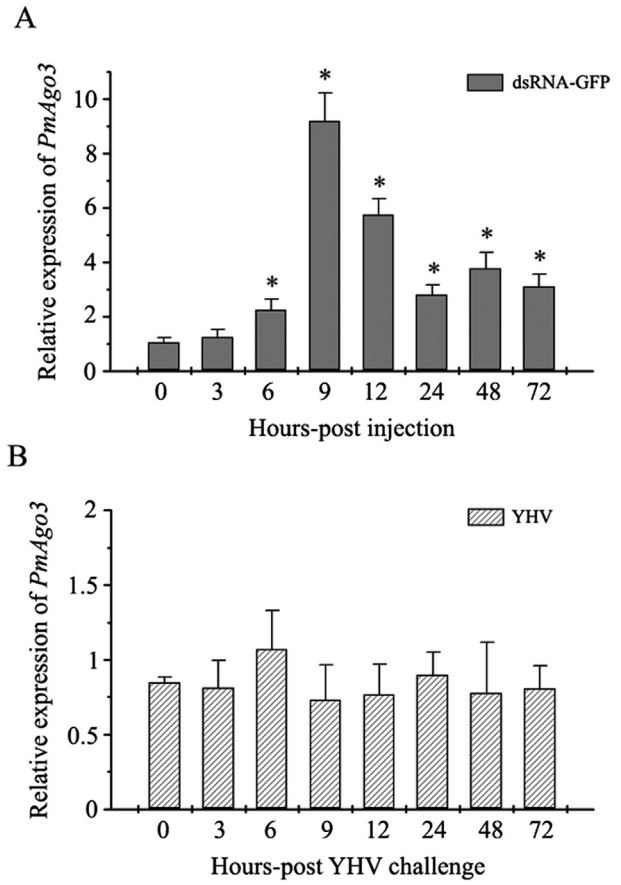


**Fig. 5.** Expression of *PmAgo3* in response to dsRNA-GFP (A) and YHV challenge (B). Hemolymph was collected from shrimps at various time points following dsRNA administration or YHV challenge. Relative expression of *PmAgo3* normalized by EF-1a was determined by qRT-PCR. Relative expression was calculated based on comparative Ct method ($2^{-\Delta\Delta Ct}$) by using zero time point as a calibrator group. Bars represent means ± SEM ($n = 6–8$). The asterisks (*) represent the significant difference ($p < 0.05$) of the relative expression of *PmAgo3* comparing to the zero time point.

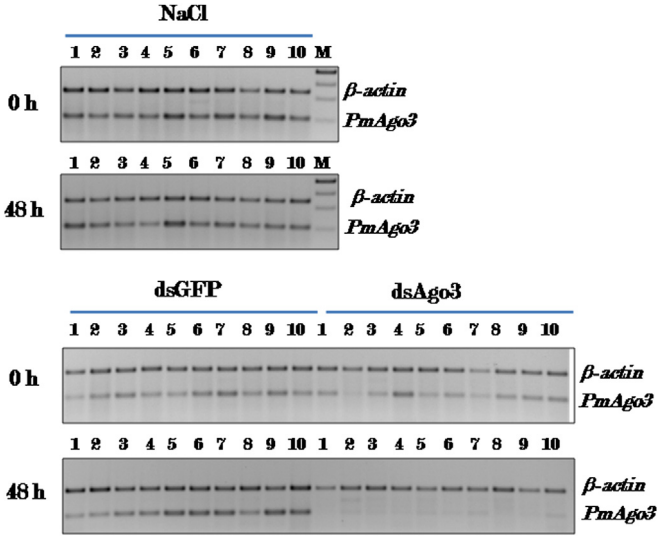


**Fig. 6.** Suppression of *PmAgo3* expression by dsRNA. Multiplex RT-PCR products of *PmAgo3* and *β-actin* amplified from hemolymph collected before (0 h) and 48 h after injection with 150 mM NaCl, 2.5 μg $g^{-1}$ shrimp of dsRNA-GFP (dsGFP) or dsRNA-*PmAgo3* (dsAgo3). The same number at 0 and 48 h for each treatment group represents the same shrimp.

prior to injection with NaCl or dsGFP (Fig. 7). The knockdown effect of *PmAgo3* still persisted at 48 h YHV challenge in *PmAgo3*-knockdown shrimps (or 4 days after dsAgo3 injection) (Fig. S3). These data implied that *PmAgo3* knockdown could inhibit YHV replication.

## 4. Discussion

In this study, we have cloned and characterized a novel Argonaute gene from *P. monodon*, *PmAgo3*. As expected, the deduced amino acid of *PmAgo3* exhibited the two signature domains of the proteins in the Argonaute family, including PAZ and PIWI domains. *PmAgo3* was classified into Ago subfamily and clustered in the same group with LvAgo2 and MjAgo2 on the bootstrapped NJ tree, while shrimp Ago1 was closely related to the miRNA class Ago proteins such as DmAgo1, BmAgo1, CeALG1 and CeALG2 [26–28]. Based on the personal communication, PmAgo2 is specifically expressed in the ovary and testis whereas PmAgo3 is ubiquitously expressed in all examined tissues. The full-length open reading frame of PmAgo2 and PmAgo3 shared approximately 40% amino acid sequence identity while the PIWI domain of both proteins shared 56% amino acid sequence identity. Expression of PmAgo2 protein (His-Ago2; 92 kDa) is different from PmAgo3 (His-Ago3; 95 kDa) as shown in Phetrungnapha et al., 2013 [29]. These results suggested that PmAgo3 is unique and distinct from PmAgo2.

Induction of Argonaute expression by dsRNA is required for efficient RNAi pathway. Choudhary et al. demonstrated that high levels of QDE-2 (Argonaute-like protein) expression induced by dsRNA were required for efficient RNAi in *Neurospora crassa*. In addition, induction of DCL-2 (Dicer-like protein) by dsRNA led to an accumulation of QDE-2, suggesting the regulatory mechanism that allowed the optimal function of the RNAi pathway [30]. In this study, we asked whether *PmAgo3* responds to dsRNA or not. Monitoring of *PmAgo3* expression in hemolymph by qRT-PCR demonstrated a strong up-regulation of its expression following dsRNA administration, suggesting its involvement in dsRNA-mediated gene silencing. Up-regulation of Ago and other

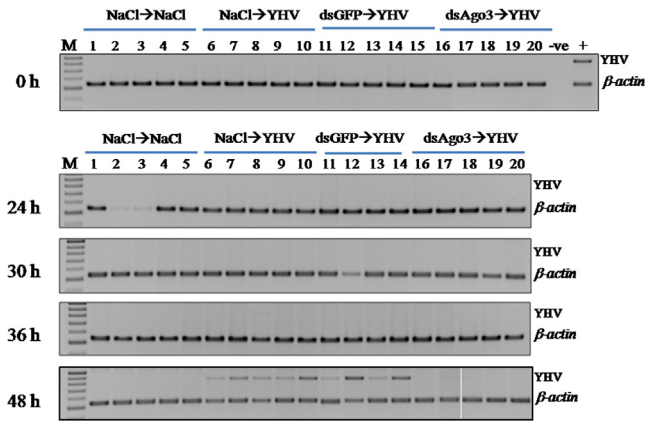


**Fig. 7.** Knockdown effect of *PmAgo3* expression on YHV replication. Multiplex RT-PCR products of *YHV* and *β-actin* amplified from hemolymph collected before (0 h) and 24, 30, 36, and 48 h after YHV challenge in shrimps prior injection of 150 mM NaCl (NaCl → YHV, lanes 6–10), 2.5 μg $g^{-1}$ shrimp of dsGFP (dsGFP → YHV, lanes 11–15) or 2.5 μg $g^{-1}$ shrimp of dsAgo3 (dsAgo3 → YHV, lanes 16–20). Shrimps injected with NaCl alone (NaCl → NaCl, lanes 1–5) were used as a control group. Lane +ve represents the positive control of RT-PCR using cDNA of YHV infected hemocytes as a template. Lane −ve represents the negative control of RT-PCR using sterile water instead of cDNA as a template. The same number at various time points for each treatment group represents the same shrimp. Shrimp #15 die after YHV challenge.

RNAi-related genes upon dsRNA administration was observed in *L. vannamei* [15,31] and *M. japonicas* (Phetrungnapha et al., unpublished data). In addition, similar pattern of Ago gene regulation was also observed in the tobacco hornworm, *Manduca sexta* Ago2 [32].

Likewise, viruses can trigger RNAi components, resulting in an antiviral response. For example, infection of the cucumber mosaic virus enhanced the accumulation of Ago1 protein in *A. thaliana* [33]. In the rare minnow, *Gobiocypris rarus*, expression of *GrAgo2* was up-regulated after infection with grass carp reovirus [34]. In this study, an alteration of *PmAgo3* expression was not observed following YHV challenge. In contrast, several studies demonstrated that RNAi components in penaeid shrimp responded to viral infection. Unajak et al. demonstrated that the expression of *PmAgo1* in lymphoid organ was increased during the early period of YHV infection [13]. In *L. vannamei*, *LvDicer-1* and *LvDrosha* were up-regulated following taura syndrome virus (TSV) and WSSV challenge, respectively [35,36]. In *Fenneropenaeus chinensis*, Fc-TRBP was up-regulated during WSSV infection [37].

RNAi is a potent antiviral defense mechanism in invertebrate [38]. The dsRNA replicative intermediates and plus-stranded viral RNAs with secondary structure are processed by Dicer, generating viral-derived siRNAs (viRNAs) which are subsequently loaded into Ago proteins and mediated the degradation of viral RNA, thereby conferring antiviral immunity [38–40]. The susceptibility of the host to viruses was increased upon suppression of RNAi machineries. For example, knockdown of Dicer or Ago increased the susceptibility of S2 cells to viral infection [41–43]. In *P. monodon*, knockdown of *PmDicer-1* expression increased the viral load of gill-associated virus, suggesting the importance of RNAi in an antiviral immunity in shrimp [44]. Therefore, to investigate the functional significance of *PmAgo3* in an antiviral immunity, *PmAgo3* was specifically knocked-down by using dsRNA and the level of YHV transcript was subsequently determined. Surprisingly, knockdown of *PmAgo3* inhibited the replication of YHV in shrimp, as the transcript of YHV could not be detected at 48 h when compared with the control groups (NaCl → YHV and dsGFP → YHV), suggesting the role of *PmAgo3* in YHV replication in shrimp. Recent studies in plants and *C. elegans* demonstrated that viRNAs not only contributed to the antiviral immunity but might involve in a viral counter-defense. Viruses utilized viRNAs to modulate cellular gene expression by mediating a potent silencing of host genes in a sequence-specific manner, thereby facilitating viral replication and production of disease symptom [45–47]. For instance, the Y-satellite of cucumber mosaic virus produced viRNAs to silence the chlorophyll biosynthetic gene, CHLI, leading to induction of viral disease production in *Nicotiana tabacum* [46]. In *M. japonicus*, the existence of the viRNAs of WSSV (WSSV-viRNAs) has been demonstrated by Huang et al. [17]. Moreover, the requirement of MjAgo2 (shared 83% amino acid sequence identity with PmAgo3) for the efficient function of WSSV-viRNAs has been also demonstrated [17]. Given the fact that YHV is a positive single-stranded RNA virus, it is plausible that YHV generates viRNAs (YHV-viRNAs) to modulate shrimp gene expression and facilitate its replication. Therefore, loss of *PmAgo3* might interfere the function of YHV-viRNAs, resulting in the inhibition of YHV replication. Identification of YHV-viRNAs should clarify this scenario better.

In conclusion, this study demonstrated that *PmAgo3* responded to dsRNA but not to YHV infection. The requirement of *PmAgo3* in YHV replication was demonstrated. Our study expands an understanding of the RNAi-based mechanisms in penaeid shrimp. Future researches are required to provide insights into the functions of Ago proteins and a regulatory mechanism in the RNAi pathway of these economically important aquatic animals.

## Acknowledgments

The authors would like to thank Dr. Witoon Tirasophon for plasmid pET-3a-stGFP, and Ms. Chaweewan Chimwai for technical assistance. This work is supported by grants from the Thailand Research Fund (RSA5480002 to C.O., DPG5680001 to S.P.), the Mahidol University Research Grant, and the Office of the Higher Education Commission and Mahidol University under the National Research University Initiatives. Student fellowship granted to A.P. by the Royal Golden Jubilee Ph.D. Program.

## Appendix A. Supplementary data

Supplementary data related to this article can be found at http://dx.doi.org/10.1016/j.fsi.2013.06.025.

## References

[1] Hutvagner G, Simard MJ. Argonaute proteins: key players in RNA silencing. Nat Rev Mol Cell Biol 2008;9:22–32.
[2] Schirle NT, MacRae IJ. The crystal structure of human Argonaute2. Science 2012;336:1037–40.
[3] Song JJ, Smith SK, Hannon GJ, Joshua-Tor L. Crystal structure of Argonaute and its implications for RISC slicer activity. Science 2004;305:1434–7.
[4] Kwak PB, Tomari Y. The N domain of Argonaute drives duplex unwinding during RISC assembly. Nat Struct Mol Biol 2012;19:145–51.
[5] Lingel A, Simon B, Izaurralde E, Sattler M. Structure and nucleic-acid binding of the *Drosophila* Argonaute 2 PAZ domain. Nature 2003;426:465–9.
[6] Ma JB, Ye K, Patel DJ. Structural basis for overhang-specific small interfering RNA recognition by the PAZ domain. Nature 2004;429:318–22.
[7] Boland A, Tritschler F, Heimstadt S, Izaurralde E, Weichenrieder O. Crystal structure and ligand binding of the MID domain of a eukaryotic Argonaute protein. EMBO Rep 2010;11:522–7.
[8] Frank F, Sonenberg N, Nagar B. Structural basis for 5′-nucleotide base-specific recognition of guide RNA by human AGO2. Nature 2010;465:818–22.
[9] Wang Y, Sheng G, Juranek S, Tuschl T, Patel DJ. Structure of the guide-strand-containing argonaute silencing complex. Nature 2008;456:209–13.
[10] Carthew RW, Sontheimer EJ. Origins and mechanisms of miRNAs and siRNAs. Cell 2009;136:642–55.
[11] Yigit E, Batista PJ, Bei Y, Pang KM, Chen CC, Tolia NH, et al. Analysis of the *C. elegans* Argonaute family reveals that distinct Argonautes act sequentially during RNAi. Cell 2006;127:747–57.
[12] Dechklar M, Udomkit A, Panyim S. Characterization of Argonaute cDNA from *Penaeus monodon* and implication of its role in RNA interference. Biochem Biophys Res Commun 2008;367:768–74.
[13] Unajak S, Boonsaeng V, Jitrapakdee S. Isolation and characterization of cDNA encoding Argonaute, a component of RNA silencing in shrimp (*Penaeus monodon*). Comp Biochem Physiol B Biochem Mol Biol 2006;145:179–87.
[14] Chen YH, Jia XT, Zhao L, Li CZ, Zhang S, Chen YG, et al. Identification and functional characterization of Dicer2 and five single VWC domain proteins of *Litopenaeus vannamei*. Dev Comp Immunol 2011;35:661–71.
[15] Labreuche Y, Veloso A, de la Vega E, Gross PS, Chapman RW, Browdy CL, et al. Non-specific activation of antiviral immunity and induction of RNA interference may engage the same pathway in the Pacific white leg shrimp *Litopenaeus vannamei*. Dev Comp Immunol 2010;34:1209–18.
[16] Huang T, Zhang X. Contribution of the argonaute-1 isoforms to invertebrate antiviral defense. PLoS One 2012;7:e50581.
[17] Huang T, Zhang X. Host defense against DNA virus infection in shrimp is mediated by the siRNA pathway. Eur J Immunol 2013;43:137–46.
[18] Robalino J, Bartlett T, Shepard E, Prior S, Jaramillo G, Scura E, et al. Double-stranded RNA induces sequence-specific antiviral silencing in addition to nonspecific immunity in a marine shrimp: convergence of RNA interference and innate immunity in the invertebrate antiviral response? J Virol 2005;79:13561–71.
[19] Robalino J, Bartlett TC, Chapman RW, Gross PS, Browdy CL, Warr GW. Double-stranded RNA and antiviral immunity in marine shrimp: inducible host mechanisms and evidence for the evolution of viral counter-responses. Dev Comp Immunol 2007;31:539–47.
[20] Robalino J, Browdy CL, Prior S, Metz A, Parnell P, Gross P, et al. Induction of antiviral immunity by double-stranded RNA in a marine invertebrate. J Virol 2004;78:10442–8.
[21] Assavalapsakul W, Smith DR, Panyim S. Propagation of infectious yellow head virus particles prior to cytopathic effect in primary lymphoid cell cultures of *Penaeus monodon*. Dis Aquat Org 2003;55:253–8.
[22] Saitou N, Nei M. The neighbor-joining method: a new method for reconstructing phylogenetic trees. Mol Biol Evol 1987;4:406–25.
[23] Ongvarrasopone C, Roshorm Y, Panyim S. A simple and cost effective method to generate dsRNA for RNAi studies in invertebrates. ScienceAsia 2007;33:35–9.

[24] Ongvarrasopone C, Chanasakulniyom M, Sritunyalucksana K, Panyim S. Suppression of PmRab7 by dsRNA inhibits WSSV or YHV infection in shrimp. Mar Biotechnol (NY) 2008;10:374–81.
[25] Pfaffl MW. A new mathematical model for relative quantification in real-time RT-PCR. Nucleic Acids Res 2001;29:e45.
[26] Grishok A, Pasquinelli AE, Conte D, Li N, Parrish S, Ha I, et al. Genes and mechanisms related to RNA interference regulate expression of the small temporal RNAs that control *C. elegans* developmental timing. Cell 2001;106:23–34.
[27] Miyoshi K, Tsukumo H, Nagami T, Siomi H, Siomi MC. Slicer function of *Drosophila* Argonautes and its involvement in RISC formation. Genes Dev 2005;19:2837–48.
[28] Wang G-H, Jiang L, Zhu L, Cheng T-C, Niu W-H, Yan Y-F, et al. Characterization of Argonaute family members in the silkworm, *Bombyx mori*. Insect Sci 2013;20:78–91.
[29] Phetrungnapha A, Panyim S, Ongvarrasopone C. *Penaeus monodon* Tudor staphylococcal nuclease preferentially interacts with N-terminal domain of Argonaute-1. Fish Shellfish Immunol 2013;34:875–84.
[30] Choudhary S, Lee HC, Maiti M, He Q, Cheng P, Liu Q, et al. A double-stranded-RNA response program important for RNA interference efficiency. Mol Cell Biol 2007;27:3995–4005.
[31] Chen YH, Zhao L, Jia XT, Li XY, Li CZ, Yan H, et al. Isolation and characterization of cDNAs encoding Ars2 and Pasha homologues, two components of the RNA interference pathway in *Litopenaeus vannamei*. Fish Shellfish Immunol 2012;32:373–80.
[32] Garbutt JS, Reynolds SE. Induction of RNA interference genes by double-stranded RNA; implications for susceptibility to RNA interference. Insect Biochem Mol Biol 2012;42:621–8.
[33] Zhang X, Yuan YR, Pei Y, Lin SS, Tuschl T, Patel DJ, et al. Cucumber mosaic virus-encoded 2b suppressor inhibits Arabidopsis Argonaute1 cleavage activity to counter plant defense. Genes Dev 2006;20:3255–68.
[34] Su J, Zhu Z, Wang Y, Jang S. Isolation and characterization of Argonaute 2: a key gene of the RNA interference pathway in the rare minnow, *Gobiocypris rarus*. Fish Shellfish Immunol 2009;26:164–70.
[35] Huang T, Xu D, Zhang X. Characterization of shrimp Drosha in virus infection. Fish Shellfish Immunol 2012;33:575–81.
[36] Yao X, Wang L, Song L, Zhang H, Dong C, Zhang Y, et al. A Dicer-1 gene from white shrimp *Litopenaeus vannamei*: expression pattern in the processes of immune response and larval development. Fish Shellfish Immunol 2010;29:565–70.
[37] Wang S, Liu N, Chen AJ, Zhao XF, Wang JX. TRBP homolog interacts with eukaryotic initiation factor 6 (eIF6) in *Fenneropenaeus chinensis*. J Immunol 2009;182:5250–8.
[38] Sabin LR, Hanna SL, Cherry S. Innate antiviral immunity in *Drosophila*. Curr Opin Immunol 2010;22:4–9.
[39] Kemp C, Imler JL. Antiviral immunity in *Drosophila*. Curr Opin Immunol 2009;21:3–9.
[40] Aliyari R, Wu Q, Li HW, Wang XH, Li F, Green LD, et al. Mechanism of induction and suppression of antiviral immunity directed by virus-derived small RNAs in *Drosophila*. Cell Host Microbe 2008;4:387–97.
[41] Wang X-H, Aliyari R, Li W-X, Li H-W, Kim K, Carthew R, et al. RNA interference directs innate immunity against viruses in adult *Drosophila*. Science 2006;312:452–4.
[42] van Rij RP, Saleh M-C, Berry B, Foo C, Houk A, Antoniewski C, et al. The RNA silencing endonuclease Argonaute 2 mediates specific antiviral immunity in *Drosophila melanogaster*. Genes Dev 2006;20:2985–95.
[43] Galiana-Arnoux D, Dostert C, Schneemann A, Hoffmann JA, Imler J-L. Essential function *in vivo* for Dicer-2 in host defense against RNA viruses in *Drosophila*. Nat Immunol 2006;7:590–7.
[44] Su J, Oanh DT, Lyons RE, Leeton L, van Hulten MC, Tan SH, et al. A key gene of the RNA interference pathway in the black tiger shrimp, *Penaeus monodon*: identification and functional characterisation of Dicer-1. Fish Shellfish Immunol 2008;24:223–33.
[45] Guo X, Li WX, Lu R. Silencing of host genes directed by virus-derived short interfering RNAs in *Caenorhabditis elegans*. J Virol 2012;86:11645–53.
[46] Smith NA, Eamens AL, Wang MB. Viral small interfering RNAs target host genes to mediate disease symptoms in plants. PLoS Pathog 2011;7:e1002022.
[47] Shimura H, Pantaleo V, Ishihara T, Myojo N, Inaba J, Sueda K, et al. A viral satellite RNA induces yellow symptoms on tobacco by targeting a gene involved in chlorophyll biosynthesis using the RNA silencing machinery. PLoS Pathog 2011;7:e1002021.

# 4. Silencing of PmYPR65 receptor prevents yellow head virus infection in *Penaeus monodon*.

Virus Research 189 (2014) 133–135

Contents lists available at ScienceDirect

Virus Research

journal homepage: www.elsevier.com/locate/virusres

Short communication

# Silencing of PmYPR65 receptor prevents yellow head virus infection in *Penaeus monodon*

Wanchai Assavalapsakul[a,*], Hoa Khanh Tran Kiem[a], Duncan R. Smith[b], Sakol Panyim[b,c]

[a] Department of Microbiology, Faculty of Science, Chulalongkorn University, Bangkok 10330, Thailand
[b] Institute of Molecular Biosciences, Mahidol University, Salaya, Nakhon Pathom 73170, Thailand
[c] Department of Biochemistry, Faculty of Science, Mahidol University, Bangkok 10400, Thailand

ARTICLE INFO

*Article history:*
Received 13 April 2014
Received in revised form 23 May 2014
Accepted 23 May 2014
Available online 2 June 2014

*Keywords:*
Yellow head virus
Receptor
RNA interference
*Penaeus monodon*

ABSTRACT

The suppression of viral replication by double-stranded RNAs (dsRNA) specific to mRNAs of either virus or host genes has been widely investigated as a possible shrimp disease therapy. PmYRP65, a yellow head virus (YHV) receptor, was previously identified and characterized in the black tiger shrimp, *Penaeus monodon*. In our previous study, entry of YHV into cells of the Oka organ of *P. monodon* required the host receptor PmYRP65 and silencing of PmYRP65 *in vitro* led to a complete suppression of YHV replication in the cells. In this study, PmYRP65 was shown to be *in vivo* suppressed by dsRNA specific for PmYRP65, leading to inhibition of YHV replication and almost complete abolition of shrimp mortality following YHV challenge. Targeting PmYRP65 could be an effective YHV antiviral shrimp strategy.



Yellow head disease, caused by Yellow head virus (YHV) a member of the genus *Okavirus*, family *Roniviridae* and order *Nidovirales*, has remained a serious disease of the black tiger shrimp *Penaeus monodon* in Thailand. YHV was first found in 1990 in Thailand and causes mass mortality in shrimp just a few days after infection (Boonyaratpalin et al., 1993). Under histopathological study, YHV can infect cells of both ectodermal and mesodermal origins (Boonyaratpalin et al., 1993; Duangsuwan et al., 2011). Genes induced by viral infection and genes whose expression is correlated with the ability of shrimp to resist viral disease have been described (Junkunlo et al., 2012; Vatanavicharn et al., 2012; Khimmakthong et al., 2013; Soowannayan et al., 2013), but the molecular mechanism underneath antiviral immunity of these organisms has not been yet uncovered. The major limitation of such studies is the lack of information regarding the shrimp genome, the lack of tools for the genetic manipulation of shrimp and the lack of continuous shrimp cell lines for *in vitro* studies. Therefore most shrimp antiviral immunity research has arisen from asking the same simple but significant question: what helps shrimp survive viral infection *in vivo*? Since virus-associated molecules are likely the targets of immune recognition in viral infection, viral proteins and double-stranded RNA (dsRNA) are of particular interest (Robalino et al., 2007). To date, no antiviral agent has been developed to prevent or protect against shrimp viruses except activation of RNA interference which is a powerful strategy for the suppression of target viral gene expression. The technique is based on the uptake of dsRNA specific to either viral mRNA or host mRNAs involved in the viral replication, resulting in an inhibition of viral replication; such technique has been applied to shrimp being infected by YHV (Yodmuang et al., 2006; Tirasophon et al., 2007; Assavalapsakul et al., 2009; Phetrungnapha et al., 2013; Píndaro et al., 2013), white spot syndrome virus (WSSV) (Robalino et al., 2005; Kim et al., 2006; Attasart et al., 2009), and hepatopancreatic parvovirus (Attasart et al., 2011).

Viruses commonly enter into cells through receptor mediated endocytosis (Thorley et al., 2010), and in a previous study we identified PmYRP65 (*Penaeus monodon* Yellow head virus receptor protein, 65 kDa) as a receptor protein mediating YHV internalization to susceptible cells, and moreover demonstrated that suppression of PmYRP65 using dsRNA specific to PmYRP65 led to inhibition of the YHV replication process *in vitro* (Assavalapsakul et al., 2006). To date, whether PmYRP65 suppression *in vivo* inhibits YHV infection remains to be determined. To address this issue, the RNAi-induced *in vivo* suppression of PmYRP65 was investigated and the effect on shrimp mortality after YHV challenge determined. To produce specific PmYRP65 dsRNA, a unique region of pmYRP65 (nucleotides 980 to 1218; pL980-1218) was cloned into pLitmus28 using the previously described primers Sense-U-P65 and

* Corresponding author at: Department of Microbiology, Faculty of Science, Chulalongkorn University, 254 Phyathai Road, Bangkok 10330, Thailand.
Tel.: +66 2218 5096; fax: +66 2252 7576.
*E-mail addresses:* wanchai.a@chula.ac.th, wanchai_at_microchula@yahoo.co.th (W. Assavalapsakul).

http://dx.doi.org/10.1016/j.virusres.2014.05.022
0168-1702/

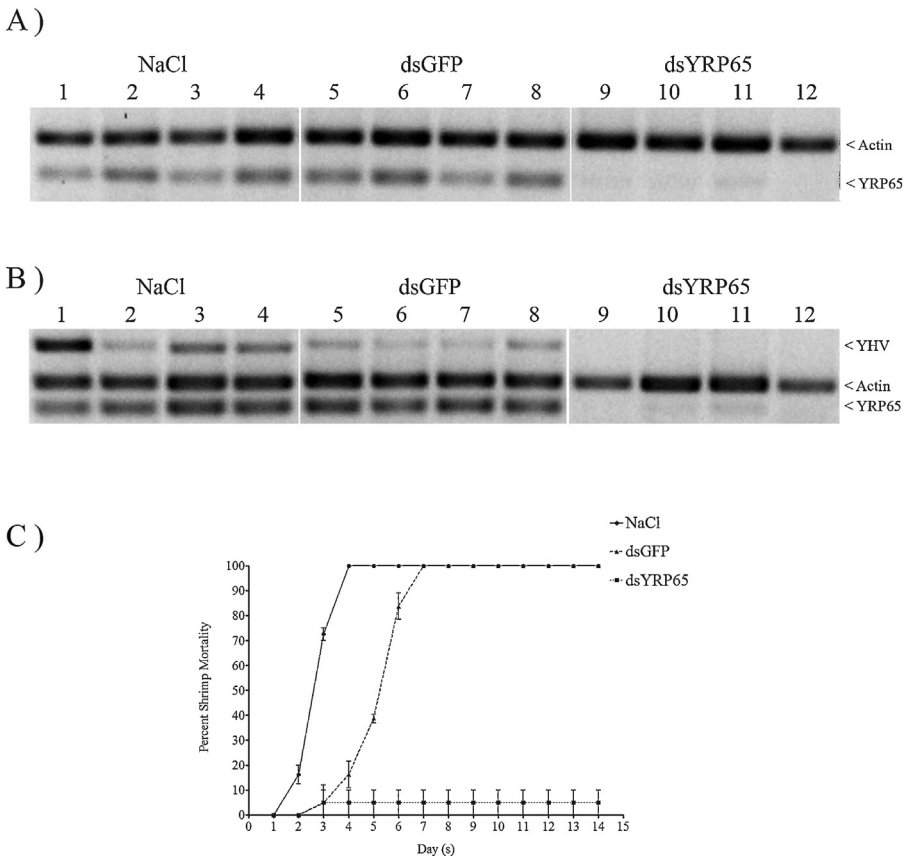


**Fig. 1.** Suppression of PmYRP65 by dsRNA. (A) Shrimp were injected with 150 mM NaCl or GFP-dsRNA or PmYRP65-dsRNA. (B) Shrimp were injected PmYRP65-dsRNA, GFP-dsRNA or 150 mM NaCl and followed by YHV injection. The YHV load and PmYRP65 expression of individual shrimp were determined by multiplex RT-PCR. (C) Percent cumulative mortality of Black tiger shrimp. Shrimp (8–10 g) were injected PmYRP65-dsRNA (▼), GFP-dsRNA (▲) or 150 mM NaCl (■) and followed by YHV injection. Shrimp mortality was recorded daily for 14 days. Percent mortality in each experimental group is presented as the mean of duplicated experiments.

anti-U-P65 (Assavalapsakul et al., 2006). The resultant recombinant plasmid pL980-1218 was linearized by restriction endonuclease digestion with either *Bgl* II or *Stu* I and purified using QIAGEN DNA purification column. Sense and antisense RNAs were produced by *in vitro* transcription using the Ribomax kit (Promega) according to the manufacturer's recommendations. Equal amounts of sense and antisense RNAs were annealed to produce dsRNA according to the protocol of Worby et al. (2001), and quantitated by UV spectroscopy.

Healthy *P. monodon* (8–10 g) were purchased and cultured in 80 L tanks containing artificial seawater at 15 ppt salinity with aeration. Shrimp were acclimated for 2–3 days at 28 ± 1 °C prior to experimental use. Three parallel individual injection treatments of PmYRP65-dsRNA, GFP-dsRNA (Tirasophon et al., 2005) and 150 mM NaCl were undertaken, in which GFP-dsRNA and 150 mM NaCl were included as negative controls. Specifically, 2.5 μg of dsRNA per gram shrimp in a total volume of 100 μL was injected into haemolymph through the arthrodial membrane of the fourth walking leg by means of a 1 mL syringe with a 29 gauge needle. After 48 h, shrimp were injected one more time and maintained for 48 h before YHV challenge with a titer of $10^5$ $TCID_{50}$ $mL^{-1}$, a challenge that induces 100% mortality within 3–4 days post-infection (Assavalapsakul et al., 2009). To determine whether PmYRP65-dsRNA was able to suppress PmYRP65 expression, haemolymph was withdrawn from four randomly selected shrimp at 96 h after the first PmYRP65-dsRNA injection (and before YHV challenge) and the level of PmYRP65 transcripts determined by semi-quantitative RT-PCR. The RT-PCR results (Fig. 1A) showed that PmYRP65 transcripts were markedly reduced as compared with the NaCl and GFP-dsRNA injection (Fig. 1A), suggesting that PmYRP65 was specifically suppressed.

After 30 h YHV challenge, haemolymph was collected from each shrimp and after extraction of RNA samples were analyzed by RT-PCR as previously described (Assavalapsakul et al., 2009). Briefly, 200 μL of haemolymph from individual shrimp was collected for RNA extraction using TRI Reagent-LS (Molecular Research Center). One microgram of total RNA was used for cDNA synthesis using Impromp II reverse transcriptase (Promega) with oligo $dT_{18}$ primer as recommended by the manufacturer. To determine YHV infection level and suppression level of PmYRP65, 2 μL of synthesized cDNA were used as a template to perform multiplex PCR amplifying portions of YHV genomic RNA and PmYRP65 mRNA respectively with primers corresponding to the YHV helicase gene (F: 5′ CAA GGA CCA CCT GGT ACC GGT AAG AC 3′ and R: 5′GCG GAA ACG ACT GAC GGC TAC ATT CAC 3′) and shrimp PmYRP65 gene (F: 5′ GCC AAA ACA GAA GCA AAG CCA GCA TCT 3′ and R: 5′ CAT AAT ACC ATC CTC CAC GGG CTG 3′). In addition, amplification of actin mRNA was used as an internal control using primers specific to the actin gene (F: 5′ GAC TCG TAC GTC GGC GAC GAG G 3′ and R: 5′ AGC AGC GGT GGT CAT CTC CTG CTC 3′). Multiplex PCR amplification was carried out as follows; 94 °C for 3 min, denaturation at 94 °C for 30 s, annealing at 55 °C for 30 s, and extension at 72 °C for 30 s; after 35 cycles, the reaction was held at 72 °C for another 10 min. The RT-PCR products were analyzed by electrophoresis through 2% agarose gels. The results showed a significant reduction in expression levels of both PmYRP65 and YHV in shrimp injected with PmYRP65-dsRNA as compared to control shrimp, indicating that PmYRP65 was successfully suppressed by PmYRP65-dsRNA and YHV replication was

consequently inhibited (Fig. 1B). In addition, injection of control GFP-dsRNA prior to YHV challenge resulted in a reduction of YHV genomes as compared to control saline injection. In 2004 Robalino and colleagues (Robalino et al., 2004) demonstrated that dsRNA can also induce an antiviral effect in shrimp in a sequence-independent manner, and they showed injection of any dsRNA, whether specific to shrimp genes or unrelated, led to increased shrimp survival after WSSV and Taura syndrome virus challenge (Robalino et al., 2004). Our results, showing a decrease in YHV genomes after GFP-dsRNA injection and YHV challenge is consistent with previous studies (Tirasophon et al., 2005; Westenberg et al., 2005; Yodmuang et al., 2006).

Shrimp were followed for 14 days following YHV challenge, and mortality was recorded daily (Fig. 1C). Control shrimp injected with saline showed 100% mortality by three days post-YHV challenge, while shrimp injected with GFP-dsRNA prior to YHV challenge showed 100% mortality after 7 days. Shrimp injected with PmYRP65-dsRNA showed 95% survival at 14 days post YHV challenge. Critically, any protection provided through non-specific RNAi induction (by GFP-dsRNA) only apparently delayed the onset of mortality rather than eliminating it almost completely as was seen with specific RNAi induction (by PmYRP65-dsRNA). This also suggests that while PmYRP65-dsRNA may induce both specific and non-specific RNAi, it is the sequence specific induction that provides long term protection against YHV challenge.

In previous studies it was shown that knock down of the *Penaeus* (*Litopenaeus*) *vannamei* laminin receptor, which has been identified as a Taura syndrome virus receptor, led to shrimp death (Senapin et al., 2010). Additionally, suppression of the *P. vannamei* SID-1 (systemic interference defective 1) transcript, which encodes a protein mediating intercellular transport of dsRNA, also results in a lethal phenotype in shrimp (Labreuche et al., 2010). However, as seen in this study, suppression of PmYRP65 resulted in 95% shrimp survival after YHV challenge on day 14, suggesting that knock down of PmYRP65 is a safe strategy for future control of YHV. These results can be further applied in commercial shrimp farming in order to generate YHV-free farmed shrimp by developing methods for administration of DNA construct expressing PmYRP65-dsRNA into shrimp *via* immersion, feeding or through plankton (Subhadra et al., 2010; Lin et al., 2011; Attasart et al., 2013; Thammasorn et al., 2013). In addition, using this strategy to protect shrimp broodstock from YHV infection, vertical transmission of YHV which is one of the major routes of viral entry into farmed shrimp, can be eliminated, giving protection to susceptible larval stages.

## Acknowledgements

This work was supported by Office of Higher Education Commission, Ministry of Education, and the Thailand Research Fund (RSA5580052 to W.A. and DPG5680001 to S.P.) The funding agencies had no role in the study design; in the collection, analysis, and interpretation of data; in the writing of the report; or in the decision to submit the paper for publication.

## References

Assavalapsakul, W., Panyim, S., Smith, D.R., 2006. Identification and characterization of a *Penaeus monodon* lymphoid cell-expressed receptor for the yellow head virus. J. Virol. 80 (1), 262–269.

Assavalapsakul, W., Chinnirunvong, W., Panyim, S., 2009. Application of YHV-protease dsRNA for protection and therapeutic treatment against yellow head virus infection in *Litopenaeus vannamei*. Dis. Aquat. Organ. 84 (2), 167–171.

Attasart, P., Kaewkhaw, R., Chimwai, C., Kongphom, U., Namramoon, O., Panyim, S., 2009. Inhibition of white spot syndrome virus replication in *Penaeus monodon* by combined silencing of viral rr2 and shrimp PmRab7. Virus Res. 145, 127–133.

Attasart, P., Kaewkhaw, R., Chimwai, C., Kongphom, U., Panyim, S., 2011. Clearance of *Penaeus monodon* densovirus in naturally pre-infected shrimp by combined ns1 and vp dsRNAs. Virus Res. 159 (1), 79–82.

Attasart, P., Namramoon, O., Kongphom, U., Chimwai, C., Panyim, S., 2013. Ingestion of bacteria expressing dsRNA triggers specific RNA silencing in shrimp. Virus Res. 171, 252–256.

Boonyaratpalin, S., Supamattaya, K., Kasornchandra, J., Direkbusaracom, S., Aekpanithanpong, U., Chantanachooklin, C., 1993. Non-occluded Baculo-like virus, the causative agent of yellow head disease in the black tiger shrimp (*Penaeus monodon*). Gyohyo Kenkyu 2, 103–109.

Duangsuwan, P., Tinikul, Y., Withyachumnarnkul, B., Chotwiwatthanakun, C., Sobhon, P., 2011. Cellular targets and pathways of yellow head virus infection in lymphoid organ of *Penaeus monodon* as studied by transmission electron microscopy. Songklanakarin J. Sci. Technol. 33, 121–127.

Junkunlo, K., Prachumwat, A., Tangprasittipap, A., Senapin, S., Borwornpinyo, S., Flegel, T.W., Sritunyalucksana, K., 2012. A novel lectin domain-containing protein (LvCTLD) associated with response of the whiteleg shrimp *Penaeus* (*Litopenaeus*) *vannamei* to yellow head virus (YHV). Dev. Comp. Immunol. 37, 334–341.

Khimmakthong, U., Kongmee, P., Deachamag, P., Leggat, U., Chotigeat, W., 2013. Activation of an immune response in *Litopenaeus vannamei* by oral immunization with phagocytosis activating protein (*PAP*) DNA. Fish Shellfish Immunol. 34, 929–938.

Kim, C.S., Kosuke, Z., Nam, Y.K., Kim, S.K., Kim, K.H., 2006. Protection of shrimp (*Penaeus chinensis*) against white spot syndrome virus (WSSV) challenge by double-stranded RNA. Fish Shellfish Immunol. 23, 242–246.

Labreuche, Y., Veloso, A., de la Vega, E., Gross, P.S., Chapman, R.W., Browdy, C.L., Warr, G.W., 2010. Non-specific activation of antiviral immunity and induction of RNA interference may engage the same pathway in the Pacific white leg shrimp *Litopenaeus vannamei*. Dev. Comp. Immunol. 34, 1209–1218.

Lin, Y.C., Yeh, S.T., Li, C.C., Chen, L.L., Cheng, A.C., Chen, J.C., 2011. An immersion of *Gracilaria tenuistipitata* extract improves the immunity and survival of white shrimp *Litopenaeus vannamei* challenged with white spot syndrome virus. Fish Shellfish Immunol. 31, 1239–1246.

Phetrungnapha, A., Ho, T., Udomkit, A., Panyim, S., Ongvarrasopone, C., 2013. Molecular cloning and functional characterization of Argonaute-3 gene from *Penaeus monodon*. Fish Shellfish Immunol. 35, 874–882.

Píndaro, Á.-R., Humberto, M.-R.C., Javier, M.-B.F., Marcial, E.-B.C., 2013. Silencing Pacific white shrimp *Litopenaeus vannamei* LvRab7 reduces mortality in brooders challenged with white spot syndrome virus. Aquac. Res. 44 (5), 772–782.

Robalino, J., Browdy, C.L., Prior, S., Metz, A., Parnell, P., Gross, P., Warr, G., 2004. Induction of antiviral immunity by double-stranded RNA in a marine invertebrate. J. Virol. 78, 10442–10448.

Robalino, J., Bartlett, T., Shepard, E., Prior, S., Jaramillo, G., Scura, E., Chapman, R.W., Gross, P.S., Browdy, C.L., Warr, G.W., 2005. Double-stranded RNA induced sequence-specific antiviral silencing inn addition to nonspecific immunity in a marine shrimp: convergence of RNA interference and innate immunity in the invertebrate antiviral response? J. Virol. 79, 13561–13571.

Robalino, J., Bartlett, T.C., Chapman, R.W., Gross, P.S., Browdy, C.L., Warr, G.W., 2007. Double-stranded RNA and antiviral immunity in marine shrimp: inducible host mechanisms and evidence for the evolution of viral counter-response. Dev. Comp. Immunol. 31, 539–547.

Senapin, S., Phiwsaiya, K., Anantasomboon, G., Sriphaijit, T., Browdy, C.L., Flegel, T.W., 2010. Knocking down a Taura syndrome virus (TSV) binding protein Lamr is lethal for the whiteleg shrimp *Penaeus vannamei*. Fish Shellfish Immunol. 29, 422–429.

Soowannayan, C., Chanarpakorn, N., Phanthura, M., Deekhlai, N., Kunasol, C., Sriurairatana, S., 2013. N-linked glycosylation is essential for the yellow head virus replication cycle. J. Gen. Virol. 94, 2458–2468.

Subhadra, B., Hurwitz, I., Fieck, A., Rao, D.V., Rao, G.S., Durvasula, R., 2010. Development of paratransgenic Artemia as a platform for control of infectious diseases in shrimp mariculture. J. Appl. Microbiol. 108, 831–840.

Thammasorn, T., Somchai, P., Laosutthipong, C., Jitrakorn, S., Wongtripop, S., Thitamadee, S., Withyachumnarnkul, B., Saksmerprome, V., 2013. Therapeutic effect of *Artemia* enriched with *Escherichia coli* expressing double-stranded RNA in the black tiger shrimp *Penaeus monodon*. Antiviral Res. 100, 202–206.

Thorley, J.A., McKeating, J.A., Rappoport, J.Z., 2010. Mechanisms of viral entry: sneaking in the front door. Protoplasma 244 (1–4), 15–24.

Tirasophon, W., Roshorm, Y., Panyim, S., 2005. Silencing of yellow head virus replication in penaeid shrimp cells by dsRNA. Biochem. Biophys. Res. Commun. 334 (1), 102–107.

Tirasophon, W., Yodmuang, S., Chinnirunvong, W., Plongthongkum, N., Panyim, S., 2007. Therapeutic inhibition of yellow head virus multiplication in infected shrimps by YHV-protease dsRNA. Antiviral Res. 74 (2), 150–155.

Vatanavicharn, T., Pongsomboon, S., Tassanakajon, A., 2012. Two plasmolipins from the black tiger shrimp, *Penaeus monodon* and their response to virus pathogens. Dev. Comp. Immunol. 38, 389–394.

Westenberg, M., heinhuis, B., Zuidema, D., Vlak, J.M., 2005. siRNA injection induces sequence-independent protection in *Penaeus monodon* against white spot syndrome virus. Virus Res. 114, 133–139.

Worby, C.A., Simonson-Leff, N., Dixon, J.E., 2001. RNA interference of gene expression (RNAi) in cultured *Drosophila* cells. Sci. STKE (95), PL1.

Yodmuang, S., Tirasophon, W., Roshorm, Y., Chinnirunvong, W., Panyim, S., 2006. YHV-protease dsRNA inhibits YHV replication in *Penaeus monodon* and prevents mortality. Biochem. Biophys. Res. Commun. 341 (2), 351–356.

# 5. Molecular characterization of a cDNA encoding red pigment-concentrating hormone in black tiger shrimp *Penaeus monodon* : Implication of its function in molt and osmoregulation.

Comparative Biochemistry and Physiology, Part A 175 (2014) 124–130

Contents lists available at ScienceDirect

Comparative Biochemistry and Physiology, Part A

journal homepage: www.elsevier.com/locate/cbpa

# Molecular characterization of a cDNA encoding red pigment-concentrating hormone in black tiger shrimp *Penaeus monodon*: Implication of its function in molt and osmoregulation

Ponsit Sathapondecha [a], Sakol Panyim [a,b], Apinunt Udomkit [a,*]

[a] Institute of Molecular Biosciences, Mahidol University, Salaya Campus, Nakhon Pathom 73170, Thailand
[b] Department of Biochemistry, Faculty of Science, Mahidol University, Rama VI Road, Bangkok 10400, Thailand

ARTICLE INFO

*Article history:*
Received 6 March 2014
Received in revised form 2 June 2014
Accepted 3 June 2014
Available online 14 June 2014

*Keywords:*
Crustacean
Eyestalk neuropeptides
Molting
Osmoregulation
$Na^+/K^+$ ATPase

ABSTRACT

Red pigment-concentrating hormone (RPCH) is a member of the AKH/RPCH peptide family present mainly in crustaceans and insects. Insect AKH is responsible for metabolic functions whereas RPCH plays a major role in the aggregation of red chromatophores in crustaceans. In this study, a full-length cDNA of RPCH of the black tiger shrimp, *Penaeus monodon* (*PmRPCH*) was cloned by Rapid Amplification of cDNA Ends strategies from the eyestalk RNA. A 770 bp full-length *PmRPCH* cDNA harbored 279 bp of an open reading frame encoding a signal peptide of 21 amino acid residues, an 8 amino acid mature RPCH peptide, followed by 61 amino acid residues of a RPCH precursor-related peptide. The highest levels of *PmRPCH* mRNA expression were detected in eyestalks while lower expression was found in other nervous tissues i.e. brain, thoracic ganglia and abdominal nerve cord. Expression of *PmRPCH* was transiently stimulated upon hypersalinity change within 12 h suggesting its osmoregulatory function. During the molting cycle, *PmRPCH* in the eyestalk was expressed at the lowest level in the early pre-molt stage ($D_0$), then gradually increased over the pre-molt period and reached the highest level in the late pre-molt ($D_4$) and post-molt (AB) stages. RPCH peptide at a dose of 100 pmol also increased gill $Na^+/K^+$ ATPase activity in 36–48 h after injection. However, PmRPCH did not accelerate the duration of molting cycle. Our results provide the first evidence on the potential function of PmRPCH in molting, probably by mediating hemolymph osmolality and ion transport enzymes during the late pre-molt stage.



## 1. Introduction

Red pigment-concentrating hormone (RPCH) is an octapeptide that belongs to the adipokinetic hormone (AKH)/red pigment-concentrating hormone (RPCH) family. The primary structure of a mature RPCH and AKH is typically composed of 8–10 amino acid residues with an N-terminal pyroglutamate and a C-terminal amidation (Gäde, 2009). In crustaceans, RPCH was mostly presented in diverse members of the order Decapoda. The crustacean RPCH was majorly expressed in nervous tissues such as the X-organ (XO) in the eyestalk (Mangerich et al., 1986; Alvarado-Alvarez et al., 1999; Chung and Webster, 2004), brain, and thoracic ganglia (Mangerich et al., 1986; Nusbaum and Marder, 1988; Chung and Webster, 2004).

The RPCH primarily functions in mediating pigment aggregation in crustaceans (Rao, 2001). Alvarado-Alvarez et al., 1999 demonstrated the biological activity of a synthetic RPCH to aggregate the tegumentary erythrophores of a crayfish *Procambarus clarkii* in vitro (Alvarado-Alvarez et al., 1999). Thereafter, several studies were successful to demonstrate in vivo the chromatophorotropic activity of the synthetic RPCH on pigment aggregation (Ribeiro and McNamara, 2009; Marco and Gäde, 2010). RPCH triggered pigment aggregation via the $Ca^{2+}$-activated cGMP signaling cascade. In the red ovarian chromatophores of the fresh water shrimp *Macrobrachium olfersi*, both the release of $Ca^{2+}$ from smooth endoplasmic reticulum (SER) and the blockage of $K^+$ influx led to membrane depolarization and thus allowed phosphorylation of downstream molecular motors essential for pigment aggregation (Milograna et al., 2010).

In addition to its major role in pigment aggregation, RPCH has also been reported to participate in other physiological processes. For instance, RPCH of the crayfish *P. clarkii* was shown to mediate retinal responsiveness to the circadian rhythm (Smith and Naylor, 1972). Sarojini et al. (1995) demonstrated that RPCH was involved in the reproductive system as a neurotransmitter that triggered the release of gonad-stimulating hormone (GSH) in the brain and/or thoracic ganglia of *P. clarkii*. In addition, a metabolic function of RPCH was investigated in an isopod, *Porcellio scaber*, where it triggered an increase in glucose level in the hemolymph (Zralá et al., 2010). These studies indicated that RPCH plays multifunctional roles in crustaceans. In *Penaeus*

* Corresponding author. Tel.: +66 2 441 9003 7x1236; fax: +66 2 441 9906.
*E-mail address:* apinunt.udo@mahidol.ac.th (A. Udomkit).

http://dx.doi.org/10.1016/j.cbpa.2014.06.001
1095-6433/

*monodon*, an amino acid sequence of the mature RPCH peptide (GenBank accession no. B3EWG0) is available but its cDNA has not yet been characterized.

Molt or ecdysis is an essential process for crustacean growth. The molting process involves several physiological mechanisms such as hormonal control, osmoregulation and metabolism (Chang and Mykles, 2011). Lipid and glucose were stored as an energy source during the intermolt stage, and were highly metabolized to supply energy for several metabolic processes during the pre-molt to post-molt stages (Siegert et al., 1993; Chamberlin et al., 1997; Galindo et al., 2009). Up-regulation of ion transport was found when the animals were just about to molt. Subsequently, water uptake became a major event during the period of post-molt (Jasmani et al., 2008; Galindo et al., 2009; Wilder et al., 2009; Jasmani et al., 2010; Bonilla-Gómez et al., 2012).

In this study a cDNA encoding RPCH of the black tiger shrimp *P. monodon* was cloned and characterized. According to its diverse function in other organisms, *PmRPCH* was investigated for its involvement in related physiological processes including salinity change and osmoregulation. In addition, our study provides the first evidence for a possible function of RPCH in the molting process of crustaceans.

## 2. Materials and methods

### 2.1. RNA extraction and cDNA synthesis

Black tiger shrimp *P. monodon* were kindly provided by Shrimp Genetic Improvement Center, Surat Thani, Thailand. They were acclimated in 5 ppt seawater until used. Shrimp tissues were freshly dissected and used for RNA extraction by Ribozol (Ameresco, USA) following the manufacturer's protocol. The amount of total RNA was determined from the absorbance at 260 nm as measured by Nanodrop 1000 (Thermo-scientific, USA). To synthesize a first-strand cDNA, 1 μg of the total RNA was mixed with 50 nM of oligo-dT primer and heated at 70 °C for 5 min then, snap cooled on ice for 3 min. The mixture composing of 1X RTase buffer, 3 mM $MgCl_2$, 0.4 mM dNTP and 1 μl of reverse-transcriptase ImpromII (Promega, USA) was added into the preheated RNA. The reaction was then incubated at 25 °C for 5 min, 42 °C for 60 min and 70 °C for 10 min. The cDNA was kept at −20 °C.

### 2.2. Cloning of a full-length PmRPCH cDNA

A full-length cDNA of *PmRPCH* was obtained by the Rapid Amplification of cDNA Ends (RACE) strategy using the first-strand cDNA from shrimp eyestalk. In 3′RACE, 1 μl of the oligo-dT-primed first-strand cDNA was amplified with 0.2 μM of 3RACE-PmRPCH-F1 and oligo-dT primers in a 25 μl reaction containing 1X *Taq* buffer + $(NH_4)_2SO_4$, 1.5 mM $MgCl_2$, 0.2 mM dNTP and 1 U *Taq* polymerase (Thermo-scientific, USA). Specific product was subsequently obtained by nested amplification using the first PCR product as a template with 3RACE-PmRPCH-F2 and PM1 primers. In 5′RACE, the first-strand cDNA was synthesized by 5RACE-PmRPCH-R1 and then tailed with dATP at the 3′end by terminal deoxytransferase (Promega, USA) using the manufacturer's protocol. The A-tailed cDNA was amplified with 5RACE-PmRPCH-R2 and oligo-dT primers in a reaction containing the same mixture as the 3′RACE reaction. Then, nested PCR was performed with the same condition as the first PCR but with 5RACE-PmRPCH-R3 and PM1 primers. The expected PCR products were ligated to a pGEM-T easy vector (Promega, USA) then, transformed into *Escherichia coli* DH5α. The nucleotide sequences of recombinant clones were determined by automated DNA sequencing at First-base Co., Ltd (Malaysia). The coding sequence of a full-length *PmRPCH* was verified by PCR using 3RACE-PmRPCH-F2 and 3UTR-PmRPCH-R primers with Phusion® high-fidelity DNA polymerase (Finnzymes, USA). Nucleotide sequences of all primers in the cloning steps are listed in Table 1.

**Table 1**
Primer pairs used in the experiments.

| Name | Objectives | Sequence (5′–3′) |
|---|---|---|
| 3RACE-PmRPCH-F1 | 3′RACE | CGGAACCATCCCAGTCACAAC |
| 3RACE-PmRPCH-F2 | 3′RACE | CTG GGGCAAGCGAGCAGCCG |
| 5RACE-PmRPCH-R1 | 5′RACE | TGATAAGYCKGTAGATGTGCATGAC |
| PmRPCH-R2 | 5′RACE and RT-PCR | TGACGGTTGTGACTG GGATGG |
| PmRPCH-R3 | 5′RACE | TGCGGCTGCTCGCTTGCC C |
| PmRPCH-F | RT-PCR | CAGATATGGTTCGTGCCGTCG |
| 3UTR-PmRPCH-R | RT-PCR | ACGAAACGGTAGATGGTTGTTG |
| Ef-1α-F | RT-PCR | GAACTGCTGACCAAGATCGACAGG |
| Ef-1α-R | RT-PCR | GAGCATACTGTTGGAAGGTCTCCA |
| ActinF | RT-PCR | GACTCGTACGTGGGCGACGAGG |
| ActinR | RT-PCR | AGCAGCGGTGGTCATCTCCTGCTC |

### 2.3. Determination of PmRPCH expression in shrimp tissues

Adult female *P. monodon* (approximately 100 g) were anesthetized on ice and various tissues including the eyestalk, brain, thoracic ganglia, abdominal nerve cord, hepatopancreas, gill, lymphoid, muscle and hemocytes were freshly collected for RNA isolation. One microgram of the total RNA was used for cDNA synthesis, and semi-quantitative RT-PCR was performed to determine the expression of *PmRPCH* with PmRPCH-F and PmRPCH-R2 (Table 1) primers using the following temperature cycles: 94 °C for 3 min, then 26 cycles of 94 °C for 30 s, 58 °C for 30 s and 72 °C for 30 s. A beta-actin transcript was amplified by Actin-F and Actin-R primers as an internal control.

### 2.4. Reverse transcription real-time PCR

The *PmRPCH* mRNA levels in shrimp eyestalk in subsequent experiments were determined by reverse transcription relative real-time PCR. The appropriate dilution of oligo-dT-primed cDNA was amplified with PmRPCH-F and PmRPCH-R2 primers. The PCR mixture was composed of a 1X KAPA SYBR Fast ABI Prism qPCR kit (KAPA Biosystems, USA), and 0.25 μM of each primer. The reaction was subjected to amplification in a real-time PCR machine (realplex$^4$, Eppendorf) using the PCR profile of 95 °C for 3 min, then 40 cycles of 95 °C for 5 s and 60 °C for 30 s. Elongation factor-1 alpha (*EF-1α*) was amplified as an internal control with EF1α-F and EF1 α-R primers using the same PCR profile. Each sample was amplified in duplication. The purified PCR products of both *PmRPCH* and *EF-1α* were diluted to $10^2$–$10^8$ copies and used as a template to establish a standard curve for each gene. The threshold cycle of both genes was calculated as copy number, and then the copy number of *PmRPCH* was normalized with that of *EF-1α*.

### 2.5. Expression of PmRPCH upon hypersalinity change

Shrimp (approximately 5 g) in the early pre-molt stage ($D_0$) were acclimated in 5 ppt seawater at 28–30 °C for one week before use. Two independent experiments were performed. The shrimp were divided into two groups; each group contained 5 shrimp. At the beginning of the experiment shrimp in the control group and the experimental group were transferred from 5 ppt seawater to a new tank filled with 5 ppt and 30 ppt seawater, respectively. Shrimp eyestalks from each group were collected at 6 h, 12 h, 24 h, 36 h and 48 h ($n = 5$ for each time point) and determined for *PmRPCH* expression by reverse transcription real-time PCR.

### 2.6. Expression of PmRPCH and gill-$Na^+$–$K^+$ ATPase activity during the molting cycle

Shrimp (approximately 10 g) were reared in 5 ppt seawater at 28–30 °C. The molting stages of the shrimp were divided into intermolt (C), early pre-molt ($D_0$), pre-molt ($D_{2-3}$), late pre-molt ($D_4$) and

post-molt (AB) stages (Promwikorn et al., 2004). *PmRPCH* mRNA expression levels were determined by reverse transcription real-time PCR. Two independent experiments were performed; each experiment was composed of three shrimp at each molting stage. Anterior (1st to 4th) and posterior (5th to 8th) gills were also collected for $Na^+$–$K^+$ ATPase activity assay.

### 2.7. Measurement of $Na^+/K^+$ ATPase activity in the gill

Activity of $Na^+/K^+$ ATPase in both anterior and posterior gills was measured by following Holliday's method (Holliday, 1985). In brief, freshly isolated gills were washed twice in cold-SEI buffer (250 mM sucrose, 10 mM EDTA and 50 mM imidazole pH 7.4) then, homogenized in 10-volumes of cold-SEI buffer containing 0.1% sodium deoxycholate. The cell debris was eliminated by centrifugation at 600 *g*, 4 °C for 5 min. The supernatant was further centrifuged at 10,000 *g* at 4 °C for another 10 min. Protein concentration in the supernatant was measured by Bradford assay (Invitrogen) before $Na^+/K^+$ ATPase activity assay. Ten microliters of each sample was added to the salt solution (130 mM NaCl, 30 mM KCl and 50 mM imidazole pH 7.4) or salt solution containing ouabain, a $Na^+/K^+$ ATPase inhibitor (130 mM NaCl, 1 mM ouabain and 50 mM imidazole pH 7.4). The reaction was pre-incubated at 37 °C for 5 min, then 0.7 mM ATP/7 mM $MgCl_2$ was added and incubated for 20 min. The reaction was stopped by adding 1 mL of cold-stop solution (8.4 mM ammonium molybdate, 3.2% v/v $H_2SO_4$ and 4.8% w/v $FeSO_4$). The concentration of phosphate was measured at $OD_{700}$. The activity unit was calculated in μmol Pi/mg protein/h.

### 2.8. Effect of synthetic RPCH on gill $Na^+/K^+$ ATPase activity

A synthetic RPCH (pyroGlu-Leu-Asn-Phe-Ser-Pro-Gly-Trp-$NH_2$) at approximately 90% of purity was produced from ChinaPeptides Company, China. The synthetic peptide was dissolved in 80% methanol to a final concentration of 1 mg/mL. The working synthetic RPCH was freshly diluted with 150 mM NaCl before use. Shrimp in the early pre-molt ($D_0$) stage reared in 5 ppt seawater were injected with 10 pmol and 100 pmol RPCH peptide, or 150 mM NaCl as a control group ($n = 5$ for each group). Anterior and posterior gills were isolated to measure $Na^+/K^+$ ATPase activity at different time points after injection (6–48 h).

### 2.9. Effect of synthetic RPCH on molt duration in shrimp

Shrimp (approximately 10 g) reared in 5 ppt seawater at 28–30 °C were allowed to molt. Three days after molt, shrimp at the late intermolt stage ($n = 7$) were injected with a single dose of synthetic RPCH at the doses of 1 pmol, 10 pmol and 100 pmol or with 150 mM NaCl. In addition, shrimp were also injected with 100 pmol synthetic RPCH or NaCl daily for 6 days. The molt duration of shrimp in both groups was recorded.

### 2.10. Statistical analysis

The expression of eyestalk *PmRPCH* under hypersalinity changes and gill $Na^+/K^+$ ATPase activity responding to RPCH peptide were determined for significant difference by two-way ANOVA and Bonferroni's test. The expression level of eyestalk *PmRPCH* mRNA and gill $Na^+/K^+$ ATPase activity in different molt stages were analyzed by one-way ANOVA and compared between groups by Duncan's test. Data analysis was performed using SPSS Statistic version 20 (IBM®, USA).

## 3. Results

### 3.1. Cloning and characterization of PmRPCH cDNA

PCR fragments of 480 bp and 358 bp were obtained from 3′ and 5′ RACE, respectively with an overlapping region of 68 bp. The combined sequence of *PmRPCH* cDNA was composed of a 129 bp 5′UTR, a 279 bp of coding region that encoded for 93 amino acid residues and a 3′UTR of 362 bp. The entire coding sequence of PmRPCH (GenBank Accession No. KC757347) was subsequently verified by PCR and characterized. The deduced amino acid sequence of PmRPCH possessed a signal peptide in the first 21 amino acid residues as predicted by VSA-QL (SignalP 4.0). The mature peptide of PmRPCH was composed of eight amino acid residues with the sequence Gln-Leu-Asn-Phe-Ser-Pro-Gly-Trp. A potential amidation site was found at the C-terminus of the mature peptide followed by a dibasic cleavage site (GKR) that, after cleavage, would produce an RPCH precursor-related peptide of 61 amino acid residues (Fig. 1). Amino acid sequence alignment showed that the PmRPCH mature peptide sequence was identical to that of RPCH of other crustaceans, whereas some variations were presented in the precursor-related peptide region. In addition, an alignment of the mature PmRPCH to the mature insect AKH peptides indicated highly conserved amino acid residues; $Gln^1$, $Leu^2$, $Phe^4$ and $Trp^8$ (Fig. 1).

### 3.2. Tissue distribution of PmRPCH expression

The *PmRPCH* mRNA expression levels in various shrimp tissues were determined by semi-quantitative RT-PCR. The result in Fig. 2 showed that *PmRPCH* mRNA was highly expressed in the eyestalk. Lower levels of *PmRPCH* expression could be detected in the brain, thoracic ganglia and abdominal nerve cord whereas the expression in other tissues i.e. hepatopancreas, lymphoid, gill, muscle and hemocytes was hardly detectable.

### 3.3. Expression of PmRPCH in response to hypersalinity change

To determine the effect of stress condition caused by hypersalinity change on *PmRPCH* expression, shrimp that had been acclimated in low salt seawater (5 ppt) were exposed to high salt seawater (30 ppt) for 6, 12, 24, 36 and 48 h. The *PmRPCH* mRNA expression level was determined by quantitative real-time PCR. The result in Fig. 3 showed that an almost three-fold change of the *PmRPCH* mRNA level was observed in the shrimp that were exposed to 30 ppt seawater for 12 h compared with that in the control shrimp that were continuingly reared in 5 ppt seawater ($p < 0.05$), before gradually declining at 24–48 h. In contrast, the expression of *PmRPCH* in the control shrimp reared in 5 ppt seawater was not changed over time courses ($p > 0.05$).

### 3.4. Relationship between PmRPCH expression and gill $Na^+/K^+$ ATPase activity during the molting cycle

The expression profile of *PmRPCH* mRNA in shrimp eyestalks at each molting stage was determined to investigate the involvement of PmRPCH in the molting process. The result showed that the *PmRPCH* mRNA level was lowest at the early pre-molt stage ($D_0$), then gradually increased and reached the highest level at the late pre-molt stage ($D_4$) and post-molt stage (AB); an approximately 4-fold increase ($p < 0.05$) compared to that in the $D_0$ stage. The expression of *PmRPCH* was then decreased after molt and remained at a low level throughout the intermolt (C) stage (Fig. 4A). In addition, gill $Na^+/K^+$ ATPase activity during the molting cycle was determined. The $Na^+/K^+$ ATPase activity in both anterior and posterior gills (Fig. 4B and C, respectively) showed the lowest activity ($45.5 \pm 5.8$ and $35.0 \pm 4.2$ μmol Pi/mg protein/h, respectively) at the pre-molt ($D_{23}$) stage. The activity was significantly raised in the late pre-molt stage ($D_4$; $118.6 \pm 25.7$ μmol Pi/mg protein/h) and post-molt stage (AB; $98.1 \pm 9.1$ μmol Pi/mg protein/h) in posterior gills, whereas the $Na^+/K^+$ ATPase activity in anterior gills remained at low levels over pre-molt stages before increasing in the post-molt stage ($124.4 \pm 25.4$ μmol Pi/mg protein/h).

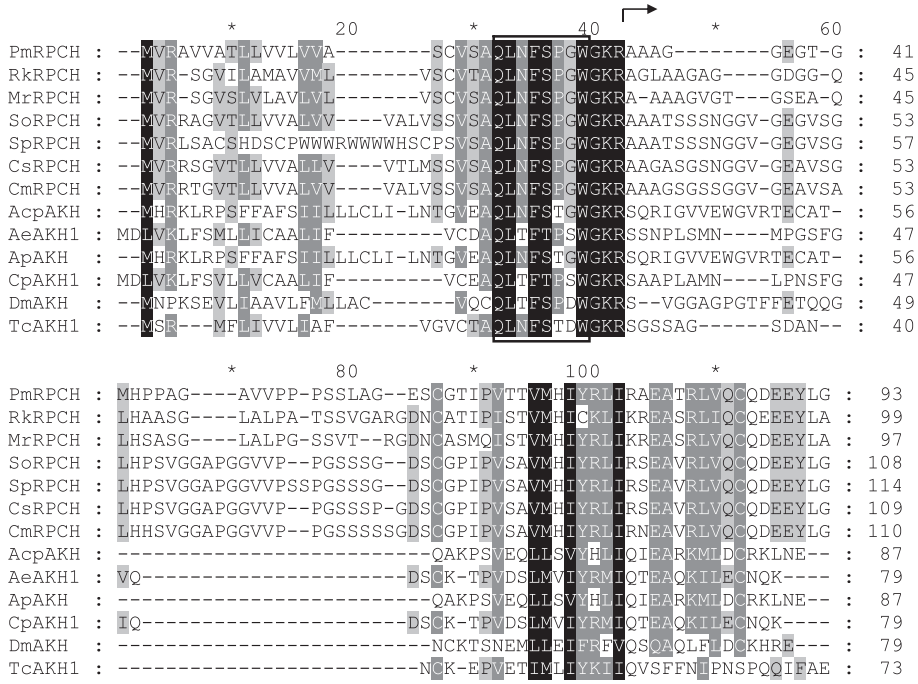


**Fig. 1.** Amino acid sequence alignment of PmRPCH with RPCH/AKH from other species. The deduced amino acid sequence of PmRPCH (GenBank accession no. KC757347) is aligned with RPCH from *Rimicaris kairei* (RkRPCH; ACZ51370), *Macrobrachium rosenbergii* (MrRPCH; ABV46765), *Scylla olivacea* (SoRPCH; ADQ73633), *Scylla paramamosain* (SpRPCH; AGW45011), *Callinectes sapidus* (CsRPCH; AAC37244) and *Carcinus maenas* (CmRPCH; AAB28133), and with insect-AKH from *Acyrthosiphon pisum* (AcpAKH; AEY77127), *Aedes aegypti* (AeAKH1; CAY77165), *Apis mellifera* (ApAKH; AEW68342), *Culex pipiens* (CpAKH1; CAY77163), *Drosophila melanogaster* (DmAKH; NP_523918), and *Tribolium castaneum* (TcAKH1; ABN79648). Amino acids that are identical or conserved in all sequences are highlighted in black color. Box and arrow indicate sequences of mature RPCH/AKH peptides and precursor-related peptide, respectively.

### 3.5. Effect of synthetic RPCH on gill $Na^+/K^+$ ATPase activity

The effect of synthetic RPCH on $Na^+/K^+$ ATPase activity in both anterior and posterior gills were determined by $Na^+/K^+$ ATPase activity assay. The result in Fig. 5 showed that the $Na^+/K^+$ ATPase activity in both anterior (A) and posterior (B) gills did not change after RPCH injection, comparing with NaCl injection in the first 24 h. At 36 h after injection, the anterior gill $Na^+/K^+$ ATPase activity was significantly increased in the shrimp injected with 100 pmol RPCH (118.9 ± 16.3 μmol Pi/mg protein/h) compared with that in NaCl-injected shrimp (49.7 ± 5.4 μmol Pi/mg protein/h). Similarly, the $Na^+/K^+$ ATPase activity in posterior gills of 100 pmol RPCH-injected shrimp (84.6 ± 10.3 μmol Pi/mg protein/h) was significantly higher than that in NaCl injected shrimp (63.4 ± 6.2 μmol Pi/mg protein/h). The posterior gill $Na^+/K^+$ ATPase activity in 100 pmol-RPCH injected shrimp continued with a significant increase at 48 h after injection (91.4 ± 12.6 μmol Pi/mg protein/h) compared with the control shrimp (47.7 ± 4.6 μmol Pi/mg protein/h).

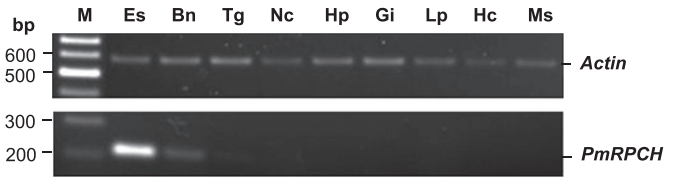


**Fig. 2.** Expression of *PmRPCH* mRNA in shrimp tissues. The expression levels of *PmRPCH* were detected by semi-quantitative RT-PCR. A representative of RT-PCR product of PmRPCH in eyestalk, Es; brain, Bn; thoracic ganglia, Tg; abdominal nerve cord, Nc; hepatopancreas, Hp; gill, Gi; lymphoid, Lp; hemocyte, Hc and muscle, Ms from one adult female *P. monodon* is shown. The upper bands (approximately 550 bp) represent the *β-actin* transcript that was used as an internal control and the lower bands (approximately 210 bp) represent *PmRPCH* RT-PCR products in each tissue. M is a 100 bp DNA ladder.

### 3.6. Effect of synthetic RPCH on molt duration

To determine whether the molting cycle was mediated by RPCH peptide, shrimp were injected with the synthetic RPCH and the duration of molt was recorded and compared to that of the shrimp injected with NaCl. Single injection of different doses of RPCH showed no significant change of molt durations compared to the control (Table 2). Similarly, six injections of the peptides also showed no significant difference of molt duration indicating that the synthetic RPCH did not affect the molting cycle of the shrimp.

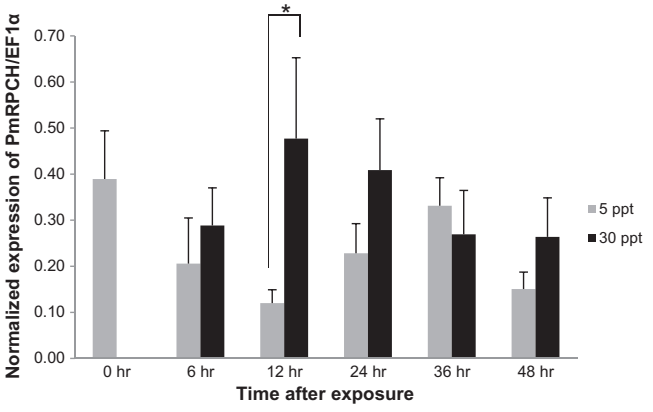


**Fig. 3.** Changes in *PmRPCH* mRNA levels under hypersalinity stress. Shrimp were acclimatized in 5 ppt seawater for one week before rearing in 30 ppt seawater (dark bars) or continuing rearing in 5 ppt seawater (gray bars). *PmRPCH* copy numbers normalized to that of *EF-1α* were determined by qRT-PCR at 6, 12, 24, 36 and 48 h. Values are shown as means ± SEM (n = 5). An asterisk depicts significant difference at $p < 0.05$ by two-way ANOVA and Bonferroni's test.

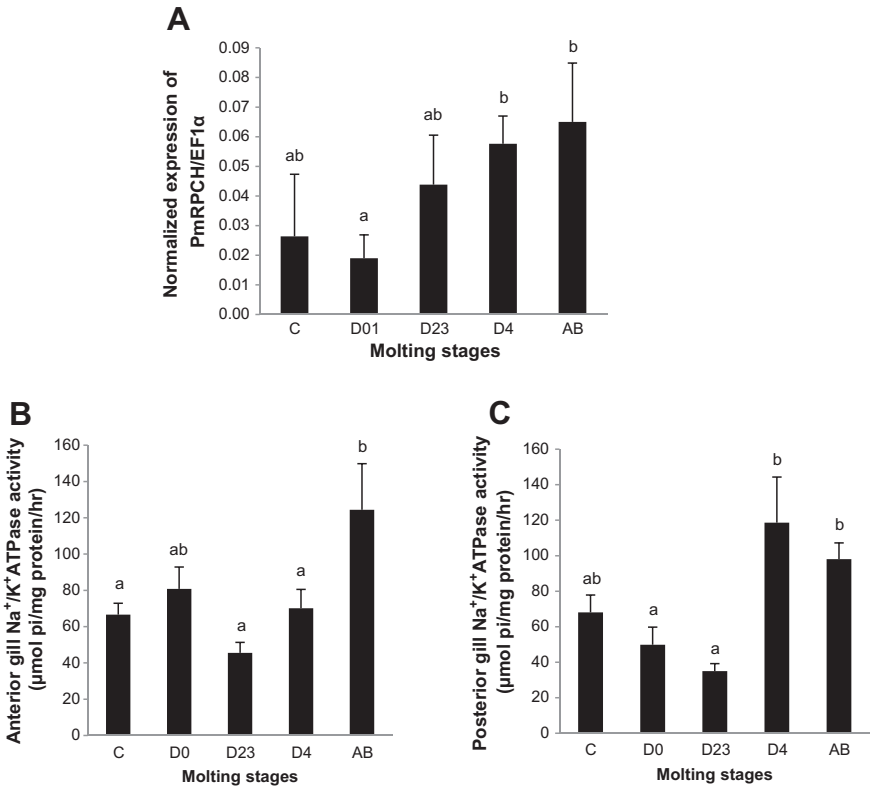


**Fig. 4.** Expression profile of eyestalk *PmRPCH* mRNA and gill $Na^+/K^+$ ATPase activity during the molting cycle. (A) *PmRPCH* mRNA expression in each stage of molt was determined by reverse transcription real-time PCR. The relative expression of *PmRPCH* compared to that of *EF-1α* in the early pre-molt stage was used as a calibrator for the relative expression values of *PmRPCH* in the other molting stages. Values are shown as means ± SEM (n = 6). Both anterior (B) and posterior (C) gill $Na^+/K^+$ ATPase activities were determined during molting cycle. The alphabets represent significant difference ($p < 0.05$) analyzed by one way ANOVA and Duncan's test. Molting stages are depicted as follows: intermolt (C); early pre-molt ($D_0$); mid pre-molt ($D_{23}$); late pre-molt ($D_4$) and post-molt (AB).

## 4. Discussion

RPCH is a crustacean neuropeptide that is structurally related to the adipokinetic hormone (AKH) in insects. Peptides in the AKH/RPCH family generally contain 8–10 amino acid residues of the mature peptide with common features including modification at the N- and C-termini by pyroglutamate and amidation, respectively. All crustacean RPCHs identified to date share identical mature peptide sequences. The fourth and eighth positions of their mature peptides usually contain aromatic amino acids Phe and Trp, respectively (Gäde, 2009). The deduced amino acid sequence of the mature PmRPCH obtained in this study shared all the aforementioned features of the RPCH peptides. Comparison of amino acid sequences revealed variations at three positions between mature RPCHs ($Asn^3$, $Pro^6$ and $Gly^7$) and AKHs ($Thr^3$, $Thr^6$ and $Ser^7$ or $Asp^7$) as shown in Fig. 1. Whereas the insect AKHs were known to be functionally involved in energy metabolism e.g. activation of glycogen phosphorylation and lipase enzymes in the fat body for energy supply, especially in the flight muscles (Gade, 2004), crustacean RPCHs primarily function in the aggregation of red pigment granules in response to environment (Rao, 2001). However, it has been demonstrated that the insect AKH could elicit pigment-concentration in prawn (Mordue and Stone, 1977). In addition, the synthetic crustacean RPCH (Panbo-RPCH) was able to trigger lipid mobilization in stinkbug, *Nezara viridula* (Gäde et al., 2003). The cross-activity between these two hormones was correlated to the similarity in their structures. In addition, this also implies that different functional activities of RPCH/AKH may require the binding of the peptides to different receptors presented in crustaceans and insects. Interestingly, Marco and Gäde (2010) recently reported that the $Lue^2$ amino acid residue was essential for the chromatophorotropic activity of RPCH since the change from $Lue^2$ to $Val^2$ resulted in a significant drop in its activity (Marco and Gäde, 2010). Further studies on the structure–function relationship as well as the ligand-receptor binding of RPCH/AKH are required for understanding detailed mechanisms of action of each peptide.

Immunohistochemical studies in several species revealed the presence of the RPCH peptide in crustacean central nervous system (CNS) e.g. optic ganglia, brain, thoracic ganglia and abdominal nerve cord (Mangerich et al., 1986; Nusbaum and Marder, 1988; Klein et al., 1995; Chung and Webster, 2004). Recent study by Kornthong et al. also confirmed the expression of RPCH in the CNS of the mud crab *Scylla olivacea* by RT-PCR and in situ hybridization (Kornthong et al., 2013). Our result showed that *P. monodon RPCH* mRNA was markedly expressed in the eyestalk and other nervous tissues such as the brain, thoracic ganglia and abdominal nerve cord (Fig. 2), thus conforming to the expression of RPCH in other crustaceans.

Besides its primary function in pigment aggregation, previous studies have demonstrated the metabolic functions of RPCH in both crustaceans and insects. For instance, injection of a synthetic RPCH increased carbohydrate, especially glucose in the hemolymph of the isopod *P. scaber* (Zralá et al., 2010). The role in osmoregulation of PmRPCH was determined under hypersalinity change in this study. The eyestalk *PmRPCH* mRNA levels were transiently increased to 3 folds after the shrimp that had been acclimated in 5 ppt seawater were transferred to 30 ppt salinity for 12 h compared with the control shrimp maintained in 5 ppt seawater (Fig. 3). This short time response of *PmRPCH* expression might involve rapid activation of the osmoregulatory system. In *P. monodon* and *Macrobrachium rosenbergii*, hemolymph osmolality was raised under hyper-osmotic condition (Wilder et al., 1998; Lin et al., 2000; Tantulo and Fotedar, 2007). Moreover, activity of ion transport enzymes, particularly $Na^+/K^+$ ATPase in gills rapidly increased within 3 h after exposing to hypersaline water in a teleost, *Fundulus heteroclitus* (Mancera and McCormick, 2000). However, in *P. monodon*

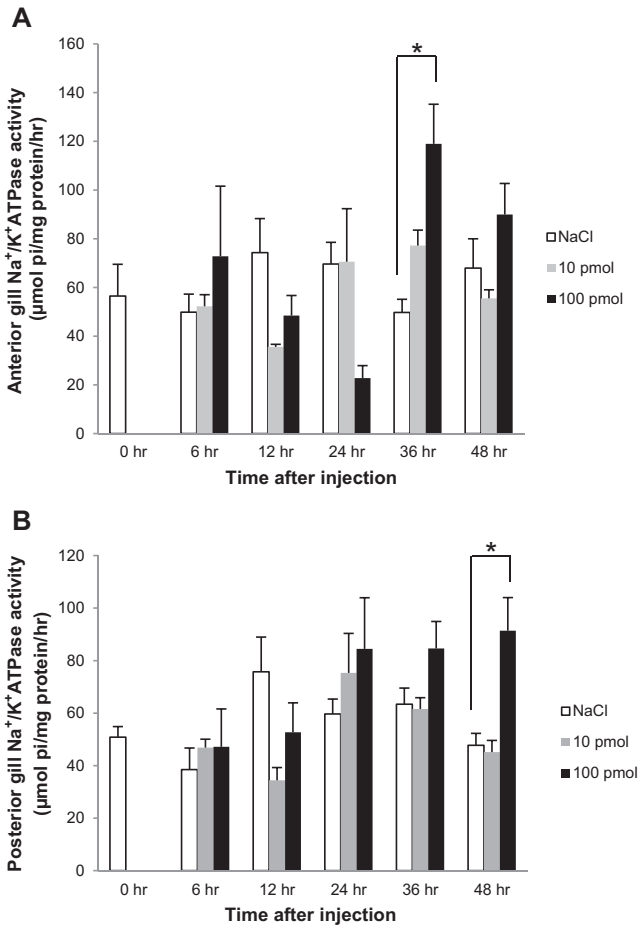


**Fig. 5.** Effect of RPCH peptide on gill $Na^+/K^+$ ATPase activity. Both anterior (A) and posterior (B) gill $Na^+/K^+$ ATPase activities were determined after injection of 10 pmol, 100 pmol RPCH or NaCl at different time courses. Values are shown as mean ± SEM (n = 5). An asterisk represents significant difference at $p < 0.05$ analyzed by two-way ANOVA and Bonferroni's test.

the activity of gill $Na^+/K^+$ ATPase measured after the shrimp were subjected to salinity changes for one week did not change comparing with the activity at the beginning (Buranajitpirom et al., 2010). Although there was no evidence about the ion transport function of RPCH at present, previous study demonstrated that RPCH could exert an overlapping function with an eyestalk's crustacean hyperglycemic hormone (CHH) in *P. scaber* (Zralá et al., 2010). As CHH belongs to the same eyestalk neuropeptide family as an ion transport peptide (ITP) (Audsley et al., 1992), our result therefore suggests that PmRPCH probably functions as an ion transport peptide, an eyestalk hormone not yet identified in *P. monodon*. However, direct evidence is needed to confirm the ion transport function of PmRPCH.

Molting is an important process required for growth in crustaceans. It involves discarding of an old exoskeleton and replacing with a new one. Dramatic changes in several physiological mechanisms, especially osmoregulation occur during the molting process (Chang, 1995). Molting is known to be regulated mainly by a molt-inhibiting hormone (MIH), an eyestalk neuropeptide that inhibits the synthesis and the release of ecdysteroids or molting hormone from the Y-organ (Chang and Mykles, 2011). In addition, other eyestalk peptides such as CHH and mandibular organ-inhibiting hormone (MO-IH) were shown to play a role in ecdysteroid synthesis (Chung, 2010). As mentioned earlier that RPCH could have overlapping functions with other eyestalk's peptides, possible involvement of PmRPCH in regulating the molting process in *P. monodon* was therefore investigated. Our result showed that injection of the synthetic RPCH did not affect the molt duration of the shrimp either by single injection or multiple injections (Table 2). Therefore it is possible that PmRPCH was not directly required for triggering or mediating the molting process. In addition, the expression levels of *PmRPCH* mRNA in shrimp eyestalk during each stage of the molting cycle were determined. A dramatic increase of *PmRPCH* mRNA expression was obviously observed from its lowest level in the early pre-molt stage ($D_0$) up to the maximum level at the late pre-molt stage ($D_4$). In the pre-molt stage, osmoregulation, one of the molting processes, was changed in crustaceans. For example, hemolymph osmolality in *Litopenaeus vannamei*, *M. rosenbergii* and *Farfantepenaeus duorarum* was increased in the late-pre-molt and molt stages (Galindo et al., 2009; Wilder et al., 2009; Bonilla-Gómez et al., 2012). Gill $Na^+/K^+$ ATPase and carbonic anhydrase activities were raised in the pre-molt stages in *Macrobrachium nipponense* and *L. vannamei* (Wang et al., 2003; Jasmani et al., 2010). Similarly, our result showed that gill $Na^+/K^+$ ATPase activity in *P. monodon* (Fig. 4 A and B) was increased in the late pre-molt through molting stages. In addition, we also demonstrated that injection of synthetic RPCH peptide stimulated $Na^+/K^+$ ATPase activity in the anterior and posterior gills at 36 h and 48 h after injection, respectively (Fig. 5A and B). Since RPCH signaling transduction raised intracellular $Ca^{2+}$ by activating some voltage-gated $Ca^{2+}$ channels (Milograna et al., 2010), it is possible that following RPCH injection, the homeostasis of $Ca^{2+}$ was regulated through a $Na^+/Ca^{2+}$ exchanger (Carafoli, 2002) resulting in a $Na^+$ influx that activated the $Na^+/K^+$ ATPase activity in the gills. Further study to determine the actual $Na^+$ flux in the shrimp is needed to explain the mechanism of action for this effect of RPCH injection. Taken together, our results provide supportive evidences for a role of PmRPCH in osmoregulatory responses during the molting process.

In summary, our current study identified and characterized a cDNA encoding RPCH in *P. monodon*. Determination of *PmRPCH* mRNA expression levels reveals that *PmRPCH* expression was transiently elevated upon hypersalinity change suggesting the role of PmRPCH in osmoregulation. Although the synthetic RPCH did not exhibit any influence on the molt duration of the shrimp, it could stimulate the activity of gill $Na^+/K^+$ ATPase. Our result further demonstrates that gill $Na^+/K^+$ ATPase activity significantly increased during the pre-molt stages. Hence, we propose that PmRPCH may not directly trigger the molting process, but is probably required for regulating hemolymph osmolality and ion transport enzymes during the molt.

**Table 2**
Duration of molt after synthetic RPCH injection.

| Injection | Group (number of shrimp) | Duration of molt (days; mean ± SD) |
|---|---|---|
| Single injection | Control (n = 7) | 10.5 ± 0.98 |
| | 1 pmol RPCH (n = 7) | 11.2 ± 1.11 |
| | 10 pmol RPCH (n = 7) | 10.8 ± 1.57 |
| | 100 pmol RPCH (n = 7) | 10.5 ± 1.13 |
| 6 injections | Control (n = 10) | 11.7 ± 1.33 |
| | 100 pmol RPCH (n = 9) | 12.0 ± 1.11 |

## Acknowledgments

The authors wish to thank Miss Somjai Wongtripop (Shrimp Genetics Improvement Center, Surat Thani, Thailand) for providing the shrimp samples. We are thankful to Ms. Chawewan Chimwai, Mrs. Suparp Hongthong and Ms. Pannee Thongboonsong for their technical assistance. This work was supported by the Thailand Research Fund (BRG5480018 to AU and DPG5680001 to SP), the Mahidol University Research Grant and the Office of the Higher Education Commission and Mahidol University under the National Research Universities Initiative. PS is the recipient of the student fellowship by the Royal Golden Jubilee Ph.D. Program (PHD/0188/2553).

## References


Alvarado-Alvarez, R., Becerra, E., Garcia, U., 1999. A high-resolution in vitro bioassay to identify neurons containing red pigment concentrating hormone. J. Exp. Biol. 202, 1777–1784.

Audsley, N., McIntosh, C., Phillips, J.E., 1992. Isolation of a neuropeptide from locust corpus cardiacum which influences ileal transport. J. Exp. Biol. 173, 261–274.

Bonilla-Gómez, J.L., Chiappa-Carrara, X., Galindo, C., Jeronimo, G., Cuzon, G., Gaxiola, G., 2012. Physiological and biochemical changes of wild and cultivated juvenile pink shrimp *Farfantepenaeus duorarum* (Crustacea: Penaeidae) during molt cycle. J. Crustac. Biol. 32, 597–606.

Buranajitpirom, D., Asuvapongpatana, S., Weerachatyanukul, W., Wongprasert, K., Namwong, W., Poltana, P., Withyachumnarnkul, B., 2010. Adaptation of the black tiger shrimp, *Penaeus monodon*, to different salinities through an excretory function of the antennal gland. Cell Tissue Res. 340, 481–489.

Carafoli, E., 2002. Calcium signaling: a tale for all seasons. Proc. Natl. Acad. Sci. U. S. A. 99, 1115–1122.

Chamberlin, M., Gibellato, C., Noecker, R., Dankoski, E., 2013. Changes in midgut active ion transport and metabolism during larval–larval molting in the tobacco hornworm (*Manduca sexta*). J. Exp. Biol. 200, 643–648.

Chang, E.S., 1995. Physiological and biochemical changes during the molt cycle in decapod crustaceans: an overview. J. Exp. Mar. Biol. Ecol. 193, 1–14.

Chang, E.S., Mykles, D.L., 2011. Regulation of crustacean molting: a review and our perspectives. Gen. Comp. Endocrinol. 172, 323–330.

Chung, J.S., 2010. Hemolymph ecdysteroids during the last three molt cycles of the blue crab. *Callinectes sapidus*: quantitative and qualitative analyses and regulation. Arch. Insect Biochem. Physiol. 73, 1–13.

Chung, J.S., Webster, S.G., 2004. Expression and release patterns of neuropeptides during embryonic development and hatching of the green shore crab, *Carcinus maenas*. Development 131, 4751–4761.

Gade, G., 2004. Regulation of intermediary metabolism and water balance of insects by neuropeptides. Annu. Rev. Entomol. 49, 93–113.

Gäde, G., 2009. Peptides of the adipokinetic hormone/red pigment-concentrating hormone family. Ann. N. Y. Acad. Sci. 1163, 125–136.

Gäde, G., Auerswald, L., Šimek, P., Marco, H.G., Kodrík, D., 2003. Red pigment-concentrating hormone is not limited to crustaceans. Biochem. Biophys. Res. Commun. 309, 967–973.

Galindo, C., Gaxiola, G., Cuzon, G., Chiappa-Carrara, X., 2009. Physiological and biochemical variations during the molt cycle in juvenile *Litopenaeus vannamei* under laboratory conditions. J. Crustac. Biol. 29, 544–549.

Holliday, C.W., 1985. Salinity-induced changes in gill Na, K-ATPase activity in the mud fiddler crab, *Uca pugnax*. J. Exp. Zool. 233, 199–208.

Jasmani, S., Jayasankar, V., Wilder, M.N., 2008. Carbonic anhydrase and Na/K-ATPase activities at different molting stages of the giant freshwater prawn *Macrobrachium rosenbergii*. Fish. Sci. 74, 488–493.

Jasmani, S., Jayasankar, V., Shinji, J., Wilder, M., 2010. Carbonic anhydrase and Na/K-ATPase activities during the molt cycle of low salinity-reared white shrimp *Litopenaeus vannamei*. Fish. Sci. 76, 219–225.

Klein, J.M., Mohrherr, C.J., Sleutels, F., Jaenecke, N., Riehm, J.P., Rao, K.R., 1995. A highly conserved red pigment-concentrating hormone precursor in the blue crab *Callinectes sapidus*. Biochem. Biophys. Res. Commun. 212, 151–158.

Kornthong, N., Chotwiwatthanakun, C., Chansela, P., Tinikul, Y., Cummins, S.F., Hanna, P.J., Sobhon, P., 2013. Characterization of red pigment concentrating hormone (RPCH) in the female mud crab (*Scylla olivacea*) and the effect of 5-HT on its expression. Gen. Comp. Endocrinol. 185, 28–36.

Lin, S.-C., Liou, C.-H., Cheng, J.-H., 2000. The role of the antennal glands in ion and body volume regulation of cannulated *Penaeus monodon* reared in various salinity conditions. Comp. Biochem. Physiol. A Mol. Integr. Physiol. 127, 121–129.

Mancera, J.M., McCormick, S.D., 2000. Rapid activation of gill $Na^+$, $K^+$-ATPase in the euryhaline teleost *Fundulus heteroclitus*. J. Exp. Zool. 287, 263–274.

Mangerich, S., Keller, R., Dircksen, H., 1986. Immunocytochemical identification of structures containing putative red pigment-concentrating hormone in two species of decapod crustaceans. Cell Tissue Res. 245, 377–386.

Marco, H.G., Gäde, G., 2010. Biological activity of the predicted red pigment-concentrating hormone of *Daphnia pulex* in a crustacean and an insect. Gen. Comp. Endocrinol. 166, 104–110.

Milograna, S.R., Bell, F.T., McNamara, J.C., 2010. Signal transduction, plasma membrane calcium movements, and pigment translocation in freshwater shrimp chromatophores. J. Exp. Zool. A Ecol. Genet. Physiol. 313, 605–617.

Mordue, W., Stone, J.V., 1977. Relative potencies of locust adipokinetic hormone and prawn red pigment-concentrating hormone in insect and crustacean systems. Gen. Comp. Endocrinol. 33, 103–108.

Nusbaum, M.P., Marder, E., 1988. A neuronal role for a crustacean red pigment concentrating hormone-like peptide: neuromodulation of the pyloric rhythm in the crab, *Cancer borealis*. J. Exp. Biol. 135, 165–181.

Promwikorn, W., Kirirat, P., Thaweethamsewee, P., 2004. Index of molt staging in the black tiger shrimp (*Penaeus monodon*). Songklanakarin J. Sci. Technol. 26, 765–772.

Rao, K.R., 2001. Crustacean pigmentary-effector hormones: chemistry and functions of RPCH, PDH, and related peptides. Am. Zool. 41, 364–379.

Ribeiro, M.R., McNamara, J.C., 2009. Cyclic guanosine monophosphate signaling cascade mediates pigment aggregation in freshwater shrimp chromatophores. Biol. Bull. 216, 138–148.

Sarojini, R., Nagabhushanam, R., Fingerman, M., 1995. A neurotransmitter role for red-pigment-concentrating hormone in ovarian maturation in the red swamp crayfish *Procambarus clarkii*. J. Exp. Biol. 198, 1253–1257.

Siegert, K.J., Speakman, J.R., Reynolds, S.E., 1993. Carbohydrate and lipid metabolism during the last larval moult of the tobacco hornworm, *Manduca sexta*. Physiol. Entomol. 18, 404–408.

Smith, G., Naylor, E., 1972. The neurosecretory system of the eyestalk of *Carcinus maenas* (Crustacea: Decapoda). J. Zool. 166, 313–321.

Tantulo, U., Fotedar, R., 2007. Osmo and ionic regulation of black tiger prawn (*Penaeus monodon* Fabricius 1798) juveniles exposed to $K^+$ deficient inland saline water at different salinities. Comp. Biochem. Physiol. A Mol. Integr. Physiol. 146, 208–214.

Wang, W.-N., Wang, A.-L., Wang, D.-M., Wang, L.-P., Liu, Y., Sun, R.-Y., 2003. Calcium, phosphorus and adenylate levels and $Na^+$–$K^+$-ATPase activities of prawn, *Macrobrachium nipponense*, during the moult cycle. Comp. Biochem. Physiol. A Mol. Integr. Physiol. 134, 297–305.

Wilder, M.N., Ikuta, K., Atmomarsono, M., Hatta, T., Komuro, K., 1998. Changes in osmotic and ionic concentrations in the hemolymph of *Macrobrachium rosenbergii* exposed to varying salinities and correlation to ionic and crystalline composition of the cuticle. Comp. Biochem. Physiol. A Mol. Integr. Physiol. 119, 941–950.

Wilder, M.N., Do Thi Thanh, H., Jasmani, S., Jayasankar, V., Kaneko, T., Aida, K., Hatta, T., Nemoto, S., Wigginton, A., 2009. Hemolymph osmolality, ion concentrations and calcium in the structural organization of the cuticle of the giant freshwater prawn *Macrobrachium rosenbergii*: changes with the molt cycle. Aquaculture 292, 104–110.

Zralá, J., Kodrík, D., Zahradníčková, H., Zemek, R., Socha, R., 2010. A novel function of red pigment-concentrating hormone in crustaceans: *Porcellio scaber* (Isopoda) as a model species. Gen. Comp. Endocrinol. 166, 330–336.

# 6. A novel gonad-specific Argonaute 4 serves as a defense against transposons in the black tiger shrimp *Penaeus monodon*.

Fish & Shellfish Immunology 42 (2015) 280–288

Contents lists available at ScienceDirect

Fish & Shellfish Immunology

journal homepage: www.elsevier.com/locate/fsi

Full length article

# A novel gonad-specific Argonaute 4 serves as a defense against transposons in the black tiger shrimp *Penaeus monodon*

Wantana Leebonoi [a], Suchitraporn Sukthaworn [a], Sakol Panyim [a, b], Apinunt Udomkit [a, *]

[a] Institute of Molecular Biosciences, Mahidol University, Salaya Campus, Nakhon Pathom, 73170, Thailand
[b] Department of Biochemistry, Faculty of Sciences, Mahidol University, Rama VI Road, Phayathai, Bangkok, 10400, Thailand

ARTICLE INFO

*Article history:*
Received 9 September 2014
Received in revised form
5 November 2014
Accepted 12 November 2014
Available online 20 November 2014

*Keywords:*
Argonaute
Shrimp
Germline
Transposons
YHV

ABSTRACT

Argonaute is a key protein of the small-RNA guided gene regulation process. The Argonaute family is generally divided into two subfamilies; AGO and PIWI. In this study, a cDNA encoding a novel type of Argonaute (PmAgo4) in the black tiger shrimp *Penaeus monodon* was identified and characterized. *PmAgo4* cDNA contained an open reading frame of 2433 nucleotides that can be translated into a deduced amino acid with the conserved PAZ and PIWI domains. PmAgo4 was phylogenetically clustered with the AGO subfamily while exhibited a gonad-specific expression pattern similar to that of proteins in the PIWI subfamily. The expression of *PmAgo4* did not change significantly in response to either double-stranded RNA or yellow head virus injection suggesting that PmAgo4 may not be the main AGO proteins that play a role in dsRNA-mediated gene silencing or antiviral defense. Interestingly, PmAgo4 appeared to participate in the control of transposons since the activation of both DNA transposon and retro-transposon was detected in the testis of *PmAgo4*-knockdown shrimp. Our study thus provided the first evidence for an unusual type of the AGO proteins that was predominantly expressed in shrimp gonad and implication of its role in protecting the shrimp genome against an invasion of transposons.


## 1. Introduction

Argonaute is a family of proteins that play central roles in small RNA-mediated gene silencing pathways. Argonaute proteins are evolutionally conserved among a wide range of organisms; from archaea and some bacteria to higher eukaryotes. Argonautes bind diverse types of small non-coding RNAs such as small-interfering RNA (siRNA), microRNA (miRNA) and piwi-interacting RNA (piRNA), and assemble into an RNA-induced silencing complex (RISC), a nucleoprotein complex that is a key mediator in RNA interference (RNAi) mechanism [1]. Argonaute proteins generally share two principal domains: PAZ and PIWI. The PAZ domain forms a specific fold that anchors two nucleotides 3'overhang of the small RNA duplex [2,3]. The PIWI domain possesses a catalytic triad Asp-Asp-His (DDH) responsible for endonucleolytic activity [4,5]. Two additional domains have also been identified; the N-domain participates in duplex unwinding of small RNAs during RISC assembly [6], and the MID domain helps anchor small RNA to Argonaute proteins [7,8].

The Argonaute family is generally categorized into AGO and PIWI proteins [9]. Members of the AGO subfamily associate with either siRNA or miRNA to mediate repression of specific gene target at transcriptional and post-transcriptional levels [10–12], whereas binding of piRNA to proteins of the PIWI sub-family is required for germ-cell maintenance, transposon repression in the germ line and spermatogenesis [13–15]. A third type of Argonaute proteins, worm-specific Argonaute (WAGO), is found only in the nematodes and act consecutively in RNAi to mediate several cellular processes [16]. Expression patterns of the AGO and PIWI in several organisms are in agreement with their established functions; AGO proteins are ubiquitously expressed while PIWI proteins are usually expressed exclusively in the germ line [9,17,18].

Numbers of Argonaute proteins vary greatly among species, ranging from a single Argonaute in *Schizosaccharomyces pombe* to as many as 27 family members in *Caenorhabditis elegans* [9]. In the black tiger shrimp *Penaeus monodon*, only members of the AGO subfamily was identified so far. *PemAgo1* was expressed in all shrimp tissues examined, and it was shown to be required for effective RNAi pathway in both the primary culture of lymphoid cells and in the animal [19,20]. In addition, the other isoform of Argonaute 1 in *P. monodon* (PmAgo1) was reported to respond to yellow head virus infection [21]. Recently, another two AGO

* Corresponding author. Tel.: +66 2 441 9003x1236; fax: +66 2 441 9906.
*E-mail address:* apinunt.udo@mahidol.ac.th (A. Udomkit).

http://dx.doi.org/10.1016/j.fsi.2014.11.014
1050-4648/

proteins were reported in *P. monodon*. The expression of *PmAgo2* was responsive to both dsRNA and ssRNA, and was activated by bacterial and viral infection [22]. PmAgo3 was shown to be involved in dsRNA-mediated gene silencing and probably play a role in yellow head virus replication in the shrimp [23]. Members of ubiquitously expressed Ago proteins were also identified in other shrimps, where their contribution to antiviral immunity was demonstrated [24,25]. In this study, we report the identification of a cDNA encoding a novel type of Argonaute in *P. monodon* (PmAgo4) that was specifically expressed in shrimp gonad. Possible involvement of PmAgo4 in different processes that are known to be regulated by Argonaute proteins was investigated.

## 2. Materials and methods

### 2.1. Animals and sample collection

Adult male and female *P. monodon* were kindly provided by Shrimp Genetic Improvement Center, Surat Thani, Thailand. Shrimp were anesthetized on ice prior to tissue dissection.

Ovarian maturation stage of *P. monodon* was defined by the presence of different types of developing oocytes as could be visualized by histochemical staining according to Ayub and Ahmed, 2002 [26] with some modifications. The progress of spermatogenesis was revealed by different categories of germ cells: spermatogonia, spermatocytes and spermatids in the seminiferous tubules.

### 2.2. Cloning of PmAgo4 cDNA from shrimp testis

A cDNA clone (TT-N-S01-0260-W) harboring partial sequence of *PmAgo4* was previously identified by BlastX homology search of the testis EST library of *P. monodon* (http://pmonodon.biotec.or.th). Total RNA extracted by Tri Reagent® (Molecular Research Center) from *P. monodon* testis was used for cloning of *PmAgo4* cDNA in this study. First strand cDNA synthesis was primed with oligo(dT) primer using Improm-II™ Reverse-Transcriptase (Promega) following the manufacturer's protocol. One microliter of the first strand cDNA was subjected to 3′ Rapid Amplification of cDNA Ends (RACE) in order to obtain the 3′ sequence of *PmAgo4* cDNA in a reaction containing 2 mM $MgCl_2$, 200 μM each dNTPs, 200 nM of PM1 primer and 3′RACE Ago4 primer designed from the nucleotide sequence of TT-N-S01-0260-W clone, 1× buffer and 1.25 unit of Taq DNA polymerase (Promega, USA). The reaction was initially denatured at 94 °C for 3 min, followed by a temperature cycle of 94 °C for 30 s, 55 °C for 30 s and 72 °C for 1 min for 35 cycles and a final extension at 72 °C for 7 min.

The complete 5′ cDNA fragment was obtained by 5′RACE-core strategy following the 5′-Full Race Core set (Takara Bio Inc.) protocol. Briefly, the first strand cDNA was synthesized using a 5′ end-phosphorylated RT-P primer followed by RNaseH digestion of the RNA template. Then the first strand cDNA was circularlized by an RNA ligase, and amplified with A2 primer and S2 primers using 2.5 units of TaKaRa LA Taq™. The entire coding sequence of *PmAgo4* was verified by amplification with primers Ago4-str and Ago4-stp. The schematic diagram of *PmAgo4* cDNA cloning strategy was shown in Fig. 1, and the nucleotide sequences of primers were shown in Table 1. The amplified cDNA fragments were cloned into pGEM T-Easy vector (Promega) and their nucleotide sequences were determined by automated DNA sequencing.

### 2.3. Tissue distribution of PmAgo4 expression

*PmAgo4* mRNA expression was detected in different tissues of adult male and female shrimp by RT-PCR with PIWI4–F and PIWI4-R primers using the following temperature profile: 94 °C for 3 min, 25 cycles of 94 °C for 30 s, 52 °C for 30 s, 72 °C for 1 min followed by 72 °C for 7 min. *Actin* transcript was amplified as an internal control with actin specific primers (Table 1).

### 2.4. Detection of PmAgo4 transcript by reverse transcription real-time PCR

*PmAgo4* transcript levels in shrimp ovary were determined by quantitative RT-PCR (qRT-PCR) using KAPA SYBR® FAST qPCR Kit (KAPABIOSYSTEMS, USA) with specific primers Ago4F3 and Ago4R3. The expression levels of *PmAgo4* were normalized to that of *EF1-α*. The expression of *PmAgo4* in shrimp male reproductive system was determined by RT-PCR as described in 2.3.

### 2.5. Affinity purification of anti-PmAgo4 PAZ polyclonal antibody

The purified recombinant PmAgo4PAZ was separated on 15% acrylamide gel and blotted onto a PVDF membrane. The membrane was stained with coomassie blue R-250, then the target band on membrane was cut into small pieces. These pieces of membrane were blocked in 5% skim milk in PBS buffer for 30 min and washed with PBS buffer for 2 min twice. The blocked membrane was incubated in 10 ml of rabbit serum containing an anti-PmAgo4PAZ polyclonal antibody (raised at Biomedical Technology Research Unit, Faculty of Associated Medical Sciences, Chiangmai University) at 4 °C overnight. After that the membrane was washed for10 min with PBS-Tween 20 and PBS for three times, 10 min each. The bound antibodies were eluted from the membrane with 1 ml of 0.1 M glycine pH 2.7. The eluted antibody was neutralized by mixing with 50 μl of 1M Tris pH 8.0 and stored at −30 °C until use.

### 2.6. Immunohistochemical detection

Shrimp ovary at each maturation stage and shrimp testis were dissected and fixed in Davidson's fixative for 24 h prior to embedding and sliced into 5 μm-sections. The paraffin sections were mounted onto HistoGrip™ (Invitrogen, USA) coated slides at 37 °C overnight. The tissue slides were then dewaxed in xylene followed by rehydration in a series of decreasing percentages of ethanol solution. The endogenous peroxidase activity was blocked with 1–3% hydrogen peroxide in 70% ethanol and washed in PBS before submerged in blocking solution (10% normal goat serum in PBS) for 1 h at room temperature. The affinity-purified anti-PmAgo4 PAZ pAb (1:5) (Supplementary data 1) were added and further incubated overnight at 4 °C. After washing in 0.4% Triton-X 100 in PBS, the sections were incubated in1:500 dilution of horseradish peroxidase-conjugated goat anti-rabbit IgG. The signal was developed with 3,3′-Diaminobenzidine (DAB) substrate, washed in PBS and counter-stained in Mayer's hematoxylin before examined and photographed under light microscope.

### 2.7. Analysis of PmAgo4 expression

Changes in *PmAgo4* expression upon double-stranded RNA (dsRNA) or viral injection were determined by injecting the shrimp (approximately 25 g in size) intramuscularly with either GFP-dsRNA at 2.5 μg/g body weight of shrimp or $10^{-2}$ dilution of yellow head virus (YHV) stock. Five individual shrimp from each group were randomly sampled at 0, 6, 9, 12, 24, 36, 48 and 72 h post-injection for determination of *PmAgo4* mRNA expression by qRT-PCR and normalized by that of *EF1-α* as described in 2.4.

**A**

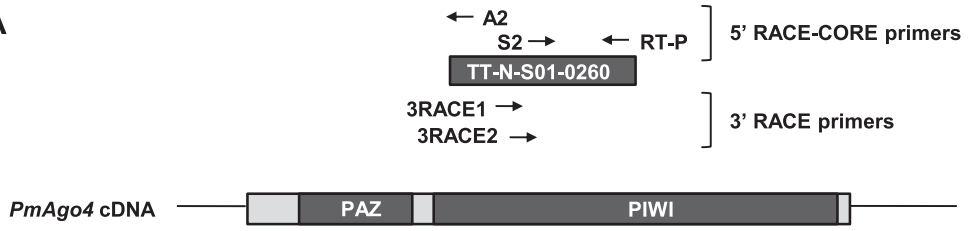


**B**

```
  ctcgcggctgctgcggacgctcctggcgctgcgcagtcgtgcggacgacactcccctggcgctgcgcagtcgtgcggtc :79
actccctcctcgcggcggcggcgctgcagttcgaagttgtgaacctctccgagcaaaatggacgcagcaaagggaagtcca :160
                                                        M  D  A  A  K  G  S  P
ggcctaaatcctccactacggctgccaagtggagctcggggaaaacctatccgtctcaacaccaattatttccctatcaaa :241
 G  L  N  P  P  L  R  L  P  S  G  A  R  G  K  P  I  R  L  N  T  N  Y  F  P  I  K
atgaaagctgaagtcaacctggtccagtatgaggtttctattaagcaagataccaagagcaatattaagatcggaaagaag :322
 M  K  A  E  V  N  L  V  Q  Y  E  V  S  I  K  Q  D  T  K  S  N  I  K  I  G  K  K
caaaatacgaaaatttttgagaaaatgaaggagaggaaccaagatgttttctcaaagcctgtggcatttgatggctttaag :403
 Q  N  T  K  I  F  E  K  M  K  E  R  N  Q  D  V  F  S  K  P  V  A  F  D  G  F  K
catgcctacagtgttgaagttctccctctctcttaagaagaagaaaactataacatttaaggtcatccttgagttagaggaa :484
 N  A  Y  S  V  E  V  L  P  S  L  K  K  K  K  T  I  T  F  K  V  I  L  E  L  E  E
ggtgatggcgatcctgtgtccttcactgtccagatttcccgaggcataaccaaaggacttagggaactaatggtatctctc :565
 G  D  G  D  P  V  S  F  T  V  Q  I  S  R  G  I  T  K  G  L  R  E  L  M  V  S  L
aaatgcactgatatgcataaaaatatttctttttacgatctttcggatgttggatacaatgctacgttaccatcgattgctc :646
 K  C  T  D  M  H  K  N  I  S  F  T  I  F  R  M  L  D  T  M  L  R  Y  H  R  L  L
agatacgaagcggttggaaagaaaagatatttcttattgaatagagaaatcaaccgtccaattgacattggaccagctgtg :727
 R  Y  E  A  V  G  K  K  R  Y  F  L  L  N  R  E  I  N  R  P  I  D  I  G  P  A  V
caaggagtcaccgggttcttcagtagcatgaaagccagcgctcatgaaaagggatcactcatgatcaacatagacctggct :808
 Q  G  V  T  G  F  F  S  S  M  K  A  S  A  H  E  K  G  S  L  M  I  N  I  D  L  A
cataccgttttctacaaggaacaacctttgttggatttcataaatataatgttctacatgtgggaaggaatgacctggatgca :889
 H  T  V  F  Y  K  E  Q  P  L  L  D  F  I  N  N  V  L  H  V  G  R  N  D  L  D  A
ccgctagacatcaaacttaggaagatattggaacgtgggcttgcagatttgagagttgagacgacacacatacctcgtacc :970
 P  L  D  I  K  L  R  K  I  L  E  R  G  L  A  D  L  R  V  E  T  T  H  I  P  R  T
tataggattattggtcttagtatgtatgggccagatcgccagatgtttccattgaataatagtgagagtggcaagattgaa :1051
 Y  R  I  I  G  L  S  M  Y  G  P  D  R  Q  M  F  P  L  N  N  S  E  S  G  K  I  E
caacgcactgttcaagattatttcgagaaggagtataaaaaaaacaatcaaatacgctagactcatctgtatacaggcatat :1132
 Q  R  T  V  Q  D  Y  F  E  K  E  Y  K  K  T  I  K  Y  P  R  L  I  C  I  Q  A  Y
cctaaggaaaaaaacatctatctaccattagagtattgtgtcgtcgcacgtggccagcgttcatttggaaacctcagcaac :1213
 P  K  E  K  N  I  Y  L  P  L  E  Y  C  V  V  A  R  G  Q  R  S  F  G  N  L  S  N
agtgaagctggaaaattcatccgctcgtccgcaattccaccgggaaagcgtcttgaacaaattaaaaacatttacaatgac :1294
 S  E  A  G  K  F  I  R  S  S  A  I  P  P  G  K  R  L  E  Q  I  K  N  I  Y  N  D
aataagtttgcaaatcatgagatgattgccagcctacagttagatgtggcaaaatctccttttaccgttaccgggcgtgtt :1375
 N  K  F  A  N  H  E  M  I  A  S  L  Q  L  D  V  A  K  S  P  F  T  V  T  G  R  V
ttatcgccgcctaaactgatgatggatcaagaagtgcagcctaaaaggggaggatggggcactcgtgacgagaagttttat :1456
 L  S  P  P  K  L  M  M  D  Q  E  V  Q  P  K  R  G  G  W  G  T  R  D  E  K  F  Y
attggagcagtagtttatacgtgggctgttatagactatacccatacatggcaaggagctctagaaagatatatccgcacc :1537
 I  G  A  V  V  Y  T  W  A  V  I  D  Y  T  H  T  W  Q  G  A  L  E  R  Y  I  R  T
ctacgctctctcggagatcgaaaaggcatggtctttaaatcaccggtcagtgtgacgaaagggattagaaagaatgtgaca :1618
 L  R  S  L  G  D  R  K  G  M  V  F  K  S  P  V  S  V  T  K  G  I  R  K  N  V  T
caacagtttcagaatctgaagaaaaaatttcctgaaattcagatgattcttgtagtgctggaagaggcagattcactatat :1699
 Q  Q  F  Q  N  L  K  K  K  F  P  E  I  Q  M  I  L  V  V  L  E  E  A  D  S  L  Y
tcccgcattaaaaccgtgggagacttagagatcagtgtcattacccagtgtgtgaagaagaggtgtatggaagaatgcaga :1780
 S  R  I  K  T  V  G  D  L  E  I  S  V  I  T  Q  C  V  K  K  R  C  M  E  E  C  R
ttcataactattggcaacctactcgtgaagataaacgcgaagatgggggggcatcaactctgtctggagtcgcagtccaaaa :1861
 F  I  T  I  G  N  L  L  V  K  I  N  A  K  M  G  G  I  N  S  V  W  S  R  S  P  K
ctgatgaaacgaagtctgatggtaatgggtgctgatgtcaatcacccatcggctggggatgccagaacaccctccatggca :1942
 L  M  K  R  S  L  M  V  M  G  A  D  V  N  H  P  S  A  G  D  A  R  T  P  S  M  A
gctatagttgcttccattgataacaattttagtaaatacgccgttgaagtaaggcctcagaaacatcgaaacgagataata :2023
 A  I  V  A  S  I  D  N  N  F  S  K  Y  A  V  E  V  R  P  Q  K  H  R  N  E  I  I
caagacgtcaaggaaatgacgaagaaccttctgaaatcgttctccattgcaaacaactctaaaccacaacgcatcatcgtt :2104
 Q  D  V  K  E  M  T  K  N  L  L  K  S  F  S  I  A  N  N  S  K  P  Q  R  I  I  V
tatcgagacggtgtaagtgacgttcagttccatcaggttctacaacacgagtttctagcgattcgtgaagcatgcaaagag :2185
 Y  R  D  G  V  S  D  V  Q  F  H  Q  V  L  Q  H  E  F  L  A  I  R  E  A  C  K  E
ctagaggaaacgtacaaacctgcaattacttttcttttggtgatgaaacgtcaccacacaagatttttcaagtagatgaa :2266
 L  E  E  T  Y  K  P  A  I  T  F  L  L  V  M  K  R  H  H  T  R  F  F  Q  V  D  E
gtagggaagaatattccaccaggcactgttgttgactcaggaattacacatcccattgagagagatttctacctgtgttcc :2347
 V  G  K  N  I  P  P  G  T  V  V  D  S  G  I  T  H  P  I  E  R  D  F  Y  L  C  S
catcaaggaatccaaggcacaagcaggccagcccattaccatgtcctgtgggatgataataatctgaccatggatcagttg :2428
 H  Q  G  I  Q  G  T  S  R  P  A  H  Y  H  V  L  W  D  D  N  N  L  T  M  D  Q  L
caagaatttacttataacatgtgccatgtgtactcaagatgtagcaagtctgtgtctttgcctgcaccagttgcgtatgca :2509
 Q  E  F  T  Y  N  M  C  H  V  Y  S  R  C  S  K  S  V  S  L  P  A  P  V  A  Y  A
catttagcagcttttcgggccaaggttcatgctatggaggtaaatatacaagagagttaactgaagcacatcaagatgatt :2590
 H  L  A  A  F  R  A  K  V  H  A  M  E  V  N  I  Q  E  S  *
agagagaaggaaatatccaataaacttattacatatagaatgttatttattgacttttattaattttatatttttta :2671
agatgactttaaggaggataccttttcaatgattcatgaaggatttcaagcaaaataaaaggatttgcagttttgttttt :2752
ggaaaatactcatcttacacttttaaaggaacaaattgtctattaaggaatatacagtatgtgcagatatgagaaactcgt :2833
gataggtttatatgattgatatttttccctcttctatgactgttttgtaatattagtgatttgaaaaattatggaaatata :2914
atggaaacatg                                                                       :2925
```

**Table 1**
Primers used in this study and their nucleotide sequences.

| Primers | Sequence (5′ to 3′) | Experiment |
|---|---|---|
| oligo(dT) | CCGGAATTCAAGCTTCTAGAGGATCCTTTTTTTTTTTTTTTT | Cloning of *PmAgo4* cDNA from shrimp testis |
| PM1 | CCGGAATTCAAGCTTCTAGAGGATCC | |
| 3′RACE Ago4-1 | ATCACC GGTCAGTGTGACGAAA | |
| 5′ end-phosphorylated RT-P | (P)-GCCGATGGGTGATTG | |
| A2 | CCCACGTATAAACTACTGC | |
| S2 | TTAAAACCGTGGGAGACTTA | |
| Ago4-str | ATGGACGCAGCAAAGGGAAG | |
| Ago4-stp | TTAACTCTCTTGTAT ATTTACCTCCATA | |
| PIWI4–F | ATGATTCTTGTAGTGCTGGA | Tissue distribution of P*mAgo4* expression |
| PIWI4-R | AACCTTGGCCCGAAAAGCT | |
| ActinF | GACTCGTACGTGGGCGACGAG | |
| ActinR | AGCAGCGGTGGTCATCTCCTGCTC | |
| Ago4F3 | TGCCAGCCTACAGTTAGATGTG | Detection of P*mAgo4* transcript by RT-realtime PCR |
| Ago4R3 | TTTCTAGAGCTCCTTGCCATGTA | |
| EF1αF | GAACTGCTGACCAAGATCGACAGG | |
| EF1αR | GAGCATACTGTTGGAGGTCTCCA | |
| MarinerF | CGGTTGGGAGAATAGGCAAATCA | Determination of the effect of *PmAgo4* knockdown on transposon expression |
| MarinerR | CCTTACAAACTGACGTTGATGGC | |
| GyPemo1bF | CTACAGCACCAACAACGTCCAA | |
| GyPemo1bR | CGTTTCCTCAAGCTGTATGAGGTG | |
| GyPemo2F | GATGCCTCAAACCTCGGGCT | |
| GyPemo2R | AACCTTGGCCCGAAAAGCT | |
| ActinF | GACTCGTACGTGGGCGACGAG | |
| ActinR | AGCAGCGGTGGTCATCTCCTGCTC | |

### 2.8. Double-strand RNA production

Double-stranded RNA targeting the PAZ coding sequence of PmAgo4 was produced as a stem-loop precursor in *Escherichia coli* expression system. The expression of the stem-loop precursor was carried out by 0.4 mM IPTG induction for 2 h, and the dsRNA was extracted by 75% EtOH according to Posiri et al., 2013 [27] before dissolving in 150 mM NaCl for further use.

### 2.9. Determination of the effect of PmAgo4 knockdown on transposon expression

To knockdown *PmAgo4* expression, juvenile shrimp (approximately 20 g) were injected with 50 μg of PmAgo4-PAZ-dsRNA. On day 14 after injection, the expression of *PmAgo4* in shrimp testis was determined by semi-quantitative RT-PCR as described in 2.3 compared with that in the control shrimp injected with 150 mM NaCl. The expression of two *P. monodon*'s gypsy elements (GyPemo1; Accession no. HF548819.1 and GyPemo2; Accession no. HF548820.1) and mariner-like sequence in the testis of the control and the *PmAgo4*-knockdown shrimp was determined by qRT-PCR with specific primers as shown in Table 1. The relative expression data was analyzed by $2^{-\Delta\Delta C}{}_{T}$ method [28], and statistical significance of values was determined by Kruskal–Wallis test followed by Mann–Whitney *U* test.

## 3. Results

### 3.1. Cloning and characterization of PmAgo4 cDNA

Two cDNA fragments were obtained from *P. monodon* testis mRNA using 3′RACE and 5′ RACE-core strategies with specific primers designed from the nucleotide sequence of the EST clone TT-N-S01-0260-W (Fig. 1A). A combined sequence of these three overlapping fragments comprised a 2925 *PmAgo4* cDNA (GenBank accession no. KF911324) containing 136 nt of a 5′UTR, a single open reading frame (ORF) of 2433 nt followed by a 3′ UTR of 356 nt (Fig. 1B). A cDNA fragment harboring the entire *PmAgo4* ORF was subsequently obtained by RT-PCR. Two signature domains of the Argonaute family; PAZ and PIWI domains were identified via http://www.ncbi.nlm.nih.gov/Structure/cdd/wrpsb.cgi [29] (Marchler-Bauer and Bryant 2004). A phylogenetic tree constructed from amino acid sequences of Argonaute proteins clearly indicated the separation of AGO and PIWI subfamilies. Within the AGO subfamily, while diverged from shrimp Ago1, PmAgo4 was placed on a separate branch in the same cluster as shrimp Ago2 and Ago3 (Fig. 2) indicating that PmAgo4 is a new member of shrimp Ago subfamily identified so far.

### 3.2. Expression of PmAgo4 in shrimp tissues

Expression of *PmAgo4* determined by RT-PCR in several tissues of male and female *P. monodon* showed that *PmAgo4* was restrictedly expressed in the gonad i.e. testis and ovary, whereas the expression of *PmAgo4* in other tissues examined was unnoticeable (Fig. 3A).

### 3.3. Expression profile of PmAgo4 during gonad maturation

The expression of *PmAgo4* that was confined to shrimp testis and ovary may suggest its function in germ cell development. Therefore, the expression levels of *PmAgo4* during gonad maturation of both male and female shrimp were determined. Our results showed that the normalized expression of *PmAgo4* in the ovary was similar in all stages of ovarian development (Fig. 3B). In male shrimp, *PmAgo4* mRNA was highly expressed in the testis whereas significantly less expression was detected in vas deferens and spermatophore (Fig. 3C).

**Fig. 1.** (A) a schematic diagram showing primers used for cloning of *PmAgo4* cDNA. Specific primers were designed from the nucleotide sequence of EST clone TT-N-S01-0260-W harboring partial *PmAgo4* cDNA sequence. The diagram at the bottom part represents the structure of *PmAgo4* cDNA. (B) Nucleotide sequence and deduced amino acids (shown in one letter symbol under corresponding codons) of PmAgo4. The N-domain is underlined, and the PAZ and PIWI domains are highlighted in light and dark gray, respectively. The asterisk marks the stop codon. Numbers on the right show coordinates of nucleotides in each line.

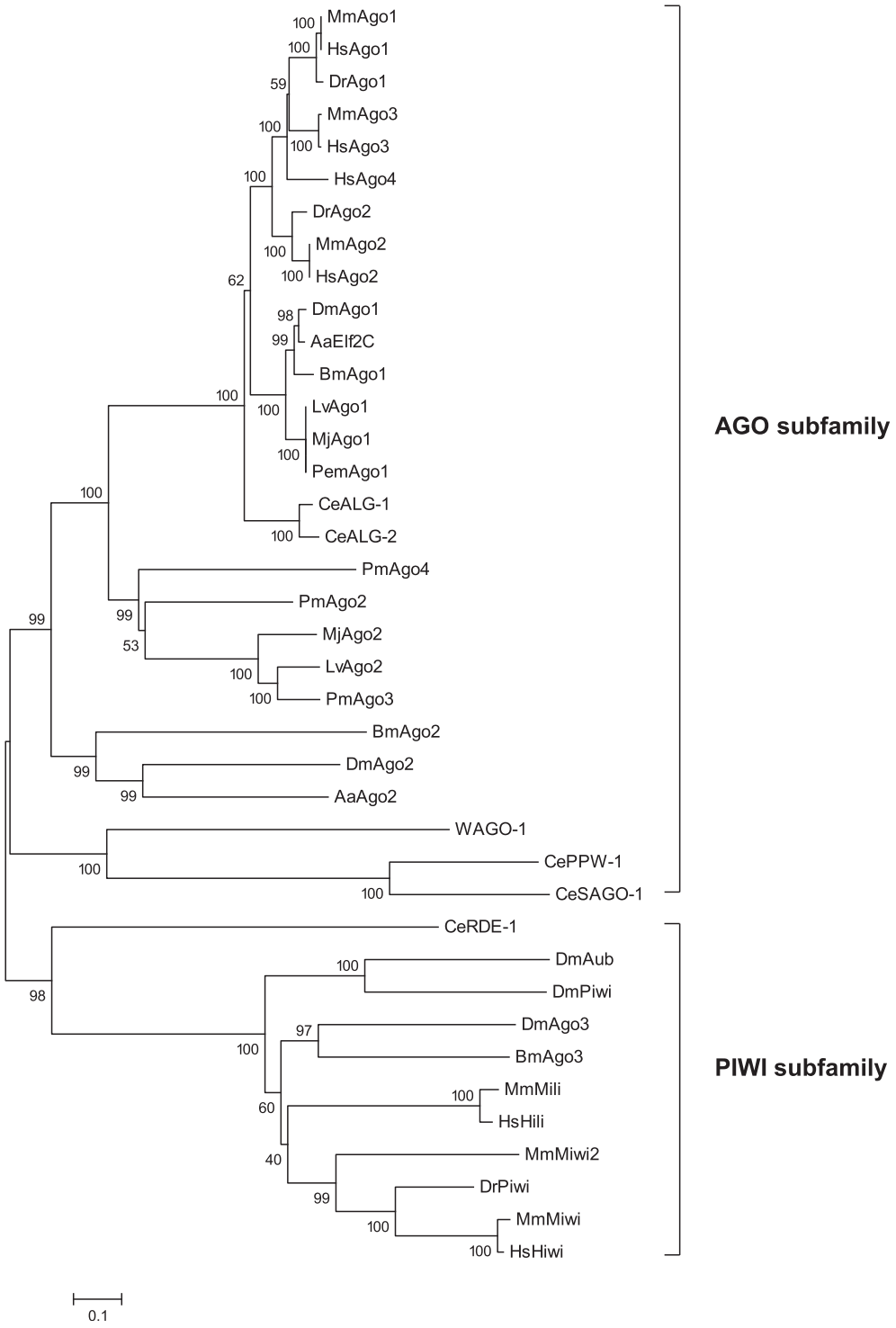


**Fig. 2.** Phylogenetic relationship of PmAgo4 and Argonaute proteins. The tree was constructed by MEGA 5.1 program with a neighbor-joining algorithm. Bootstrap values from 1000 reiterations are indicated. AaElf2C, *Aedes aegypti* eukaryotic translation initiation factor 2c (XP_001662554.1); AaAgo2, *Aedes aegypti* Argonaute 2 (ACR56327.1); BmAgo1, *Bombyx mori* Argonaute 1 (BAF73719.1); BmAgo2, *Bombyx mori* Argonaute 2 (BAD91160.2); BmAgo3, *Bombyx mori* Argonaute 3 (BAF73717.2); CeALG-1, *Caenorhabditis elegans* ALG-1 (CAA93496.2); CeALG-2, *Caenorhabditis elegans* ALG-2 (CCD73271.1); CeRDE-1, *Caenorhabditis elegans* RDE-1 (CAB05546.2); CePPW-1, *Caenorhabditis elegans* PPW-1 (CCD65142.1); CeWAGO-1, *Caenorhabditis elegans* WAGO-1 (CAA95839.1); CeSAGO-1, *Caenorhabditis elegans* SAGO-1 (CCD70367.1); DmAgo1, *Drosophila melanogaster* Argonaute 1 (AAF58314.1); DmAgo2, *Drosophila melanogaster* Argonaute 2 (AAF49620.2); DmAgo3, *Drosophila melanogaster* Argonaute 3 (ABO27430.1); DmAub, *Drosophila melanogaster* Aubergine (AAF53046.1); DmPiwi, *Drosophila melanogaster* Piwi (AAF53043.1); DrAgo1, *Danio rerio* Argonaute 1 (AFU66007.1); DrAgo2, *Danio rerio* Argonaute 2 (AFU66008.1); DrPiwi, *Danio rerio* Piwi-like protein (NP_899181.1); HsAgo1, *Homo sapiens* Argonaute 1 (NP_036331.1); HsAgo2, *Homo sapiens* Argonaute 2 (NP_036286.2); HsAgo3, *Homo sapiens* Argonaute 3 (NP_079128.2); HsAgo4, *Homo sapiens* Argonaute 4 (NP_060099.2); HsHiwi, *Homo sapiens* HIWI (AAC97371.2); HsHili, *Homo sapiens* HILI (Argonaute 2 (BAM37459.1); MmAgo1, *Mus musculus* Argonaute 1 (NP_700452.2); MmAgo2, *Mus musculus* Argonaute 2 (NP_694818.3); MmAgo3, *Mus musculus* Argonaute 3 (NP_700451.2); MmMili, *Mus musculus* Mili (BAA93706.1); MmMiwi, *Mus munsculus* Miwi (AAL31014.1); MmMiwi2, *Mus musculus* Miwi2 (AAN75583.1); PemAgo1, *Penaeus monodon* Argonaute 1 (ABG66640.1); PmAgo2, *Penaeus monodon* Argonaute 2 (AHB63227.1); PmAgo3, *Penaeus monodon* Argonaute 3 (AGC95229.1).

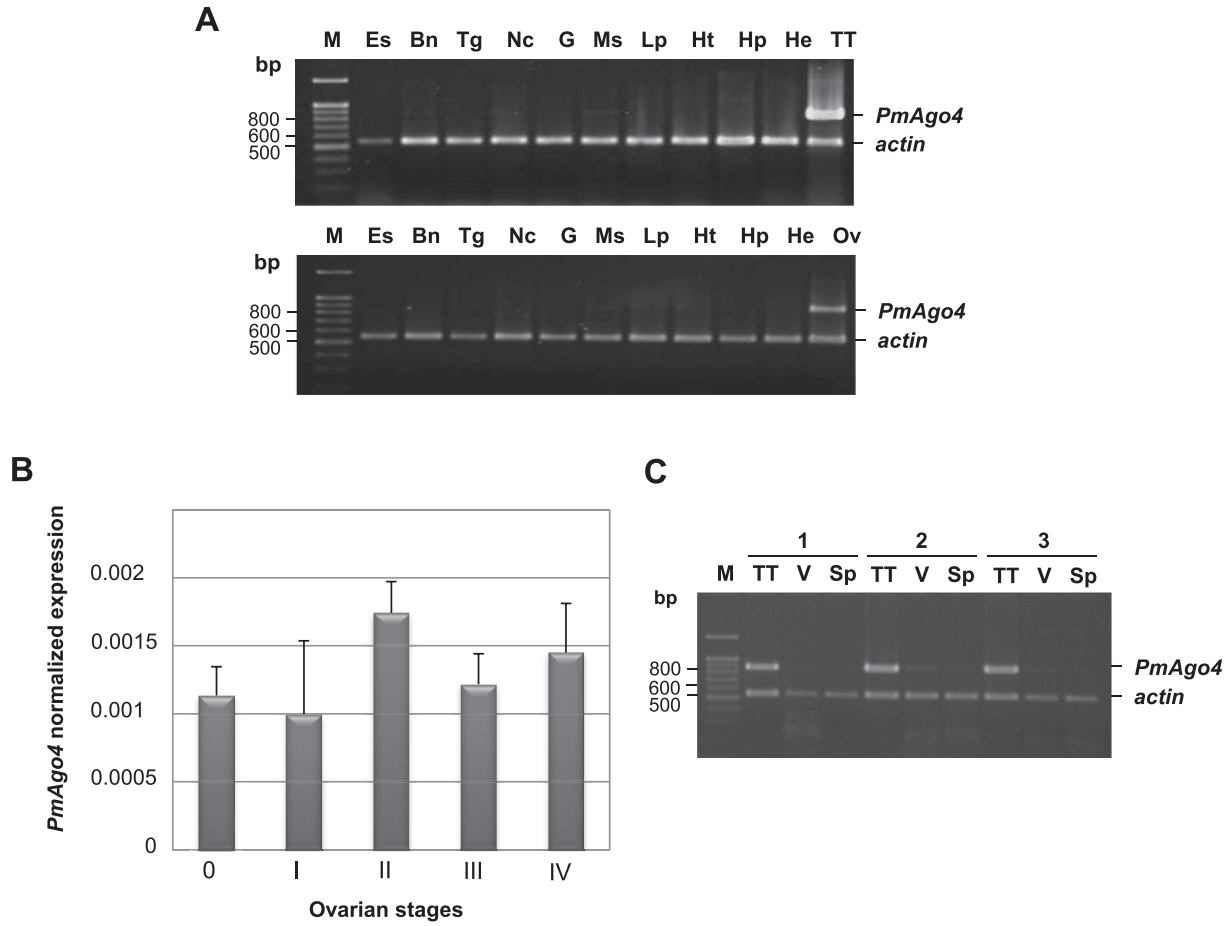


**Fig. 3.** Expression of *PmAgo4* in shrimp tissues. (A) RT-PCR was performed to detect *PmAgo4* expression in several tissues of male (upper panel) and female (lower panel) *P. monodon*. M, 100-bp DNA ladder; Es, eyestalk; Bn, brain; Tg, thoracic ganglia; Nc, abdominal nerve cord; G, gill; Ms, muscle; Lp, lymphoid organ; Ht, heart; Hp, hepatopancreas; He, hemolymph; TT, testis; Ov, ovary. The *Actin* transcript was amplified as an internal control. (B) Expression level of *PmAgo4* normalized with that of *EF1-α* in the ovary at different developmental stages was determined by qRT-PCR. (C) Expression level of *PmAgo4* and *actin* in different parts of male reproductive system: TT, testis; V, vas deferens; Sp, spermatophore as detected by RT-PCR. The numbers 1, 2 and 3 refer to different shrimp.

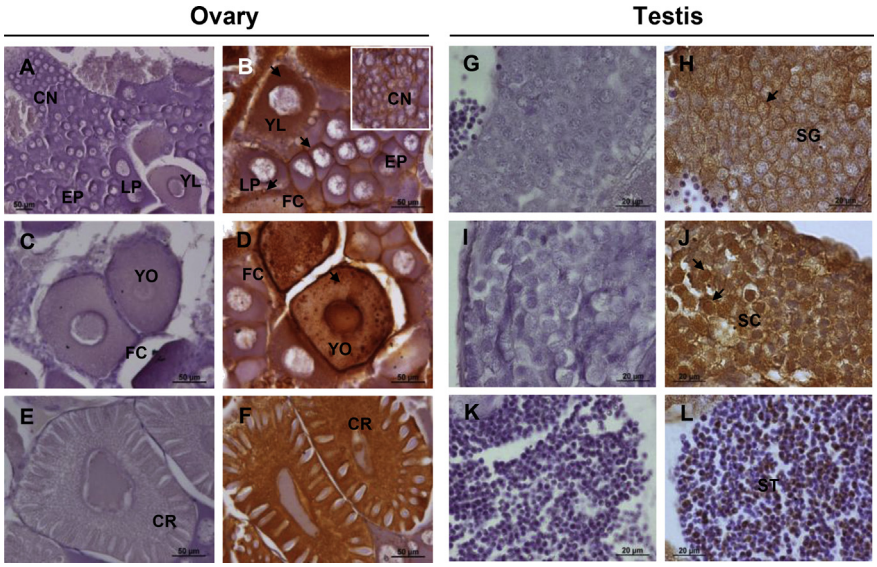


**Fig. 4.** Localization of *PmAgo4* in the ovary (A–F) and testis (G–L) of *P. monodon*. Positive signal of PmAgo4 (arrows) was detected by immunohistochemical staining with affinity-purified anti-PmAgo4 PAZ antibody in the germ cells undergoing oogenesis and spermatogenesis in shrimp ovary and testis, respectively. Negative staining in the absence of affinity-purified PmAgo4 PAZ antibody (A, C, E, G, I, K) was included. FC, follicular cells; CN, chromatin nucleolar oocytes; EP, early perinucleolar oocytes; LP, late perinucleolar oocytes; YL,yolkless oocytes; YO, yolky oocytes; CR, cortical rod oocytes; SG, spermatogonia; SC, spermatocytes; ST, spermatid.

### 3.4. Localization of PmAgo4 in shrimp testis and ovary

In order to further investigate the correlation between PmAgo4 and gonad maturation in *P. monodon*, immunohistochemical staining with the affinity-purified anti-PmAgo4 PAZ pAb was employed to visualize and to localize PmAgo4 protein in oocytes and spermatocytes at different stages of maturation.

The specificity of the affinity-purified PmAgo4 PAZ pAb was demonstrated by western blot analysis (Fig. S1). Immunohistochemical staining revealed PmAgo4-positive signal in the peripheral cytoplasm of chromatin nucleolar oocytes. (Fig. 4B; in set). Perinucleolar oocytes were stained with PmAgo4 signal in the peripheral cytoplasm with some diffused signal in the cytoplasmic region. (Fig. 4B). The PmAgo4 signal was also detected in follicular cells surrounding some of the late perinuclolar oocytes (arrow in Fig. 4B). PmAgo4 was evenly distributed in the cytoplasmic region of the oocytes throughout the higher maturation stages (Fig. 4B, D and F).

In the male reproductive system, the signal of PmAgo4 stained the cytoplasm at the peripheral of spermatogonia (Fig. 4H), and became more pronounced in the nucleus of spermatocytes where the chromatin were rather condensed (Fig. 4J). As the sperm further developed, most of the spermatids lost PmAgo4 positive signal (Fig. 4L).

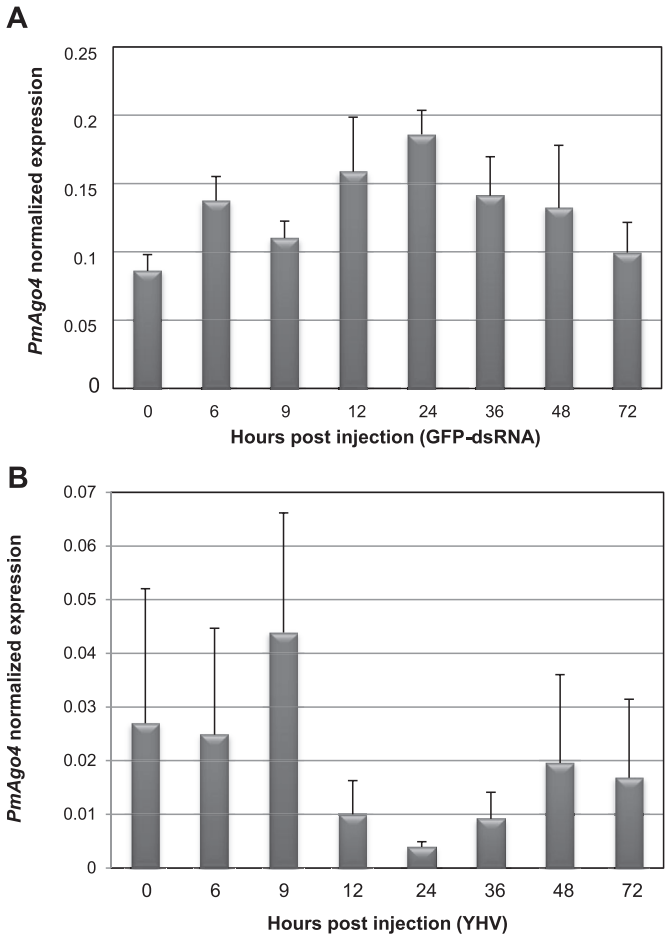


**Fig. 5.** Expression of *PmAgo4* in response to GFP-dsRNA and YHV challenge. The histograms show expression level of *PmAgo4* normalized with that of *EF1-α* in the testis of *P. monodon* at different time points after injected with either GFP-dsRNA (A) or YHV (B). Each histogram represents mean ± SEM ($n = 5$). The expression levels of *PmAgo4* at every time points are not significantly different ($p > 0.05$) as analyzed by Kruskal–Wallis test followed by Mann–Whitney *U* test.

### 3.5. Expression of PmAgo4 in response to dsRNA or YHV injection

To determine whether *PmAgo4* expression was influenced by dsRNA or YHV challenge, *PmAgo4* mRNA levels in shrimp testis at different time points post injection were measured by qRT-PCR. The detection of gp116 transcript of YHV in the shrimp at each time point after YHV injection revealed that the shrimp were actually infected (Fig. S2). The result in Fig. 5 showed that the expression levels of *PmAgo4* did not change significantly upon either GFP-dsRNA injection or YHV challenge ($p > 0.05$) at any time point during the course of experiment.

### 3.6. Knockdown of PmAgo4 derepressed transposon expression in shrimp testis

Functional analysis of PmAgo4 was performed by knocking down *PmAgo4* expression with specific dsRNA. After dsRNA injection, only the transcript level of *PmAgo4*, but not *PemAgo1* or *PmAgo3* was reduced (Fig. S3), suggesting that the dsRNA specifically knockdown only its *PmAgo4* target. The result showed that expression of *PmAgo4* in three out of six shrimp could be suppressed completely on day 14 after dsRNA injection (Fig. 6A). The expression of three transposons including two gypsy-like elements (GyPemo1 and 2) and mariner-like sequences in these *PmAgo4*-knockdown shrimp was dramatically increased when compared with the levels in the control shrimp (Fig. 6B). Interestingly, incomplete suppression of *PmAgo4* in the other three shrimp could not rescue the expression of all transposons examined.

## 4. Discussion

In shrimp, three members of AGO proteins were identified. While shrimp Ago1 is phylogenetically related to invertebrate Ago1

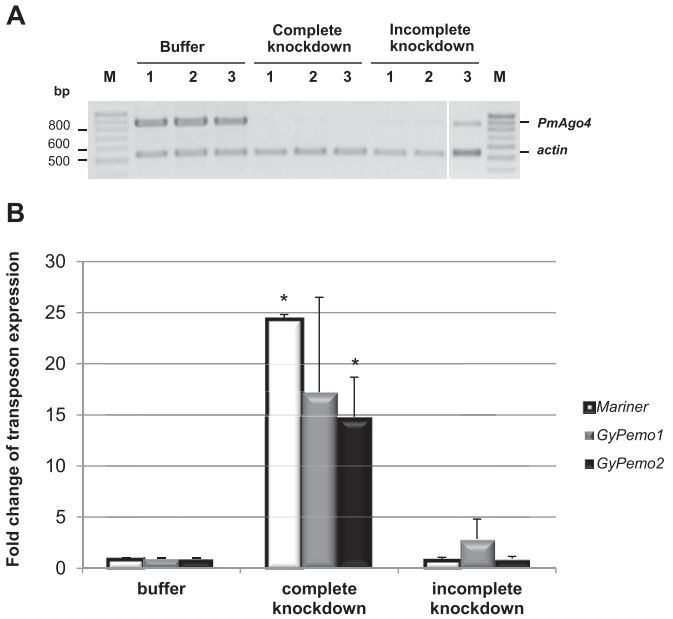


**Fig. 6.** Expression of transposons in the testis of *PmAgo4*-knockdown shrimp. (A) Suppression of *PmAgo4* expression by *PmAgo4*-dsRNA was determined by RT-PCR compared with that of *actin* in the testis of shrimp on day 14 following dsRNA injection. The shrimp injected with 150 mM NaCl (Buffer) were included as the control group. The complete and incomplete knockdown of *PmAgo4* expression was placed in separated groups. (B) Relative expression of three types of transposon (mariner, GyPemo1, GyPemo2) to that of *EF1-α* in the complete and incomplete PmAgo4-knockdown shrimp were determined by qRT-PCR. Asterisks (*) indicate significant fold changes ($p < 0.05$) in the relative expression (mean ± SEM; $n = 3$) of each transposon compared with that of the control group.

cluster, the PmAgo4 (previously called PmAgo2 in [23]) identified in the present study is located in the same cluster, but on a distinct branch from shrimp Ago2 and Ago3. Interestingly, although the primary structure of PmAgo4 placed it into the same subfamily as AGO proteins, its restrict expression only in shrimp gonad was more similar to that of the PIWI proteins. Our results thus indicate that PmAgo4 is a novel and unique member of shrimp AGO subfamily.

All the previously identified shrimp AGO proteins were either responsive to dsRNA or involved in antiviral defense [19,21–25]. A possible involvement of PmAgo4 in both dsRNA-mediated gene silencing and antiviral response was therefore investigated by determining the expression of *PmAgo4* in shrimp testis in response to dsRNA injection or yellow head virus (YHV) challenge. Non-significant change in the levels of *PmAgo4* expression following both treatments indicated that PmAgo4 may not play a vital role in gene silencing or antiviral defense through a dsRNA (in particular siRNA)-mediated pathway. However, a non-responsive expression upon YHV did not absolutely imply that PmAgo4 is not involved in shrimp immunity; a more detailed investigation is needed to demonstrate the relationship of PmAgo4 and immunological response in the shrimp. In addition, the possibility that PmAgo4 may be involved in other small RNA-related gene silencing pathways cannot be excluded unless the small RNA associated with PmAgo4 is identified.

The specific expression of *PmAgo4* in the ovary and testis of *P. monodon* suggested a possible function of PmAgo4 in germ cell development. The intense staining of PmAgo4 in the cytoplasm of developing oocytes and follicle cells was similar to that of *Drosophila* Ago1. The *ago1*-mutant flies were defective in oocyte formation and germline cell division [30]. These defects were shared by null mutants of *dcr-1*, *Drosha* and *Pasha* suggesting that Ago-1 together with its partner proteins in miRNA biogenesis pathway is required for *Drosophila* oogenesis. In the mouse, in addition to the role of Ago2 in siRNA-mediated mRNA expression [31], Ago2-deficient oocytes affected global miRNA expression and also disrupted expression pattern of several downstream genes [32]. Although the steady expression of *PmAgo4* in shrimp ovary suggested that PmAgo4 is required at all oocyte developmental stages, whether or not PmAgo4 has function in regulating gene expression during shrimp oogenesis needs further investigation.

A high mRNA expression level in shrimp testis but not in the vas deferens and spermatophores conformed to the localization of PmAgo4 in spermatogonia and spermatocytes rather than in the spermatids, and implied its potential role during spermatogenesis. In general, PIWI members represent a germ line-specific subfamily of Argonaute proteins that is essential for germ cells division and act as a key regulator in the germ line to safeguard the genome from the intruding effect of transposable elements during gametogenesis in insect and animal [33]. However, some plant AGO proteins are also exclusively expressed in the germline and function in germ cell development [34,35]. The preferential localization of PmAgo4 in the nucleus of spermatocytes suggested that PmAgo4 probably plays a role in transcriptional gene regulation process during spermatogenesis. The presence of AGO subfamily in the nucleus is not uncommon as a number of AGO proteins were found in both the cytoplasm and nucleus [36–38]. In yeast and plants, these nuclear AGOs mediate transcriptional gene silencing by facilitating chromatin modification via either RNA-directed DNA methylation or heterochromatin formation [39–43]. In addition, mammalian AGOs were demonstrated to mediate transcriptional gene silencing by targeting at the promoter [11,44]. Moreover, nuclear AGOs also associate with transcriptional machineries at the transcriptionally active loci to prevent RNA pol II-elongation complex [36,45]. Alternative nuclear functions of AGO proteins such as alternative splicing and double-strand break repair were also demonstrated as reviewed by Meister [46]. The RNAi-mediated transcription gene silencing mechanism in shrimp is still unknown; whether or not PmAgo4, a shrimp nuclear AGO is involved in this process awaits more thoroughly investigation.

One of the major functions of Argonaute proteins, especially those in the PIWI subfamily, in nuclear silencing process is to maintain genome integrity against transposable elements [47,48]. The activation of transposon expression in loss-of-function mutants of *Piwi* gene in animals suggested that PIWI proteins are essential for transposon repression [49,50]. In addition to PIWI proteins, some proteins belonging to the AGO subfamily also exhibited transposon silencing function via the RNAi process [51–53]. Our results demonstrated that the expression of both DNA transposon (marine-like element) and retrotransposon (Gypsy-like elements) were elevated in *PmAgo4*-knockdown shrimp implicating the involvement of PmAgo4 in transposon control in the shrimp. Identification of small-RNAs associated with PmAgo4 in shrimp germ cells will provide an insight into the pathway by which PmAgo4 used to direct transposon repression.

In conclusion, a novel member of AGO proteins that is exclusively expressed in shrimp germline has been identified. In addition to its possible role in spermatogenesis, silencing of PmAgo4 led to derepression of transposon in shrimp testis. Our study demonstrates for the first time the potential role of an Argonaute protein in the defense against transposons in the shrimp.

## Acknowledgments

We thank Dr. Jaruwan Poljaroen and Asst. Prof. Yotsawan Tinikul (Mahidol University) for their suggestion on immunohistochemical staining technique; Ms. Somjai Wongtripop (Shrimp Genetic Improvement Center, Thailand) for providing shrimp samples; Ms. Chawewan Chimwai and Ms. Orathai Namramoon for technical assistance. This work was supported by a grant under the program Strategic Scholarships for Frontier Research Network for the Joint Ph.D. Program Thai Doctoral degree from the Office of the Higher Education Commission; Thailand Research Fund (BRG5480018 to AU and DPG5680001 to SP); and Mahidol University Research Grant.

## Appendix A. Supplementary data

Supplementary data related to this article can be found at http://dx.doi.org/10.1016/j.fsi.2014.11.014

## References

[1] Hutvagner G, Simard MJ. Argonaute proteins: key players in RNA silencing. Nature 2008;9:22–32.
[2] Lingel A, Simon B, Lzaurralde E, Sattler M. Nucleic acid 3′-end recognition by the Argonaute2 PAZ domain. Nat Struct Mol Biol 2004;11:576–7.
[3] Song JJ, Liu J, Tolia NH, Schneiderman J, Smith SK, Martienssen RA, et al. The crystal structure of the Argonaute2 PAZ domain reveals an RNA-binding motif in RNAi effector complex. Nat Struct Biol 2003;10:1026–32.
[4] Parker JS, Roe SM, Barford D. Crystal structure of a PIWI protein suggests mechanism for siRNA recognition and slicer activity. EMBO J 2004;23:4727–37.
[5] Song JJ, Smith SK, Hannon GJ, Joshua-Tor L. Crystal structure of argonaute and its implications for RISC slicer activity. Science 2004;305:1434–7.
[6] Kwak PB, Tomari Y. The N domain of Argonaute drives duplex unwinding during RISC assembly. Nat Struct Mol Biol 2012;19:145–51.
[7] Collins RE, Cheng X. Structural domains in RNAi. FEBS Lett 2005;579:5841–9.
[8] Frank F, Sonenberg N, Nagar B. Structural basis for 5'-nucleotide base-specific recognition of guide RNA by human AGO2. Nature 2010;465:818–22.
[9] Höck J, Meister G. The Argonaute protein family. Genome Biol 2008;9:210. 1-210.8.
[10] Chen PY, Meister G. MicroRNA-guided posttranscriptional gene regulation. Biol Chem 2005;386:1205–18.

[11] Janowski BA, Huffman KE, Schwartz JC, Ram R, Nordsell R, Shames DS, et al. Involvement of AGO1 and AGO2 in mammalian transcriptional silencing. Nat Struct Mol Biol 2006;13:787–92.
[12] Hammond SM, Bernstein E, Beach D, Hannon GJ. An RNA-directed nuclease mediates post-transcriptional gene silencing in *Drosophila* cells. Nature 2000;404:293–6.
[13] Deng W, Lin H. Miwi, a murine homolog of piwi, encodes a cytoplasmic protein essential for spermatogenesis. Dev Cell 2002;2:819–30.
[14] Kalmykova AI, Klenov MS, Gvozdev VA. Argonaute protein PIWI controls mobilization of retrotransposons in the *Drosophila* male germline. Nucleic Acids Res 2005;33:2052–9.
[15] Kuramochi-Miyagawa S, Kimura T, Ijiri TW, Isobe T, Asada N, Fujita Y, et al. Mili, a mammalian member of piwi family gene, is essential for spermatogenesis. Development 2004;131:839–49.
[16] Yigit E, Batista PJ, Bei Y, Pang KM, Chen CC, Tolia NH, et al. Analysis of the *C. elegans* Argonaute family reveals that distinct Argonautes act sequentially during RNAi. Cell 2006;127:747–57.
[17] Brennecke J, Aravin AA, Stark A, Dus M, Kellis M, Sachidanandam R, et al. Discrete small RNA-generating loci as master regulators of transposon activity in *Drosophila*. Cell 2007;128:1089–103.
[18] Sasaki T, Shiohama A, Minoshima S, Shimizu N. Identification of eight members of the Argonaute family in the human genome. Genomics 2003;82:323–30.
[19] Dechklar M, Udomkit A, Panyim S. Characterization of Argonaute cDNA from *Penaeus monodon* and implication of its role in RNA interference. Biochem Biophys Res Commun 2008;367:768–74.
[20] Phetrungnapha A, Panyim S, Ongvarrasopone C. *Penaeus monodon* tudor staphylococcal nuclease preferentially interacts with N-terminal domain of Argonaute-1. Fish Shellfish Immunol 2013;34:875–84.
[21] Unajak S, Boonsaeng V, Jitrapakdee S. Isolation and characterization of cDNA encoding Argonaute, a component of RNA silencing in shrimp (*Penaeus monodon*). Comp Biochem Physiol B Biochem Mol Biol 2006;145:179–87.
[22] Yang L, Li X, Jiang S, Qiu L, Zhou F, Liu W, et al. Characterization of Argonaute2 gene from black tiger shrimp (*Penaeus monodon*) and its responses to immune challenges. Fish Shellfish Immunol 2014;36:261–9.
[23] Phetrungnapha A, Ho T, Udomkit A, Panyim S, Ongvarrasopone C. Molecular cloning and functional characterization of Argonaute-3 gene from *Penaeus monodon*. Fish Shellfish Immunol 2013;35:874–82.
[24] Labreuche Y, Veloso A, de la Vega E, Gross PS, Chapman RW, Browdy CL, et al. Non-specific activation of antiviral immunity and induction of RNA interference may engage the same pathway in the Pacific white leg shrimp *Litopenaeus vannamei*. Dev Comp Immunol 2010;34:1209–18.
[25] Huang T, Zhang X. Contribution of the Argonaute-1 isoforms to invertebrate antiviral defense. e50581 PLoS One 2012;7(11).
[26] Ayub Z, Ahmed M. A description of the ovarian development stages of penaeid shrimps from the coast of Pakistan. Aquac Res 2002;33:767–76.
[27] Posiri P, Ongvarrasopone C, Panyim S. A simple one-step method for producing dsRNA from *E. coli* to inhibit shrimp virus replication. J Virol Methods 2013;188:64–9.
[28] Pfaffl MW. A new mathematical model for relative quantification in real-time RT-PCR. e45 Nucleic Acids Res 2001;29.
[29] Marchler-Bauer A, Bryant SH. CD-search: protein domain annotations on the fly. Nucleic Acids Res 2004;32:327–31.
[30] Azzam G, Smibert P, Lai EC, Liu J-L. Drosophila Argonaute 1 and its miRNA biogenesis partners are required for oocyte formation and germline cell division. Dev Biol 2012;365:384–94.
[31] Watanabe T, Totoki Y, Toyoda A, Kaneda M, Kuramochi-Miyagawa S, Obata Y, et al. Endogenous siRNAs from naturally formed dsRNAs regulate transcripts in mouse oocytes. Nature 2008;453:539–43.
[32] Masahiro K, Tang F, O'Carroll D, Lao K, Surani MA. Essential role for Argonaute 2 protein in mouse oogenesis. Epigenetics Chromatin 2009;2:9.
[33] Aravin AA, Hannon GJ, Brennecke J. The Piwi-piRNA pathway provides an adaptive defense in the transposon arms race. Science 2007;318:761–4.
[34] Borges F, Pereira PA, Slotkin RK, Martienssen RA, Becker JD. MicroRNA activity in the *Arabidopsis* male germline. J Exp Bot 2011;62:1611–20.
[35] Nonomura K, Morohoshi A, Nakano M, Eiguchi M, Miyao A, Hirochika H, et al. A germ cell specific gene of the ARGONAUTE family is essential for the progression of premeiotic mitosis and meiosis during sporogenesis in rice. Plant Cell 2007;19:2583–94.
[36] Cernilogar FM, Onorati MC, Kothe GO, Burroughs AM, Parsi KM, Breiling A, et al. Chromatin -associated RNA interference components contribute to transcriptional regulation in *Drosophila*. Nature 2011;480:391–5.
[37] Gagnon KT, Li L, Chu Y, Janowski BA, Corey DR. RNAi factors are present and active in human cell nuclei. Cell Rep 2014;6:211–21.
[38] Wierzbicki AT, Ream TS, Haag JR, Pikaard CS. RNA polymerase V transcription guides ARGONAUTE4 to chromatin. Nat Genet 2009;41:630–4.
[39] Chan SW, Zilberman D, Xie Z, Johansen LK, Carrington JC, Jacobsen SE. RNA silencing genes control de novo DNA methylation. Science 2004;303:1336.
[40] He XJ, Hsu YF, Zhu S, Wierzbicki AT, Pontes O, Pikaard CS, et al. An effector of RNA-directed DNA methylation in *Arabidopsis* is an ARGONAUTE 4- and RNA-binding protein. Cell 2009;137:498–508.
[41] Matzke MA, Birchler JA. RNAi-mediated pathways in the nucleus. Nat Rev Genet 2005;6:24–35.
[42] Motamedi MR, Verdel A, Colmenares SU, Gerber SA, Gygi SP, Moazed D. Two RNAi complexes, RITS and RDRC, physically interact and localize to noncoding centromeric RNAs. Cell 2004;119:789–802.
[43] Verdel A, Jia S, Gerber S, Sugiyama T, Gygi S, Grewal SIS, et al. RNAi-mediated targeting of heterochromatin by the RITS complex. Science 2004;303:672–6.
[44] Kim DH, Villeneuve LM, Morris KV, Rossi JJ. Argonaute-1 directs siRNA-mediated transcriptional gene silencing in human cells. Nat Struct Mol Biol 2006;13:793–7.
[45] Guang S, Bochner AF, Burkhart KB, Burton N, Pavelec DM, Kennedy S. Small regulatory RNAs inhibit RNA polymerase II during the elongation phase of transcription. Nature 2010;465:1097–101.
[46] Meister G. Argonaute proteins: functional insights and emerging roles. Nat Rev Genet 2013;14:447–59.
[47] Castañeda J, Genzor P, Bortvin A. piRNAs, transposon silencing, and germline genome integrity. Mutat Res 2011;714:95–104.
[48] Guo M, Wu Y. Fighting an old war with a new weapon-silencing transposons by Piwi-interacting RNA. IUBMB Life 2013;65:739–47.
[49] Carmell MA, Girard A, van de Kant HJ, Bourc'his D, Bestor TH, de Rooij DG, et al. MIWI2 is essential for spermatogenesis and repression of transposons in the mouse male germline. Dev Cell 2007;12:503–14.
[50] Houwing S, Kamminga LM, Berezikov E, Cronembold D, Girard A, van den Elst H, et al. A role for Piwi and piRNAs in germ cell maintenance and transposon silencing in zebrafish. Cell 2007;129:69–82.
[51] Czech B, Malone CD, Zhou Z, Stark A, Schlingeheyde C, Dus M, et al. An endogenous small interfering RNA pathway in *Drosophila*. Nature 2008;453:798–802.
[52] Sijen T, Plasterk RH. Transposon silencing in the *Caenorhabditis elegans* germ line by natural RNAi. Nature 2003;426:310–4.
[53] Vastenhouw NL, Fischer SE, Robert VJ, Thijssen KL, Fraser AG, Kamath RS, et al. A genome-wide screen identifies 27 genes involved in transposon silencing in *C. elegans*. Curr Biol 2003;13:1311–6.

# 7. Correlation between gonad-inhibiting hormone and vitellogenin during ovarian maturation in the domesticated *Penaeus monodon*..

Aquaculture 437 (2015) 1–9

Contents lists available at ScienceDirect

Aquaculture

journal homepage: www.elsevier.com/locate/aqua-online

# Correlation between gonad-inhibiting hormone and vitellogenin during ovarian maturation in the domesticated *Penaeus monodon*

Sittichai Urtgam [a], Supattra Treerattrakool [a,*], Sittiruk Roytrakul [b], Somjai Wongtripop [c], Juthatip Prommoon [c], Sakol Panyim [a,d], Apinunt Udomkit [a,**]

[a] Institute of Molecular Biosciences, Mahidol University, Salaya Campus, Nakhon Pathom 73170, Thailand
[b] Genome Institute, National Center for Genetic Engineering and Biotechnology (BIOTEC), Pathum Thani 12120, Thailand
[c] Shrimp Genetic Improvement Center, National Center for Genetic Engineering and Biotechnology (BIOTEC), Pathum Thani 12120, Thailand
[d] Department of Biochemistry, Faculty of Science, Mahidol University, Rama VI Road, Bangkok 10400, Thailand

ARTICLE INFO

*Article history:*
Received 6 June 2014
Received in revised form 4 November 2014
Accepted 14 November 2014
Available online 20 November 2014

*Keywords:*
Black tiger shrimp
Eyestalk
Gonad-inhibiting hormone
Vitellogenesis
Ovarian maturation

ABSTRACT

Vitellogenesis in crustaceans is a process by which a major yolk protein, vitellin (Vn) is proteolytically produced from vitellogenin (Vg) and deposited into developing oocytes. Vitellogenesis is regulated by a gonad-inhibiting hormone (GIH) produced in the eyestalk ganglia. In this study, *Vg* and *GIH* mRNA expression and their physiological concentrations at the protein level were examined during ovarian maturation in domesticated broodstock of *Penaeus monodon*. *GIH* mRNA was expressed at the highest level in the eyestalk ganglia of the shrimp with immature ovary while the GIH peptide was actively released into the hemolymph. The release of GIH dropped dramatically at stage I of the ovary onwards conforming to its negative regulatory function on Vg synthesis. *Vg* mRNA expression study confirmed that Vg was synthesized in both the ovary and the hepatopancreas of *P. monodon*. The expression of *Vg* increased as ovarian maturation progressed similarly to that demonstrated in the wild broodstock. Vg protein was found in the hemolymph since stage I of ovarian maturation suggesting a rapid release of Vg into the hemolymph before deposition into oocytes as shown by a significant increase of Vn in the ovary at the following stage. Unlike previous studies in wild *P. monodon* broodstock, Vn was localized to follicle cells of late perinucleolar oocytes and to both follicle cells and ooplasm of the vitellogenic oocytes of domesticated broodstock. We speculate that the incorporation of Vn from follicle cells to the oocytes occurred more slowly in domesticated shrimp; this may account for the retarded reproductive maturation of the domesticated broodstock comparing with the wild broodstock. Our study thus provides insights on vitellogenesis in domesticated *P. monodon* that will be useful for improvement of their reproductive maturation.



## 1. Introduction

Ovarian maturation in oviparous animals occurs by two phases of vitellogenesis: the synthesis of a yolk precursor, vitellogenin (Vg) in vitellogenic organs and the accumulation of a major yolk protein called vitellin (Vn) into oocyte cells. In penaeid shrimps, Vg is synthesized as a large precursor molecule in both the ovary and the hepatopancreas (Avarre et al., 2003; Phiriyangkul and Utarabhand, 2006; Tsang et al., 2003; Tseng et al., 2001; Tsutsui et al., 2000; Xie et al., 2009). Following its synthesis in the hepatopancreas, Vg is cleaved into two subunits that are subsequently released into the hemolymph. The Vg subunits in the hemolymph are further processed by proteolytic cleavage before deposition into developing oocytes where they undergo biochemical modifications such as glycosylation and conjugation to lipid and carotenoids into vitellin that serves as a nutrient source during embryogenesis (Sappington and Raikhel, 1998; Wilder et al., 2010).

Vitellogenin synthesis in crustaceans is controlled by two antagonistic hormones; one stimulates and another inhibits ovarian development. It was demonstrated that implantation of thoracic ganglion or injection of the ganglion extract could induce vitellogenesis in previtellogenic shrimp (Yano, 1992; Yano et al., 1998), indicating that thoracic ganglion contains the substance that can induce Vg synthesis and/or Vg release into the hemolymph. However, identification of such vitellogenesis-stimulating factor has not been successful so far. On the other hand, vitellogenin expression is inhibited by a well characterized eyestalk's hormone called gonad-inhibiting hormone (GIH) (Nagaraju, 2011; Yano, 1998). GIH is synthesized and secreted by the x-organ-sinus gland neurosecretory system in crustacean eyestalk. Although it is generally known that a decrease in the amount of GIH by eyestalk ablation can induce ovarian maturation in shrimp, the mechanism by which GIH regulates vitellogenesis is still unclear. It

* Corresponding author at: S. Treerattrakool, Institute of Molecular Biosciences, Mahidol University, Nakhon Pathom 73170, Thailand.
** Correspondence to: A. Udomkit, Institute of Molecular Biosciences, Mahidol University, Phutthamonthon 4 Rd., Nakhon Pathom 73170, Thailand. Tel.: +66 2441 9003x1236; fax: +66 2441 9906.
*E-mail addresses:* tsupattra@gmail.com (S. Treerattrakool), apinunt.udo@mahidol.ac.th (A. Udomkit).

http://dx.doi.org/10.1016/j.aquaculture.2014.11.014
0044-8486/

was shown that GIH level in the hemolymph of an American lobster *Homarus americanus* was high during the immature and previtellogenic stage and decreased in vitellogenic stage (de Kleijn et al., 1998). Correspondingly, *Vg* mRNA expression in both the ovary and hepatopancreas as well as the hemolymph Vg levels of the kuruma shrimp *Marsupenaeus japonicus* were low at previtellogenic stage and drastically increased during vitellogenesis (Okumura et al., 2007). These results, though studied in different crustaceans, evidently suggest the inhibitory role of GIH on vitellogenesis. The investigation of Vg and GIH at both mRNA expression and protein levels during vitellogenesis in a single crustacean species will lead to a more thorough understanding of the regulation of this important reproductive process.

The black tiger shrimp *Penaeus monodon* is one of the important aquatic animals in Thailand and worldwide. The production of *P. monodon* larvae generally relies on eyestalk ablation of the female broodstock (Browdy, 1992). Since removal of the eyestalk not only impedes the production of GIH but also other hormones of physiological importance, other hormonal manipulation approaches have been examined in an attempt to substitute for eyestalk ablation. For instance, the injection of progesterone could stimulate ovarian development in *Metapenaeus ensis* (Yano, 1985). A neurotransmitter serotonin or 5-hydroxytryptamine could also induce ovarian maturation in Penaeid shrimps (Vaca and Alfaro, 2000; Wongprasert et al., 2006). More recently, specific inhibition of GIH expression by dsRNA was demonstrated as a potential alternative to eyestalk ablation to induce vitellogenin expression as well as ovarian maturation in *P. monodon*, especially in the wild broodstock (Treerattrakool et al., 2011). Although these studies provide promising results, an in depth knowledge about the mechanism controlling vitellogenesis process in shrimp is necessary for application of these hormonal manipulation methods to achieve maximum reproductive performance of this shrimp.

In order to understand the control mechanism of vitellogenesis in *P. monodon*, the present study investigates the relationships between GIH and Vg transcripts and protein levels during ovarian maturation in domesticated *P. monodon*. This information will be useful for future development of an alternative method to induce ovarian maturation in female shrimp broodstock.

## 2. Materials and methods

### 2.1. Experimental animals and tissue preparation

Domesticated, pond-reared female broodstock of *P. monodon* were kindly provided by the Shrimp Genetic Improvement Center, Suratthani, Thailand. The developmental stages of the ovaries were determined by both the gonado-somatic index (GSI) and histochemical staining with hematoxylin and eosin according to Tan-Fermin and Pudadera (1989), and could be classified into immature (stage 0; GSI = 0.97 ± 0.08%), previtellogenic (stage I; GSI = 1.79 ± 0.06% containing chromatin nucleolar and perinucleolar oocytes), early vitellogenic (stage II; GSI = 2.46 ± 0.09% containing yolkless oocytes as a majority), late vitellogenic (stage III; GSI = 3.88 ± 0.33% mostly composing of yolky oocytes) and mature (stage IV: GSI = 6.24 ± 0.70% as indicated by the massive population of cortical rod oocytes) stages. Tissue samples i.e. eyestalk ganglia, lateral lobe of the ovary and the hepatopancreas were freshly dissected, and immediately frozen in liquid nitrogen and stored at −80 °C. About 2–4 ml of the hemolymph was drawn from dorsal hemolymph sinuses of the shrimp using a syringe and needle containing modified Alsever's solution or anticoagulant-I buffer (27 mM sodium citrate, 450 mM NaCl, 115 mM glucose, 10 mM EDTA, pH is 7.0). The hemolymph samples were centrifuged at 830 ×*g* for 30 min at 4 °C and then transferred to a new tube and stored at −80 °C. All animal experiments were carried out in accordance with animal care and use protocol of the Mahidol University Animal Care and Use Committee.

### 2.2. RNA isolation and quantitative reverse transcription real-time polymerase chain reaction

About 50 mg of shrimp tissues (ovary and hepatopancreas) or an optic lobe from eyestalk were homogenized in 500 μl of TRI-REAGENT® (Molecular Research Center, Inc.), and the RNA was extracted following the manufacturer's protocol. RNA concentration was estimated by spectrophotometry and the quality of the RNA was determined by 1.2% TAE agarose gel electrophoresis.

One microgram of RNA was used as a template in first-strand cDNA synthesis reaction with an oligo$(dT)_{16}$ primer using ImProm-II™ reverse transcriptase enzyme (Promega, USA) according to the manufacturer's protocol. Then 1 μl of 1:10 dilution of the cDNA was used in quantitative real-time PCR to detect *GIH* and *Vg* transcript levels. Quantitative real time PCR was performed using KAPA SYBR® FAST qPCR kit with specific primers for *GIH* (GIH-F: 5′-AACATC CTGGACAGCAAATGCAGGG-3′ and GIH-R: 5′-GGCCTCGCGCT TGGCCG AGTG-3′) and *Vg* (Vg-F: 5′-TCCATCTGCAGCACCAATCTTCGC-3′ and Vg-R: 5′-GCAACAGCCTTCATTCTGATGCCA-3′) and following KAPA SYBR® FAST qPCR protocol (KAPABIOSYSTEMS, USA). The reaction composing of 1 × KAPA SYBR® FAST qPCR Master Mix, 200 nM each of forward and reverse primers was carried out in a real-time PCR machine ABI7500-prism model. The expression levels of *GIH* and *Vg* were normalized with, and expressed as a relative level to that of *EF-1α* mRNA determined by EF-1α F (5′-GAACTGCTG ACCAAGATCG ACAGG-3′) and EF-1α R (5′-GAGCATACTGTTGGAAGGT CTCCA-3′) primers. The real-time PCR data was analyzed by $2^{-\Delta CT}$ method.

### 2.3. Immunohistochemistry

The dissected tissues were fixed in Davidson's fixative (31% Ethanol, 22% Formalin, and 11.5% Glacial acetic acid) for 48 h before processed by paraffin sectioning procedure into 5 μm-thick tissue sections, then histological features of the tissues were determined by hematoxylin and eosin staining according to Bell and Lightner (1988). For localization of Vg/Vn in shrimp ovary and hepatopancreas, the tissue sections were immersed in 0.1% $H_2O_2$ in PBS to eliminate endogenous peroxidase. Non-specific signal was then blocked by incubating the sections in PBS containing 10% fetal bovine serum prior to incubating with monoclonal antibody raised against *P. monodon* Vn protein (anti-Vn mAb) that reacts to the 140 kDa subunits of both Vg and Vn (Longyant et al., 2000) (kindly provided by Prof. Paisarn Sithigorngul and Asst. Prof. Siwaporn Longyant, Srinakharinwirot University, Thailand) for 16 h at 4 °C and washed in PBS containing 0.1% tween 20. The sections were incubated with 1:1000 dilution of horseradish peroxidase (HRP)-conjugated anti-mouse IgG for 90 min at 37 °C. The signal was developed by diaminobenzidine and the reaction was terminated in PBS. The sections were mounted with permount and visualized under the light microscope.

### 2.4. Immunofluorescence staining

The eyestalks were fixed in Davidson's fixative and processed by paraffin sectioning procedure as described earlier. For immunofluorescence staining, the sections were rehydrated with decreasing percentages of ethanol from 100% to 50% followed by PBS. The tissues were permeabilized in 0.1% Triton X-100 in PBS for 5 min and washed in PBS. Non-specific signal was then blocked by incubating the sections in PBS containing 10% fetal bovine serum prior to incubating with 1:50 dilution of monoclonal antibody specific to *P. monodon* GIH protein (anti-GIH mAb) in PBS containing 1% fetal bovine serum (Treerattrakool et al., 2014) for 16 h at 4 °C, and washed in PBS containing 0.05% tween 20. Subsequently, the sections were incubated with 1:100 dilution in PBS of the Alexa flour 488-conjugated anti-mouse IgG for 2 h at room temperature. The sections were mounted with ProLong® Gold Antifade reagent and visualized under the Olympus FluoView™ FV1000 confocal microscope.

### 2.5. Preparation of vitellogenin from shrimp ovaries

Vitellogenin was prepared from stage IV ovary of *P. monodon* according to the method described by Ramachandra Reddy et al. (2006). One gram of ovarian tissues was homogenized in 10 ml (10% w/v) of homogenization buffer (0.1 M NaCl, 0.05 M Tris–Cl, 1 mM EDTA and 0.1% Tween 20 with Protease Inhibitor Cocktail (Sigma, USA); pH 7.8). After centrifuged at 4000 ×*g* for 5 min at 4 °C, the supernatant was collected and centrifuged again at 20,000 ×*g* for 20 min at 4 °C. Ammonium sulphate was added to the supernatant with constant stirring until a final of 25% ammonium sulphate solution was obtained, and further incubated for 1 h at 4 °C. The solution was centrifuged at 20,000 ×*g* for 10 min at 4 °C and the supernatant was collected to a new tube. Ammonium sulphate was added to produce 40%, 50% and 60% saturation as described above. The pellets at 60% saturation were re-suspended in homogenization buffer and dialyzed against homogenization buffer at 4 °C for 12 h for three times. The purified vitellogenin was analyzed by 8% SDS-PAGE and stored at −30 °C.

### 2.6. Protein extraction from shrimp tissues

An eyestalk ganglia was homogenized in 500 μl of PBS (pH 7.4), and approximately 50 mg of ovary and hepatopancreas tissues were homogenized in 500 μl of 0.5 mM EDTA in PBS (pH 7.4). Tissue homogenate was subsequently centrifuged at 10,000 ×*g* for 30 min at 4 °C. The soluble fraction was collected and stored at −80 °C.

### 2.7. Enzyme-linked immunosorbent assay (ELISA)

The competitive ELISA for Vg/Vn was performed by coating each well of the ELISA plate with 1 μg of vitellogenin for 16 h at 4 °C. After washing with PBS containing 0.1% tween 20, the plate was blocked with 5% skim milk in PBS. To each well, 50 μl of protein sample and 50 μl of anti-Vn mAb at a dilution of 1:3000 were added and incubated at 4 °C for a further period of 6 h. After washing with PBS containing 0.1% tween 20, 50 μl of peroxidase-conjugated anti-mouse IgG (whole molecule) (Sigma, USA) at a dilution of 1:3000 was added and incubated for 3 h at 37 °C. Finally, the plate was incubated with 100 μl of 0.1 mg/ml of 3,3′,5,5′-Tetramethylbenzidine (Sigma, USA) in substrate buffer (10% (v/v) DMSO, 45 mM Phosphate-Citrate, pH 5 and 0.005% (v/v) hydrogen peroxide). The reaction was stopped with 2 N $H_2SO_2$ and detected by an ELISA plate reader (Spectra Max 190) at 450 nm.

### 2.8. Determination of GIH concentrations in the eyestalk and hemolymph by LC–MS/MS

To prepare protein samples for determination of GIH concentration in shrimp eyestalks, the neuronal ganglia of the eyestalks were extracted with PBS, followed by centrifugation at 10,000 rpm for 10 min. Proteins in the supernatant were separated by SDS-PAGE and further processed as described below. The protein sample of the hemolymph was prepared by mixing the hemolymph samples with acetonitrile to a final concentration of 60% acetonitrile. The mixture was vigorously shaken and subsequently centrifuged at 6000 ×*g* for 30 min at 4 °C. The soluble fraction was dried for 48 h at 4 °C with Univapor concentrator centrifugation, and dissolved in sample buffer (200 mM Tris–Cl pH 6.8, 2% SDS, 4% Glycerol, 0.03% bromophenol blue, 2% β-mercaptoethanol). Protein samples from both the eyestalks and hemolymph were separated in SDS-polyacrylamide gel, and visualized by silver staining. The band of GIH at approximately 9 kDa of each sample was excised and destained with 5% $H_2O_2$ followed by sterile water before extracted with 100% acetonitrile. After removing acetonitrile, the gel slice was allowed to dry and immersed in 20 μl of 10 mM dithiothreitol in 10 mM $NH_4HCO_3$ at 56 °C to reduce disulfide bonds. Subsequently, 20 μl of 100 mM iodoacetamide in 10 mM $NH_4HCO_3$ was added and kept in the dark for 1 h at room temperature. After washing twice in 100% acetonitrile, the gel slice was incubated with 10 μl of 10 ng/μl of trypsin in 50% acetonitrile/10 mM $NH_4HCO_3$ for 20 min at room temperature followed by 3 h incubation in 20 μl of 30% acetonitrile at 37 °C. The peptides were finally extracted in 30 μl of 50% acetonitrile containing 0.1% formic acid. The solution was dried overnight at 40 °C, and the pellet was stored at −80 °C. The protein samples were then subjected to LC–MS/MS analysis by LC–MS/MS machine model Ultimate 3000 LC System (Dionex, USA) coupled to ESI-Ion Trap MS (HCT Ultra PTM Discovery System (Bruker, Germany)) at Proteomics Research Laboratory, BIOTEC, NSTDA Thailand.

### 2.9. Statistical analysis

The results are presented in a box-and-whisker diagram (box plot). Non-parametric statistics were used to analyze a non-normal distribution data. The statistical significance of values was determined by Kruskal–Wallis test followed by Mann–Whitney U test (SPSS 20 for Window). Significance was accepted at $p < 0.05$.

## 3. Results

### 3.1. Expression of GIH mRNA during ovarian maturation of P. monodon

The expression of *GIH* mRNA in the eyestalk ganglia of individual domesticated, pond-reared *P. monodon* female broodstock at each stage of ovarian development (n = 13–24 for each stage) was detected by reverse transcription real-time PCR. *GIH* mRNA was expressed at the highest level in the shrimp at the immature stage (stage 0), and then gradually decreased as the ovary developed (Fig. 1). *GIH* mRNA expression reached the minimum level ($p < 0.05$) at early vitellogenic stage (stage II) and remained at relatively low levels throughout the maturation period until stage IV of ovarian development.

### 3.2. Expression of Vg mRNA in the ovary and hepatopancreas during ovarian maturation of P. monodon

*Vg* mRNA levels were determined in both of its major synthesis sites; the ovary and the hepatopancreas of *P. monodon*. In both tissues the expression of *Vg* changed with regard to ovarian maturation. *Vg* mRNA expression in the ovary increased continuously with significant difference

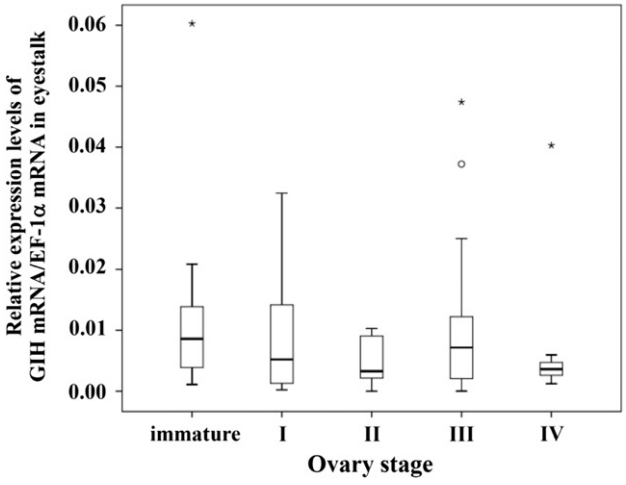


**Fig. 1.** Expression levels of *GIH* mRNA in the eyestalk during ovarian development in domesticated *P. monodon*. The relative mRNA expression levels of *GIH* to that of *EF-1α* in the eyestalk ganglia of female shrimp at different ovarian maturation stages (n = 13–24 for each stage) were determined by reverse transcription real-time PCR using KAPA™ SYBR® FAST qPCR kit. Boxes show values between 25th and 75th percentiles; horizontal lines show the median; error bars show minimum and maximum values excluded outliers; open circle and asterisk show outliers and extreme outliers, respectively.

from stage 0 to stage IV (Fig. 2a). *Vg* mRNA in the hepatopancreas was at unnoticeable level in immature shrimp, then slightly but significantly went up until stage III before showing a sharp increase ($p < 0.001$) in the mature stage (Fig. 2b). Noticeably, although a rise of *Vg* mRNA expression in the hepatopancreas seemed to delay when compared with that in the ovary, the relative expression level of *Vg* at the maturation stage in the hepatopancreas was more than twice the level in the ovary.

### 3.3. Localization of GIH and Vg in shrimp tissues

To examine the location of GIH in shrimp eyestalk, a monoclonal antibody specific to *P. monodon*'s GIH (anti-GIH mAb) (Treerattrakool et al., 2014) was used in the immunofluorescence detection. The results showed positive signals in the sinus gland of the eyestalk (Fig. 3, top row). Moreover, GIH signals were also detected in some of the perikarya in the medulla terminalis X-organ cell bodies, the expected site of GIH synthesis (Fig. 3, middle row) as well as in the organ of Bellonci (Fig. 3, bottom row).

Anti-Vn mAb was used to study the localization of Vg/Vn in both the ovary and hepatopancreas. In the ovary, Vn-positive signals were detected in the follicle cells surrounding some late perinucleolar (LPO), early vitellogenic (Y1) and late (Y2) vitellogenic oocytes, but not those surrounding early perinulcleolar oocytes (PO) and the oocytes with cortical rods. No Vn signal was detected in perinucleolar oocytes, but the signal started to accumulate in the ooplasm of the oocytes at all vitellogenic stages including Y1, Y2 and oocytes with cortical rods (Fig. 4).

In the hepatopancreas, Vg-positive signals were localized mainly in the intertubular space. The Vg signal was observed in the hepatopancreas since stage I of ovarian maturation despite its very low levels of mRNA expression. The levels of Vg signal increased in shrimp with more mature stages of ovarian development (Fig. 5).

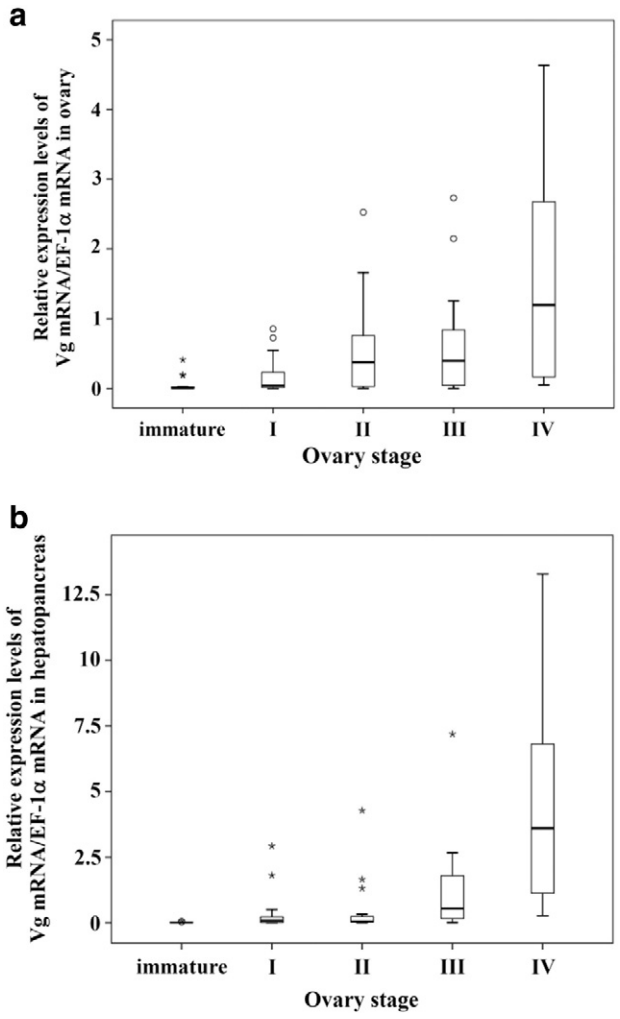


**Fig. 2.** Expression levels of *Vg* mRNA in ovary (a) and hepatopancreas (b) of domesticated female broodstock of *P. monodon* at each ovarian maturation stage. The relative mRNA expression levels of *Vg* to that of *EF-1α* were determined by reverse transcription real-time PCR using KAPA™ SYBR® FAST qPCR kit. Boxes show values between 25$^{th}$ and 75$^{th}$ percentiles; horizontal lines show the median; error bars show minimum and maximum values excluded outliers; open circle and asterisk show outliers and extreme outliers, respectively.

### 3.4. Changes in GIH concentration in shrimp eyestalk during ovarian maturation

Since the amount of GIH peptide in the eyestalk was lower than the sensitivity of ELISA detection in this study, an alternative method employing the advantage of LC–MS/MS to precisely detect low amount of the peptide was developed and used for determination of GIH concentration in this study. The highest amount of GIH peptide was found in the eyestalk of shrimp possessing stage 0 and stage I ovaries. Subsequently, the GIH peptide concentration in the eyestalk declined when the ovary developed to later stages with the lowest level at stage III of ovarian maturation (Fig. 6a).

### 3.5. Vitellogenin/Vitellin concentrations at the sites of synthesis during ovarian maturation cycle of female shrimp

The dynamic of Vg/Vn during ovarian maturation in female shrimp was also studied. Vg/Vn concentrations in its synthesis organs i.e. ovary and hepatopancreas at different stages of ovarian maturation were determined by competitive ELISA. The result in Fig. 6b showed that Vn concentration in the ovary was undetectable in stage 0 and significantly increased at later stages of developing ovaries ($p < 0.001$). The highest concentration of Vn was seen in stage III of ovarian development, and decreased a little bit in the final stage (stage IV) of the ovary. However, Vg protein in the hepatopancreas was at undetectable level as detected by competitive ELISA at all stages of ovarian development.

### 3.6. Concentrations of GIH peptide and vitellogenin in the hemolymph of female shrimp at different ovarian stages

To obtain complete information about the relationship of GIH and Vg during ovarian maturation in female shrimp, the effective concentrations of circulating GIH and Vg in the hemolymph of *P. monodon* at each ovarian developmental stage were determined. The result in Fig. 6c showed a high concentration of hemolymph GIH at the immature stage (stage 0) of the ovary. The GIH concentrations decreased as the ovary developed to the next stage and remained at low levels in the hemolymph all through the maturation cycle.

The concentration of hemolymph Vg was low in the shrimp with immature ovary and getting higher in stage I. A significant increase in the hemolymph Vg concentration was reached at stage II and maintained at relatively high levels in subsequent maturation stages (Fig. 6d).

In addition, a bivariate correlation analysis revealed a significant inverse correlation between GIH and Vg concentrations in the hemolymph, and also between GIH concentration in the hemolymph and Vn in the ovary (Supplementary Fig. 1).

## 4. Discussion

Shrimp larva production relies mostly on wild-caught broodstock because of its high reproductive performance although the quality of the wild broodstock varies upon size, age, season and geographic heterogeneity (Crocos and Coman, 1997; Hansford and Marsden, 1995;

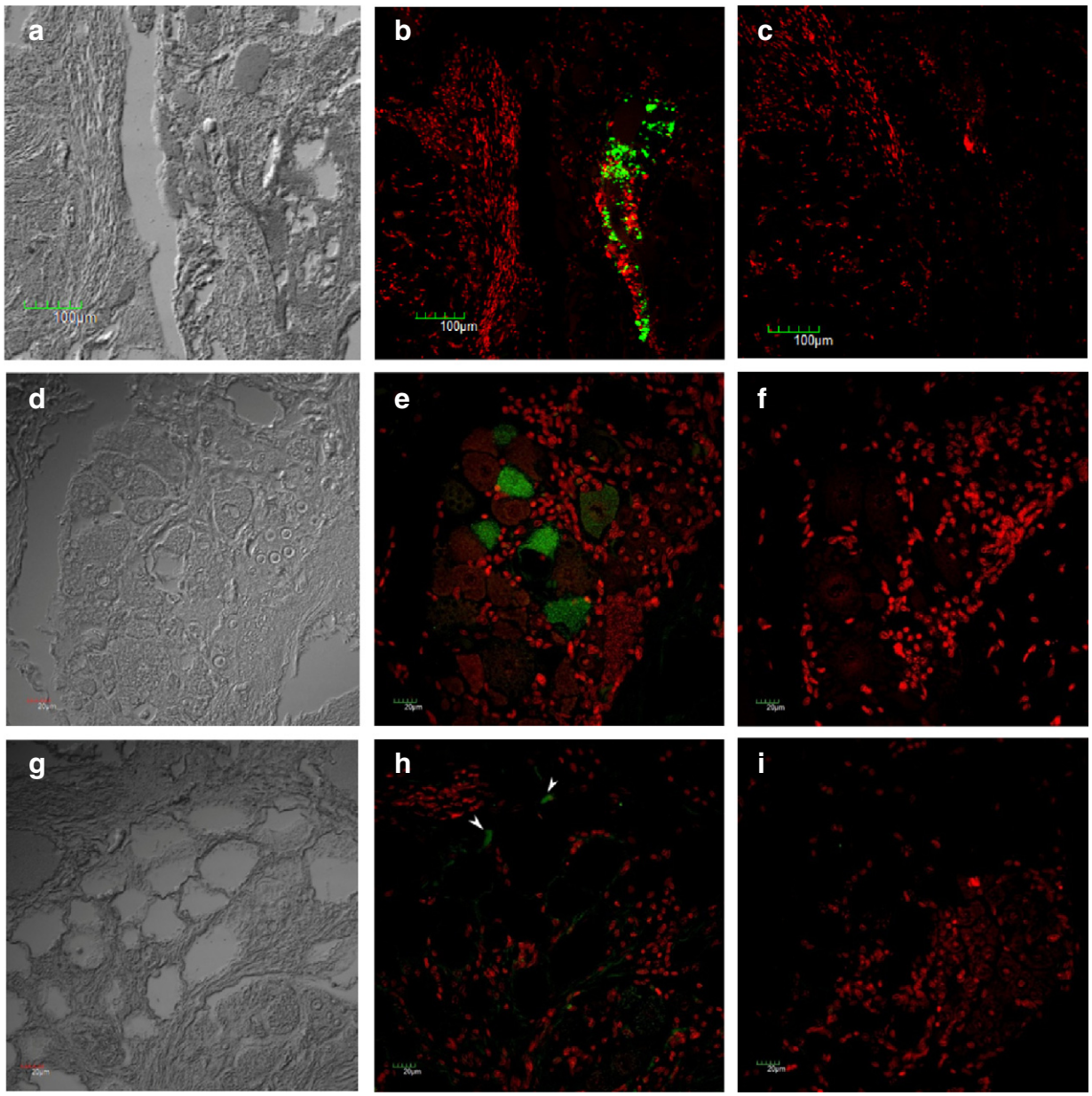


**Fig. 3.** Immunofluorescence detection of GIH peptide in the eyestalk ganglia of female *P. monodon*. Localization of GIH by anti-GIH mAb was illustrated in the sinus gland (top row), the cell bodies of the organ of Hanström (middle row) and the organ of Bellonci (bottom row). White arrow heads indicate positive staining signals (green). The immunoreactive staining sections are shown in the middle panels (b, e and h), whereas differential interference contrast images of corresponding sections are shown in the left panels (a, d and g) and the negative staining (PBS) of adjacent sections are shown in the right panels (c, f and i).

Menasveta et al., 1994). In addition, utilization of wild broodstock not only leads to a decline in natural resources but also introduces pathogens/diseases to the hatcheries (Craig, 1998). Successful domestication of a specific pathogen-free and high quality broodstock is currently a high priority for a sustainable shrimp aquaculture. Therefore, in this study the biology of ovarian maturation was investigated in the domesticated *P. monodon* broodstock in order to assist the improvement of reproduction performance in this pond-reared stock of the breeders. Moreover, eyestalk ablated and unablated adult *P. monodon* showed different performances on maturation (Emmerson, 1983). Therefore, the relationship between GIH and Vg during ovarian maturation was examined in intact broodstock to allow ovarian development to occur by natural process without influences from eyestalk ablation.

The high expression level of *GIH* mRNA in the eyestalk ganglia as well as the high level of GIH peptide in both the eyestalk and hemolymph at the immature stage of the ovary indicated that GIH was actively produced and instantly released into the hemolymph of the shrimp with undeveloped ovary. A drastic decrease in the hemolymph level of GIH peptide at the onset of vitellogenesis (stage I) and the continuous low levels throughout the maturation cycle confirming its inhibitory function on vitellogenesis (Huberman, 2000). In an American lobster *H. americanus*, the expression pattern of *GIH* mRNA as well as the hemolymph level of GIH during ovarian maturation cycle was different from that of *P. monodon* reported in this study. The lowest level of *GIH* mRNA in *H. americanus* with immature ovary and the resumption of the high hemolymph level at maturation (de Kleijn et al., 1998) suggest that the control of GIH could be slightly different in diverse species.

The immunoreactivity to anti-GIH mAb was localized in the axon terminals of the sinus gland as well as in some of the perikarya in the

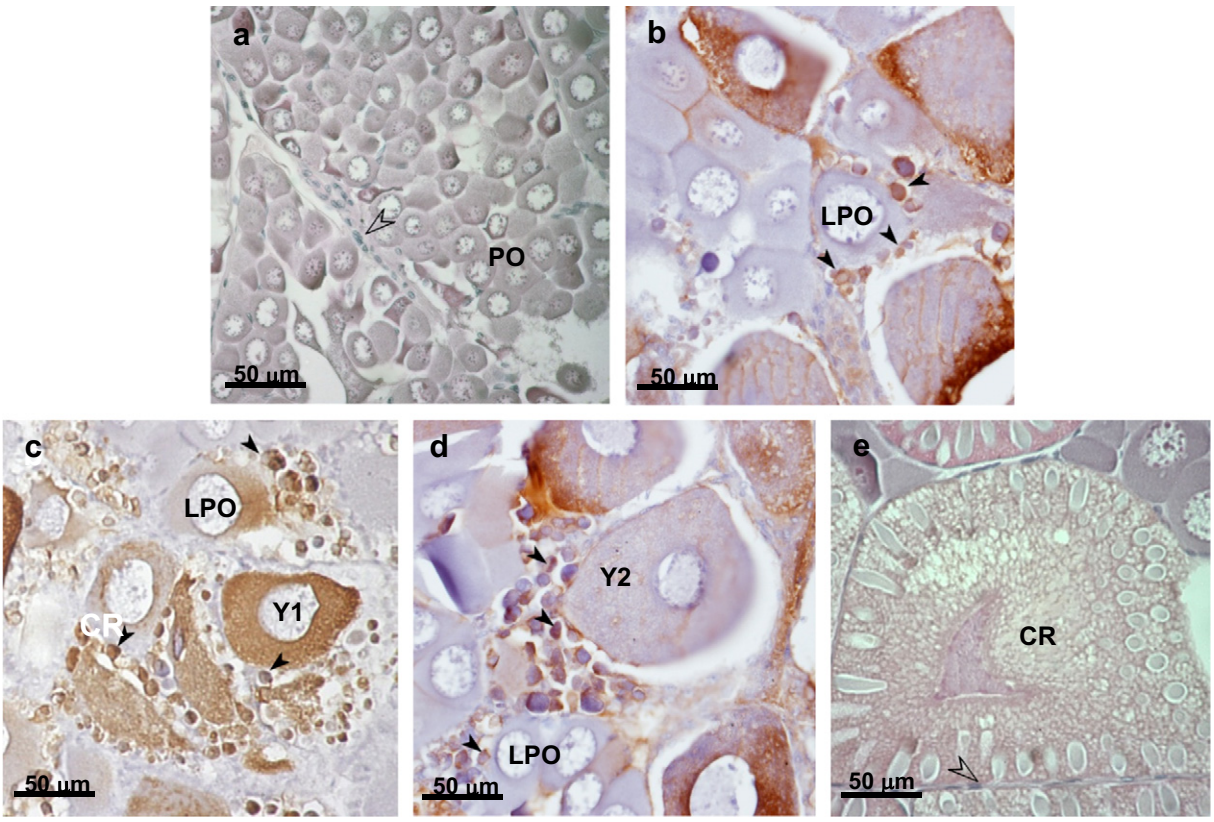


**Fig. 4.** Localization of Vg/Vn in different stages of shrimp ovaries. The anti-Vn mAb was used in the immunohistochemical detection of Vg/Vn in the ovary of domesticated female broodstock of *P. monodon* at different ovarian maturation stages. Open and black arrow heads indicate the negative (a and e) and positive stain (b, c and d), respectively in the follicle cells. PO = perinucleolar oocytes; LPO = late perinucleolar oocytes; Y1 = early vitellogenic (yolkless) oocytes; Y2 = late vitellogenic (yolky) oocytes; CR = cortical rod oocytes.

medulla terminalis ganglionic X-organ (MT-XO) similar to that previously reported in other decapod crustaceans (Marco and Gäde, 1999). Immunohistochemical localization of the other two neuropeptides in the same family as GIH i.e. CHH and MIH revealed similar immunoreactive patterns to that of GIH (Giulianini et al., 2002; Gu et al., 2001; Sithigorngul et al., 1999). Although these crustacean neuropeptides are located in the perikarya of neurons in the MT-XO, they seem to be localized in different neuron cells. In *H. americanus*, most of the CHH-immunoreactive neurons were localized centrally to the X-organ surrounded by GIH-positive cells while co-localization of CHH and GIH was observed in only a few neurons (Rotllant et al., 1993). No co-localization was also observed for CHH and MIH of the crab *Carcinus maenas* at both RNA and protein levels (Klein et al., 1993). These results suggest that neuropeptides in the CHH family are synthesized in separate cells and probably regulated by different pathways. In *P. monodon*, whether or not GIH is localized in different perikarya of the MT-XO from CHH and MIH needs further investigation.

We next investigated whether there is a correlation between hemolymph GIH concentration and Vg synthesis. Our results demonstrated a rise of *Vg* mRNA expression in both the ovaries and hepatopancreas upon a deprivation of hemolymph GIH concentration at previtellogenic stage, and continuingly increased as the ovary developed to higher maturation stages. However, a significant rise in *Vg* expression levels occurred earlier in the ovary than in the hepatopancreas. High Vg expression levels in both tissues during vitellogenesis were also reported in other penaeid shrimp such as *M. japonicus* (Okumura et al., 2007), *Penaeus semisulcatus* (Avarre et al., 2003) and *Fenneropenaeus merguiensis* (Phiriyangkul et al., 2007) although with slightly difference in the time when the expression reached a peak in each shrimp. These results confirm that a rapid decrease of GIH concentration in the hemolymph triggers *Vg* mRNA expression that is required for the onset of vitellogenesis.

The contribution of the ovary and hepatopancreas in vitellogenesis does not seem to be universal as comparative expression levels of *Vg* between both tissues differed among shrimp species. Expression of *Vg* was much higher in the ovary than in the hepatopancreas of *Litopenaeus vannamei* and *F. merguiensis* (Phiriyangkul et al., 2007; Raviv et al., 2006). In contrast, the *Vg* mRNA level in the hepatopancreas of *M. japonicus* was greater than that in the ovary at every stage of vitellogenesis (Tsutsui et al., 2000). Our result in domesticated *P. monodon* broodstock also demonstrated that higher levels of *Vg* mRNA were expressed in the hepatopancreas compared with that in the ovary. Recent study in wild-caught *P. monodon* broodstock revealed even more than 25-fold greater relative expression levels of *Vg* mRNA in shrimp hepatopancreas than that in the ovary (Hiransuchalert et al., 2013). In *M. ensis*, multiple copies of *Vg* gene were detected; among these, two *Vg* genes (*MeVg1* and *MeVg2*) were cloned and characterized (Kung et al., 2004; Tsang et al., 2003). While *MeVg1* was expressed in the ovary and hepatopancreas, *MeVg2* transcript was detected solely in the hepatopancreas. In addition to the 7.8–8 kb of *MeVg1* and *MeVg2* transcripts, smaller transcripts of both *MeVg1* and *MeVg2* were found in the hepatopancreas as detected by Northern blot hybridization (Tiu et al., 2006; Tsang et al., 2003). The presence of these smaller transcripts in large quantity suggests that alternative splicing or processing of *Vg* transcripts in the hepatopancreas is probably required for providing major contribution to vitellogenesis. Whether or not multiple *Vg* genes or transcripts are present in other penaeid shrimp, including *P. monodon* needs further investigation. Specific detection of these transcripts and their protein products are important to understand how Vg from the ovary and hepatopancreas coordinately contribute to vitellogenesis.

Variation of Vg concentration in the hemolymph during ovarian maturation cycle was opposed to changes in the hemolymph concentration of GIH. Hemolymph Vg concentration rose in previtellogenic

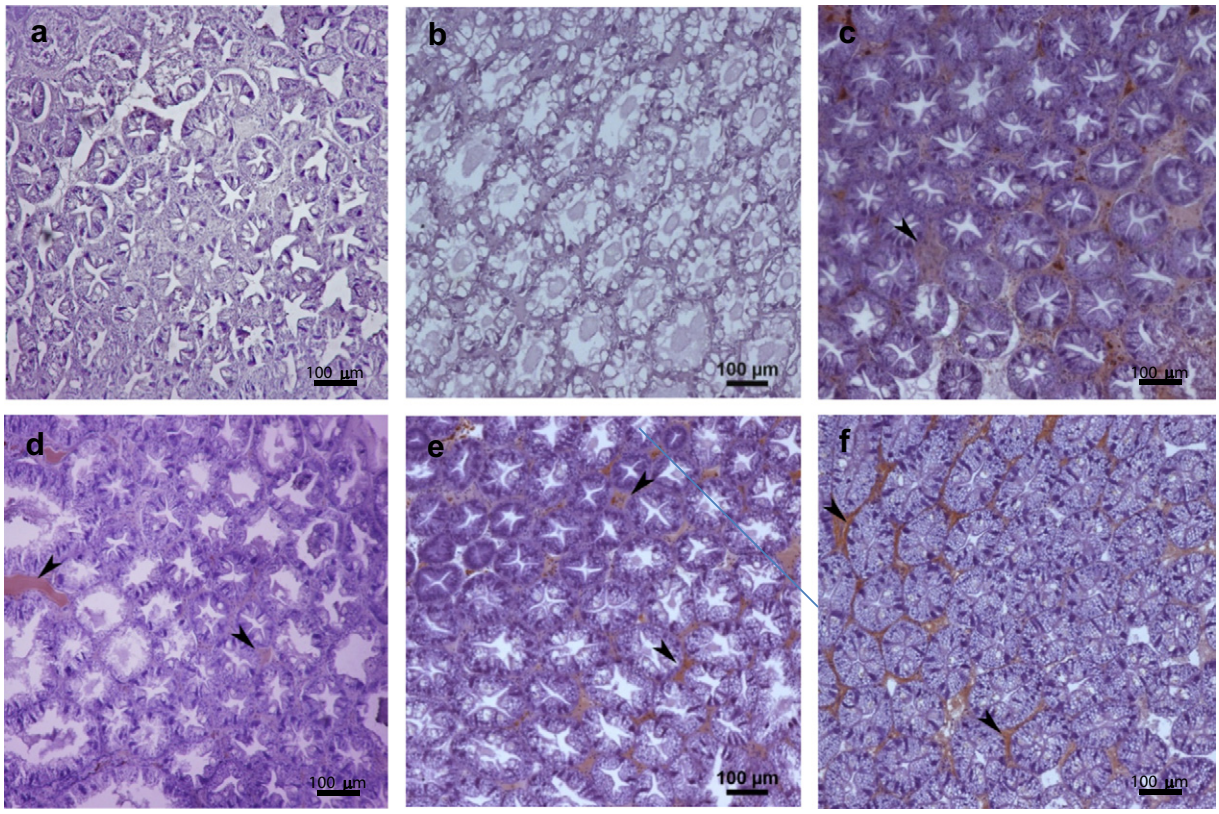


**Fig. 5.** Immunohistochemical detection of Vg in the hepatopancreas of female shrimp during ovarian development. Vg was detected by anti-Vn mAb in the hepatopancreas of *P. monodon* domesticated female broodstock at immature stage (b), stage I (c), stage II (d), stage III (e) and stage IV (f) of ovarian maturation. Detection in the absence of anti-Vn mAb was included as a negative control (a). Arrow heads indicate Vg-positive signals.

shrimp, and persisted at high levels throughout the rest of ovarian maturation cycle. Similar pattern of hemolymph Vg concentration during ovarian development have been reported in *M. japonicus* (Okumura et al., 2007), *Litopenaeus merguiensis* (Auttarat et al., 2006) and the fresh water prawn *Macrobrachium rosenbergii* (Revathi et al., 2012). A rapid increase of hemolymph Vg concentration at the early vitellogenic stage suggested that the *Vg* mRNA was actively translated into Vg protein and instantly released into the hemolymph for further processing into smaller subunits of vitellin before being incorporated into the ovaries; as reflected by an increase in vitellin (Vn) concentration in the ovaries. The persistence of relatively high hemolymph Vg levels during all vitellogenic stages indicates that Vg sequestration into the ovaries was probably balanced by a high *Vg* mRNA expression and the continuing release of Vg into the hemolymph throughout oocyte development.

In the present study, the detection of Vg protein in the hepatopancreas by ELISA was not successful. Hiransuchalert et al. (2013) also reported that proteins from hepatopancreas of *P. monodon* did not give immunoreactive band of Vg as detected by western blot analysis indicating very low amount of Vg in the hepatopancreas. These results support our postulation that the Vg synthesized in the hepatopancreas was rapidly released from its site of synthesis. This was further confirmed by immunohistochemical staining of Vg in the hepatopancreas that revealed immunoreactive signals to anti-Vn mAb only in the intertubular space.

In previous reports, Vn concentration in the ovaries was found to increase in accordance with ovarian developmental stages with the highest level at late-vitellogenic or maturation stage (Ferré et al., 2012; Vazquez Boucard et al., 2002). Our result also showed an increased Vn concentration in developing oocytes, but with a noticeable decrease at maturation stage. The reason for this is unclear as the diminishing of accumulated Vn in the mature ovaries seems unlikely. One possible explanation is that Vn accumulation was completed in the cortical rod oocytes while cortical rod proteins were produced; the amount of Vn per gram of ovarian tissue was therefore apparently lower than that in the earlier ovarian stages. Alternatively, although the monoclonal antibody was raised against Vn protein and reacted with a 140 kDa subunit in both Vn and Vg by western blot analysis (Longyant et al., 2000), modification of Vg into Vn by the addition of polysaccharides and lipids may possibly render lower immunoreactivity of antibody on the modified Vn (Spaziani et al., 1995).

Previous reports in wild *P. monodon* broodstock indicated that *Vg* mRNA was first detected in the ovarian follicle cells surrounding the vitellogenic oocytes, but not in the oocytes (Hiransuchalert et al., 2013), whereas the immunoreactive signal of Vn protein was observed only in the ooplasm of the oocytes (Hiransuchalert et al., 2013; Tiu et al., 2008). However, our results illustrated the immunoreactive signal of Vn in the follicle cells since the late perinulceolar stage of the ovaries of domesticated broodstock, while the accumulation of Vn signal started to be detectable in the ooplasm of early vitellogenic oocytes. These results indicated that the translocation of follicular Vn protein to ooplasms occur more rapidly in the wild broodstock than in the domesticated ones. This could be one factor that contributes to the difference in reproductive performance between the broodstock from the two sources that was demonstrated in several Penaied shrimp (Keys and Crocos, 2006; Marsden et al., 2013; Waikhom and Pillai, 2011).

In summary, we demonstrated that an inverse correlation between hemolymph GIH and Vg concentration is required for ovarian maturation in domesticated *P. monodon* broodstock. Although the overall patterns of *Vg* mRNA expression and Vg concentration in the hemolymph were similar to that previously reported in the wild broodstock, slight variations in the stage at which the expression reached the peak level were observed. This, together with the apparently slower sequestration of Vn into the ooplasm, may explain a poorer reproductive performance

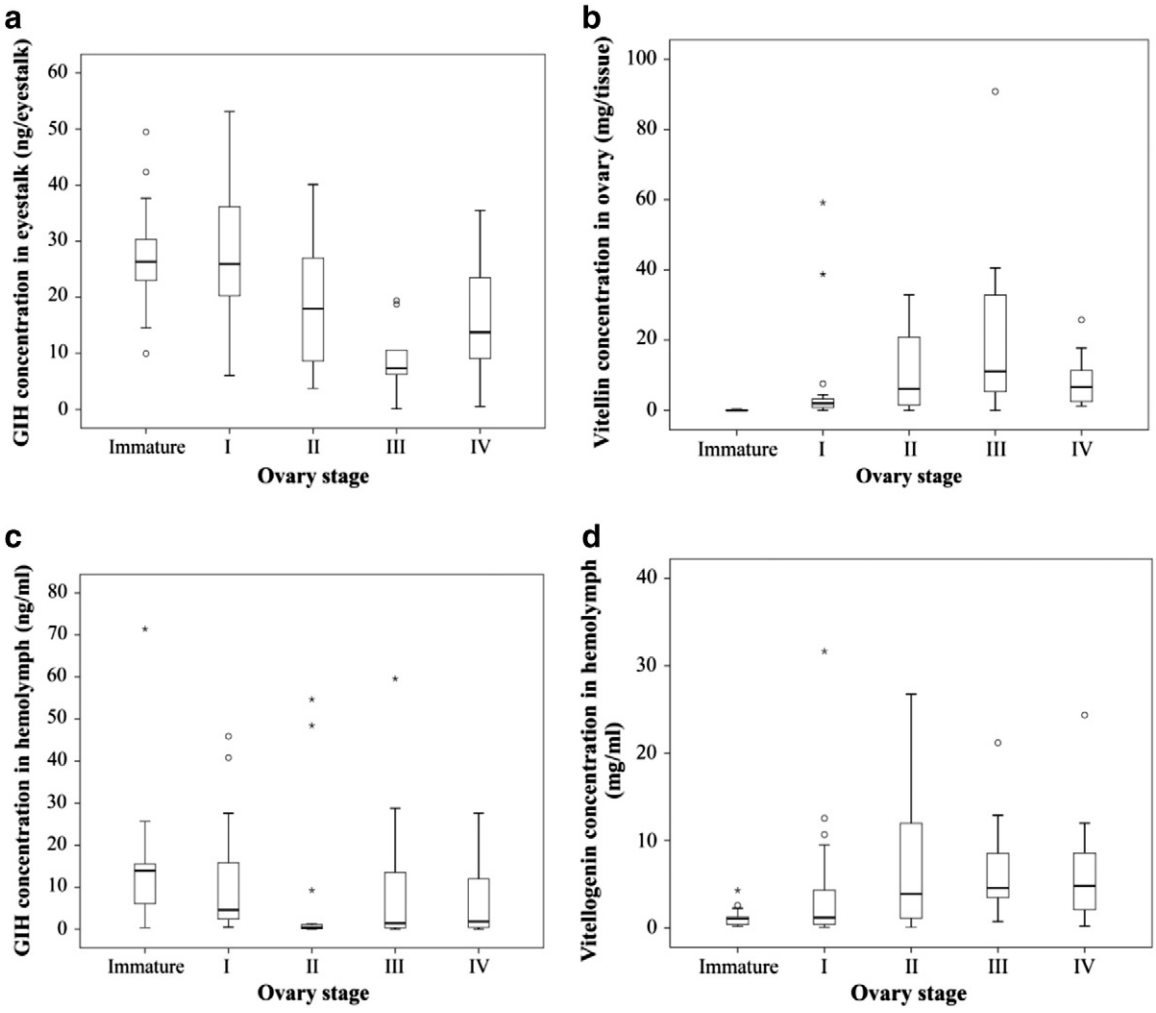


**Fig. 6.** Concentrations of GIH peptide and Vg/Vn during ovarian development of domesticated *P. monodon*. The GIH concentration in shrimp eyestalks (a) and hemolymph (c) as well as Vn concentration in the ovaries (b) and Vg concentration in the hemolymph (d) at each ovarian maturation stage were determined by competitive ELISA. Boxes show values between 25$^{th}$ and 75$^{th}$ percentiles; horizontal lines show the median; error bars show minimum and maximum values excluded outliers; open circle and asterisk show outliers and extreme outliers, respectively.

of the domesticated female broodstock. Our studies provide useful information for the further improvement of reproductive maturation in domesticated *P. monodon* broodstock and the quality of their offspring.

Supplementary data to this article can be found online at http://dx.doi.org/10.1016/j.aquaculture.2014.11.014.

## Acknowledgments

The authors would like to thank Prof. Prasert Sobhon and Prof. Timothy Flegel for their comments on immunohistochemical staining results. We thank Assoc. Prof. Chalermporn Ongvarrasopone for providing the Alexa flour 488-conjugated anti-mouse IgG. We also thank Dr. Benjamart Pratoomthai for her suggestion on immunofluorescence technique, and Mr. Chartchai Chaichana and Ms. Narumon Phaonakrop (BIOTEC, Thailand) for their kind help in in-gel tryptic digestion and LC–MS/MS analysis. This work was supported by grants under the program Strategic Scholarships for Frontier Research Network for the Joint Ph.D. Program Thai Doctoral degree from the Office of the Higher Education Commission, Thailand Research Fund (BRG5480018 to AU, DPG5680001 to SP and TRG5680002 to ST), Mahidol University Research Grant, The Office of the Higher Education Commission and Mahidol University under the National Research Universities Initiative and the Cluster and Program Management Office, NSTDA, Thailand.

## References

Auttarat, J., Phiriyangkul, P., Utarabhand, P., 2006. Characterization of vitellin from the ovaries of the banana shrimp *Litopenaeus merguiensis*. Comp. Biochem. Physiol. 143B, 27–36.

Avarre, J.C., Michelis, R., Tietz, A., Lubzens, E., 2003. Relationship between vitellogenin and vitellin in a marine shrimp (*Penaeus semisulcatus*) and molecular characterization of vitellogenin complementary DNAs. Biol. Reprod. 69, 355–364.

Bell, T., Lightner, D., 1988. Handbook of Normal Penaeid Shrimp Histology. The World Aquaculture Society, Louisiana, USA.

Browdy, C.L., 1992. A review of the reproductive biology of *Penaeus* species: perspectives on controlled shrimp maturation system for high quality nauplii production. In: Wyban, J. (Ed.), Proceeding of the Special Session on Shrimp Farming. Baton Rouge, LA, pp. 22–51.

Craig, L.B., 1998. Recent development in penaeid broodstock and seed production technologies: improving the outlook for superior captive stocks. Aquaculture 164, 3–21.

Crocos, P.J., Coman, G.J., 1997. Seasonal and age variability in the reproductive performance of *Penaeus semisulcatus* broodstock: optimising broodstock selection. Aquaculture 155, 55–67.

de Kleijn, D.P.V., Janssen, K.P.C., Waddy, S.L., Hegeman, R., Lai, W.Y., Martens, G.J.M., Van Herp, F., 1998. Expression of the crustacean hyperglycemic hormones and the gonad-inhibiting hormone during the reproductive cycle of the female American lobster *Homarus americanus*. J. Endocrinol. 156, 291–298.

Emmerson, W.D., 1983. Maturation and growth of ablated and unablated *Penaeus monodon* Fabricius. Aquaculture 32, 235–241.
Ferré, L.E., Medesani, D.A., Garcia, C.F., Grodzielski, M., Rodriguez, E.M., 2012. Vitellogenin levels in hemolymph, ovary and hepatopancreas of the fresh water crayfish *Cherax quadricarinatus* (Decapoda: Parastacidae) during the reproductive cycle. Rev. Biol. Trop. 60, 253–261.
Giulianini, P.G., Pandolfelli, N., Lorenzon, S., Ferrero, E.A., Edomi, P., 2002. An antibody to recombinant crustacean hyperglycemic hormone of *Nephrops norvegicus* cross-reacts with neuroendocrine organs of several taxa of malacostracan Crustacea. Cell Tissue Res. 307, 243–254.
Gu, P.-L., Chu, K.H., Chan, S.-M., 2001. Bacterial expression of the shrimp molt-inhibiting hormone (MIH): antibody production, immunocytochemical study and biological assay. Cell Tissue Res. 303, 129–136.
Hansford, S., Marsden, G., 1995. Temporal variation in egg and larval productivity *of Penaeus monodon* eyestalk ablated spawners. J. World Aquacult. Soc. 26, 396–405.
Hiransuchalert, R., Thamniemdee, N., Khamnamtong, B., Yamano, K., Klinbunga, S., 2013. Expression profiles and localization of vitellogenin mRNA and protein during ovarian development of the giant tiger shrimp *Penaeus monodon*. Aquaculture 412–413, 193–201.
Huberman, A., 2000. Shrimp endocrinology. A review. Aquaculture 191, 191–208.
Keys, S.J., Crocos, P.J., 2006. Domestication, growth and reproductive performance of wild, pond and tank-reared brown tiger shrimp *Penaeus esculentus*. Aquaculture 1–4, 232–240.
Klein, J.M., de Kleijn, D.P.V., Hunemeyer, G., Keller, R., Weidemann, W., 1993. Demonstration of the cellular expression of genes encoding molt-inhibiting hormone and crustacean hyperglycemic hormone in the eyestalk of the shore crab *Carcinus maenas*. Cell Tissue Res. 274, 515–519.
Kung, S.Y., Chan, S.M., Hui, J.H., Tsang, W.S., Mak, A., He, J.G., 2004. Vitellogenesis in the sand shrimp, *Metapenaeus ensis*: the contribution from the hepatopancreas-specific vitellogenin gene (MeVg2). Biol. Reprod. 71, 863–870.
Longyant, S., Sithigorngul, P., Thammapalerd, N., Sithigorngul, W., Menasveta, P., 2000. Characterization of vitellin and vitellogenin of giant tiger prawn *Penaeus monodon* using monoclonal antibodies specific to vitellin subunits. Invert. Reprod. Dev. 37, 211–221.
Marco, H.G., Gäde, G., 1999. A comparative immunocytochemcal study of the hyperglycemic, moult-inhibiting and vitellogenesis-inhibiting neurohormone family in three species of decapods crustacean. Cell Tissue Res. 295, 171–182.
Marsden, G., Richardson, N., Mather, P., Knibb, W., 2013. Reproductive behavioral differences between wild-caught and pond-reared *Penaeus monodon* prawn broodstock. Aquaculture 402–403, 141–145.
Menasveta, P., Sangpradub, S., Piyatiratitivorakul, S., Fast, A.W., 1994. Effects of broodstock size and source on ovarian maturation and spawning of giant tiger prawn *Penaeus monodon* Fabricius from Gulf of Thailand. J. World Aquacult. Soc. 25, 41–49.
Nagaraju, G.P.C., 2011. Reproductive regulators in decapods crustaceans: an overview. J. Exp. Biol. 214, 3–16.
Okumura, T., Yamano, K., Sakiyama, K., 2007. Vitellogenin gene expression and hemolymph vitellogenin during vitellogenesis, final maturation, and oviposition in female kuruma prawn, *Marsupenaeus japonicus*. Comp. Biochem. Physiol. 147A, 1028–1037.
Phiriyangkul, P., Utarabhand, P., 2006. Molecular characterization of a cDNA encoding vitellogenin in the banana shrimp, *Penaeus* (*Litopenaeus*) *merguiensis* and sites of vitellogenin mRNA expression. Mol. Reprod. Dev. 73, 410–423.
Phiriyangkul, P., Puengyam, P., Jakobsen, I.B., Utarabhand, P., 2007. Dynamics of vitellogenin mRNA expression during vitellogenesis in the banana shrimp *Penaeus* (*Fenneropenaeus*) *merguiensis* using real-time PCR. Mol. Reprod. Dev. 74, 1198–1207.
Ramachandra Reddy, P., Kiranmayi, P., Thanuja Kumari, K., Sreenivasula Reddy, P., 2006. 17α-Hydroxyprogesterone induced ovarian growth and vitellogenesis in the freshwater rice field crab *Oziotelphusa senex senex*. Aquaculture 254, 768–775.
Raviv, S., Parnes, S., Segall, C., Davis, C., Sagi, A., 2006. Complete sequence of *Litopenaeus vannamei* (Crustacea: Decapoda) vitellogenin cDNA and its expression in endocrinologically induced sub-adult females. Gen. Comp. Endocrinol. 145, 39–50.
Revathi, P., Iyapparaj, P., Munuswamy, N., Krishnan, M., 2012. Vitellogenesis during the ovarian development in freshwater female prawn *Macrobrachium resenbergii* (De Man). Int. J. Aqua. Sci. 3, 13–27.
Rotllant, G., De Kleijn, D., Charmantier-Daures, M., Charmantier, G., Van Herp, F., 1993. Localization of crustacean hyperglycemic hormone (CHH) and gonad-inhibiting hormone (GIH) in the eyestalk of *Homarus gammarus* larvae by immunocytochemistry and *in situ* hybridization. Cell Tissue Res. 271, 507–512.
Sappington, T.W., Raikhel, A.S., 1998. Molecular characteristics of insect vitellogenins and vitellogenin receptors. Insect Biochem. Mol. Biol. 28, 277–300.
Sithigorngul, P., Panchan, N., Vilaivan, T., Sithigorngul, W., Petsom, A., 1999. Immunochemical analysis and immunocytochemical localization of crustacean hyperglycemic hormone from the eyestalk of *Macrobrachium resenbergii*. Comp. Biochem. Physiol. 124B, 73–80.
Spaziani, E., Wang, W.L., Novy, L.A., 1995. Serum high-density lipoproteins in the crab *Cancer antennaris*—IV. Electrophoretic and immunological analyses of apolipoproteins and a question of female-specific lipoproteins. Comp. Biochem. Physiol. 111B, 265–276.
Tan-Fermin, J.D., Pudadera, R.A., 1989. Ovarian maturation stages of the wild giant tiger prawn, *Penaeus monodon* Fabricius. Aquaculture 77, 229–242.
Tiu, S.H., Hui, J.H., He, J.G., Tobe, S.S., Chan, S.M., 2006. Characterization of vitellogenin in the shrimp *Metapenaeus ensis*: expression studies and hormonal regulation of MeVg1 transcription *in vitro*. Mol. Reprod. Dev. 73, 424–436.
Tiu, S.H., Benzie, J., Chan, S.M., 2008. From hepatopancreas to ovary: molecular characterization of a shrimp vitellogenin receptor involved in the processing of vitellogenin. Biol. Reprod. 79, 66–74.
Treerattrakool, S., Panyim, S., Udomkit, A., 2011. Induction of ovarian maturation and spawning in *Penaeus monodo*n broodstock by double-stranded RNA. Mar. Biotechnol. 13, 163–169.
Treerattrakool, S., Boonchoy, C., Urtgam, S., Panyim, S., Udomkit, A., 2014. Functional characterization of recombinant gonad-inhibiting hormone (GIH) and implication of antibody neutralization on induction of ovarian maturation in marine shrimp. Aquaculture 428–429, 166–173.
Tsang, W.S., Quackenbush, L.S., Chow, B.K., Tiu, S.H., He, J.G., Chan, S.M., 2003. Organization of the shrimp vitellogenin gene: evidence of multiple genes and tissue specific expression by the ovary and hepatopancreas. Gene 303, 99–109.
Tseng, D.Y., Chen, Y.N., Kou, G.H., Lo, C.F., Kuo, C.M., 2001. Hepatopancreas is the extraovarian site of vitellogenin synthesis in black tiger shrimp, *Penaeus monodon*. Comp. Biochem. Physiol. 129A, 909–917.
Tsutsui, N., Kawazoe, I., Ohira, T., Jasmani, S., Yang, W.J., Wilder, M.N., Aida, K., 2000. Molecular characterization of a cDNA encoding vitellogenin and its expression in the hepatopancreas and ovary during vitellogenesis in the Kuruma prawn, *Penaeus japonicus*. Zool. Sci. 17, 651–660.
Vaca, A., Alfaro, J., 2000. Ovarian maturation and spawning in the white shrimp, *Penaeus vannamei*, by serotonin injection. Aquaculture 182, 373–385.
Vazquez Boucard, C.G., Levy, P., Ceecaldi, H.J., Brogren, C.-H., 2002. Developmental changes in concentrations of vitellin, vitellogenin, and lipids in hemolymph, hepatopancreas, and ovaries from different ovarian stages of Indian white prawn *Fenneropenaeus indicus*. J. Exp. Mar. Biol. Ecol. 281, 63–75.
Waikhom, G., Pillai, S.M., 2011. Comparative reproductive performance of captive-reared Indian stocks of *Fenneropenaeus merguiensis* (De Man) with wild-caught broodstock. J. Inland Fish. Soc. India 43, 73–78.
Wilder, M.N., Okumura, T., Tsutsui, N., 2010. Reproductive mechanisms in crustacean focusing on selected prawn species: vitellogenin structure, processing and synthetic control. Aqua-BioSci. Monogr. 3, 73–110.
Wongprasert, K., Asuvapongpatana, S., Poltana, P., Tiensuwan, M., Withyachumnarnkul, B., 2006. Serotonin stimulates ovarian maturation and spawning in the black tiger shrimp *Penaeus monodon*. Aquaculture 261, 1447–1454.
Xie, S., Sun, L., Liu, F., Dong, B., 2009. Molecular characterization and mRNA transcript profile of vitellogenin in Chinese shrimp, *Fenneropenaeus chinensis*. Mol. Biol. Rep. 36, 389–397.
Yano, I., 1985. Induced ovarian maturation and spawning in greasyback shrimp, *Metapenaeus ensis*, by progesterone. Aquaculture 47, 223–229.
Yano, I., 1992. Effect of thoracic ganglion on vitellogenin secretion in kuruma prawn, *Penaeus japonicus*. Bull. Natl. Res. Inst. Aquacult. 21, 9–14.
Yano, I., 1998. Hormonal control of vitellogenesis in penaeid shrimp. In: Flegel, T.W. (Ed.), Advances in Shrimp Biotechnology. Proceedings to the Special Session on Shrimp Biotechnology 5th Asian Fisheries Forum, November 11–14,1998. National Center for Genetic Engineering and Biotechnology, Bangkok, Chiengmai, Thailand, pp. 29–31.
Yano, I., Tsukimura, B., Sweeney, J.N., Wyban, J.A., 1998. Induced ovarian maturation of *Penaeus vannamei* by implantation of lobster ganglion. J. World Aquacult. Soc. 19, 204–209.

# 8. Molecular cloning and characterization of Mj-mov-10, a putative RNA helicase involved in RNAi of kuruma shrimp.

Fish & Shellfish Immunology 44 (2015) 241–247

Contents lists available at ScienceDirect

Fish & Shellfish Immunology

journal homepage: www.elsevier.com/locate/fsi

Full length article

# Molecular cloning and characterization of Mj-mov-10, a putative RNA helicase involved in RNAi of kuruma shrimp

Amnat Phetrungnapha [a], Hidehiro Kondo [b], Ikuo Hirono [b], Sakol Panyim [c, d], Chalermporn Ongvarrasopone [c, *]

[a] Department of Biochemistry, Faculty of Medical Science, Naresuan University, Phitsanulok 65000, Thailand
[b] Laboratory of Genome Science, Graduate School of Tokyo University of Marine Science and Technology, Minato, Tokyo, Japan
[c] Institute of Molecular Biosciences, Mahidol University, Phutthamonthon 4 Road, Salaya, Nakhon Pathom 73170, Thailand
[d] Department of Biochemistry, Faculty of Science, Mahidol University, Rama VI Road, Phayathai, Bangkok 10400, Thailand

ARTICLE INFO

*Article history:*
Received 27 November 2014
Received in revised form
15 February 2015
Accepted 16 February 2015
Available online 24 February 2015

*Keywords:*
RISC
White spot syndrome virus
Double stranded RNA
RNAi
Shrimp

ABSTRACT

Identification and characterization of the RNAi-related genes is the key to understanding RNAi mechanism in shrimp. In this study, we have identified and characterized a novel putative RNA helicase gene, *Mj-mov*-10 from the kuruma shrimp, *Marsupenaeus japonicus* and its implication in shrimp RNAi was demonstrated. The full-length *Mj-mov-10* gene contained 3536 bp, including 239 bp of 5′UTR, 2895 bp of the open reading frame (ORF) and 402 bp of 3′UTR, respectively. An ORF of *Mj-mov-10* could be translated to a 109-kDa protein which consists of a single helicase core domain containing seven signature motifs of the RNA helicase superfamily-1. Mj-MOV-10 protein shared 47% and 40% identity with mammalian MOV-10 and plant SDE3, respectively. Expression of *Mj-mov-10* gene was significantly up-regulated upon dsRNA and white spot syndrome virus (WSSV) challenge. *In vivo* gene knockdown of *Mj-mov-10* resulted in an increase of a susceptibility of shrimp to WSSV infection. Our results implied the functional significance of Mj-MOV-10 in dsRNA-mediated gene silencing and antiviral defense mechanism in shrimp.


## 1. Introduction

Discovery of RNA interference (RNAi) in penaeid shrimp provides great benefits for research and application in this economically important aquaculture species. RNAi is a post-transcriptional gene silencing mechanism in eukaryotes. This mechanism utilizes double-stranded RNAs (dsRNA), including short-interfering RNAs (siRNA) and microRNAs (miRNA) as a guide to target mRNAs in a sequence specific manner and inactivate the encoded gene by mRNA degradation or translational repression [1,2]. RNAi regulates gene expression in several cellular processes such as cell cycle, cell death, cellular metabolism, signal transduction, and development [3–6]. In invertebrates, RNAi is employed as a major defense system against viruses [7,8]. Several studies demonstrated that induction of shrimp RNAi pathway by using either siRNA or long dsRNA corresponding to viral genes can inhibit viral infection, such as white spot syndrome virus (WSSV), yellow head virus (YHV), and *Penaeus monodon* densovirus [9–12]. Therefore, RNAi has been considered as a new promising tool for developing an approach for sustainable shrimp cultivation. In addition, RNAi has also been employed for studying gene function in shrimp. Genes involved in shrimp cellular processes such as immune system [13,14], apoptosis [15], endocytosis [16], development [17], and molting [18] were silenced by using RNAi for functional characterization. Even though, RNAi has been widely used in research and application in shrimp, the mechanism by which the RNAi operates in shrimp cells is not yet completely understood. Two key proteins in shrimp RNAi pathway, Dicer and Argonaute (AGO), were identified and characterized [19–22]; however, there are still many questions remaining about additional protein players involved in this pathway and the mechanisms of action at each step. Therefore, identification and characterization of the RNAi-related genes is the key to understanding RNAi mechanism in shrimp.

Moloney leukemia virus 10 (MOV-10) was first identified as a GTP-binding protein which prevents Moloney murine leukemia virus infection in mice [23]. It belongs to the UPF1-like family of the

* Corresponding author. Institute of Molecular Biosciences, Mahidol University (Salaya Campus), 25/25 Phutthamonthon 4 Rd., Salaya, Phutthamonthon district, Nakhon Pathom 73170, Thailand. Tel.: +66 2 800 3624x1280; fax: +66 2 4419906.
*E-mail address:* chalermporn.ong@mahidol.ac.th (C. Ongvarrasopone).

http://dx.doi.org/10.1016/j.fsi.2015.02.028
1050-4648/

ATP-dependent RNA helicase superfamily 1 (SF-1) [24]. MOV-10 is a homolog of silencing defective protein 3 (SDE3), a protein which is necessary for post-transcriptional gene silencing in *Arabidopsis* [25]. Armitage, a *Drosophila* homolog of MOV-10, was identified as a component of the RNA-induced silencing complex (RISC) which required for RISC maturation and RISC activity [26]. MOV-10 was also reported to be an essential component of RISC in human. It is a P-body marker protein which interacts and co-localizes with AGO1 and AGO2, and is required for miRNA-guided mRNA cleavage *in vivo* [27,28]. It has been recently reported that a homolog of MOV-10 which is specifically expressed in germ cells, MOV-10-like 1 protein (MOV-10L1), interacts with the Piwi proteins, MILI and MIWI, and plays a crucial role in piRNA-directed retrotransposon silencing in mouse [29]. In addition, MOV-10 was found to be a cellular factor that is involved in the replication process of RNA viruses. Perturbation of MOV-10 expression inhibits human hepatitis delta virus and HIV-1 replications [30,31]. However, the controversial data revealed that MOV-10 overexpression substantially decreased the production of infectious retrovirus particles [32].

As mentioned earlier, identification and characterization of the RNAi-related genes is the key to understanding RNAi mechanism in shrimp. In this study, a novel putative RNA helicase gene, Moloney leukemia virus 10 from kuruma shrimp, *Marsupenaeus japonicus* (*Mj-mov-10*) was identified and characterized. The expression of *Mj-mov-10* gene in response to dsRNA administration and WSSV challenge was studied. The functional significance of *Mj-mov-10* was also investigated in order to implicate the role of Mj-MOV-10 in shrimp RNAi pathway.

## 2. Materials and methods

### 2.1. Experimental shrimp

The kuruma shrimps, *M. japonicus* (~10 g body weight) were purchased from a local commercial shrimp farm in Miyazaki, Japan. They were reared in the laboratory tanks containing artificial seawater with continuous aeration. Water temperature and salinity were maintained at ~25 °C and 30 ppt, respectively. Shrimps were fed *ad libitum* for a week with the commercial shrimp feed to acclimate the laboratory condition.

### 2.2. Cloning of the full-length Mj-mov-10 cDNA

The partial sequence of *Mj-mov-10* was preliminarily identified from an in-house *M. japonicus* cDNA library. Rapid Amplification of the cDNA Ends (RACE) was performed in order to obtain the full-length *Mj-mov-10* cDNA. Shrimp hemocytes were prepared as described by Hipolito et al. [33]. Total RNA was extracted from shrimp hemocytes by using RNAiso (Takara) following the manufacturer's instruction. RACE-PCR was performed using SMARTer® RACE 5′/3′ kit (Clontech). Briefly, Total RNA (1 μg) was reverse transcribed to cDNA. Reverse transcription was performed in a 20-μl reaction with 5′-CDS primer A and SMARTer® II A oligonucleotide (Clontech), according to the manufacturer's instruction. cDNA was subsequently used for 5′RACE. The first 5′RACE-PCR was performed with 5-mov-R1 primer and universal primer mix (UPM; Clontech). The nested 5′RACE-PCR was performed with 5-mov-R2 primer and UPM. For 3′RACE-PCR, cDNA was synthesized by using reverse transcription with 3′-CDS primer, following the manufacturer's instruction. The first 3′RACE-PCR was performed with UPM and 3-mov-F1. The nested 3′RACE-PCR was performed with UPM and 3-mov-F2. All primers used for RACE-PCR are listed in Table 1. The PCR products from 5′ and 3′RACE-PCR were purified from the gel by using QIAquick gel extraction kit (Qiagen). The purified PCR products were cloned into pGEM®-T Easy vector (Promega) and subsequently subjected for DNA sequencing.

### 2.3. Sequence analysis

The nucleotide and deduced amino acid sequences of *Mj-mov-10* were compared with the known sequences in the GenBank database using blastn and blastp, respectively. The protein domain features of *Mj-mov-10* were predicted by using Conserved Domain Architecture Retrieval Tool (CDART) [34]. Molecular weight and isoelectric point of the protein were predicted by tools in the Expasy website (www.expasy.org). Multiple sequence alignment (MSA) and phylogenetic analysis were performed by using MEGA 5.05 [35]. Phylogenetic tree was constructed based on Neighbor-joining methods with Bootstrap values of 1000.

### 2.4. Tissue distribution study

Expression of *Mj-mov-10* in different shrimp tissues was evaluated by RT-PCR. Tissues including hemocytes, lymphoid organ, gills, hepatopancreas, stomach, and muscle were dissected out from healthy shrimps ($n = 3$) and flash frozen in liquid nitrogen. Total RNA was then extracted as described above. One microgram of total RNA was used for cDNA synthesis. Reverse transcription was performed with M-MLV reverse transcriptase (Invitrogen) and oligo-dT primer (Table 1), following the manufacturer's protocol. RT-PCR was performed with MOV10-F and MOV10-R primers under the following condition: denaturation at 94 °C for 5 min, followed by 28 cycles of 94 °C for 30 s, 55 °C for 30 s, and 72 °C for 30 s. The final extension was carried out at 72 °C for 7 min. PCR products were analyzed by using agarose gel electrophoresis, stained with ethidium bromide, and visualized under UV light. *EF1-α* was used as an internal control gene in this study.

### 2.5. Preparation of double-stranded RNA

Double-stranded RNA corresponding to *Mj-mov-10* (dsMOV-10) was designed. The target site of dsMOV-10 located at nucleotide 1414-1808 of the *Mj-mov-10* gene. The dsMOV-10 was synthesized by *in vitro* transcription using T7 RiboMAX™ Express Large Scale RNA Production System (Promega), following the manufacturer's instructions. Briefly, sense and anti-sense DNA template strands for *in vitro* transcription were synthesized by PCR using a set of primers containing T7 RNA polymerase promoter sequences (primers; dsMOV-FT7 and dsMOV-R for sense DNA template and dsMOV-F and dsMOV-RT7 for antisense DNA template, Table 1). Each of the sense and anti-sense DNA template strands was purified and used for single-stranded RNA (ssRNA) synthesis. Then, DNA templates were removed by incubating with RQ1 DNase (Promega). Equal amount of the sense and anti-sense ssRNA were combined and annealed to produce dsRNA by incubating at 95 °C for 2 min. Then, the temperature was decreased to 25 °C at the rate of 0.1 °C/s and hold at 25 °C for 30 min. The remaining ssRNA was subsequently degraded by incubating with RNase A (US Biological). The dsMOV-10 was further purified by using RNAiso (Takara), according to the manufacturer's instructions. For non-specific dsRNA, bacterial expression system was used for synthesis of dsRNA corresponding to green fluorescent protein (dsRNA-GFP or dsGFP), as described by Ongvarrasopone et al. [36]. The quality and quantity of dsRNAs were determined by agarose gel electrophoresis and NanoDrop Lite spectrophotometer (Thermo Scientific), respectively.

**Table 1**
Primers used in this study. T7 promoter sequences are underlined.

| Primers | Sequences (5′ → 3′) | Experiments |
|---|---|---|
| PRT-oligo | CCGGAATTCAAGCTTCTAGAGGATCCTTTTTTTTTTTTTTTT | RT-PCR |
| 5-mov-R1 | CTGGAGTGACGTTGACTGATACAGTCC | 5′ RACE |
| 5-mov-R2 | GCCACTTCACTCTATGCTCTTCCGTCG | 5′ RACE |
| 3-mov-F1 | GCAGAACATCATCTCTGGGACC | 3′ RACE |
| 3-mov-F2 | GACCGTCACAGTTGTAGAGGCA | 3′ RACE |
| CDS-F | ATGAACAGAAGCTTACGATTTCTC | RT-PCR |
| CDS-R | CATGGCAGAGAGCCACTATTC | RT-PCR |
| MOV10-F | GAGGGATTCGTTCCTGGAATTG | RT-PCR, qRT-PCR |
| MOV10-R | TTGGCTTCATGTCGGACTTCAT | RT-PCR, qRT-PCR |
| EF1-F | ATTGCCACACCGCTCACA | RT-PCR, qRT-PCR |
| EF1-R | TCGATCTTGGTCAGCAGTTCA | RT-PCR, qRT-PCR |
| dsMOV-FT7 | TAATACGACTCACTATAGGCTGAAGAAGACTCTCTGGCTCG | dsRNA synthesis |
| dsMOV-R | TGCCTCTACAACTGTGACGGTC | dsRNA synthesis |
| dsMOV-F | CTGAAGAAGACTCTCTGGCTCG | dsRNA synthesis |
| dsMOV-RT7 | TAATACGACTCACTATAGGTGCCTCTACAACTGTGACGGTC | dsRNA synthesis |
| VP28–F | ATGAAAACCTCCGCATTCCTG | WSSV detection |
| VP28-R | CCAAGGTGTCGCTGTCAAAG | WSSV detection |

### 2.6. In vivo gene silencing

*In vivo* gene silencing of *Mj-mov-10* was conducted by injecting 20 μg of dsMOV-10 (2 μg per g of shrimp) via intramuscular injection. Expression of *Mj-mov-10* in hemocytes was verified by RT-PCR before and 1, 3, and 5 days post dsRNA injection. Shrimp injected with dsGFP were used as a control group. Total RNA extraction and cDNA synthesis were performed as described above. qRT-PCR was then used for determination of the silencing effect of dsMOV-10. qRT-PCR was performed in an ABI 7500 real-time detection system (Applied Biosystems) by using Thunderbird™ SYBR® qPCR mix (Toyobo) with MOV10-F and MOV10-R primers. *EF1-α* was used as an internal control gene for normalization. qRT-PCR was carried out in triplicate for each sample in a 20-μl reaction containing 10 μl of Thunderbird™ SYBR® qPCR mix, 5 μl of 1:50 diluted cDNA, 0.2 μM each of the primers, 0.4 μl of 50X ROX reference dye, and sterile water up to 20 μl qRT-PCR was performed under the following conditions: enzyme activation at 95 °C for 3 min, followed by 40 cycles of 95 °C for 10 s and 60 °C for 31 s. The specificity of primers was determined by melting curve analysis from the ABI Prism 7500 detection system. The expression ratio of each gene was determined by comparative Ct method ($2^{-\Delta\Delta Ct}$) [37].

### 2.7. Gene expression analysis

To determine the temporal expression of *Mj-mov-10* mRNA upon dsRNA administration, shrimps ($n = 5$) were intramuscularly injected with 20 μg dsGFP. Hemolymph was collected individually before and 3, 6, 9, 12, 24, 48, 72, and 96 h post injection (hpi). The temporal expression of *Mj-mov-10* upon WSSV infection was also evaluated. Shrimps ($n = 5$) were intramuscularly injected with 100 μl of WSSV ($10^{-5}$ dilution). Viral dilution corresponding to LD50 condition was prepared as described by Maningas et al. [38]. Hemolymph was collected individually before and 3, 6, 12, 24, 48 and 72 hpi. Shrimps injected with PBS ($n = 5$) were used as a control group for both experiments. Total RNA extraction, reverse transcription and qRT-PCR of *Mj-mov-10* were performed as described above. *EF1-α* was used as an internal control gene for normalization. The expression ratio of each gene was determined by comparative Ct method ($2^{-\Delta\Delta Ct}$). RT-PCR of *vp28* gene of WSSV using primers; VP28-F and VP28-R (Table 1) was performed under the following condition: denaturation at 94 °C for 5 min, followed by 28 cycles of 94 °C for 30 s, 55 °C for 30 s, and 72 °C for 30 s. The final extension was carried out at 72 °C for 7 min.

### 2.8. Cumulative mortality assay

To further investigate the functional significance of *Mj-mov-10* during WSSV infection, cumulative mortality assay was performed. First, shrimp were divided into four groups ($n = 18$/group), including PBS→PBS, PBS → WSSV, dsMOV-10 → WSSV, and dsGFP → WSSV. Then, the dsMOV-10 → WSSV and dsGFP → WSSV groups were injected with 20 μg of dsMOV-10 and dsGFP, respectively. Three days later, they were challenged with 100 μl of WSSV ($10^{-5}$ dilution). The control groups PBS → PBS and PBS → WSSV were injected with PBS. Three days later, they were injected with PBS, or challenged with WSSV ($10^{-5}$ dilution), respectively. Cumulative mortality was recorded daily for 10 days after WSSV challenge. The experiment was performed in duplicate. Amplification of *vp28* gene of WSSV was performed as described above.

### 2.9. Statistical analysis

The data from qRT-PCR was expressed as mean ± standard error of mean (SEM). The statistical analysis was performed using one-way ANOVA in Sigma Stat 3.5 program. The probability ($p$) value less than 0.05 ($p < 0.05$) was generally accepted as statistical significance.

## 3. Results

### 3.1. Cloning of the full-length Mj-mov-10 gene

A partial sequence of *Mj-mov-10* gene of 1656 bp was previously identified from an in-house *M. japonicus* hemocytes cDNA library. Therefore, 5′ and 3′ RACE-PCR were performed to obtain the full-length cDNA of this gene. The DNA fragments of 510 bp and 1750 bp were obtained from 5′ and 3′ RACE-PCR, respectively (data not shown). After combining with a partial sequence of *Mj-mov-10* from cDNA library, the full-length *Mj-mov-10* gene was obtained and contained 3536 bp, including 239 bp of 5′UTR, 2895 bp of the open reading frame (ORF) and 402 bp of 3′UTR, respectively. The entire ORF of *Mj-mov-10* gene could be amplified, confirming the cloning and sequencing results (Supplementary Fig. 1). Kozak's sequence and polyadenylation signal were also identified (Supplementary Fig. 2). The ORF encoded the polypeptide of 964 amino acids, with a molecular weight of 109.7 kDa and p*I* of 7.87. Motif scanning by cDART demonstrated that Mj-MOV-10 protein composed of a single helicase core domain. The full-length cDNA of

*Mj-mov-10* gene was submitted to the GenBank under the accession number **KP128064**.

### 3.2. Sequence and phylogenetic analysis

Amino acid sequences of MOV-10 and its homologs were retrieved from GenBank database. Multiple sequence alignment of the helicase core domain revealed that Mj-MOV-10 contains seven conserved motifs of the RNA helicase superfamily 1, including motif I (aa 510–517), Ia (aa 534–549), II (aa 630–633), III (aa 654–662), IV (aa 711–716), V (aa 836–844), and VI (aa 879–884) (Fig. 1). The nucleotide triphosphate-binding and hydrolysis motifs are located in motif I, II, and VI. The nucleic acid-binding motif are located in motif Ia, III, IV and V. Mj-MOV-10 shared 47% amino acid sequence identity with mammalian MOV-10, and 48% identity with *Gallus gallus* and *Xenopus tropicalis* MOV-10. *Arabidopsis* and rice SDE shared 40% identity with Mj-MOV-10. In addition, the *Drosophila* Armitage shared only 31% identity with Mj-MOV-10. Phylogenetic analysis revealed that Mj-MOV-10 formed a sister group with vertebrate MOV-10 (Fig. 2). In addition, plant SDE3 formed a sister group with animal MOV-10 clade. Armitage was found to be clustered in a different clade of MOV-10 and SDE3.

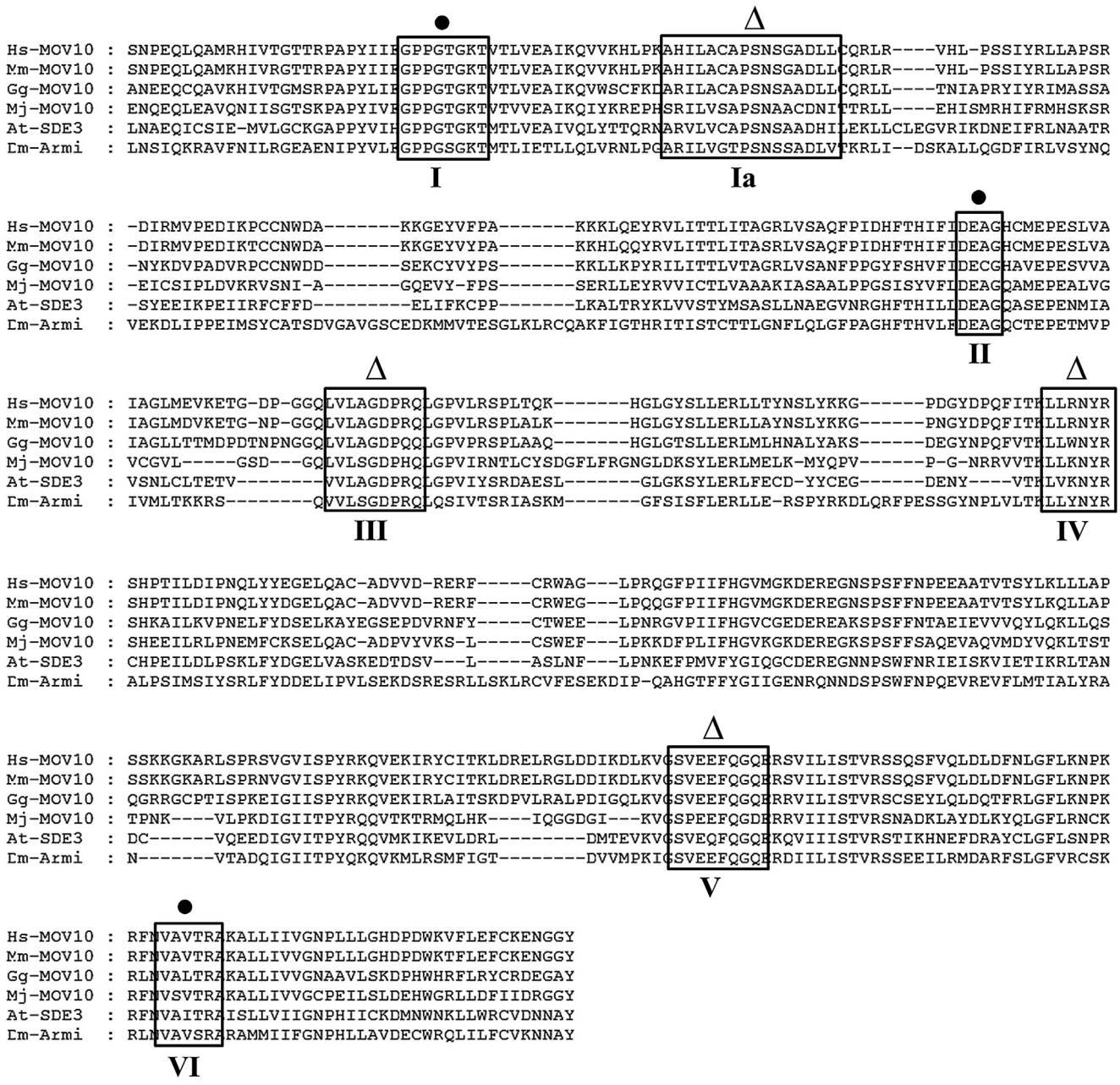


**Fig. 1.** Multiple sequence alignment of the helicase domain (amino acid 485–916) from shrimp MOV-10 and the representative MOV-10 homologs by Clustal W. Seven conserved motifs of the RNA helicase superfamily 1, including I (aa 510–517), Ia (aa 534–549), II (630–633), III (654–662), IV (aa 711–716), V (aa 836–844), and VI (aa 879–884). The conserved motifs are boxed. The circles (●) represent the nucleotide triphosphate-binding and hydrolysis motifs. The triangles (Δ) represent the nucleic acid-binding motif. GenBank accession number of each species is in the parenthesis: *Homo sapiens*, Hs-MOV-10 (NP_001123551.1); *Mus musculus* MOV-10, Mm-MOV-10 (NP_001156912.1); *Gallus gallus* MOV-10, Gg-MOV-10 (NP_001012861.1); *Marsupenaeus japonicus* MOV-10, Mj-MOV-10 (**KP128064**); *Arabidopsis thaliana* SDE3, At-SDE3 (NP_172037.1); *Drosophila melanogaster* Armitage, Dm-Armi (NP_647816.2).

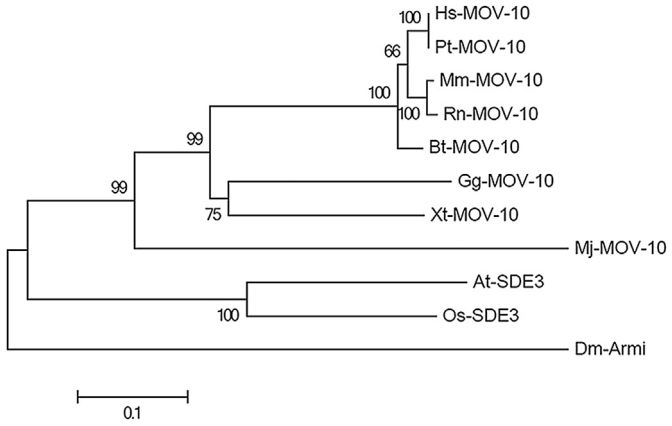


**Fig. 2.** Phylogenetic analysis of MOV-10 proteins and homologs. The Neighbor-joining tree was constructed based on multiple sequence alignment of the helicase domain with bootstrap value of 1000. GenBank accession number of each species is in the parenthesis: *Homo sapiens*, Hs-MOV-10 (NP_001123551.1); *Pan troglodytes*, Pt-MOV-10 (XP_513630.3); *Mus musculus*, Mm-MOV-10 (NP_001156912.1); *Rattus norvegicus*, Rn-MOV-10 (NP_001101181.1); *Bos taurus*, Bt-MOV-10 (NP_001069307.1); *Gallus gallus*, Gg-MOV-10 (NP_001012861.1); *Xenopus tropicalis*, Xt-MOV-10 (XP_002932163.1); *Arabidopsis thaliana*, At-SDE3 (NP_172037.1); *Oryza sativa*, Os-SDE3 (NP_001049037.1); *Drosophila melanogaster*, Dm-Armi (NP_647816.2); *Marsupenaeus japonicus*, Mj-MOV-10 (**KP128064**).

### 3.3. Tissue distribution study

By using RT-PCR, the result demonstrated that *Mj-mov-10* mRNA was expressed in all examined tissues, including hemocytes, lymphoid organ, gills, hepatopancreas, stomach, and muscle at similar levels of expression. The representative gel of *Mj-mov-10* tissue distribution study is shown in Fig. 3.

### 3.4. Mj-mov-10 up-regulated upon dsRNA and WSSV challenge

Temporal expression of *Mj-mov-10* mRNA in response to dsRNA administration and WSSV challenge was determined by using qRT-PCR. The results demonstrated that the expression of *Mj-mov-10* in shrimp hemocytes was up-regulated upon dsRNA administration (Fig. 4A). Its expression level was significantly increased at 9 dpi and then reached the peak at 48 hpi ($p < 0.05$). Similar result was observed when shrimp were challenged with WSSV (Fig. 4B). Expression of *Mj-mov-10* in shrimp hemocytes was gradually increased after WSSV challenge and then significantly increased to the peak at 72 hpi ($p < 0.05$). Expression of *vp28* gene confirmed that shrimp was infected by WSSV (Supplementary Fig. 3).

### 3.5. Gene silencing of Mj-mov-10 increased shrimp mortality

The dsRNA corresponding to *Mj-mov-10* (dsMOV-10) was designed and used for *in vivo* gene silencing in shrimp. The results in Fig. 5 showed that expression of *Mj-mov-10* was significantly

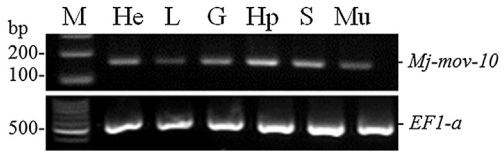


**Fig. 3.** mRNA expression of *Mj-mov-10* mRNA in different shrimp tissues. A representative gel represents RT-PCR products of *Mj-mov-10* and *EF1-α*. M, 100 bp DNA ladder; He, hemolymph; L, lymphoid organ; G, gill; Hp, hepatopancreas; S, stomach; Mu, abdominal muscle.

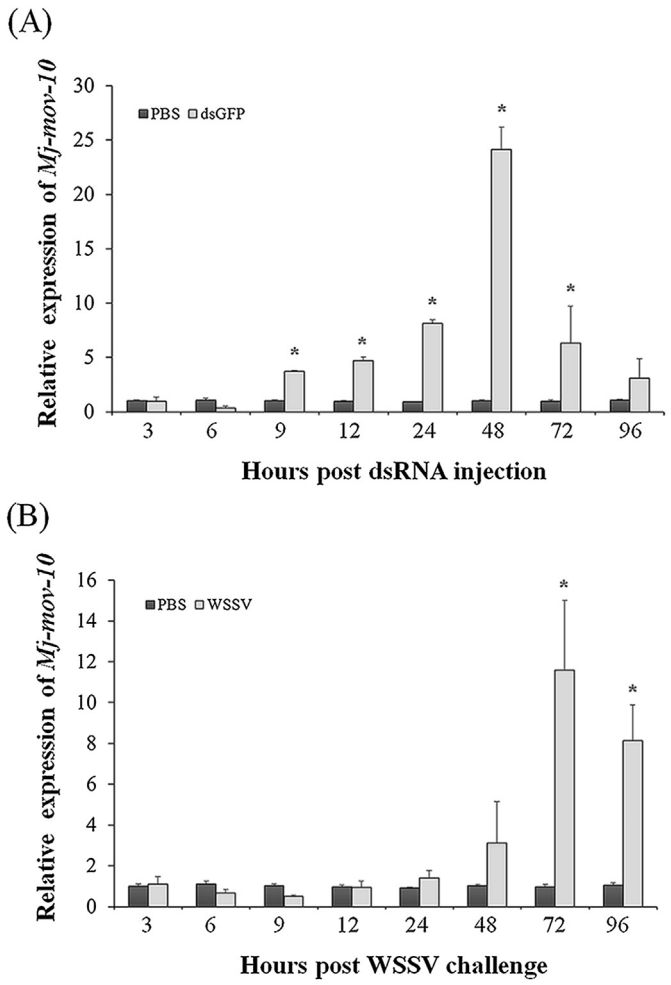


**Fig. 4.** Temporal mRNA expression of *Mj-mov-10*mRNA upon dsRNA administration (A) and WSSV challenge (B). *Mj-mov-10* expression in shrimp hemocytes ($n = 3$) was validated at 0, 3, 6, 9, 12, 24, 48, 72 and 96 hpi by using qRT-PCR. *EF1-α* was used as an internal control gene. The expression of *Mj-mov-10* was calculated by using comparative Ct method ($2^{-\Delta\Delta Ct}$). The data were analyzed by one-way ANOVA and presented as mean ± S.E. Asterisks indicate significant differences between experimental and control PBS groups ($p < 0.05$).

decreased upon dsMOV-10 injection ($p < 0.05$), while no silencing effect was observed in shrimp injected with non-specific dsRNA, dsGFP. *Mj-mov-10* was most effectively silenced at 3 days-post dsMOV-10 injection, as 67% reduction of *Mj-mov-10* expression was observed when compared to that of the control. Subsequently, cumulative mortality assay was performed to observe the effect of *Mj-mov-10* silencing on WSSV infection. Three days after silencing *Mj-mov-10*, shrimp were challenged with WSSV. The results in Fig. 6 demonstrated that shrimp injected with dsMOV-10 followed by WSSV (dsMOV-10 → WSSV) died more rapidly than the WSSV control group (PBS → WSSV). Shrimp injected with dsMOV-10 → WSSV showed more than 80% cumulative mortality at day-5 post infection and almost 100% died at day-6 post infection. In contrast, shrimp injected with PBS → WSSV showed 61% cumulative mortality at day-5 and almost 100% died at day-9 post infection. In addition, injection of dsGFP could significantly protect shrimp from WSSV infection, as 58% cumulative mortality was observed in dsGFP → WSSV group at day-10 post infection. Significance difference ($p < 0.05$) among dsMOV-10 → WSSV group and the control groups (PBS → WSSV and dsGFP → WSSV) was shown by ANOVA. Expression of *vp28* of WSSV was observed in all

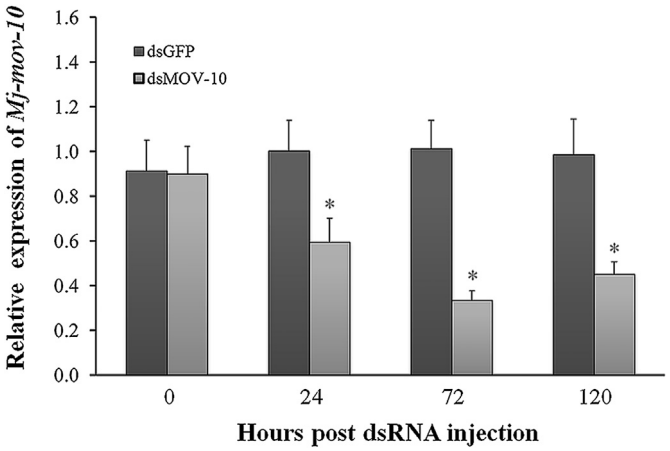


**Fig. 5.** *In vivo* gene silencing of *Mj-mov-10* in shrimp. Twenty micrograms of dsMOV-10 was injected into shrimp ($n = 3$). *Mj-mov-10* expression was validated at 0, 1, 3 and 5 dpi by using qRT-PCR. *EF1-α* was used as an internal control gene. Shrimp injected with dsGFP were used as a control group. The expression of *Mj-mov-10* was calculated by using comparative Ct method ($2^{-\Delta\Delta Ct}$). The data were analyzed by one-way ANOVA and presented as mean ± S.E. Asterisks indicate significant differences between experimental and control groups ($p < 0.05$).

death shrimp from dsMOV-10 → WSSV group (Supplementary Fig. 4).

## 4. Discussion

RNA helicases are the most abundant group of enzymes involved in RNA metabolism in eukaryotes [39]. RNA helicases have been implicated in transcription, RNA degradation, gene regulation, RNA export, and RNAi [40]. In this study, the novel RNA helicase gene, Moloney leukemia virus 10 from *M. japonicus* (*Mj-mov-10*) was identified, and its implication in shrimp RNAi pathway was also investigated. The *Mj-mov-10* ORF could be translated into a polypeptide which contains a single helicase core domain. By using multiple sequence alignment, seven signature helicase motifs in helicase core domain, including I, Ia, II, III, IV, V, and VI was observed, suggesting that Mj-MOV-10 belonged to the RNA helicase superfamily-1 (SF-1) [24]. SF-1 helicase separates RNA–RNA or DNA–RNA duplex into single strands in an ATP-dependent reaction. Seven conserved motifs of SF-1 helicase directly participate in nucleotide triphosphate-binding and hydrolysis (motif I, II and VI) and RNA binding and recognition (Ia, III, IV, and V) [24,41]. Phylogenetic analysis indicated that Mj-MOV-10 is closely related to vertebrate MOV-10, and plants SDE3 forms a sister group with MOV-10 clade. Surprisingly, Armitage, a *Drosophila* homolog of MOV-10, was located on different clade of MOV-10 and SDE3. Our result indicates that Armitage is a protein in SF-1 helicase which shares low sequence similarity with MOV-10 and SDE3 rather than a homolog.

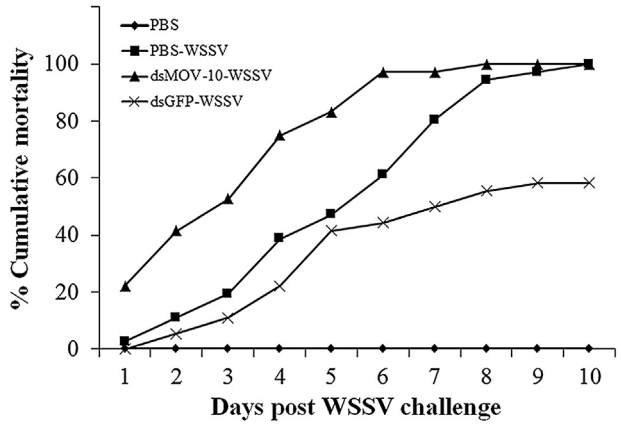


**Fig. 6.** Gene silencing of *Mj-mov-10* increases the susceptibility of shrimp to WSSV. Shrimp were divided into four groups ($n = 18$). WSSV was injected into positive control (PBS → WSSV), non-specific dsRNA control (dsGFP → WSSV) and *Mj-mov-10*-silenced groups (dsMOV-10 → WSSV). The untreated shrimps (PBS → PBS) were used as a negative control group. Cumulative mortality was observed for 10 days after WSSV challenged. The data were analyzed by one-way ANOVA and expressed as mean of two sets of experiment.

Induction of proteins in an RNAi pathway is required for an efficient RNAi mechanism. An induction of DCL-2 (Dicer-like protein) and QDE-2 (Argonaute-like protein) expression by dsRNA was required for an effectiveness of dsRNA-meditaed gene silencing in *Neurospora crassa* [42]. In addition, up-regulation of RNAi-related genes upon dsRNA administration such as *LvAgo2, LvSid-1, LvPasha* and *PmAgo3* was previously demonstrated in shrimp [20,43,44]. Similarly, if Mj-MOV-10 is involved in the mechanism of shrimp RNAi pathway, its expression would be modified during the course of dsRNA injection. The result showed that *Mj-mov-10* expression was significantly increased after dsRNA injection, suggesting the involvement of Mj-MOV-10 in dsRNA-mediated gene silencing mechanism. In human, MOV-10 is one of the RISC components and is essential for miRNA-mediated gene silencing. It associates with AGO1 and AGO2 protein and co-localizes to P-bodies [27,28]. In *Arabidopsis*, SDE3, a homolog of MOV-10, is essential for post-transcriptional gene silencing (PTGS). *Arabidopsis* plants carrying mutations at the *SDE3* locus have defective PTGS [25]. Recent work from Garcia et al. revealed that SDE3 interacted with AGO via its GW motifs, and acted downstream of RNA-dependent RNA polymerase 6 (RDR6) in amplified silencing [45].

Accumulating evidence demonstrates that RNAi plays a crucial role in an antiviral defense mechanism in penaeid shrimp. Several studies revealed that suppression of RNAi components significantly increases a susceptibility of shrimp to viral infection. For example, knockdown of *PmDicer-1* expression increased the viral load of gill-associated virus in *P. monodon* [21]. Knockdown of TRBP, a protein partner of Dicer, and eIF6, a component of RISC, resulted in an increase of WSSV virion copies in *M. japonicus* [46]. Similar result was also observed in this study. Shrimp injected with dsMOV-10 were more susceptible to WSSV infection than normal shrimp, as they died more rapidly after WSSV challenge. Recently, a shrimp miRNA, miR-7, has been shown to play a crucial role in an antiviral defense against WSSV infection by targeting the 3′UTR of the viral early gene, wsv447. Blocking of endogenous miR-7 by AMO-miR-7 resulted in an increase of WSSV genome copies in WSSV-infected shrimp [47]. In addition, suppression of miR-100 expression induced apoptosis and decreased WSSV genome copies in shrimp [48]. Referring to the model organism, MOV-10 plays an important role in miRNA pathway by acting as a P-body marker protein that associates with the Argonaute proteins, the core component of the RISC [27,28]. It is plausible that silencing of *Mj-mov-10* might disrupt or interfere the proper functions of the RNAi-related proteins, especially in RISC and P-bodies. An increase of the susceptibility of shrimp to WSSV might come from the failure of miRNA-mediated gene silencing to protect shrimp from viral infection.

In this study, the up-regulation of *Mj-mov-10* expression was demonstrated upon WSSV challenge. In human, MOV-10 has also been reported to be a type I interferon-stimulated genes [30]. Overexpression of MOV-10 inhibits a wide range of retrovirus replication, including HIV-1, simian immunodeficiency virus, murine leukemia virus, and equine infectious anemia virus [49]. Whether Mj-MOV-10 functions as an inhibitor of viral replication in shrimp remained to be elucidated.

In summary, *Mj-mov-10*, a novel putative RNA helicase gene from *M. japonicus* was identified and characterized. The results demonstrated the functional significance of Mj-MOV-10 in shrimp RNAi pathway and WSSV infection. This study expands an understanding of the RNAi mechanisms in penaeid shrimp. Further study is required for better understanding of the underlying mechanism of Mj-MOV-10 in shrimp RNAi pathway.

## Acknowledgment

This project is supported by the Office of the Higher Education Commission and Mahidol University under the National Research Universities Initiative and grants from the Thailand Research Fund (RSA5480002 and BRG5780006 to C.O. and DPG5680001 to S.P.).

## Appendix A. Supplementary data

Supplementary data related to this article can be found at http://dx.doi.org/10.1016/j.fsi.2015.02.028.

## References

[1] Carthew RW, Sontheimer EJ. Origins and mechanisms of miRNAs and siRNAs. Cell 2009;136:642–55.
[2] Meister G, Tuschl T. Mechanisms of gene silencing by double-stranded RNA. Nature 2004;431:343–9.
[3] Rottiers V, Naar AM. MicroRNAs in metabolism and metabolic disorders. Nat Rev Mol Cell Biol 2012;13:239–50.
[4] Sayed D, Abdellatif M. MicroRNAs in development and disease. Physiol Rev 2011;91:827–87.
[5] Subramanian S, Steer CJ. MicroRNAs as gatekeepers of apoptosis. J Cell Physiol 2010;223:289–98.
[6] Carleton M, Cleary MA, Linsley PS. MicroRNAs and cell cycle regulation. Cell Cycle 2007;6:2127–32.
[7] Sabin LR, Hanna SL, Cherry S. Innate antiviral immunity in *Drosophila*. Curr Opin Immunol 2010;22:4–9.
[8] Ding SW, Voinnet O. Antiviral immunity directed by small RNAs. Cell 2007;130:413–26.
[9] Attasart P, Kaewkhaw R, Chimwai C, Kongphom U, Namramoon O, Panyim S. Inhibition of *Penaeus monodon* densovirus replication in shrimp by double-stranded RNA. Arch Virol 2010;155:825–32.
[10] Xu J, Han F, Zhang X. Silencing shrimp white spot syndrome virus (WSSV) genes by siRNA. Antivir Res 2007;73:126–31.
[11] Tirasophon W, Yodmuang S, Chinnirunvong W, Plongthongkum N, Panyim S. Therapeutic inhibition of yellow head virus multiplication in infected shrimps by YHV-protease dsRNA. Antivir Res 2007;74:150–5.
[12] Yodmuang S, Tirasophon W, Roshorm Y, Chinnirunvong W, Panyim S. YHV-protease dsRNA inhibits YHV replication in *Penaeus monodon* and prevents mortality. Biochem Biophys Res Commun 2006;341:351–6.
[13] Amparyup P, Wiriyaukaradecha K, Charoensapsri W, Tassanakajon A. A clip domain serine proteinase plays a role in antibacterial defense but is not required for prophenoloxidase activation in shrimp. Dev Comp Immunol 2010;34:168–76.
[14] Shockey JE, O'Leary NA, de la Vega E, Browdy CL, Baatz JE, Gross PS. The role of crustins in *Litopenaeus vannamei* in response to infection with shrimp pathogens: an in vivo approach. Dev Comp Immunol 2009;33:668–73.
[15] Rijiravanich A, Browdy CL, Withyachumnarnkul B. Knocking down caspase-3 by RNAi reduces mortality in Pacific white shrimp *Penaeus (Litopenaeus) vannamei* challenged with a low dose of white-spot syndrome virus. Fish Shellfish Immunol 2008;24:308–13.
[16] Ongvarrasopone C, Chanasakulniyom M, Sritunyalucksana K, Panyim S. Suppression of PmRab7 by dsRNA inhibits WSSV or YHV infection in shrimp. Mar Biotechnol (NY) 2008;10:374–81.
[17] Lee JH, Momani J, Kim YM, Kang CK, Choi JH, Baek HJ, et al. Effective RNA-silencing strategy of Lv-MSTN/GDF11 gene and its effects on the growth in shrimp, *Litopenaeus vannamei*. Comp Biochem Physiol B Biochem Mol Biol 2014;179C:9–16.
[18] Hui JH, Tobe SS, Chan SM. Characterization of the putative farnesoic acid O-methyltransferase (LvFAMeT) cDNA from white shrimp, *Litopenaeus vannamei*: evidence for its role in molting. Peptides 2008;29:252–60.
[19] Yang L, Li X, Jiang S, Qiu L, Zhou F, Liu W, et al. Characterization of Argonaute2 gene from black tiger shrimp (*Penaeus monodon*) and its responses to immune challenges. Fish Shellfish Immunol 2014;36:261–9.
[20] Phetrungnapha A, Ho T, Udomkit A, Panyim S, Ongvarrasopone C. Molecular cloning and functional characterization of Argonaute-3 gene from *Penaeus monodon*. Fish Shellfish Immunol 2013;35:874–82.
[21] Su J, Oanh DT, Lyons RE, Leeton L, van Hulten MC, Tan SH, et al. A key gene of the RNA interference pathway in the black tiger shrimp, *Penaeus monodon*: identification and functional characterisation of Dicer-1. Fish Shellfish Immunol 2008;24:223–33.
[22] Unajak S, Boonsaeng V, Jitrapakdee S. Isolation and characterization of cDNA encoding Argonaute, a component of RNA silencing in shrimp (*Penaeus monodon*). Comp Biochem Physiol B Biochem Mol Biol 2006;145:179–87.
[23] Mooslehner K, Muller U, Karls U, Hamann L, Harbers K. Structure and expression of a gene encoding a putative GTP-binding protein identified by provirus integration in a transgenic mouse strain. Mol Cell Biol 1991;11:886–93.
[24] Fairman-Williams ME, Guenther UP, Jankowsky E. SF1 and SF2 helicases: family matters. Curr Opin Struct Biol 2010;20:313–24.
[25] Dalmay T, Horsefield R, Braunstein TH, Baulcombe DC. SDE3 encodes an RNA helicase required for post-transcriptional gene silencing in Arabidopsis. EMBO J 2001;20:2069–78.
[26] Tomari Y, Du T, Haley B, Schwarz DS, Bennett R, Cook HA, et al. RISC assembly defects in the *Drosophila* RNAi mutant armitage. Cell 2004;116:831–41.
[27] Landthaler M, Gaidatzis D, Rothballer A, Chen PY, Soll SJ, Dinic L, et al. Molecular characterization of human Argonaute-containing ribonucleoprotein complexes and their bound target mRNAs. RNA 2008;14:2580–96.
[28] Meister G, Landthaler M, Peters L, Chen PY, Urlaub H, Luhrmann R, et al. Identification of novel argonaute-associated proteins. Curr Biol 2005;15:2149–55.
[29] Zheng K, Xiol J, Reuter M, Eckardt S, Leu NA, McLaughlin KJ, et al. Mouse MOV10L1 associates with Piwi proteins and is an essential component of the Piwi-interacting RNA (piRNA) pathway. Proc Natl Acad Sci U S A 2010;107:11841–6.
[30] Schoggins JW, Wilson SJ, Panis M, Murphy MY, Jones CT, Bieniasz P, et al. A diverse range of gene products are effectors of the type I interferon antiviral response. Nature 2011;472:481–5.
[31] Furtak V, Mulky A, Rawlings SA, Kozhaya L, Lee K, Kewalramani VN, et al. Perturbation of the P-body component Mov10 inhibits HIV-1 infectivity. PLoS One 2010;5:e9081.
[32] Serquina AK, Das SR, Popova E, Ojelabi OA, Roy CK, Gottlinger HG. UPF1 is crucial for the infectivity of human immunodeficiency virus type 1 progeny virions. J Virol 2013;87:8853–61.
[33] Hipolito SG, Shitara A, Kondo H, Hirono I. Role of *Marsupenaeus japonicus* crustin-like peptide against *Vibrio penaeicida* and white spot syndrome virus infection. Dev Comp Immunol 2014;46:461–9.
[34] Geer LY, Domrachev M, Lipman DJ, Bryant SH. CDART: protein homology by domain architecture. Genome Res 2002;12:1619–23.
[35] Kumar S, Nei M, Dudley J, Tamura K. MEGA: a biologist-centric software for evolutionary analysis of DNA and protein sequences. Brief Bioinform 2008;9:299–306.
[36] Ongvarrasopone C, Roshorm Y, Panyim S. A simple and cost effective method to generate dsRNA for RNAi studies in invertebrates. ScienceAsia 2007;33:35–9.
[37] Pfaffl MW. A new mathematical model for relative quantification in real-time RT-PCR. Nucleic Acids Res 2001;29:e45.
[38] Maningas MB, Kondo H, Hirono I, Saito-Taki T, Aoki T. Essential function of transglutaminase and clotting protein in shrimp immunity. Mol Immunol 2008;45:1269–75.
[39] Anantharaman V, Koonin EV, Aravind L. Comparative genomics and evolution of proteins involved in RNA metabolism. Nucleic Acids Res 2002;30:1427–64.
[40] Ambrus AM, Frolov MV. The diverse roles of RNA helicases in RNAi. Cell Cycle 2009;8:3500–5.
[41] Cheng Z, Muhlrad D, Lim MK, Parker R, Song H. Structural and functional insights into the human Upf1 helicase core. EMBO J 2007;26:253–64.
[42] Choudhary S, Lee HC, Maiti M, He Q, Cheng P, Liu Q, et al. A double-stranded-RNA response program important for RNA interference efficiency. Mol Cell Biol 2007;27:3995–4005.
[43] Chen YH, Zhao L, Jia XT, Li XY, Li CZ, Yan H, et al. Isolation and characterization of cDNAs encoding Ars2 and Pasha homologues, two components of the RNA interference pathway in *Litopenaeus vannamei*. Fish Shellfish Immunol 2012;32:373–80.
[44] Labreuche Y, Veloso A, de la Vega E, Gross PS, Chapman RW, Browdy CL, et al. Non-specific activation of antiviral immunity and induction of RNA interference may engage the same pathway in the Pacific white leg shrimp *Litopenaeus vannamei*. Dev Comp Immunol 2010;34(11):1209–18.
[45] Garcia D, Garcia S, Pontier D, Marchais A, Renou JP, Lagrange T, et al. Ago hook and RNA helicase motifs underpin dual roles for SDE3 in antiviral defense and silencing of nonconserved intergenic regions. Mol Cell 2012;48:109–20.
[46] Wang S, Chen AJ, Shi LJ, Zhao XF, Wang JX. TRBP and eIF6 homologue in *Marsupenaeus japonicus* play crucial roles in antiviral response. PLoS One 2012;7:e30057.
[47] Huang T, Zhang X. Functional analysis of a crustacean microRNA in host-virus interactions. J Virol 2012;86:12997–3004.
[48] Yang L, Yang G, Zhang X. The miR-100-mediated pathway regulates apoptosis against virus infection in shrimp. Fish Shellfish Immunol 2014;40:146–53.
[49] Izumi T, Burdick R, Shigemi M, Plisov S, Hu WS, Pathak VK. Mov10 and APOBEC3G localization to processing bodies is not required for virion incorporation and antiviral activity. J Virol 2013;87:11047–62.

# 9. Successful yellow head virus infection of *Penaeus monodon* requires clathrin heavy chain.

Aquaculture 435 (2015) 480–487

Contents lists available at ScienceDirect

Aquaculture

journal homepage: www.elsevier.com/locate/aqua-online

# Successful yellow head virus infection of *Penaeus monodon* requires clathrin heavy chain

Pratsaneeyaporn Posiri [a], Hidehiro Kondo [b], Ikuo Hirono [b], Sakol Panyim [a,c], Chalermporn Ongvarrasopone [a,*]

[a] Institute of Molecular Biosciences, Mahidol University (Salaya Campus), Nakhon Pathom 73170 Thailand
[b] Laboratory of Genome Science, Tokyo University of Marine Science and Technology, Tokyo, Japan
[c] Department of Biochemistry, Faculty of Science, Mahidol University, Bangkok 10400, Thailand

ARTICLE INFO

*Article history:*
Received 31 August 2014
Received in revised form 10 October 2014
Accepted 12 October 2014
Available online 22 October 2014

*Keywords:*
Yellow head virus
Endocytosis
Double stranded RNA
RNAi
Black tiger shrimp

ABSTRACT

Viral disease caused by the Yellow head virus (YHV) had great impact on economic loss in the aquaculture industry. Prevention or curing YHV disease is still not possible due to the lack of understanding of the basic mechanisms of YHV infection. In this report, the endocytosis inhibitors (chlorpromazine (CPZ), amiloride and methyl-β-cyclodextrin (MβCD)) were used to identify the cellular entry pathway of YHV. Pretreating shrimp with CPZ but not amiloride or MβCD followed by YHV challenge resulted in a significant reduction of YHV levels, suggesting that YHV entered the shrimp cells via clathrin-mediated endocytosis. Next, the major component of the clathrin-coated vesicle, *Penaeus monodon* clathrin heavy chain (*Pm*CHC) was cloned and characterized. The complete coding sequence of PmCHC is 5055 bp encoding a putative protein of 1684 amino acids. Specific silencing of PmCHC mRNA by dsRNA-PmCHC showed an inhibition of YHV replication for 48 h post YHV injection as well as exhibiting a delay in shrimp mortality. These results indicated that PmCHC was an essential component for YHV infection of shrimp cells.



## 1. Introduction

Yellow head virus (YHV) is one of the most devastating shrimp pathogens as it causes mortality within 3 days. This virus was first identified in 1992 from moribund shrimp from southern Thailand (Boonyaratpalin et al., 1993). The virus was named from symptoms of the disease in which the moribund shrimp would present a yellowish cephalothorax and very sallow overall coloration. YHV can infect various penaeid shrimp such as *Penaeus aztecus*, *Penaeus duorarum*, *Penaeus merguiensis*, *Penaeus monodon*, *Penaeus setiferus*, *Penaeus stylirostris* and *Litopenaeus vannamei* (Flegel, 1997). The infected moribund shrimp shows nuclear condensation as well as pyknosis and karyorrhexis which are signs of cell apoptosis (Khanobdee et al., 2002). YHV has a positive-sense single-stranded RNA genome of approximately 27 kb with a poly (A) tail. It belongs to the genus *Okavirus*, family *Roniviridae* in the order *Nidovirales*. The morphology of YHV reveals an enveloped bacilliform which has a particle size about 50–60 × 190–200 nm, containing the internal helical nucleocapsid which is closely surrounded by an envelope studded with prominent peplomers or spikes (Nadala et al., 1997; Sittidilokratna et al., 2008). YHV contains two major structural transmembrane glycoproteins (gp116 and gp64) and a nucleoprotein (p20) (Jitrapakdee et al., 2003). Antiserum against the gp116 but not gp64 can neutralize YHV infectivity in the primary lymphoid cells of *Penaeus monodon* (Assavalapsakul et al., 2005). In addition, injection of double-stranded RNA (dsRNA) targeting to the YHV-binding protein, YRP65, inhibited YHV replication (Assavalapsakul et al., 2006). Also, suppression of PmRab7 (a late endosomal marker involved in trafficking) resulted in inhibition of YHV replication (Ongvarrasopone et al., 2008). These results imply that for successful infection, YHV requires receptor mediated endocytosis as a route of entry and takes advantage of the host cell machineries for endosomal trafficking and replication. Therefore, better understanding of the endocytosis and trafficking pathway of YHV will shed light on the mechanism of YHV infection and replication and thus will lead to the development of an antiviral agent or strategy to combat YHV infection.

Many viruses utilize well-characterized cellular endocytic mechanisms including clathrin-mediated endocytosis, lipid raft caveola-dependent endocytosis and macropinocytosis to internalize into host cells. For instance, several positive-sense ssRNA viruses such as severe acute respiratory syndrome virus (Inoue et al., 2007), hepatitis C, dengue and semliki forest virus use clathrin-mediated endocytosis (Marsh and Helenius, 2006; Meertens et al., 2006; Mercer et al., 2010) as a route of entry. In clathrin-mediated endocytosis, the cargo is trafficked through the cell via the coated vesicle which is surrounded by the polymerized clathrin in a basket-like structure. The formation of the endocytic clathrin-coated vesicles occurs through the interaction of clathrin, heterotetrameric adaptor protein-2 (AP-2), and several

* Corresponding author at: Institute of Molecular Biosciences, Mahidol University (Salaya Campus), 25/25 Phutthamonthon 4 Rd. Salaya, Phutthamonthon District, Nakhon Pathom 73170, Thailand. Tel.: +66 2 800 3624x1280; fax: +66 2 4419906.
*E-mail address:* chalermporn.ong@mahidol.ac.th (C. Ongvarrasopone).

http://dx.doi.org/10.1016/j.aquaculture.2014.10.018
0044-8486/

accessory proteins such as Epsin, Eps15, AP180/CALM and dynamin. Clathrin, in which the light chain and heavy chain form a unique structure called the clathrin triskelion, as well as AP-2 are recruited by epsin to the plasma membrane in response to receptor-mediated internalization signals. Epsin then mediates the assembly of a clathrin cage, which results in membrane curvature induced by the coated-pit formation. Once assembled, the clathrin-coated pits are pinched off from the plasma membrane by dynamin to form clathrin-coated vesicles which are then trafficked to endosomes (Doherty and McMahon, 2009; Mousavi et al., 2004). Whether YHV utilizes this pathway as a route of entry into shrimp cells remained to be investigated. Therefore, one purpose of this study was to characterize the YHV entry pathway by using several trafficking inhibitors. *P. monodon* clathrin heavy chain (*Pm*CHC), a major protein component in the clathrin-dependent pathway was cloned and characterized. The suppression effect of PmCHC in YHV-challenged shrimp also was investigated.

## 2. Materials and methods

### 2.1. P. monodon (black tiger shrimp) culture

Juvenile shrimp were obtained from Manoach's farm in Nakhon Pathom province, Thailand. Shrimp were sampled to determine that they were free from YHV and white spot syndrome virus (WSSV) infection using Diagnosis Strip Test YHV + WSSV (Pacific Biotech Co., Ltd, Thailand). In addition, shrimp were acclimatized for at least 5 days before use in experiments. They were maintained in large containers with oxygenated sea water at 5 ppt salinity before the experiment and fed with commercial feed every day. Half of the water was changed every 2 days.

### 2.2. Yellow head virus preparation

Virus stock was prepared from hemolymph of YHV infected moribund shrimp. The moribund shrimp showed signs of YHV infection for example, a yellowish cephalothorax. To confirm that the hemolymph was collected from the moribund shrimp infected with YHV not other viruses, total RNA was extracted and reverse transcription-PCR analysis was performed to detect the helicase gene of YHV and other viruses such as VP28 gene of WSSV. To prepare the viral stock, hemolymph was collected with AC-1 solution (27 mM Sodium citrate, 34.33 mM NaCl, 104.5 mM Glucose, 198.17 mM EDTA, pH 7.0), ratio 1:1, and the virus was obtained by ultracentrifugation (100,000 ×*g*) for 1 h. Viral pellet was dissolved in 150 mM NaCl and stored at −80 °C until use. The virus titer that causes 100% mortality within 3–4 days was used in this experiment.

### 2.3. Screening of YHV entry pathways by using drug inhibitors

The entry pathways of YHV were screened by using drug inhibitors. Various inhibitors of clathrin-dependent endocytosis, macropinocytosis and caveolar endocytosis such as chlorpromazine (CPZ), amiloride and methyl-β-cyclodextrin (MβCD), respectively, were employed at a dose of 0.25 mM $g^{-1}$ shrimp (9 shrimp per group). The inhibitors were injected into the hemolymph using 0.5 ml U-100 insulin syringe with 29 gauge needle. Injection of PBS was used as control. At 12 h post-injection, shrimp were challenged with YHV. Then at 24 h post YHV injection, gills from individual shrimp were collected to extract the total RNA and YHV levels were determined using quantitative RT-PCR.

### 2.4. Cloning of the full-length of P. monodon clathrin heavy chain (PmCHC)

Specific primers, cdfullCHC-F and cdfullCHC-R (Table 1), were used to amplify PmCHC from hemocytes of *P. monodon* and were designed based on the nucleotide sequences obtained from *Marsupenaeus japonicus* clathrin heavy chain. The cDNA of PmCHC coding sequences was amplified by using Taq DNA polymerase (New England Biolabs). The PCR was performed by hot-start at 95 °C for 5 min; 30 cycles of 95 °C for 30 s, 60 °C for 30 s, and 68 °C for 6 min; followed by 68 °C for 7 min. The cDNA was cloned into pGEM-T easy vector (Promega). The recombinant plasmid containing PmCHC was sequenced using T7, SP6, walkCHC-F1, walkCHC-F2, walkCHC-R1 as primers (Table 1) by First Base Co., Ltd. (Malaysia).

**Table 1**
Primer sequences used in the experiments.

| Primers | Sequences (5′- - → 3′) | Experiments |
|---|---|---|
| cdfullCHC-F | GGGGTACCATGACACAGGCGTTACCC | Full length PmCHC coding region |
| cdfullCHC-R | GGAATTCCATATGTTACATGCTGTAGCCTTG | Full length PmCHC coding region |
| walkCHC-F1 | TGTATTCTTCCCACCAGAGGC | Sequencing primers |
| walkCHC-F2 | ACGTCTGCCAGTTGTTGTGG | Sequencing primers |
| walkCHC-R1 | CCTTGAAGTGTGACTCTCGCC | Sequencing primers |
| mjCHC-F | AGTGCTTTGCTGAAACTGGTC | Partial PmCHC cDNA region |
| mjCHC-R | CATGAATACGAGATTCCAGCC *Xba*I | Partial PmCHC cDNA region |
| sCHC-F1 | GCTCTAGACGAAATGTAATGCGTGTC *Kpn*I | dsRNA-PmCHC construction |
| lpCHC-R1 | GGGGTACCCTATCTGCACTACAATCTGTAG *Eco*RI | dsRNA-PmCHC construction |
| asCHC-F2 | GGAATTCCGAAATGTAATGCGTGTC *Kpn*I | dsRNA-PmCHC construction |
| asCHC-R2 | GGGGTACCGACCAACCATTCTGGGTT | dsRNA-PmCHC construction |
| PmCHC-F | CTTCTCCCAAGAACCAGAGGTGCAC | Detection of PmCHC mRNA |
| PmCHC-R | ATTCCTCTTCTCCACCTCTTCCACC | Detection of PmCHC mRNA |
| PRT-oligo dT | CCGGAATTCAAGCTTCTAGAGGATCC$(T)_{16}$ | Reverse transcription |
| YHV(hel)-F | CAAGGACCACCTGGTACCGGTAAGAC | Detection of YHV mRNA |
| YHV(hel)-R | GCGGAAACGACTGACGGCTACATTCAC | Detection of YHV mRNA |
| PmActin-F | GACTCGTACGTGGGCGACGAGG | Detection of PmActin mRNA |
| PmActin-R | AGCAGCGGTGGTCATCTCCTGCTC | Detection of PmActin mRNA |
| qYHV-F | ATCATCAGCTCACAGGCAAGTTCC | Real time PCR |
| qYHV-R | GGGTCTAAATGGAGCTGGAAGACC | Real time PCR |
| EF-1α-F | GAACTGCTGACCAAGATCGACAGG | Real time PCR |
| EF-1α-R | GAGCATACTGTTGGAAGGTCTCCA | Real time PCR |

### 2.5. Sequence analysis

The nucleotide sequence analysis was performed with BLASTN (http://blast.ncbi.nlm.nih.gov). The deduced amino acid sequence of PmCHC was used to search the NCBI database (http://www.ncbi.nlm.nih.gov/Structure/cdd/wrpsb.cgi) to predict the conserved domains. Predictions of molecular weight and isoelectric point (pI) of the protein were performed by Expert Protein Analysis System (www.expasy.org). Sequences of proteins from several organisms were obtained from GenBank database. Multiple amino acid sequence alignments were performed by VectorNTI program (Invitrogen). Phylogenetic analysis (http://www.phylogeny.fr/version2_cgi/phylogeny.cgi) was based on the neighbor-joining method (Dereeper et al., 2008, 2010).

### 2.6. Construction of the recombinant plasmid expressing dsRNA-PmCHC

Recombinant plasmid containing stem-loop of dsRNA was constructed in pGEM-3Zf+ (Promega) and pET-17b (Novagen) vectors. Sense-loop region of the dsRNA was amplified from the first-strand cDNA by specific primers, sCHC-F1 and lpCHC-R1 (Table 1). The antisense region was amplified by asCHC-F2 and asCHC-R2 (Table 1). Both PCR fragments were gel-purified and subjected to restriction enzyme digestion. The purified fragment of the sense-loop was cloned into the linearized fragment of pGEM-3Zf+ (digested by *Xba*I and *Kpn*I). Then, this recombinant plasmid containing the sense-loop region of PmCHC

was digested by *Kpn*I and *Eco*RI and ligated with *Kpn*I and *Eco*RI digested antisense fragment. The recombinant plasmid containing sense-loop-antisense fragments of PmCHC (pGEM-3Zf+-PmCHC) was obtained. Then, the sense-loop-antisense fragment of PmCHC was subcloned into pET-17b vector at *Xba*I and *Eco*RI sites to construct recombinant plasmid pET17b-PmCHC which was used for dsRNA production by in vivo bacterial expression.

### 2.7. Production of dsRNA by in vivo bacterial expression

Recombinant plasmid pET17b-PmCHC was transformed into a RNase III mutant HT115 *Escherichia coli* strain. This strain is modified to express T7 RNA polymerase from an isopropyl-β-D thiogalactopyranoside (IPTG) inducible promoter. Therefore, dsRNAs can be produced in the HT115 bacterial host after induction with IPTG. Double-stranded RNA was extracted and purified as previously described (Ongvarrasopone et al., 2007; Posiri et al., 2013). The quality of dsRNA was characterized by ribonuclease digestion assay using RNase A and RNase III. dsRNA concentration was estimated by agarose gel electrophoresis by comparing to the intensity of 100 bp DNA marker.

### 2.8. Suppression of PmCHC by dsRNA-PmCHC

The knockdown effect of dsRNA-PmCHC was tested by injection of dsRNA into hemolymph. Shrimp were injected with 2.5 μg $g^{-1}$ shrimp of dsRNA-PmCHC or an unrelated gene of dsRNA-GFP dissolved in 150 mM NaCl. Injection of 150 mM NaCl was used as control. After 24 h post dsRNA injection, gills of individual shrimp were collected to extract total RNA. Suppression effect of dsRNA was analyzed by reverse-transcription PCR (RT-PCR) to determine PmCHC mRNA level. To study the knockdown effect of PmCHC in YHV-challenged shrimp, shrimp were injected with dsRNA-PmCHC for 24 h before YHV challenge. Forty-eight hours later, gills of individual shrimp were collected to extract total RNA to detect YHV (helicase gene) and PmCHC mRNA expression levels. PmActin mRNA was used as an internal control.

### 2.9. Shrimp mortality assay

The mortality of shrimp injected with dsRNA followed by YHV challenge were observed every 6 h. Shrimp were about 1 g with 15 shrimp per group. Three independent experiments were performed. Shrimp were injected with 150 mM NaCl, 2.5 μg $g^{-1}$ shrimp of dsRNA-PmCHC or dsRNA-GFP. After 24 h post injection, shrimp were challenged with YHV. Mortality was plotted every 12 h.

### 2.10. RNA isolation and RT-PCR analysis

Total RNA from gill tissues was isolated by Trizol® reagent (Molecular Research Center) following the manufacturer's procedure. The RNA concentration was measured by Nanodrop ND-1000 spectrophotometer (Nanodrop Technologies). Total RNA (2 μg) was used to generate first-strand cDNA by Improm-II™ reverse transcriptase (Promega) and PRT primer (Table 1). PmCHC mRNA level was amplified by primers; PmCHC-F1 and PmCHC-R1 (Table 1). PmActin mRNA expression, used as internal control, was amplified by specific primers, PmActin-F and PmActin-R1 (Table 1). Multiplex PCR for PmCHC and PmActin was performed according to this condition: 95 °C for 5 min; 25 cycles of 95 °C for 30 s, 60 °C for 30 s, and 72 °C for 45 s; followed by 72 °C for 7 min. YHV mRNA level was amplified using primers, YHV(hel)-F and YHV(hel)-R (Table 1). The multiplex PCR condition for YHV and PmActin was as above except that the annealing temperature was changed to 55 °C for 30 s. The PCR products were analyzed on 1.5% agarose gel. The intensity of each band after subtracting the background was quantified by using ImageJ analysis program (version 1.46r). The relative expression level of PmCHC and YHV was normalized with PmActin levels and expressed as an arbitrary unit.

### 2.11. Quantitative real time PCR (qPCR)

Total RNA 2 μg was used for the first-strand cDNA synthesis by Improm-II™reverse transcriptase (Promega) using PRT primer. Dilution of cDNA at 1:32 was mixed with qPCR reaction using KAPA™ SYBR®Fast master mix (2×) ABI Prism™ (KAPA Biosystems) following the manufacturer's protocol. qYHV-F and qYHV-R specific primers (Table 1) were used to amplify YHV mRNA; EF1-α (EF1α-F and EF1α-R) is used as internal control: 95 °C for 3 min; 40 cycles of 95 °C for 5 s, 60 °C for 30 s. The qPCR was analyzed in an ABI 7500 real-time detection system (Applied Biosystems). The cycle threshold (Ct) value of YHV and EF1-α was compared and calculated by $2^{-\Delta\Delta C}{}_T$ method (Livak and Schmittgen, 2001).

### 2.12. Statistical analysis

The relative mRNA levels of PmCHC or YHV normalized with PmActin and fold change in PmCHC expression were presented as mean ± SEM. Cumulative percent mortality was plotted as mean ± SEM. In addition, significant differences of each experimental group were tested by using analysis of variance (ANOVA). A probability ($P$) value of 0.05 was used to define significant difference.

## 3. Results

### 3.1. Analysis of YHV entry pathway

To identify the pathway for YHV internalization into shrimp cell, shrimp of about 2 g were pretreated with inhibitors of clathrin-mediated endocytosis (chlorpromazine, CPZ), macropinocytosis (amiloride) or the caveolar dependent pathway (methyl-β-cyclodextrin, MβCD), and this was followed by YHV challenge. All shrimp receiving inhibitors survived throughout the experiment. Quantitative RT-PCR of the shrimp pretreated with chlorpromazine showed a significant reduction of YHV mRNA levels, approximately 77%, when compared to the PBS-YHV injected group, whereas shrimp pretreated with amiloride and MβCD demonstrated no significant difference to the YHV control group (Fig. 1).

### 3.2. Cloning of PmCHC coding region and sequence analysis

The sequence of *M. japonicus* clathrin heavy chain was used to design specific-primers to amplify the full-length coding region of *P. monodon*

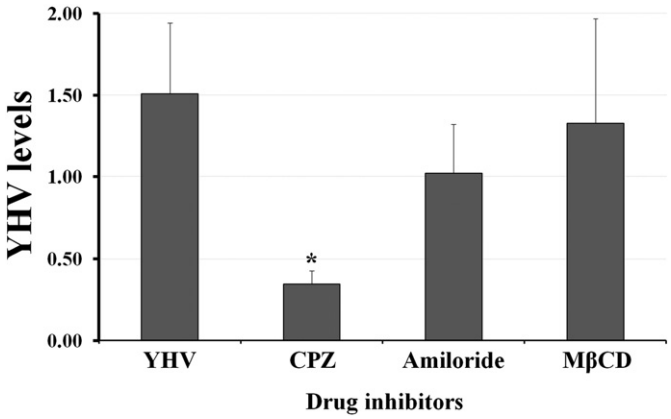


**Fig. 1.** Effect of inhibitors on YHV internalization into shrimp cell. Graphs represent the quantitative RT-PCR of YHV mRNA levels (fold change) of YHV-challenged shrimp pretreated with inhibitors which are chlorpromazine (CPZ), amiloride and methyl-β-cyclodextrin (MβCD). Nine shrimp per group were analyzed. (*) represents significant difference ($P < 0.05$) of YHV mRNA levels compared between the YHV- challenged groups pretreated with or without inhibitors.

**Table 2**
Accession number of organisms used for phylogenetic analysis.

| Organisms | Accession number |
|---|---|
| *Acromyrmex echinator* | EGI60613 |
| *Aedes aegypti* | XP_001656878 |
| *Bombyx mori* | NP_001136443 |
| *Bos taurus* | AAC48524 |
| *Ciona intestinalis* | XP_002130279 |
| *Culex quinquefasciatus* | EDS40945 |
| *Danaus plexippus* | EHJ79063 |
| *Danio rerio* | NP_001005391 |
| *Drosophila melanogaster* | NP_001096993 |
| *Gallus gallus* | NP_001073586 |
| *Glycine max* | AAC49294 |
| *Homo sapiens* | NP_004850 |
| *Medicago truncatula* | AES71175 |
| *Penaeus monodon* | KJ700941 |
| *Populus trichocarpa* | EEF02372 |
| *Rattus norvegicus* | AAA40874 |
| *Riptortus pedestris* | BAN20627 |
| *Sus scrofa* | NP_001139599 |
| *Theobroma cacao* | EOY34523 |
| *Tribolium castaneum* | XP_967829 |
| *Zea mays* | AGC82051 |

clathrin heavy chain from hemocytes. The open reading frame of PmCHC is 5055 bp, encoding a protein of 1684 amino acids, with an estimated molecular weight of 192.5 kDa and a pI of 5.53. The nucleotide sequence is deposited in the GenBank database under the accession number KJ700941. The protein contains several conserved domains: clathrin propeller repeat (amino acid: 205–241, 259–295, 303–337), clathrin heavy chain linker (amino acid 338–361), clathrin-H-link (amino acid 363–428), and clathrin heavy chain repeat homology (amino acid: 544–682, 693–831, 844–978, 986–1127, 1139–1275, 1281–1423, 1434–1572) (Supplementary Fig. 1). For most organisms (Table 2, Fig. 2), conserved domains of CHC consist of a seven CHC repeat homology, one CHC H-linker and one CHC linker. One clathrin propeller repeat is observed in plants including *Zea mays* and *Theobroma cacao*. However, three to four clathrin propeller repeats are found in both invertebrate and vertebrate species including *P. monodon*, *Aedes aegypti*, *Drosophila melanogaster*, *Homo sapiens* and *Danio rerio* (Table 2). Phylogenetic tree analysis clustered organisms in three groups which are plants, invertebrates and vertebrates. PmCHC was clustered into an invertebrate group (Fig. 3).

### 3.3. Production of dsRNA-PmCHC and its suppression effect

Recombinant plasmid pET17b containing a stem loop of PmCHC was constructed and transformed into HT115 *E. coli* strain to be used as template for *Pm*CHC dsRNA production (dsRNA-PmCHC) by in vivo bacterial expression. Then, hairpin dsRNA-PmCHC was extracted using an ethanol method (Posiri et al., 2013). The quality of dsRNA-PmCHC was characterized by ribonuclease III (RNase III) and by ribonuclease A (RNase A) digestion assay. DsRNA-GFP was also produced for nonspecific dsRNA injection. The hairpin dsRNA-PmCHC and dsRNA-GFP could be cleaved by RNase III but not by RNase A, suggesting that good quality dsRNA were obtained (Fig. 4A). Injection of dsRNA-PmCHC resulted in a significant reduction of PmCHC mRNA levels, approximately 90% when compared to the NaCl injected group ($P < 0.01$; $n = 5$). In contrast, no significant difference in PmCHC expression levels was observed between dsRNA-GFP- and NaCl-injected groups (Fig. 4B and 4C).

### 3.4. Suppression effect of PmCHC in YHV-challenged shrimp inhibited YHV mRNA levels

To determine whether PmCHC is required for YHV internalization into shrimp cells, the PmCHC-knockdown shrimp were challenged with YHV. After 48 h, gills were collected for total RNA extraction and RT-PCR analysis to determine mRNA expression of YHV and PmCHC. The results demonstrated the suppression effect of PmCHC, by dsRNA-PmCHC, and resulted in almost complete inhibition of YHV mRNA expression. However, high levels of YHV mRNA were still observed in both NaCl-injected and dsRNA-GFP injected groups (Fig. 5A and B).

### 3.5. Suppression of PmCHC in YHV-challenged shrimp delayed mortality

Shrimp receiving dsRNA-*Pm*CHC, followed by YHV challenge, reached 100% cumulative mortality at 120 h post YHV injection (hpi) whereas NaCl- and dsRNA-GFP-injected groups gave 100% mortality at 108 hpi. Furthermore, shrimp injected with dsRNA-PmCHC followed by YHV challenge showed significant reduction in cumulative percent mortality at 84–108 hpi when compared with the NaCl injection group (Fig. 6A). This result suggested that clathrin heavy chain is required for YHV infection. However, shrimp injected with dsRNA-PmCHC at 2.5 μg $g^{-1}$ shrimp without YHV challenge reached 100% mortality at 156 h post dsRNA injection whereas shrimp injected with NaCl or dsRNA-GFP showed no mortality (Fig. 6B). In addition, shrimp injected with dsRNA-PmCHC at lower dosage, 1.25 μg $g^{-1}$ shrimp,

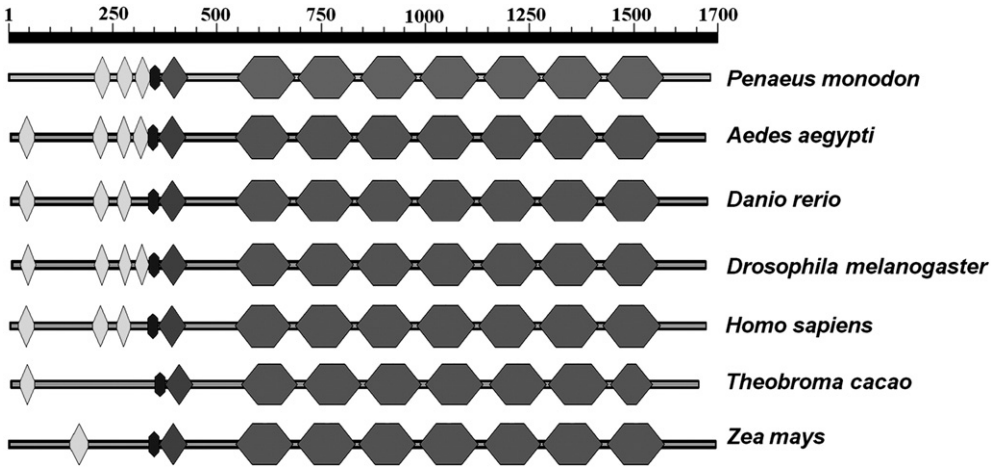


**Fig. 2.** Comparison of the clathrin heavy chain protein domains among several organisms. The protein domains comprising of clathrin propeller repeat (), clathrin heavy chain linker (), clathrin-H-link (), clathrin heavy chain repeat homology (). *Aedes aegypti*, *Drosophila melanogaster*, *Homo sapiens*, *Danio rerio*, *Zea mays* and *Theobroma cacao* were compared to *Penaeus monodon*.

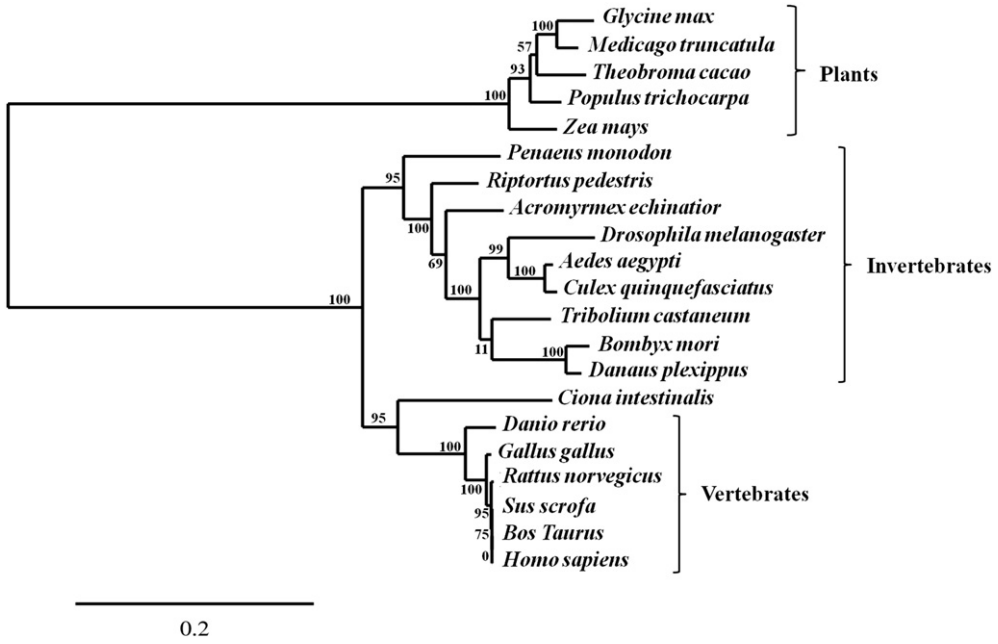


**Fig. 3.** Phylogenetic analysis of the clathrin heavy chain based on amino acid sequence of various species (*Glycine max*, *Medicago truncatula*, *Theobroma cacao*, *Populus trichocarpa*, *Zea mays*, *Penaeus monodon*, *Riptortus pedestris*, *Acromyrmex echinatior*, *Drosophila melanogaster*, *Aedes aegypti*, *Culex quinquefasciatus*, *Tribolium castaneum*, *Bombyx mori*, *Danaus plexippus*, *Ciona intestinalis*, *Danio rerio*, *Gallus gallus*, *Rattus norvegicus*, *Sus scrofa*, *Bos taurus*, and *Homo sapiens*) using neighbor-joining distance analysis. The GenBank accession numbers of CHC from each organism are in Table 2. Bootstrap values from 1000 replicates are indicated at the node.

without YHV challenge reached 100% mortality at a later time, 180 h post dsRNA injection. A 75% mortality was observed in shrimp injected with dsRNA-PmCHC at 0.63 μg $g^{-1}$ without YHV challenge during 144–240 h post dsRNA injection (Supplementary Fig. 2). Dead shrimp were sampled for viral load detection. The results showed that dsRNA-PmCHC → YHV group (Fig. 6C (b)) demonstrated lower YHV mRNA levels when compared to NaCl → YHV group (Fig. 6C (a)) and dsRNA-GFP → YHV group (Fig. 6C (c)). All dead shrimp except samples from lanes 2, 3, 8, 11, and 12 in the dsRNA-PmCHC → YHV group showed the presence of YHV. This suggested that the shrimps in lanes 2, 3, 8,

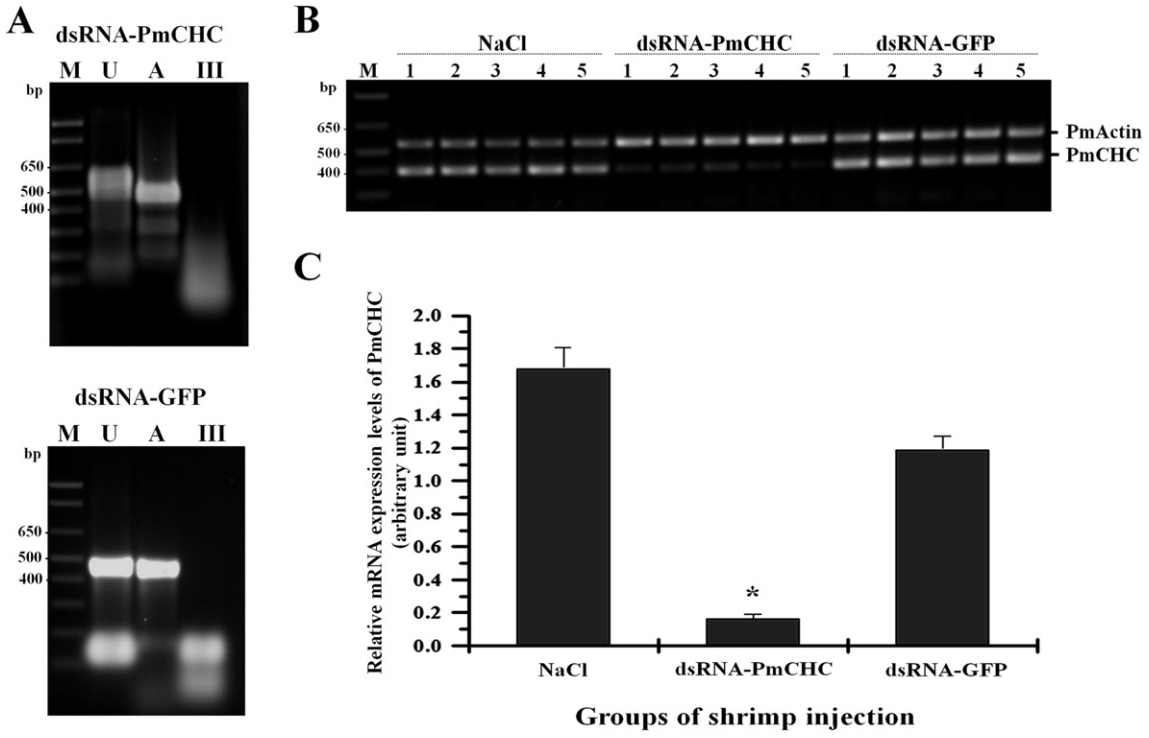


**Fig. 4.** Effectiveness of dsRNA-PmCHC on silencing of PmCHC mRNA. (A) Quality of dsRNA-PmCHC and dsRNA-GFP produced by in vivo bacterial expression. M is 1 kb plus DNA ladder. U, A and III are undigested dsRNA, dsRNA treated with RNase A and dsRNA treated with RNase III, respectively. (B) Representative agarose gel of RT-PCR products of PmCHC and PmActin expression of NaCl control, injected with dsRNA-PmCHC or dsRNA-GFP groups. M is 1 kb plus DNA marker. (C) The relative mRNA expression levels of PmCHC when normalized with PmActin are presented as mean ± SEM (n = 5). (*) Statistically significant difference between dsRNA-CHC compared to NaCl injected group ($P < 0.01$).

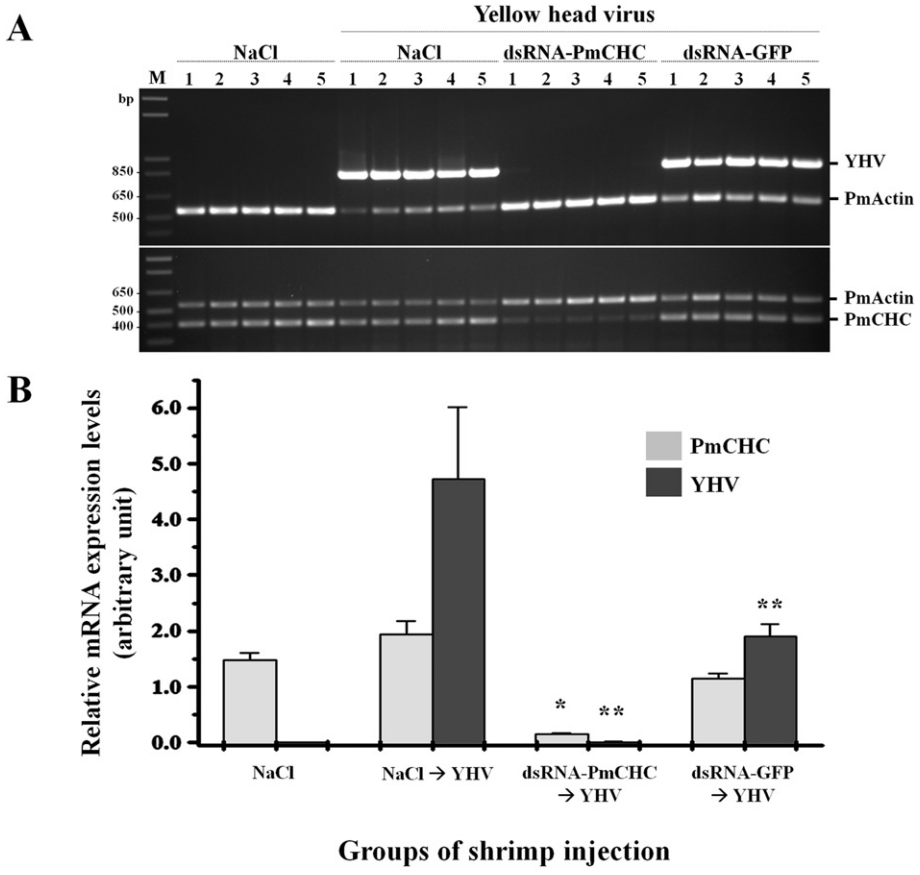


**Fig. 5.** Suppression effect of PmCHC upon YHV infection. (A) A representative gel of RT-PCR products of YHV (top panel) and PmCHC (bottom panel) mRNA levels. PmActin was used as an internal control. Shrimp were divided into 4 groups: NaCl alone and NaCl + YHV challenge, dsRNA-PmCHC + YHV challenge or dsRNA-GFP + YHV challenge (n = 5 per group). M is 1 kb plus DNA marker. (B) The relative mRNA expression levels of PmCHC (gray bar) and YHV normalized with PmActin (light black bar). Data is expressed as mean ± SEM in an arbitrary unit. (*) represents significant difference ($P < 0.05$) of PmCHC mRNA levels between dsRNA-PmCHC → YHV and NaCl injected group. (**) represents statistically significant difference ($P < 0.05$) of YHV mRNA levels between dsRNA-injected group and NaCl → YHV group.

11, and 12 were protected from YHV infection but were dead from the PmCHC knockdown. Taken together, the results strongly suggested that clathrin heavy chain is essential for YHV infection.

## 4. Discussion

Clathrin heavy chain (CHC) is a major protein in clathrin-coated pit and clathrin-coated vesicle. Clathrin heavy and light chains are assembled to form a three-legged structure, called a triskelion. Clathrin heavy chain together with adaptor and accessory proteins, including AP2, EPS15, AP-180, epsin or dynamin (McMahon and Boucrot, 2011; Mousavi et al., 2004; Young, 2007) are involved in endocytosis. The functions of clathrin heavy chain are believed to be involved in sorting cargo protein in the membrane and membrane curvature.

In black tiger shrimp, the role of clathrin heavy chain in virus infection has not been previously investigated. In this study, we have cloned *P. monodon* clathrin heavy chain (*Pm*CHC). The function of PmCHC especially for yellow head virus (YHV) infection was tested to study the major route for YHV internalization. RNA interference (RNAi) was used as a tool to study the function of PmCHC. Shrimp injected with dsRNA-PmCHC showed reduction of PmCHC mRNA levels up to 90% when compared to the NaCl-injected control group. In addition, knockdown of PmCHC mRNA in YHV-challenged shrimp exhibited low levels of YHV expression (Figs. 5 and 6C) and a delay in shrimp mortality up to 24 h post YHV injection (84–108 hpi) (Fig. 6A). These effects may be due to suppression of PmCHC gene (Fig. 6B and Supplementary Fig. 2). After knocking down of PmCHC mRNA, low levels of PmCHC present may slow down the entry of YHV into the cell, thus resulting in a delay of shrimp mortality. Moreover, the shrimp death may also be due to the depletion of clathrin heavy chain (Fig. 6B and Supplementary Fig. 2). This is because clathrin heavy chain has diverse cellular functions such as transportation of cargo inside the cell, cytokinesis and glucose metabolism (Brodsky, 2012). Depletion of PmCHC may inhibit some cellular functions which are essential for cell survival. Several studies have shown that some viruses require clathrin heavy chain for infection (Bhattacharyya et al., 2010; Hongliang and Chengyu, 2009; Hussain et al., 2011). For instance, confocal microscopy demonstrated the colocalization between rhesus rhadinovirus and clathrin heavy chain (Zhang et al., 2010). Similar to this study, suppression of the clathrin heavy chain by small interfering RNA exhibited a reduction of viral load in the host cells, including influenza A virus, severe acute respiratory syndrome coronavirus or human enterovirus 71 (Hongliang and Chengyu, 2009; Hussain et al., 2011; Inoue et al., 2007). It has been shown that the cargo molecules that can be transported via clathrin-meditated endocytosis are size dependent, approximately 200 nm (Rejman et al., 2004) which nicely fit with the YHV virion, whose size is ~50–60 × 190–200 nm (Nadala et al., 1997). In addition, a recent report showed the reduction of YHV level in clathrin coat AP17 knockdown shrimp (Jatuyosporn et al., 2014). Moreover, by using various inhibitors (CPZ, MβCD and amiloride), only the YHV-challenged shrimp pretreated with CPZ showed a significant reduction of YHV levels. These results suggested that the major route of YHV into the shrimp cells was via clathrin-mediated endocytosis pathway.

In shrimp, a previous study has identified a protein in the endocytosis pathway, *P. monodon* Rab7 (PmRab7) (Sritunyalucksana et al, 2006). Rab7 is a small GTPase protein and plays a crucial role to regulate the

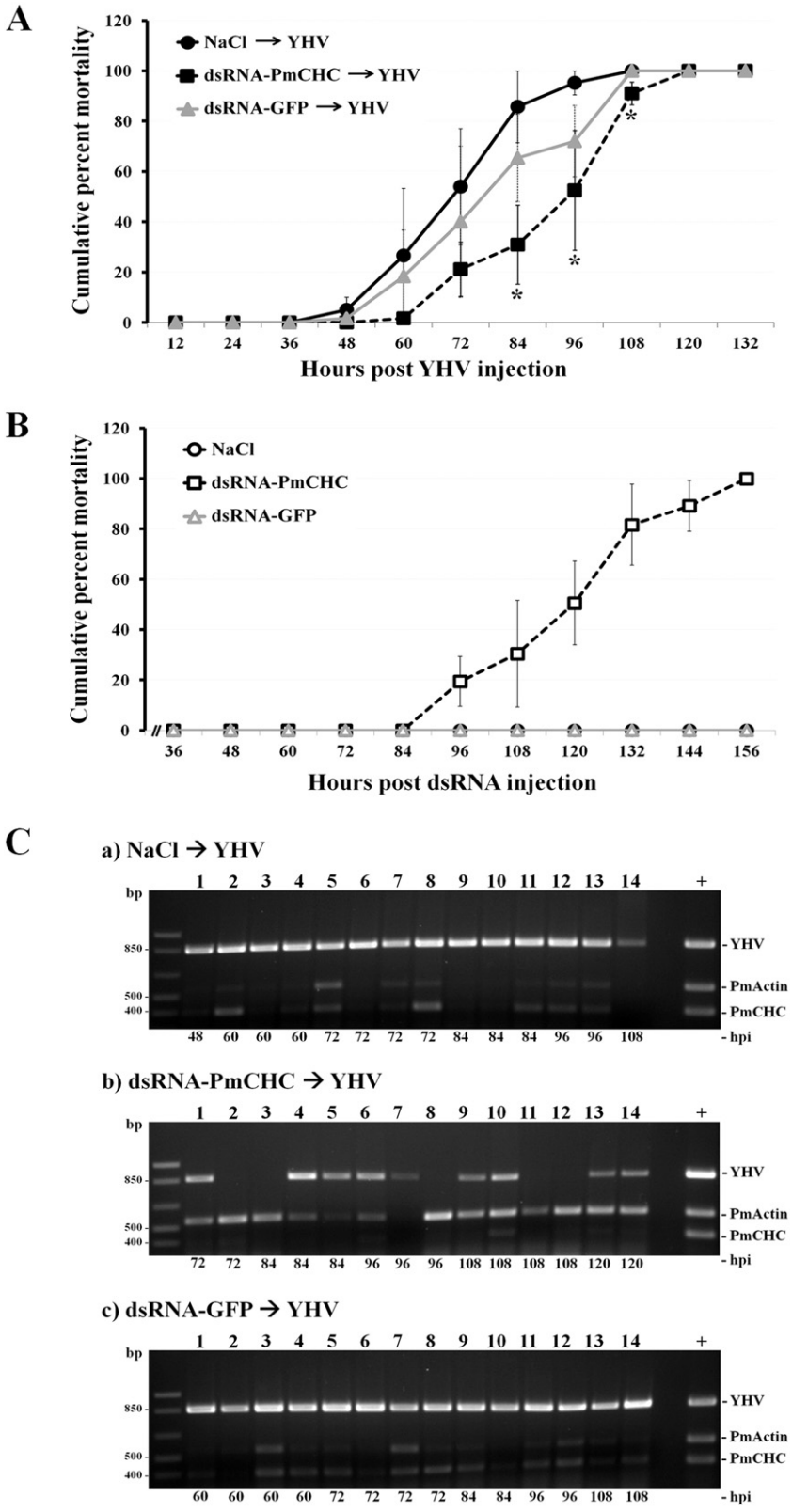


**Fig. 6.** The cumulative percent mortality of shrimp injected with NaCl, dsRNA-PmCHC, or dsRNA-GFP followed by YHV challenge (A) or without YHV challenge (B). (*) represents significant difference between dsRNA-PmCHC → YHV and NaCl → YHV group. (C) A representative gel of RT-PCR products of YHV and PmCHC mRNA levels of dead shrimp. a) NaCl → YHV group, b) dsRNA-PmCHC → YHV group and c) dsRNA-GFP → YHV group. PmActin was used as internal control. The number on the bottom of the each lane represents the time (hours of post YHV challenge, hpi) that the shrimp die. The expression of PmActin in dead shrimp samples that showed high expression levels of YHV were very faint. This result was also demonstrated in a previous study (Posiri et al., 2011).

transportation from late endosome to lysosome during endosome maturation (Huotari and Helenius, 2011). In addition, PmRab7 is required for several shrimp viruses such as white spot syndrome virus (WSSV), taura syndrome virus (TSV) Laem-Singh virus (LSNV) or YHV for intracellular trafficking inside the cell (Ongvarrasopone et al., 2008, 2010, 2011). Therefore based on the previous evidence and this study, the

mechanism of YHV entry and intracellular trafficking can be proposed. YHV enters the shrimp cells by using the envelop protein gp116 to bind to YHV binding protein, PmYRP65 (Assavalapsakul et al., 2006). Then, many adaptor proteins which are involved in clathrin-coated pit formation including AP2, AP17 and PmCHC are recruited to induce membrane invagination to form clathrin-coated vesicles which then transport YHV to the early endosome which also may require Rab5 protein (Hutagalung and Novick, 2011; Stenmark, 2009). After that, YHV may be transported toward the late endosome and lysosome via the regulation by PmRab7 for viral uncoating. The intracellular trafficking process of YHV may be similar to that of semliki forest virus (SFV) which is internalized via clathrin mediated endocytosis and requires Rab7 for transportation inside the cell (Vonderheit and Helenius, 2005).

Taken together, this study demonstrated that PmCHC is an essential protein required for YHV internalization into the shrimp cell. Knockdown of PmCHC by dsRNA-PmCHC resulted in inhibition of YHV levels suggesting that clathrin-mediated endocytosis is a major route for YHV infection.

Supplementary data to this article can be found online at http://dx.doi.org/10.1016/j.aquaculture.2014.10.018.

## Acknowledgments

We would like to thank Assoc. Prof. Albert Ketterman and Asst. Prof. Dr. Kusol Pootanakit for critically reading the manuscript, and Ms. Chaweewan Chimawei, Mrs. Suparb Hongthong and Ms. Punnee Tongboonsong for technical assistance in culturing shrimp. This work was supported by grants from Mahidol University and Thailand Research Fund (BRG5780006 to C.O. and DPG5680001 to S.P.). PP is supported by the grant DPG5680001.

## References

Assavalapsakul, W., Tirasophon, W., Panyim, S., 2005. Antiserum to the gp116 glycoprotein of yellow head virus neutralizes infectivity in primary lymphoid organ cells of *Penaeus monodon*. Dis. Aquat. Org. 63, 85–88.

Assavalapsakul, W., Smith, D.R., Panyim, S., 2006. Identification and characterization of a *Penaeus monodon* lymphoid cell-expressed receptor for the yellow head virus. J. Virol. 80 (1), 262–269.

Bhattacharyya, S., Warfield, K.L., Ruthel, G., Bavari, S., Aman, M.J., Hope, T.J., 2010. Ebola virus uses clathrin-meditated endocytosis as and entry pathway. Virology 401, 18–28.

Boonyaratpalin, S., Supamattaya, K., Kasornchandra, J., Direkbusaracom, S., Aekpanithanpong, U., Chantanachooklin, C., 1993. Non-occluded baculo-like virus, the causative agent of yellow head disease in the black tiger shrimp (*Penaeus monodon*). Fish Pathol. 28 (3), 103–109.

Brodsky, F.M., 2012. Diversity of clathrin function: new tricks for an old protein. Annu. Rev. Cell Dev. Biol. 28, 309–336.

Dereeper, A., Guignon, V., Blanc, G., Audic, S., Buffet, S., Chevenet, F., Dufayard, J.-F., Guindon, S., Lefort, V., Lescot, M., Claverie, J.-M., Gascuel, O., 2008. Phylogeny.fr: robust phylogenetic analysis for the non-specialist. Nucleic Acids Res. 36, W465–W469.

Dereeper, A., Audic, S., Claverie, J.-M., Blanc, G., 2010. BLAST-EXPLORER helps you building datasets for phylogenetic analysis. BMC Evol. Biol. 12, 10:8.

Doherty, G.J., McMahon, H.T., 2009. Mechanisms of endocytosis. Annu. Rev. Biochem. 78, 31.1–31.46.

Flegel, T.W., 1997. Major viral diseases of the black tiger prawn (*Penaeus monodon*) in Thailand. World J. Microbiol. Biotechnol. 13, 433–442.

Hongliang, W., Chengyu, J., 2009. Influenza A virus H5N1 entry into host cells is through clathrin-dependent endocytosis. Sci. China C Life Sci. 52 (5), 464–469.

Huotari, J., Helenius, A., 2011. Endosome maturation. EMBO J. 30 (17), 3481–3500.

Hussain, K.M., Leong, K.L., Ng, M.M., Chu, J.J., 2011. The essential role of clathrin-mediated endocytosis in the infectious entry of human enterovirus 71. J. Biol. Chem. 286 (1), 309–321.

Hutagalung, A.H., Novick, P.J., 2011. Role of Rab GTPases in membrane traffic and cell physiology. Physiol. Rev. 91, 119–149.

Inoue, Y., Tanaka, N., Tanaka, Y., Inoue, S., Morita, K., Zhuang, M., Hattori, T., Sugamura, K., 2007. Clathrin-dependent entry of severe acute respiratory syndrome coronavirus into target cells expressing ACE2 with the cytoplasmic tail deleted. J. Virol. 81 (16), 8722–8729.

Jatuyosporn, T., Supungul, P., Tassanakajon, A., Krusong, K., 2014. The essential role of clathrin-mediated endocytosis in yellow head virus propagation in the black tiger shrimp *Penaeus monodon*. Dev. Comp. Immunol. 44, 100–110.

Jitrapakdee, S., Unajak, S., Sittidilokratna, N., Hodgson, R.A., Cowley, J.A., Walker, P.J., Panyim, S., Boonsaeng, V., 2003. Identification and analysis of gp116 and gp64 structural glycoproteins of yellow head nidovirus of *Penaeus monodon* shrimp. J. Gen. Virol. 84, 863–873.

Khanobdee, K., Soowannayan, C., Flegel, T.W., Ubol, S., Withyachumnarnkul, B., 2002. Evidence for apoptosis correlated with mortality in the giant black tiger shrimp *Penaeus monodon* infected with yellow head virus. Dis. Aquat. Org. 48, 79–90.

Livak, K.J., Schmittgen, T.D., 2001. Analysis of relative gene expression data using real-time quantitative PCR and the $2^{-\Delta\Delta CT}$ method. Methods 25, 402–408.

Marsh, M., Helenius, A., 2006. Virus entry: open sesame. Cell 124, 729–740.

McMahon, H.T., Boucrot, E., 2011. Molecular mechanism and physiological functions of clathrin-mediated endocytosis. Nat. Rev. Mol. Cell Biol. 12, 517–533.

Meertens, L., Bertaux, C., Dragic, T., 2006. Hepatitis C Virus entry requires a critical postinternalization step and delivery to early endosomes via clathrin-coated vesicles. J. Virol. 80 (23), 11571–11578.

Mercer, J., Schelhaas, M., Helenius, A., 2010. Virus entry by endocytosis. Annu. Rev. Biochem. 79, 803–833.

Mousavi, S.A., Malerod, L., Berg, T., Kjeken, R., 2004. Clathrin-dependent endocytosis. Biochem. J. 377, 1–16.

Nadala Jr., C.B., Tapay, L.M., Loh, P.C., 1997. Yellow-head virus: a rhabdovirus-like pathogen of penaeid shrimp. Dis. Aquat. Org. 31, 141–146.

Ongvarrasopone, C., Roshorm, Y., Panyim, S., 2007. A simple and cost effective method to generate dsRNA for RNAi studies in invertebrates. ScienceAsia 33, 35–39.

Ongvarrasopone, C., Chanasakulniyom, M., Sritunyalucksana, K., Panyim, S., 2008. Suppression of PmRab7 by dsRNA inhibits WSSV or YHV infection in shrimp. Mar. Biotechnol. 10 (4), 374–381.

Ongvarrasopone, C., Chomchay, E., Panyim, S., 2010. Antiviral effect of PmRab7 knockdown on inhibition of Laem-Singh virus replication in black tiger shrimp. Antiviral Res. 88, 116–118.

Ongvarrasopone, C., Saejia, P., Chanasakulniyom, M., Panyim, S., 2011. Inhibition of Taura syndrome virus replication in *Litopenaeus vannamei* through silencing LvRab7 gene by double-stranded RNA. Arch. Virol. 156, 1117–1123.

Posiri, P., Ongvarrasopone, C., Panyim, S., 2011. Improved preventive and curative effects of YHV infection in *Penaeus monodon* by a combination of two double stranded RNAs. Aquaculture 314, 34–38.

Posiri, P., Ongvarrasopone, C., Panyim, S., 2013. A simple one-step method for producing dsRNA from *E. coli* to inhibit shrimp virus replication. J. Virol. Methods 188, 64–69.

Rejman, J., Oberle, V., Zuhorn, I.S., Hoekstra, D., 2004. Size-dependent internalization of particles via the pathways of clathrin and caveolae-mediated endocytosis. Biochem. J. 377, 159–169.

Sittidilokratna, N., Dangtip, S., Cowley, J.A., Walker, P.J., 2008. RNA transcription analysis and completion of the genome sequence of yellow head nidovirus. Virus Res. 136, 157–165.

Sritunyalucksana, K., Wannapapho, W., Lo, C.F., Flegel, T.W., 2006. PmRab7 is a VP28-binding protein involved in white spot syndrome virus infection in shrimp. J. Virol. 80 (21), 10734–10742.

Stenmark, H., 2009. Rab GTPases as coordinators of vesicle traffic. Nat. Rev. Mol. Cell Biol. 10, 513–525.

Vonderheit, A., Helenius, A., 2005. Rab7 associates with early endosomes to mediate sorting and transport of semliki forest virus to late endosomes. PLoS Biol. 3 (7), 1225–1238.

Young, A., 2007. Structural insights into the clathrin coat. Semin. Cell Dev. Biol. 18, 448–458.

Zhang, W., Zhou, F., Greene, W., Gao, S.-J., 2010. Rhesus rhadinovirus infection of rhesus fibroblasts occurs through clathrin-mediated endocytosis. J. Virol. 84 (22), 11709–11717.

# 10. A novel function of bursicon in stimulation of vitellogenin expression in black tiger shrimp, *Penaeus monodon*.

Aquaculture 446 (2015) 80–87

Contents lists available at ScienceDirect

Aquaculture

journal homepage: www.elsevier.com/locate/aqua-online

# A novel function of bursicon in stimulation of vitellogenin expression in black tiger shrimp, *Penaeus monodon*

Ponsit Sathapondecha [a], Sakol Panyim [a,b], Apinunt Udomkit [a,*]

[a] Institute of Molecular Biosciences, Mahidol University, Salaya Campus, Nakhon Pathom 73170, Thailand
[b] Department of Biochemistry, Faculty of Science, Mahidol University, Rama VI Road, Bangkok 10400, Thailand

ARTICLE INFO

*Article history:*
Received 28 February 2015
Received in revised form 23 April 2015
Accepted 25 April 2015
Available online 2 May 2015

*Keywords:*
Cystine knot
Vitellogenesis
Shrimp
Gonad-stimulating hormone
Gonadotropins

ABSTRACT

Bursicon is a cystine knot glycoprotein hormone that is composed of two subunits; alpha and beta. Bursicon plays several physiological roles in insects and crustaceans such as cuticle tanning, wing expansion and molting process. Because of its structural similarity with vertebrate gonadotropins, this study therefore aimed to investigate a novel function of bursicon in vitellogenin (Vg) stimulation in reproductive female shrimp, *Penaeus monodon*. Full-length cDNAs encoding the alpha and beta subunits of bursicon in *P. monodon* (Pmbursα and Pmbursβ) were obtained by rapid-amplification of cDNA ends. Both *Pmbursα* and *Pmbursβ* mRNA levels were dominantly expressed in subesophageal ganglia and thoracic ganglia. The expression of *Pmbursα* and *Pmbursβ* in subesophageal ganglia was significantly increased in early-vitellogenic stage of ovarian development suggesting a possible role of bursicon in vitellogenesis. To study the function of bursicon in shrimp reproduction, recombinant Pmbursα (rbursα), Pmbursβ (rbursβ) and Pmbursαβ (rbursαβ) were successfully expressed in the methylotrophic yeast, *Pichia pastoris*. A treatment of shrimp ovarian cells with recombinant Pmburs showed that only rbursαβ could induce the expression of *Vg* mRNA. In addition, injection of rbursαβ into female *P. monodon* broodstock caused an increase of *Vg* mRNA expression in the ovary as well as stimulated ovarian development. This study provides the first evidence for a reproductive role, most likely as an invertebrate neuropeptide gonad-stimulating hormone, of the heterodimeric bursicon in *P. monodon*.

*Statement of relevance*

Useful information for improvement of shrimp reproduction.



## 1. Introduction

Oocyte development is an important physiological process in female reproduction. In crustaceans, the oocyte development can be divided into two major phases; primary vitellogenesis and secondary vitellogenesis. The primary vitellogenesis involves oocyte growth and follicular development whereas the secondary vitellogenesis precedes by the synthesis and accumulation of vitellogenin (Vg), a precursor of yolk protein, and oocyte maturation (Charniaux-Cotton, 1985). Vitellogenesis in both phases is regulated by several factors such as peptide hormones, steroid hormones and neurotransmitters. A neuropeptide gonad-inhibiting hormone (GIH) is well-characterized in its function of vitellogenesis inhibition in several crustaceans including *Penaeus monodon*, *Litopenaeus vannamei* and *Homarus americanus* (Chen et al., 2014; de Kleijn et al., 1994; Treerattrakool et al., 2008). In contrast, a putative gonad-stimulating hormone (GSH) is believed to be synthesized and secreted from brain and/or thoracic ganglia of crustaceans. For instances, the injection of thoracic ganglia extract prepared from vitellogenic female shrimp, *Penaeus japonicus*, resulted in an increase in the hemolymph Vg level (Yano, 1992). In addition, ovarian maturation in *Penaeus vannamei* was induced after the injection of brain extract from vitellogenic female American lobster, *H. americanus* (Yano and Wyban, 1992). In addition, in the red swamp crayfish, *Procambarus clarkii*, oocyte growth could be stimulated by a neurotransmitter serotonin in the ovarian explants that was co-incubated with brain or thoracic ganglia, but not in the serotonin-treated ovarian explants alone (Sarojini et al., 1996). This result suggested that serotonin stimulated the secretion of a putative GSH from brain and thoracic ganglia that was required for oocyte growth. These evidences suggested the existence of putative GSH in the brain and thoracic ganglia of crustaceans though none has been identified and characterized so far.

In vertebrates, gonad development is controlled by gonadotropins such as follicle-stimulating hormone (FSH), luteinizing hormone (LH) and chorionic gonadotropin (CG) (Burger et al., 2004). These hormones are heterodimeric glycoprotein hormone composing of alpha and beta subunits. Each subunit forms a conserved cystine knot-containing tertiary structure (Boime and Ben-Menahem, 1999; Milton and Peter,

* Corresponding author. Tel.: +66 2 441 9003 7x1236; fax: +66 2 441 9906.
*E-mail address:* apinunt.udo@mahidol.ac.th (A. Udomkit).

http://dx.doi.org/10.1016/j.aquaculture.2015.04.027
0044-8486/

2000). The function of FSH and LH are known to stimulate follicular development, steroid hormone production, and ovulation (Ulloa-Aguirre and Timossi, 1998; Weghofer et al., 2007). In crustaceans, the existence of vertebrate gonadotropin-like hormone in brain and thoracic ganglia was demonstrated by a number of studies. The FSH and LH-like peptide were detected in the brain and thoracic ganglia tissues of the swimming crab, *Portunus trituberculatus* using the monoclonal antibody against human FSH or LH (Huang et al., 2008). Moreover, FSH-like peptide in the hemolymph of *Marsupenaeus japonicas* was also detected by ELISA, and its level was increased in vitellogenic stage of ovarian development suggesting the involvement of FSH-like peptide in gonad-stimulation in the shrimp (Ye et al., 2011). Nevertheless, a vertebrate gonadotropin-like peptide in crustaceans has not yet been identified.

An invertebrate cystine knot glycoprotein, bursicon (burs) was first discovered in the blowflies and was demonstrated for its role in cuticle tanning (Fraenkel and Hsiao, 1965). Since then, diverse functions of bursicon have been elucidated such as wing expansion (Huang et al., 2007; Nathan et al., 2008) and development in insects (Loveall and Deitcher, 2010), and cuticle hardening during the molting cycle of crustaceans (Chung et al., 2012; Webster et al., 2013; Wilcockson and Webster, 2008). Bursicon is a heterodimeric protein comprising of alpha (bursα) and beta (bursβ) subunits. Both subunits are mainly synthesized at thoracic ganglia in crustaceans (Chung et al., 2012; Sharp et al., 2010; Webster et al., 2013; Wilcockson and Webster, 2008) and at ventral nervous tissues in insects (Honegger et al., 2011; Luo et al., 2005). Each burs subunit contains a cystine knot conserved sequence C–X–G–X–C, which forms a cystine knot structure by 3 disulfide bonds similar to that of other cystine knot growth factors such as vertebrate gonadotropins and transforming growth factor (Avsian-Kretchmer and Hsueh, 2004; Honegger et al., 2008). This structural homology of bursicon to other growth factors therefore suggests its possible roles in growth and reproductive processes.

This study is aimed to investigate a reproductive function of bursicon in female black tiger shrimp, *P. monodon*. A full-length cDNA of both *P. monodon bursα* (*Pmbursα*) and *bursβ* (*Pmbursβ*) was cloned, and the correlation between their expression and ovarian development was investigated. A recombinant *P. monodon*'s bursicon was expressed in the yeast *Pichia pastoris* and was used to demonstrate its function in gonad-stimulation in the shrimp.

## 2. Material and methods

### 2.1. RNA extraction and cDNA synthesis

Adult female black tiger shrimp, *P. monodon* were provided from Shrimp Genetic Improvement Center, Suratthani, Thailand. All animal experiments were carried out in accordance with animal care and use protocol of the Mahidol University Animal Care and Use Committee. Shrimp tissues were freshly isolated from the shrimp that had been anesthetized on ice, and the total RNA was extracted by Ribozol reagent (Ameresco, USA) according to the manufacturer's protocol. The RNA concentration was measured by Nanodrop (ND-1000, Thermoscientific). The total RNA was treated with 0.5 U DNase I (Thermoscientific) at 37 °C for 15 min, then heated at 65 °C for 5 min before converting into the first-stranded cDNA. The cDNA synthesis was primed with an oligo-dT primer in a reaction containing 1X reverse transcriptase buffer (Promega), 3 mM $MgCl_2$, 0.5 mM dNTP and 1 μl Impromp II reverse transcriptase (Promega). The reverse transcription reaction was incubated at 25 °C for 5 min, 42 °C for 60 min and 70 °C for 10 min. The cDNA was kept at −20 °C until use.

### 2.2. Cloning of full-length PmBursα and PmBursβ cDNAs

The nucleotide sequence of *L. vannamei* EST clone (Accession No. FE173462) that showed high homology to bursα of *Homarus gammarus* (Accession No. HM113369) was aligned with that of bursα of *H. gammarus*, *Carcinus maenas* and *Callinectes sapidus*, and the conserved sequences were selected to design specific primers for obtaining Pmbursα partial nucleotide sequence. While the conserved sequences among the translated amino acid sequence of bursβ of *H. gammarus*, *C. maenas* and *C. sapidus* was used to design degenerate primers to obtain partial sequence of Pmbursβ (data not shown). These partial nucleotide sequences of Pmbursα and Pmbursβ were used to design specific primers for the cloning of full-length cDNA encoding each subunit as described below.

A full-length cDNA of PmBursα and PmBursβ was obtained by rapid amplification of cDNA ends (RACE). In 3′ RACE, the cDNA synthesized from thoracic ganglia RNA was used to amplify with PmBursα-F1 or PmBursβ-F1 and oligo-dT (PRT) primers in a PCR reaction mixture containing 1X *Taq* DNA polymerase buffer with 2 mM $MgCl_2$, 0.2 mM dNTP, 0.2 μM primers and 1 U *Taq* DNA polymerase (New England Laboratory). The PCR reaction was performed at 94 °C for 3 min, then 35 cycles of 94 °C for 30 s, 60 °C for 30 s and 72 °C for 30 s followed by a final extension at 72 °C for 5 min. The PCR product was used as a template in nested PCR with PmBursα-F2 or PmBursβ-F2 and PM1 primers with the same temperature profile. For 5′ RACE, two microgram of thoracic ganglia RNA was used to synthesize the first-stranded cDNA with PmBursα-R1 or PmBursβ-R1 primer. The cDNA was 3′-tailed with dATP by terminal deoxynucleotidyl transferase (TdT) reaction composing of 1X TdT buffer, 0.2 mM dATP and 1 U TdT (Promega). The reaction was incubated at 37 °C for 30 min, then 65 °C for 5 min. The poly A-tailed cDNA was used as a template in the PCR with PmBursα-R2 or PmBursβ-R2 and oligo-dT primer pair. The PCR product was subsequently used to amplify with nested primers (PmBursα-R3 or PmBursβ-R3 and PM1 primer pair). These PCR products were ligated to pGemT-easy vector (Promega), and used to transform into *Escherichia coli* DH5α. The nucleotide sequences of the cloned cDNAs were determined by 1st-Base company, Malaysia. Nucleotide sequences of all primers were shown in Table 1.

### 2.3. Expression of Pmbursα and Pmbursβ in shrimp tissues

Determination of mRNA levels was performed by quantitative real-time RT-PCR. The cDNA from different tissues of adult female *P. monodon* was used as a template in a PCR mixture that was composed

**Table 1**
List of nucleotide sequence of primers used in this study.

| Primer | Sequence (5′ → 3′) | Experiment |
|---|---|---|
| PRT | CCGGAATTCAAGCTTCTAGAGGATCCTTTTTTTTTTT TTTTTT | cDNA, RACE |
| PM1 | CCGGAATTCAAGCTTCTAGAGGATCC | RACE |
| Pmbursβ-F1 | TGCAACCATCCGTCAACACTC | 3′RACE,qPCR |
| Pmbursβ-F2 | GGATTCCTGAAGGACTGCC | 3′RACE |
| Pmbursβ-R1 | AGTGGGATCGAACTCCTTATCGG | 5′RACE.qPCR |
| Pmbursβ-R2 | GGCAGTCCTTCAGGAATCC | 5′RACE |
| Pmbursβ-R3 | GAGTGTTGACGGATGGTTGC | 5′RACE |
| matPmbursβ-F | CCGCTCGAGAAAAGACACACCTACGGCTCAGAATG | Protein expression |
| matPmbursβ-R | GCTTCTAGATTATCGGATCGAATTCCCGCAC | Protein expression |
| Pmbursα-F1 | TGCATGTGTTGCCAGGAGTC | 3′RACE |
| Pmbursα-F2 | CGCCCATTGACTGCATGTG | 3′RACE,qPCR |
| Pmbursα-R1 | GAGATCACAGGTCGGCAACG | 5′RACE.qPCR |
| Pmbursα-R2 | AAGGGCGTGGTGGTCATTAC | 5′RACE |
| Pmbursα-R3 | AAGTTGGCGATCTCCTGCG | 5′RACE |
| matPmbursα-F | CCGCTCGAGAAAAGAGACGAATGCTCCCTGACG | Protein expression |
| matPmbursα-R | GCTTCTAGATTACTTCAGGAATGGGACG | Protein expression |
| EF1α-F | GAACTGCTGACCAAGATCGACAGG | qPCR |
| EF1α-R | GAGCATACTGTTGGAAGGTCTCCA | qPCR |
| Vg-F | TCCATCTGCAGCACCAATCTTCGC | qPCR |
| Vg-R | GCAACAGCCTTCATTCTGATGCCA | qPCR |
| 5′ AOX1 | GACTGGTTCCAATTGACAAGC | PCR |
| 3′ AOX1 | GCAAATGGCATTCTGACATCC | PCR |

of 1X SYBR fast ABI Prism® qPCR (KAPA Biosystem) and 0.25 μM of each gene-specific primer shown in Table 1. The PCR reaction was carried out in real-time PCR machine (realplex$^4$, Eppendorf) with the temperature profile of 95 °C for 3 min, then 40 cycles of 95 °C for 5 s and 60 °C for 30 s. Subsequently, the melting curve analysis was performed by incubation of the PCR product at 95 °C for 30 s, 60 °C for 30 s and 95 °C for 30 s. The Ct value of the target gene and reference gene (Elongation factor 1α, *EF1α*) was calculated for its copy number from the standard curve of each gene that was constructed from the Ct values of the amplification of each gene at different copy numbers ranging from $10^2$ to $10^8$ copies. The relative expression of the target gene was presented as a ratio of its copy number to that of the reference gene.

### 2.4. Construction of recombinant PmBursα, PmBursβ and PmBursαβ expression vector

The nucleotide sequences encoding mature peptide of either Pmbursα or PmBursβ were amplified with matPmbursα-F and matPmbursα-R or matPmbursβ-F and matPmbursβ-R primer pairs, respectively (Table 1). The cDNA from subesophageal ganglia was used as a template in a PCR reaction mixture containing of 1X *Pfu* polymerase buffer with 1.5 mM $MgCl_2$, 0.2 mM dNTP, 0.2 μM each primer and 1 U *Pfu* polymerase (Promega). The PCR reaction was performed at 94 °C for 3 min, then 35 cycles of 94 °C for 30 s, 60 °C for 30 s and 72 °C for 1 min. The PCR product of the mature Pmbursα and Pmbursβ coding sequences were digested with *Xho* I and *Xba* I prior to ligation to pPICZαA plasmid (Invitrogen) that had been digested with the same restriction enzymes to produce pmatPmbursα and pmatPmbursβ recombinant plasmids. Both recombinant plasmids were individually transformed into *E. coli* DH5α. The nucleotide sequences of the cloned fragments were determined by automated DNA sequencing (1st Base Company, Malaysia). To construct a dual expression plasmid containing both matPmbursα and matPmbursβ expression cassettes, the pmatPmbursα plasmid was linearized with *Bam*H I and dephosphorylated by alkaline phosphatase enzyme. Due to the size of the matPmbursβ expression cassette excised with *Bam*H I and *Bgl* II was very close to that of the vector backbone, the matPmbursβ expression cassette was excised from the pmatPmbursβ plasmid by digestion with *Bgl* II, *Bam*H I and also with *Nco*I that cut within the vector backbone sequence in order to eliminate the backbone such that the matPmbursβ expression cassette would be purified more easily. The matPmbursβ cassette was then ligated into the linearized pmatPmBursα with T4 ligase enzyme. The resulting recombinant plasmid, pmatPmbursαβ, was verified by restriction enzyme analysis with *Eco*R I, *Bgl* II and *Bam*H I enzymes. Approximately 50 ng of pmatPmBursα and pmatPmbursβ were linearized with *Dra* I as well as 500 ng of undigested pmatPmbursαβ prior to transformation into the *P. pastoris* KM71 by electroporation using a condition of 2 kV and 25 μF. The transformants were cultured on YPD (1% w/v yeast extract, 2% w/v peptone and 2% w/v D-glucose) containing 100 μg/ml zeocin (Invitrogen) agar. The genomic DNA of *P. pastoris* recombinants was extracted following Lõoke et al., 2011. Integration of each matPmburs expression cassette into the yeast genomic was then verified by PCR with 5′AOX1 and 3′AOX1 primers (Table 1).

### 2.5. Expression and purification of recombinant Pmburs in P. pastoris

The expression of Pmburs proteins from recombinant *P. pastoris* KM71 was induced by methanol induction. A single colony of recombinant *P. pastoris* KM71 was cultured in YPD medium containing 100 μg/ml zeocin at 30 °C for 2 days. The starter culture was inoculated in BMGY medium (1% w/v yeast extract, 2% w/v peptone, 100 mM phosphate buffer pH 6.0, 1% v/v glycerol, 0.67% w/v YNB and 0.00004% w/v biotin) at the $OD_{600}$ of 0.1. The yeast culture was incubated at 30 °C for 12–13 h until the $OD_{600}$ reached 6–8. Approximately 30–35 $OD_{600}$/ml of *P. pastoris* culture were induced in BMMY medium (1% w/v yeast extract, 2% w/v peptone, 100 mM phosphate buffer pH 6.0, 3% v/v methanol, 0.67% w/v YNB and 0.0004% w/v biotin) at 30 °C for 2 days. The culture medium was then collected, and recombinant Pmburs proteins were subsequently precipitated by 40–50% saturated ammonium sulfate. The ammonium sulfate precipitated proteins were further purified by anion exchange chromatography by dissolving in 20 mM Tris pH 7.4 and subjected into a Hitrap Q HP column (GE Healthcares). After washing the column with 20 mM Tris pH 7.4, a step-wise elution was performed with 20 mM Tris pH 7.4 containing different concentration of NaCl ranging from 0.1 to 0.5 M. The purified rPmbursα and rPmbursβ were identified by liquid chromatography and mass spectrometry (LC-MS/MS). Analysis of dimeric formation of the purified recombinant Pmburs was performed by SDS-PAGE either with or without the reducing agent, β-mercaptoethanol and native polyacrylamide gel.

### 2.6. Functional assay of recombinant Pmburs proteins in P. monodon

The function of Pmburs in the stimulation of vitellogenin expression was studied both in the primary culture of ovarian cells and in the shrimp. To prepare the ovarian cells, previtellogenic ovaries were freshly isolated from adult female *P. monodon*, excised into small pieces and rinsed with the culture medium (Leibovitz's L-15 powder, 0.5% w/v NaCl, 1% w/v D-glucose, 3.33% w/v lactalbumin, 10% v/v FBS, 10% v/v shrimp meat extract) containing 100 U penicillin/streptomycin. The ovary pieces were washed several times in the culture medium containing 1000 U and 2000 U penicillin/streptomycin, and subsequently chopped by scissors until homogeneous suspension was obtained. Approximately $7.5 \times 10^5$ oocyte cells were seeded in 1 ml culture medium at 28 °C. After seeded the cells for overnight, the culture medium was discarded and replaced with fresh culture medium containing 200 ng of either rbursα, rbursβ or rbursαβ whereas the Tris/NaCl buffer (20 mM Tris pH 7.4, 200 mM NaCl) was added to the control cells. This amount of recombinant protein was based on twice amount of the bursicon in hemolymph at ecdysis stage of the crab, *C. maenas* (Webster et al., 2013). After treatment for 24 h, approximately 1 ml of ovarian cells was collected to determine *Vg* expression levels. The culture medium of the remaining 24-h treated ovarian cells was then replaced with 500 μl of the fresh culture medium containing the same concentration of the recombinant proteins, and cultured for another 24 h before collecting the cells. Total RNA was extracted from the cells that were treated with each rPmburs protein for 24 and 48 h as well as from the control cells, and the *Vg* mRNA level was determined by real-time RT-PCR as described above.

For *in vivo* study, previtellogenic female shrimp (~90 g) were injected with 6 μg of rbursαβ (equivalent to approx. 60 ng/g shrimp body weight) or Tris/NaCl buffer. Two days later, the shrimp were injected for the second time with the same treatment. Ovaries were isolated on day 4 after the first injection to determine for *Vg* mRNA expression by real-time RT-PCR using EF1α as an internal control as described previously. The developmental stage of the ovary was observed by the appearance of the ovary through the dorsal skeleton under the torchlight as described by Tan-Fermin and Pudadera, 1989.

## 3. Results and discussion

### 3.1. Characterization of Pmbursα and Pmbursβ cDNAs

A heterodimeric glycoprotein hormone, bursicon has been identified and characterized in several insects such as *Calliphora erythrocephala*, *Drosophila melanogaster*, *Anopheles gambiae* and *Bombyx mori* (Fraenkel and Hsiao, 1965; Honegger et al., 2011; Huang et al., 2007; Luo et al., 2005) and crustaceans including *H. gammarus*, *C. maenas* and *C. sapidus* (Chung et al., 2012; Sharp et al., 2010; Wilcockson and Webster, 2008).

Total RNA from thoracic ganglia was used as a source for cDNA cloning of *P. monodon*'s bursicon in this study because bursicon was commonly found in the thoracic ganglia of several crustaceans. The full-length cDNA encoding Pmbursα and Pmbursβ in *P. monodon* (GenBank accession no. KP191597 and KP191598, respectively) were

successfully obtained by RACE technique. The *Pmbursα* cDNA contains a 423 bp open reading frame coding for a putative signal peptide and a mature peptide of 20 and 121 amino acids, respectively. A 432 bp open reading frame of *Pmbursβ* cDNA encodes 29 amino acids residues of a signal peptide and a 115 amino acids mature peptide of Pmbursβ. An alignment of the deduced amino acid sequences of Pmbursα and Pmbursβ to those of other arthropods indicated high levels of similarity (Fig. 1A and B). Pmbursα and Pmbursβ share the highest identity of 84% and 83%, respectively to that of *H. gammarus*. The amino acid sequences of both Pmburs subunit peptides contain 11 conserved cysteine residues including a conserved sequence of cystine knot-containing proteins, C–X–G–X–C, that is found in other cystine knot growth factors such as vertebrate gonadotropins and transforming growth factor (Avsian-Kretchmer and Hsueh, 2004; Honegger et al., 2008). In addition, three intra-molecular disulfide bridges were found in both bursicon subunits which were paired between C1 and C7, C3 and C9, and C4 and C10 (Fig. 1). Structurally, two of these disulfide bonds form a knot-ring and another pass through the ring resulting in three-loop formation. This was similar to other cystine knot-containing proteins including glycoprotein hormone family, transforming growth factor beta and bone morphogenetic protein (BMP) antagonist (Roch and Sherwood, 2014). Moreover, additional disulfide bond between C2 and C8 formed a seat-belt like structure, which was similar to that of human CGβ (Hearn and Gomme, 2000) and *Drosophila* bursicon (Luo et al., 2005).

### 3.2. Expression of bursicon mRNAs in *P. monodon*

Bursicon peptide was detected in the ventral nerve cord of insects by immunohistostaining (Luo et al., 2005), whereas the mRNA detection by either semi-quantitative RT-PCR or *in situ* hybridization demonstrated

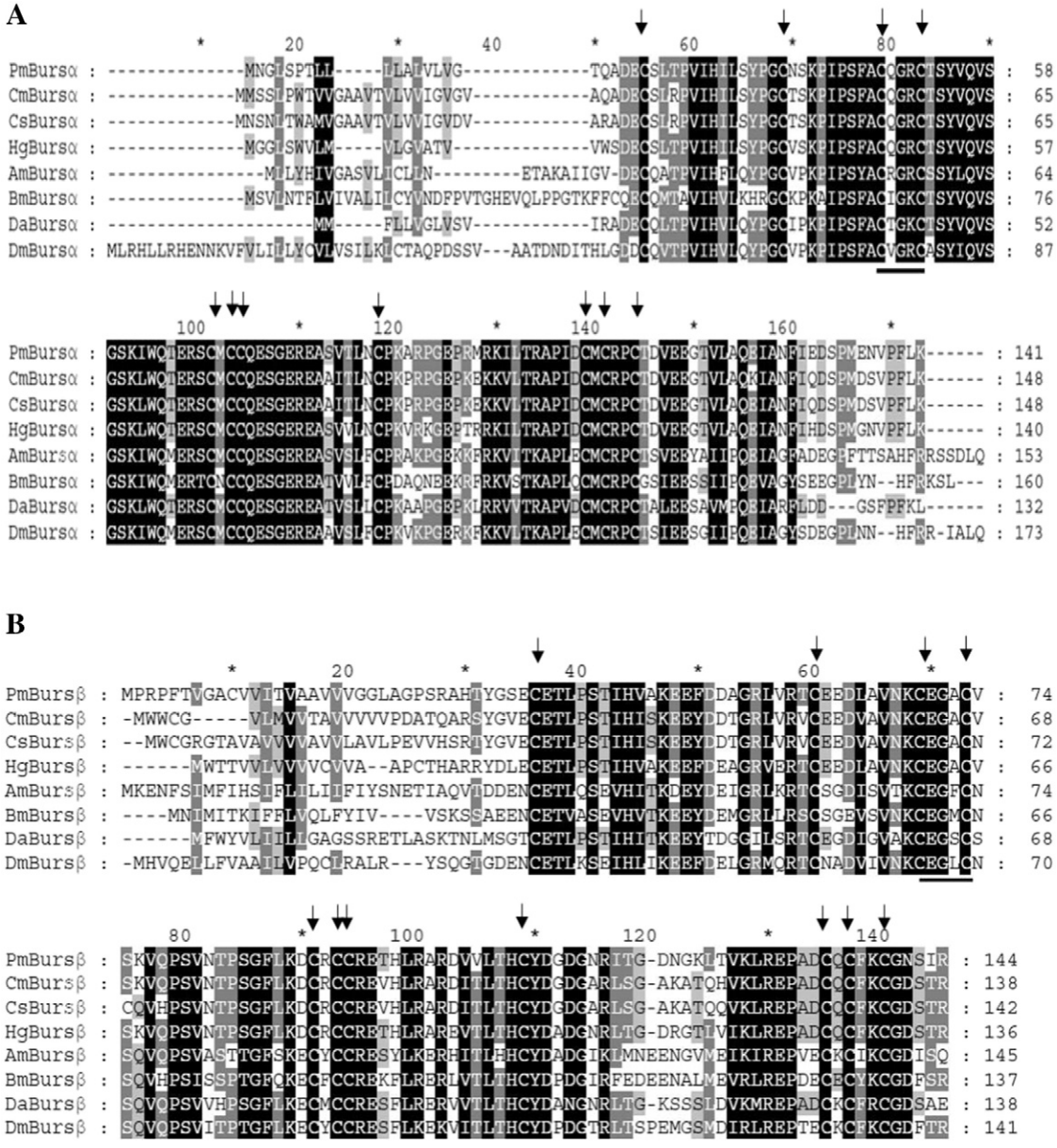


**Fig. 1.** Alignment of deduced amino acid sequences of bursα and bursβ. The deduced amino acid sequence of Pmbursα (A) and Pmbursβ (B) were aligned with those of other insects and crustaceans by Clustal X program. The sequences include bursicons of *C. maenas* (Cmbursα: EU139428 and Cmbursβ: EU139429), *C. sapidus* (Csbursα: EU677191 and Csbursβ: EU677190), *H. gammarus* (Hgbursα: HM113369 and Hgbursβ: HM113370), *Apis mellifera* (Ambursα: NM_001098234 and Ambursβ: NM_001040262), *B. mori* (Bmbursα: NM_001098375 and Bmbursβ: NM_001043824), *Daphnia arenata* (Dabursα: EU139431 and Dabursβ: EU139430) and *D. melanogaster* (Dmbursα: NM_142726 and Dmbursβ: NM_135868). The amino acids that were identical in all sequences are highlighted in black. The lesser degrees of identity are highlighted in different shades of gray. Arrows indicate conserved cysteine residues in cystine knot proteins. The conserved sequence of cystine knot protein is underlined.

the expression of both bursicon subunits in the thoracic ganglia of crustaceans (Chung et al., 2012; Sharp et al., 2010; Wilcockson and Webster, 2008). Similarly, the quantitative real-time PCR detection of bursicon mRNA in *P. monodon* revealed that both *Pmbursα* and *Pmbursβ* mRNA were dominantly expressed in subesophageal ganglia and thoracic ganglia whereas the expression in other tissues including eyestalk, brain, hepatopancreas, gills, ovary and muscle was not detectable (Fig. 2). This indicated a common source of bursicon production in crustaceans. In addition, the mRNA expression level of *Pmbursα* and *Pmbursβ* in subesophageal ganglia and each node of thoracic ganglia of previtellogenic female shrimp were determined. The result showed that both *Pmbursα* and *Pmbursβ* transcripts were expressed at higher level in subesophageal ganglia than in the thoracic ganglia, and that each node of thoracic ganglia expressed similar levels of *Pmbursα* and *Pmbursβ* transcripts (Fig. 3). This is similar to the mRNA expression of bursicon in the lobster, *H. gammarus* where no difference in the expression level in each node of either thoracic ganglia or abdominal nerve cords was reported (Sharp et al., 2010).

In order to investigate the correlation between bursicon expression and ovarian development in the shrimp, the expression of both *Pmbursα* and *Pmbursβ* in subesophageal ganglia of female *P. monodon* at different stages of ovarian development was determined by real-time RT-PCR. The result in Fig. 4 showed that *Pmbursα* and *Pmbursβ* expression was significantly increased approximately two-folds in early vitellogenic shrimp compared with that in pre-vitellogenic ovary (Fig. 4). The expression of *Pmbursα* and *Pmbursβ* in higher stages of ovarian development was then reduced again to the levels similar to that in previtellogenic stage. This result implicated that bursicon may play a role during early vitellogenesis in the shrimp. Although no direct evidence for the reproduction-related function of bursicon has been shown so far, our expression study of *bursicon* during ovarian developmental cycle in *P. monodon* together with its cystine knot structure that is conserved among vertebrate gonadotropins, which is involved in gonad-stimulation (Roch and Sherwood, 2014) suggesting that bursicon may play a role in reproduction of female shrimp, particularly in vitellogenin synthesis during ovarian development.

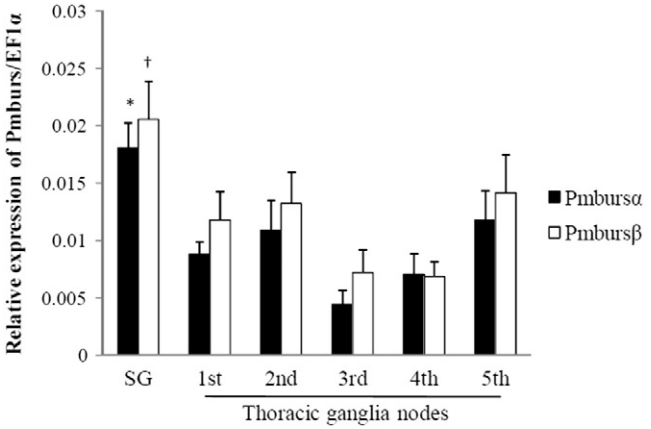


**Fig. 3.** Expression pattern of *Pmburs* mRNA in the ganglia of shrimp. Relative expression of *Pmbursα* (black bar) and *Pmbursβ* (open bar) in subesophageal ganglia and each node of thoracic ganglia of female *P. monodon* at previtellogenic stage of ovarian development were determined by real-time RT-PCR. The relative expression levels of *Pmburs* to that of *EF1α* are represented as mean ± SEM (n = 7). Asterisk and cross depict significant difference at $p < 0.05$ between groups by random complete block design ANOVA and pair-wise comparison with Tukey's HSD test of *Pmbursα* and *Pmbursβ*, respectively.

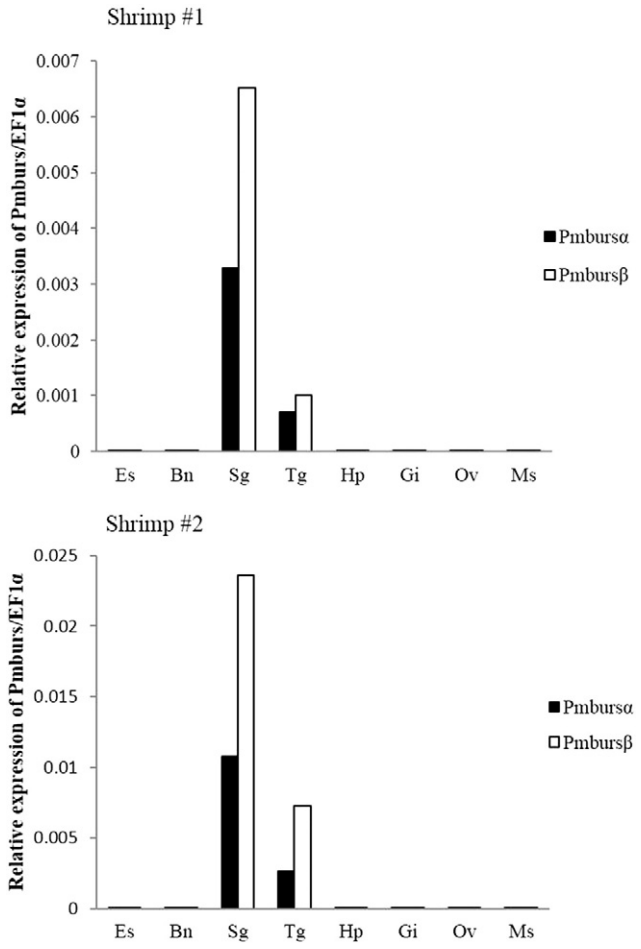


**Fig. 2.** Determination of *Pmburs* mRNA expression in various shrimp tissues. The *Pmbursα* (black bar) and *Pmbursβ* (open bar) mRNA expression were determined in *P. monodon* tissues including eyestalk (Es), brain (Bn), subesophageal ganglia (Sg), thoracic ganglia (Tg), hepatopancreas (Hp), gill (Gi), ovary (Ov) and muscle (Ms) by real-time RT-PCR. The expression in two shrimp is shown individually. The values are shown as relative expression level of *Pmburs* to that of *EF1α*.

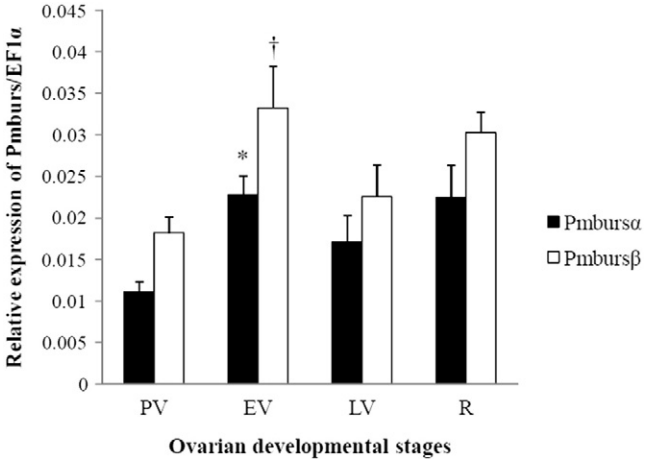


**Fig. 4.** Expression pattern of *Pmburs* mRNA in subesophageal ganglia at different stages of ovarian development. The subesophageal ganglia of female broodstock shrimp at each stage of ovarian development was determined for *Pmbursα* (black bar) and *Pmbursβ* (open bar) mRNA level by real-time RT-PCR. The ovarian stages are composed of previtellogenic (PV), early vitellogenic (EV), late vitellogenic (LV) and ripe stages (R). The relative expression levels of *Pmburs* to that of *EF1α* are represented as mean ± SEM (n = 7–9). Asterisk and cross depict significant difference at $p < 0.05$ between groups by one-way ANOVA and pair-wise comparison with Tukey's HSD test of *Pmbursα* and *Pmbursβ*, respectively.

### 3.3. Production of recombinant P. monodon's bursicon in P. pastoris

To study the function of bursicon in *P. monodon*, recombinant proteins of Pmbursα (rbursα) and Pmbursβ (rbursβ) were expressed in the yeast, *P. pastoris* either individually to produce a homodimeric form of each subunit or co-expressed together to produce a heterodimeric Pmbursαβ (rbursαβ). Because the homodimeric form of either bursα or bursβ could occur after expression in mammalian cells system (An et al., 2012; Luo et al., 2005), therefore the expression cassette of Pmbursα and Pmbursβ was cloned into the same plasmids for heterodimeric rbursαβ expression instead of *in vitro* dimerization of both rbursα and rbursβ subunits so as to prevent self-formation of homodimeric proteins. After ammonium sulfate precipitation, the expressed rbursα, rbursβ and rbursαβ were further purified by anion exchange Hitrap Q HP column (GE Healthcares). Only rbursβ and rbursαβ could be purified by anion exchange chromatography whereas rbursα seemed to be unstable under the condition used in the purification step, and thus could not be recovered after purification. Accordingly, the anion exchange purified rbursβ and rbursαβ and the ammonium sulfate precipitated rbursα were used in further studies.

Analysis by SDS-PAGE indicated that rbursα was expressed as two bands at the molecular weight of 16–18 kDa, which was similar to *Drosophila* bursα expressed in HEK293 cells (Luo et al., 2005), while a single band of rbursβ was presented at approximately 20 kDa.

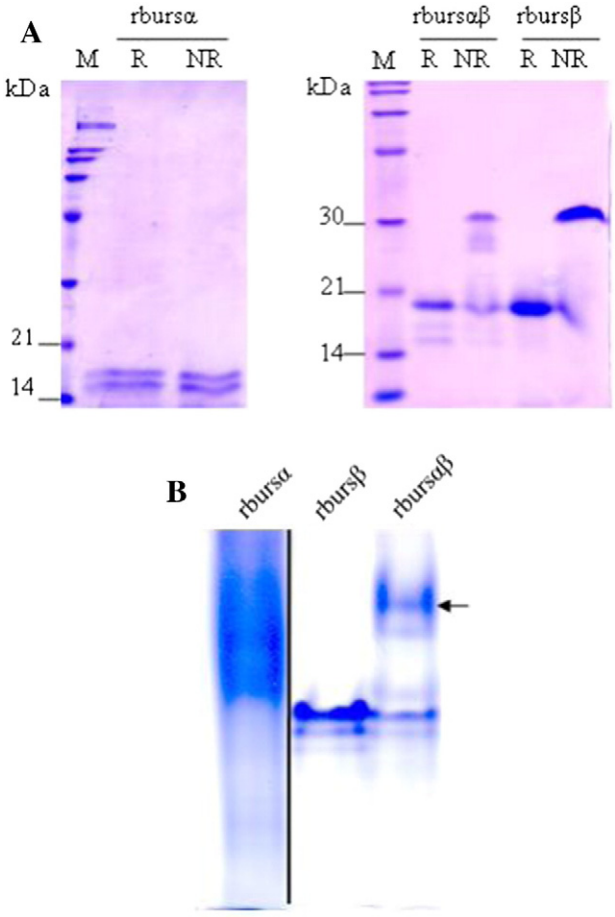


**Fig. 5.** Analysis of recombinant Pmburs peptides on polyacrylamide gel electrophoresis. Approximately 2 μg of rbursα, rbursβ and rbursαβ were analyzed by denaturing SDS-PAGE and native gel. The purified recombinant peptides treated with (R) or without (NR) reducing agent were separated on 15% SDS-PAGE (A). Analysis of the purified recombinant Pmburs in the native gel were performed by 7.5% polyacrylamide gel electrophoresis without SDS (B). M is a broad-range protein marker (Bio-rad). An arrow shows a heterodimer of rbursαβ.

The rbursαβ showed the band pattern corresponding to that of both rbursα and rbursβ (Fig. 5A). The protein bands of both rbursα and rbursβ were verified by LC-MS/MS, and the result revealed similarity to bursicons of the crab, *C. maenas* with 14% and 9% coverage, respectively (data not shown). When analyzed under reduced and non-reduced conditions, a protein band of rbursβ appeared at higher molecular weight of approximately 32 kDa under the non-reduced condition compared with that under the reduced condition (Fig. 5A) suggesting the formation of a homodimeric rbursβ via an intermolecular disulfide bond. The expected size of the homodimeric rbursβ was not well correlated with that of the monomeric form could possibly due to the difference in the structure of the monomer subunit or post-translational modifications, particularly glycosylation. Under the non-reduced condition, the strong intramolecular disulfide bonds might still hold the cystine knot structure of each monomer subunit of the homodimeric rbursβ, whereas the monomeric form under reduced condition did not retain the cystine knot structure. In contrast to rbursβ, rbursα showed the same protein pattern under both conditions suggesting that rbursα might not form a homodimer. However, when analyzed by native gel, rbursα appeared to be slightly larger than rbursβ (Fig. 5B) implying that rbursα was presented as homodimer that was likely formed by a non-disulfide bond.

In addition, the co-expression of rbursα and rbursβ resulted in the formation of rbursαβ heterodimer as recognized under the non-reduced condition (Fig. 5A). However, the homodimer of rbursβ and the free rbursα subunits were also present. The formation of rbursαβ when both subunits were co-expressed was confirmed by the presence of an extra band, as indicated by an arrow in Fig. 5B, in the native gel that did not appear in either rbursα or rbursβ alone. The expression of recombinant shrimp bursicon in *P. pastoris* suggested either homodimeric or heterodimeric formation of recombinant bursicon similar to the recombinant *Drosophila* bursicon expressed in HEK293 cells (An et al., 2012; Luo et al., 2005), except that the formation of shrimp rbursα homodimer might not occur by disulfide bond. This was probably due to the difference in the expression system and translational modification in different host systems.

### 3.4. Reproductive function of P. monodon bursicon

In order to study a possible involvement of bursicon in the reproduction in female *P. monodon*, its effect on vitellogenin expression and oocyte development were investigated. Vitellogenin (Vg), a precursor

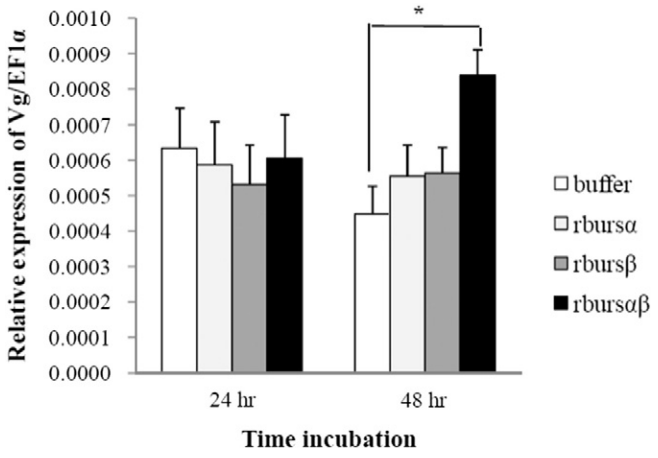


**Fig. 6.** Effect of recombinant Pmburs on vitellogenin mRNA expression in ovarian cells. The primary ovarian cells were treated with approximately 200 ng/ml rbursα, rbursβ, rbursαβ or Tris/NaCl buffer, and incubated at 28 °C for 24 and 48 h. After incubation, *Vg* mRNA level in the ovarian cells were determined by real-time RT-PCR. The relative expression levels of *Vg* to that of *EF1α* is presented as mean ± SEM of three independent experiments. Asterisk represents significant difference at $p < 0.05$ between groups by two-way ANOVA and pairwise comparison with Duncan's test.

of yolk protein, was used as a biomarker to determine the effect of bursicon on gonad stimulation. In primary ovarian cells, *Vg* mRNA levels after the treatment with rbursα, rbursβ or rbursαβ for 24 h did not change significantly when compared to that of the control cells. However, the *Vg* mRNA expression level was significantly elevated approximately two-folds in rbursαβ-treated ovarian cells at 48 h after treatment whereas the cells treated with rbursα or rbursβ still expressed the same level of *Vg* to the control cells (Fig. 6). This study indicated that only the heterodimeric rbursαβ, but not rbursα or rbursβ homodimer alone could stimulate *Vg* expression in ovarian cells of *P. monodon*. This effect of Pmburs on Vg stimulation is analogous to that of putative gonad-stimulating hormone from the brain and thoracic ganglia extracts previously reported in a few decapods (Thangaraj and Prakash Vincent, 2004; Yano, 1992; Yano and Wyban, 1992). The up-regulation of *Vg* induced by bursicon at 48 h after treatment might suggest that bursicon is required to mediate the stimulation of vitellogenesis. Although there was no evidence revealing downstream process activated by bursicon in crustaceans, one of the roles of other glycoprotein hormones, especially FSH was to regulate the expression and increase the activity of a steroidogenic enzyme aromatase that converts androgens to estrogens (Erickson and Hsueh, 1978; Hearn and Gomme, 2000; Parakh et al., 2006). Moreover, vertebrate steroid hormone such as 17β-estradiol was also demonstrated to stimulate Vg synthesis in the oocyte of *M. japonicus* (Yano and Hoshino, 2006) as well as increase Vg level in the hemolymph of the crayfish, *Cherax albidus* (Coccia et al., 2010). It is therefore possible that bursicon may regulate *Vg* expression in crustacean ovary via steroidogenesis. It was demonstrated that serotonin, a neurotransmitter that is known to stimulate ovarian maturation in crustacean (Kulkarni et al., 1992; Vaca and Alfaro, 2000; Wongprasert et al., 2006) exert its function via stimulating the release of GSH from brain and/or thoracic ganglia (Sarojini et al., 1995, 1996). Whether or not serotonin also takes part in bursicon stimulation is not known and awaits further investigation.

To study the function of bursicon in the shrimp, previtellogenic female *P. monodon* were injected with rbursαβ or Tris/NaCl buffer twice on day 0 and day 2. The effect of rbursαβ on gonad stimulation was then investigated on day 4. The result in Fig. 7A showed that *Vg* mRNA expression in the ovary was significantly elevated more than three-folds in the rbursαβ-injected shrimp compared with that in the buffer-injected shrimp. Consistent with the *Vg* expression, approximately 75% of the buffer-injected shrimp were retained in previtellogenic stage whereas the majority (>60%) of the shrimp injected with rbursαβ could develop to late vitellogenic and mature stages (Fig. 7B). These results suggested that bursicon plays a role in ovarian maturation by stimulating Vg synthesis in *P. monodon*. This biological function is related to the elevated mRNA expression level of *Pmburs* in subesophageal ganglia at early vitellogenic stage of ovarian development. Concentration of circulating bursicon in the hemolymph at different molting stages was studied in the crabs, and the highest level (~4000 fmol/ml in *C. maenas* and ~100 fmol/ml in *C. sapidus*) was found at ecdysis stage (Chung et al., 2012; Webster et al., 2013). This suggests that the effective hemolymph concentrations of bursicon could be different between different species. However, because rbursαβ was produced as a mixture with monomeric and homodimeric forms the effective concentration of rbursαβ that caused up-regulation of *Vg* expression and ovarian development in *P. monodon* is presently not known, and further study with a higher purity of rbursαβ should be performed.

The effect of Pmburs on ovarian maturation is similar to that of a number of mammalian gonadotropins in crustaceans. For example, FSH and LH showed stimulating effect on the ovary of the sand shrimp, *Crangon crangon* (Żukowska-Arendarczyk, 1981). In the fresh water prawn *Macrobrachium lamerrii*, injection of FSH led to an increase in follicle cell number and size as well as the accumulation of yolk granules in the oocytes (Sarojini et al., 1988). The human chorionic gonadotropin (hCG) also had the influence on gonad maturation and spawning in *Penaeus semisulcatus* (Aktas and Kumlu, 2005).

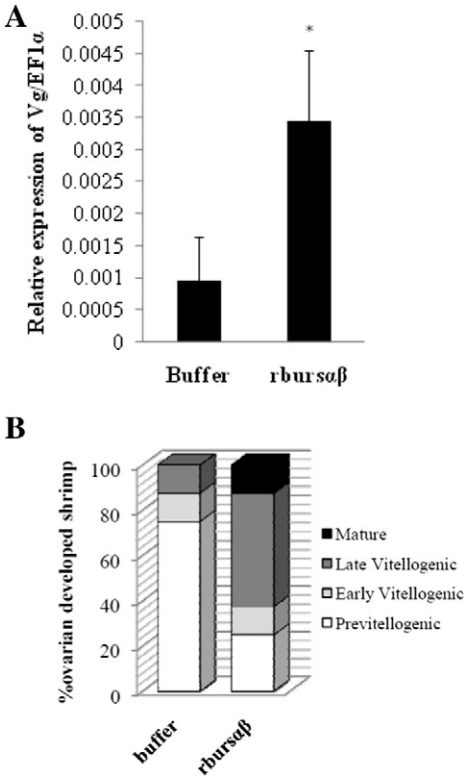


**Fig. 7.** Effect of recombinant bursαβ on vitellogenin expression in shrimp. Female *P. monodon* broodstock (approximately 90 g body weight) at previtellogenic stage of ovarian development were injected twice with approximately 60 ng/g bogy weight shrimp of rbursαβ or Tris/NaCl buffer on day 0 and 2. (A) The relative *Vg* mRNA expression to that of *EF1α* in the ovary was determined by real-time RT-PCR. An asterisk represents significant difference at $p < 0.05$ by Mann–Whitney U test. The values were presented as mean ± SEM (n = 8). (B) Ovarian developmental stage of individual shrimp in each group was observed and determined by morphology of the ovary. The results are presented as a percentage of shrimp at each ovarian developmental stage to the total number of shrimp in each group.

In addition, mode of action of gonadotropins involves the binding of the hormones to their specific receptors, a leucine-rich repeated G protein-coupled receptor (GPCR), which triggers adenylyl cyclase activation resulting in an increase of cAMP and subsequently activates protein kinase A (Milton and Peter, 2000). Interestingly, a specific bursicon receptor was identified in *D. melanogaster* to be a leucine-rich repeated GPCR type 2, and binding of recombinant bursicon to the receptor triggered cAMP production resulting in cuticle tanning stimulation (Luo et al., 2005). Besides, the expression of the bursicon-specific receptor was found in nervous tissues (Diao and White, 2012), epidermis (Davis et al., 2007) and muscle (Harwood et al., 2014). Similarly, the FlyAtlas database revealed that the bursicon receptor was expressed in several tissues including brain, thoracic ganglia, fat body, ovary and testis in adult *D. melanogaster* (Chintapalli et al., 2007). The ubiquitous expression of bursicon receptor in those tissues conformed to the multiple roles of bursicon including cuticle tanning (Fraenkel and Hsiao, 1965), wing expansion (Huang et al., 2007; Nathan et al., 2008) and development (Loveall and Deitcher, 2010). Accordingly, the expression of bursicon receptor found in the ovary might suggest another role of bursicon on an ovarian developmental process. These evidences imply that Pmburs might induce vitellogenin expression via similar signaling pathway to that used by gonadotropin to trigger ovarian maturation.

In conclusion, our study demonstrated for the first time the reproductive function of bursicon in the shrimp. Its structural similarity to vertebrate gonadotropins as well as its effect on the stimulation of *Vg* expression suggests that Pmburs is an invertebrate gonadotropin

homolog, and is likely one of putative gonad-stimulating factors in *P. monodon*.

## Acknowledgments

We thank Ms. Somjai Wongtripop (Shrimp Genetic Improvement Center, Thailand) for providing shrimp samples. This study was supported by the Thailand Research Fund (Basic Research Grant to AU and DPG5680001 to SP), the Office of the Higher Education Commission and Mahidol University under the National Research Universities Initiative, and Mahidol University Research Grant. PS is the recipient of the student fellowship by the Royal Golden Jubilee Ph. D. program (PHD/0188/2553) under the Thailand Research Fund and Mahidol University.

## References

Aktas, M., Kumlu, M., 2005. Gonadal maturation and spawning in *Penaeus semisulcatus* de Hann, 1844 by hormone injection. Turk. J. Zool. 29, 193–199.

An, S., Dong, S., Wang, Q., Li, S., Gilbert, L.I., Stanley, D., Song, Q., 2012. Insect neuropeptide bursicon homodimers induce innate immune and stress genes during molting by activating the NF-κB transcription factor relish. PLoS One 7, e34510.

Avsian-Kretchmer, O., Hsueh, A.J.W., 2004. Comparative genomic analysis of the eight-membered ring cystine knot-containing bone morphogenetic protein antagonists. Mol. Endocrinol. 18, 1–12.

Boime, I., Ben-Menahem, D., 1999. Glycoprotein hormone structure—function and analog design. Recent Prog. Horm. Res. 54, 271–288.

Burger, L.L., Haisenleder, D.J., Dalkin, A.C., Marshall, J.C., 2004. Regulation of gonadotropin subunit gene transcription. J. Mol. Endocrinol. 33, 559–584.

Charniaux-Cotton, H., 1985. Vitellogenesis and its control in malacostracan crustacea. Am. Zool. 25, 197–206.

Chen, T., Zhang, L.P., Wong, N.K., Zhong, M., Ren, C.H., Hu, C.Q., 2014. Pacific white shrimp (*Litopenaeus vannamei*) vitellogenesis-inhibiting hormone (VIH) is predominantly expressed in the brain and negatively regulates hepatopancreatic vitellogenin (VTG) gene expression. Biol. Reprod. 90 (47) (41-10).

Chintapalli, V.R., Wang, J., Dow, J.A.T., 2007. Using FlyAtlas to identify better *Drosophila melanogaster* models of human disease. Nat. Genet. 39, 715–720.

Chung, J.S., Katayama, H., Dircksen, H., 2012. New functions of arthropod bursicon: inducing deposition and thickening of new cuticle and hemocyte granulation in the blue crab, *Callinectes sapidus*. PLoS One 7, e46299.

Coccia, E., de Lisa, E., Di Cristo, C., Di Cosmo, A., Paolucci, M., 2010. Effect of estradiol and progesterone on the reproduction of the freshwater crayfish *Cherax albidus*. Biol. Bull. 218, 36–47.

Davis, M.M., O'Keefe, S.L., Primrose, D.A., Hodgetts, R.B., 2007. A neuropeptide hormone cascade controls the precise onset of post-eclosion cuticular tanning in *Drosophila melanogaster*. Development 134, 4395–4404.

de Kleijn, D.P.V., Sleutels, F.J.G.T., Martens, G.J.M., Van Herp, F., 1994. Cloning and expression of mRNA encoding prepro-gonad-inhibiting hormone (GIH) in the lobster *Homarus americanus*. FEBS Lett. 353, 255–258.

Diao, F., White, B.H., 2012. A novel approach for directing transgene expression in *Drosophila*: T2A-Gal4 in-frame fusion. Genetics 190, 1139–1144.

Erickson, G.F., Hsueh, A.J., 1978. Stimulation of aromatase activity by follicle stimulating hormone in rat granulosa cells *in vivo* and *in vitro*. Endocrinology 102, 1275–1282.

Fraenkel, G., Hsiao, C., 1965. Bursicon, a hormone which mediates tanning of the cuticle in the adult fly and other insects. J. Insect Physiol. 11, 513–556.

Harwood, B.N., Draper, I., Kopin, A.S., 2014. Targeted inactivation of the rickets receptor in muscle compromises *Drosophila* viability. J. Exp. Biol. 217, 4091–4098.

Hearn, M.T.W., Gomme, P.T., 2000. Molecular architecture and biorecognition process of the cystine knot protein superfamily: part I. The glycoprotein hormones. J. Mol. Recognit. 13, 223–278.

Honegger, H., Dewey, E., Ewer, J., 2008. Bursicon, the tanning hormone of insects: recent advances following the discovery of its molecular identity. J. Comp. Physiol. A. 194, 989–1005.

Honegger, H., Estévez-Lao, T.Y., Hillyer, J.F., 2011. Bursicon-expressing neurons undergo apoptosis after adult ecdysis in the mosquito *Anopheles gambiae*. J. Insect Physiol. 57, 1017–1022.

Huang, J., Zhang, Y., Li, M., Wang, S., Liu, W., Couble, P., Zhao, G., Huang, Y., 2007. RNA interference-mediated silencing of the bursicon gene induces defects in wing expansion of silkworm. FEBS Lett. 581, 697–701.

Huang, H., Ye, H., Li, S., Wang, G., 2008. Immunocytological evidence for the presence of vertebrate FSH- and LH-like substances in the brain and thoracic ganglion of the swimming crab, *Portunus trituberculatus*. Prog. Nat. Sci. 18, 1453–1457.

Kulkarni, G.K., Nagabhushanam, R., Amaldoss, G., Jaiswal, R.G., Fingerman, M., 1992. *In vivo* stimulation of ovarian development in the red swamp crayfish, *Procambarus clarkii* (Girard), by 5-hydroxytryptamine. Invertebr. Reprod. Dev. 21, 231–239.

Lõoke, M., Kristjuhan, K., Kristjuhan, A., 2011. Extraction of genomic DNA from yeasts for PCR-based applications. Biotechniques 50, 325–328.

Loveall, B., Deitcher, D., 2010. The essential role of bursicon during *Drosophila* development. BMC Dev. Biol. 10, 92.

Luo, C., Dewey, E., Sudo, S., Ewer, J., Hsu, S., Honegger, H., Hsueh, A., 2005. Bursicon, the insect cuticle-hardening hormone, is a heterodimeric cystine knot protein that activates G protein-coupled receptor LGR2. Proc. Natl. Acad. Sci. U. S. A. 102, 2820–2825.

Milton, T.W.H., Peter, T.G., 2000. Molecular architecture and biorecognition process of the cystine knot protein superfamily: part I. The glycoprotein hormones. J. Mol. Recognit. 13, 223–278.

Nathan, C.P., Diao, F., Kuan, H., Wang, H., Dewey, E.M., Honegger, H.-W., Benjamin, H.W., 2008. Bursicon functions within the *Drosophila* central nervous system to modulate wing expansion behavior, hormone secretion and cell death. J. Neurosci. 28, 14379–14391.

Parakh, T.N., Hernandez, J.A., Grammer, J.C., Weck, J., Hunzicker-Dunn, M., Zeleznik, A.J., Nilson, J.H., 2006. Follicle-stimulating hormone/cAMP regulation of aromatase gene expression requires β-catenin. Proc. Natl. Acad. Sci. U. S. A. 103, 12435–12440.

Roch, G.J., Sherwood, N.M., 2014. Glycoprotein hormones and their receptors emerged at the origin of metazoans. Genome Biol. Evol. 6, 1466–1479.

Sarojini, R., Jayalakshmi, K., Sambasivarao, S., Nagabhushanam, R., 1988. Stimulation of oogenesis in the freshwater prawn, *Macrobrachium lamerri* by prostagalndin $E_2$ and follicle stimulating hormone. Indian J. Fish. 25, 283–287.

Sarojini, R., Nagabhushanam, R., Fingerman, M., 1995. Mode of action of the neurotransmitter 5-hydroxytryptamine in stimulating ovarian maturation in the red swamp crayfish, *Procambarus clarkii*: an in vivo and in vitro study. J. Exp. Zool. 271, 395–400.

Sarojini, R., Nagabhushanam, R., Fingerman, M., 1996. In vitro inhibition by dopamine of 5-hydroxytryptamine-stimulated ovarian maturation in the red swamp crayfish, *Procambarus clarkii*. Experientia 52, 707–709.

Sharp, J.H., Wilcockson, D.C., Webster, S.G., 2010. Identification and expression of mRNAs encoding bursicon in the plesiomorphic central nervous system of *Homarus gammarus*. Gen. Comp. Endocrinol. 169, 65–74.

Tan-Fermin, J.D., Pudadera, R.A., 1989. Ovarian maturation stages of the wild giant tiger prawn, *Penaeus monodon* Fabricius. Aquaculture 77, 229–242.

Thangaraj, M., Prakash Vincent, S.G., 2004. Assessment of vitellogenin stimulating activity in extracts of brain and sub-oesophageal ganglia of tiger shrimp, *Penaeus monodon*. Indian J. Fish. 51, 133–138.

Treerattrakool, S., Panyim, S., Chan, S.M., Withyachumnarnkul, B., Udomkit, A., 2008. Molecular characterization of gonad-inhibiting hormone of *Penaeus monodon* and elucidation of its inhibitory role in vitellogenin expression by RNA interference. FEBS J. 275, 970–980.

Ulloa-Aguirre, A., Timossi, C., 1998. Structure-function relationship of follicle-stimulating hormone and its receptor. Hum. Reprod. Update 4, 260–283.

Vaca, A.A., Alfaro, J., 2000. Ovarian maturation and spawning in white shrimp, *Penaeus vannamei*, by serotonin injection. Aquaculture 182, 373–385.

Webster, S.G., Wilcockson, D.C., Mrinalini, Sharp, J.H., 2013. Bursicon and neuropeptide cascades during the ecdysis program of the shore crab, *Carcinus maenas*. Gen. Comp. Endocrinol. 182, 54–64.

Weghofer, A., Schnepf, S., Barad, D., Gleicher, N., 2007. The impact of luteinizing hormone in assisted reproduction: a review. Curr. Opin. Obstet. Gynecol. 19, 253–257.

Wilcockson, D.C., Webster, S.G., 2008. Identification and developmental expression of mRNAs encoding putative insect cuticle hardening hormone, bursicon in the green shore crab *Carcinus maenas*. Gen. Comp. Endocrinol. 156, 113–125.

Wongprasert, K., Asuvapongpatana, S., Poltana, P., Tiensuwan, M., Withyachumnarnkul, B., 2006. Serotonin stimulates ovarian maturation and spawning in the black tiger shrimp *Penaeus monodon*. Aquaculture 261, 1447–1454.

Yano, I., 1992. Effect of thoracic ganglion on vitellogenin secretion in kuruma prawn, *Penaeus japonicus*. Bull. Natl. Res. Inst. Aquac. 21, 9–14.

Yano, I., Hoshino, R., 2006. Effect of 17 β-estradiol on the vitellogenin synthesis and oocyte development in the ovary of kuruma prawn (*Marsupenaeus japonicus*). Comp. Biochem. Physiol. A 144, 18–23.

Yano, I., Wyban, J.A., 1992. Induced ovarian maturation of *Penaeus vannamei* by injection of lobster (*Homarus americanus*) brain extract. Bull. Natl. Res. Inst. Aquac. 21, 1–7.

Ye, H., Ma, J., Lin, Q., Wang, G., 2011. Occurrence of follicle-stimulating hormone-like substance in the kuruma prawn, *Marsupenaeus japonicus*, during ovarian maturation. Mar. Biol. Res. 7, 304–309.

Żukowska-Arendarczyk, M., 1981. Effect of hypophyseal gonadotropins (FSH and LH) on the ovaries of the sand shrimp *Crangon crangon* (Crustacea: Decapoda). Mar. Biol. 63, 241–247.

# 11. A formulated double-stranded RNA diet for reducing *Penaeus monodon* densovirus infection in black tiger shrimp.

Journal of Invertebrate Pathology 134 (2016) 23–26

Contents lists available at ScienceDirect

Journal of Invertebrate Pathology

journal homepage: www.elsevier.com/locate/jip

Short Communication

# A formulated double-stranded RNA diet for reducing *Penaeus monodon* densovirus infection in black tiger shrimp

Chaweewan Chimwai [a], Punnee Tongboonsong [a], Orathai Namramoon [a], Sakol Panyim [a,b], Pongsopee Attasart [a,*]

[a] Institute of Molecular Biosciences, Mahidol University, Salaya, Nakhon Pathom 73170, Thailand
[b] Department of Biochemistry, Faculty of Science, Mahidol University, Bangkok 10400, Thailand

ARTICLE INFO

*Article history:*
Received 1 September 2015
Revised 30 December 2015
Accepted 4 January 2016
Available online 5 January 2016

*Keywords:*
*Penaeus monodon* densovirus
Shrimp
RNAi
Double-stranded RNA
Oral delivery
*Pm*DNV inhibition

ABSTRACT

*Penaeus monodon* densovirus (*Pm*DNV) is one of the major causes of stunted shrimp in the aquaculture industry in Thailand. Significant reductions in levels of *Pm*DNV as assessed by PCR analysis of shrimp hepatopancreas were seen in both prophylactic and curative experiments after feeding shrimp with a formulated diet containing mixed inactivated bacteria harboring dsRNAs corresponding to the *Pm*DNV ns1 and vp genes. Significant reductions of approximately 88% (prophylactic) and 64% (curative) of *Pm*DNV were observed, suggesting that this diet has a high potential for application in commercial aquaculture for reducing *Pm*DNV associated stunted growth of shrimp.



Shrimp with a slow growth rate and a stunted appearance remain a problem of the shrimp aquaculture industry in Thailand. *Penaeus monodon* densovirus (*Pm*DNV) (formerly called hepatopancreatic parvovirus or HPV) is one of the causative pathogens of this syndrome (Flegel et al., 1999). While the use of specific pathogen free (SPF) broodstock, discarding *Pm*DNV infected post larvae and exclusion of carrier animals in culture systems are effective methods to avoid outbreaks of this pathogen, high stocking density, poor water quality and improper farm management can contribute to the introduction and spread of the pathogen. Therefore, the development of an efficient approach for *Pm*DNV management is needed.

In the past decade, a number of studies have demonstrated efficient RNA interference (RNAi) based approaches for controlling shrimp viruses. Exogenous double-stranded RNAs (dsRNAs) targeted to viral genes (Robalino et al., 2005; Yodmuang et al., 2006) or endogenous shrimp genes (Ongvarrasopone et al., 2008) essential for viral infection/replication are administered into shrimp prior to virus challenge. As a result, the corresponding messenger RNAs to the introduced dsRNAs are then degraded by the RNase activity of Ago in the siRNA-RISC complex. Consequently the replication of the particular virus is suppressed, significantly reducing shrimp mortality. In the case of *Pm*DNV, a single-stranded DNA non-enveloped virus (Lightner and Redman, 1985; Bonami et al., 1995), two dsRNAs (dsRNA-ns1 and dsRNA-vp) specific to non-structural protein gene (ns1) and structural protein gene (vp), respectively, have shown both protective (Attasart et al., 2010) and therapeutic effects (Attasart et al., 2011) against *Pm*DNV infection in black tiger shrimp. However, the dsRNAs were introduced into shrimp by injection which is not a feasible methodology for application at an industrial shrimp aquaculture scale. Moreover, the successful use of *Escherichia coli* (HT115) as a carrier to deliver specific dsRNA into shrimp via oral feeding has recently been demonstrated (Attasart et al., 2013). Therefore, in this work, a shrimp diet containing a combination of two inactivated HT115 harboring dsRNA-ns1 and dsRNA-vp was formulated and used to feed shrimp (*P. monodon*) before and after challenge with *Pm*DNV and suppression of *Pm*DNV in both prophylactic and curative modes was evaluated.

Prior to starting the experiment, batches of juvenile stage shrimp (200–300 mg) obtained from a hatchery farm were sampled randomly and screened for *Pm*DNV infection by PCR. Total DNA of the hepatopancreas of each shrimp was isolated using DNAzol (Life Technologies) following the manufacturer's protocol. The total DNA pellet was finally resuspended in sterile distilled water at 60 °C and quantitated by UV spectroscopy. Approximately

* Corresponding author.
*E-mail addresses:* pongsopee.att@mahidol.ac.th, attasart_aung@hotmail.com (P. Attasart).

http://dx.doi.org/10.1016/j.jip.2016.01.003
0022-2011/

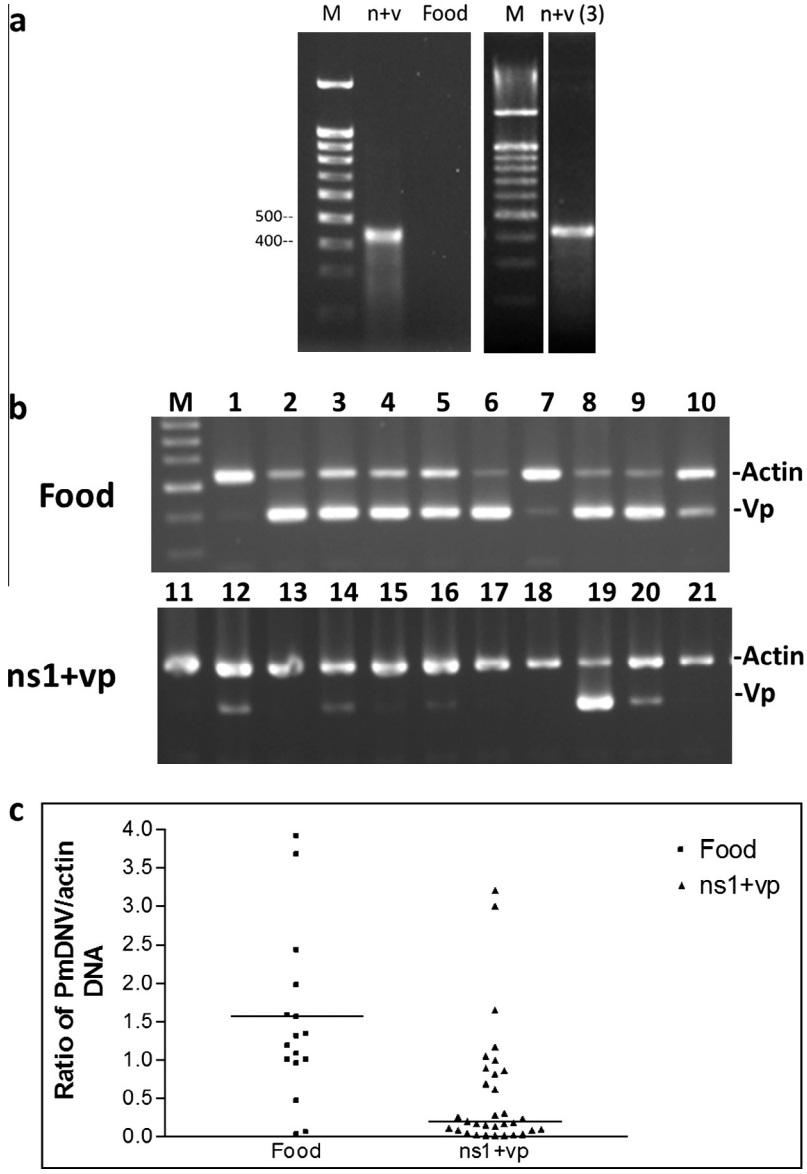


**Fig. 1.** Protective effect of a dsRNA formulated diet on *Pm*DNV infection. (a) Total RNA was extracted from a formulated diet containing a combination of bacteria expressing dsRNA-ns1 and dsRNA-vp ($n + v$) or after 3 months storage ($n + v$ (3)) or commercial food pellet (Food) by Ribozol. After RNase A treatment, the integrity of dsRNA was visualized by 1.5% agarose gel electrophoresis. M: 100-bp ladder. (b) The amount of *Pm*DNV in each shrimp was determined by multiplex PCR using viral specific primers (vp) together with primers to shrimp actin (for normalization). Lanes 1–10 represent individual shrimp fed with commercial food (Food), lanes 11–21 represent individual shrimp fed the formulated diet. M: 100-bp ladder. (c) The relative amount of normalized *Pm*DNV of individual shrimp is shown together with the median line. The $p$ value is less than 0.0001.

200 ng total DNA was used as a template for vp amplification using vp-s (5′AATCTGCAGGGTACGGAAAAAAC3′) and vp-a (5′TGTGGAAC CATCTCAAATGCC 3′) primers. As an internal control, shrimp actin primers; F (5′GACTCGTACGTCGGGCGACGA GG 3′) and R (5′AGCA GCGGTGGTCATCACCTGCTC3′), were included in the amplification. The PCR amplification procedure was carried out as follows: 94 °C for 2 min, denaturation at 94 °C for 10 sec, annealing at 55 °C for 30 sec, and extension at 72 °C for 1 min. After 30 cycles, the reaction was held at 72 °C for another 5 min. The PCR products were analyzed by agarose gel electrophoresis (data not shown). Batches of shrimp were designated as *Pm*DNV free (no PCR product) or *Pm*DNV infected (presence of the 400 bp viral PCR product) based on the screening results, and were subsequently used in the preventive and curative experiments.

Two recombinant plasmids, pET17b-stns1 and pET17b-stvp (Attasart et al., 2010), were used for the production of dsRNA-ns1 and dsRNA-vp, respectively. Each dsRNA was synthesized in RNaseIII deficient bacteria (HT115) according to the protocol of Ongvarrasopone et al. (2007). The overnight culture was diluted and grown at 37 °C until the $OD_{600}$ reached 0.4 before induction with 0.4 mM of isopropyl-β-D-thiogalactopyranoside (IPTG) for 4 h. The bacterial cells were then centrifuged at 6000*g* for 5 min at 4 °C. For environmental safety, the bacterial cells were inactivated by treatment with 0.5% formaldehyde in PBS and cells were subsequently kept at −20 °C until use. The diet was formulated using the conditions previously described (Attasart et al., 2013). To prepare the diet, the two inactivated bacteria preparations containing dsRNA-ns1 and dsRNA-vp were combined at a 1:1 $OD_{600}$ ratio before centrifugation. The bacterial pellet was then mixed with ground commercial shrimp food (CP, Thailand) and pellet binder (fresh ripe banana (Nam-wa variety)) at a 1:1:1 weight ratio before being extruded through a syringe and air-dried overnight

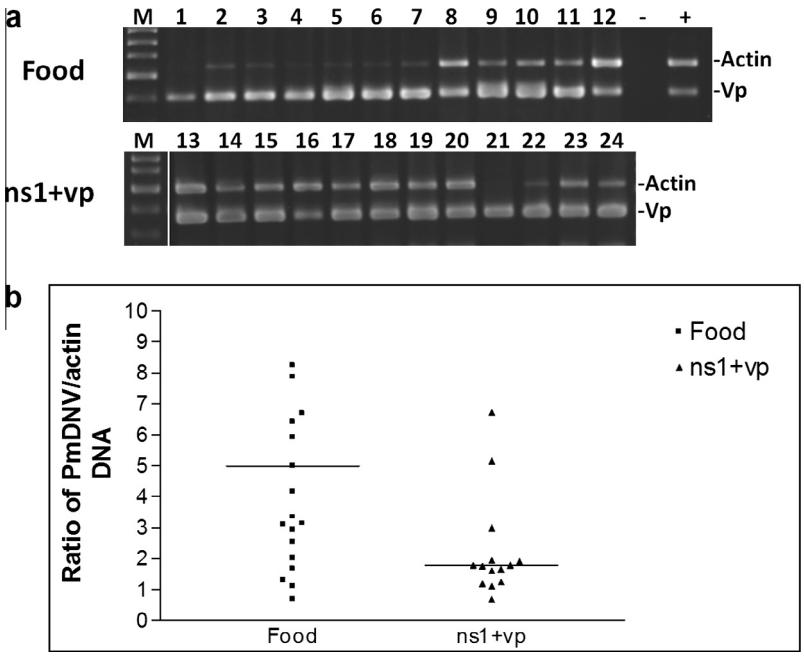


**Fig. 2.** Therapeutic effect of a dsRNA formulated diet on *Pm*DNV infection. (a) Naturally *Pm*DNV infected shrimp were fed a control diet or a formulated diet for two weeks after which the amount of *Pm*DNV in each shrimp was determined by multiplex PCR using viral specific primers (vp) together with primers to shrimp actin (for normalization). Lanes 1–12 represent individual shrimp fed with commercial food (Food), lanes 13–24 represent individual shrimp fed the formulated diet. M: 100-bp ladder. (b) The relative amount of normalized *Pm*DNV of individual shrimp is shown together with median line. The *p* value is 0.01.

at room temperature. The dry strings were then broken into small pieces consistent with commercial shrimp food pellets and kept at room temperature or in a refrigerator until use. To evaluate the integrity of the dsRNA during preparation of the shrimp diet, total RNA was extracted from 10 milligrams (mg) of dry pellets which contained approximately 2.6–3 $\times$ $10^9$ bacterial cells. The pellets were ground in 250 μl of 0.1% sodium dodecyl sulfate (SDS) in phosphate buffer saline (PBS) and the homogenate was boiled for 2 min and quickly cooled on ice. The RNA was treated with RNaseA (1 μg) in the presence of 1X RNase buffer (300 mM Sodium acetate, 10 mM Tris-Cl pH7.5) for 30 min to degrade unwanted single-stranded RNAs before extraction using Ribozol (Amresco). The extracted dsRNAs were dissolved in 150 mM NaCl and analyzed by electrophoresis though a 1.5% agarose gel. As shown in Fig. 1a, a clear band of dsRNA was observed at approximately 400 bp in the formulated diet but not in the control food without dsRNA. By comparison with the DNA marker, the amount of mixed dsRNAs was approximately 7.5 micrograms (μg) per milligram dry weight of diet. This formulated diet can be kept for up to 3 months without degradation of dsRNAs (Fig. 1a), similar to other diets previously presented (Attasart et al., 2013), suggesting a high stability of the formulated diet, which is suitable for commercial applications.

To test the preventive effect of this diet, *Pm*DNV free shrimp (200–300 mg body weight) were divided into two groups (10 shrimp for control and 20 shrimp for feeding diet, in duplicate) and reared in separate cages in 10 parts per thousand (ppt) sea water. Shrimp were fed with 30 mg of the diet-ns1 + vp or commercial food twice a day for 14 days. During this period, shrimp were challenged with *Pm*DNV by injection on days 7 and 8. To prepare the *Pm*DNV lysate for injection, the hepatopancreas of a *Pm*DNV infected shrimp was homogenized in TN buffer (20 mM Tris-HCl, 400 mM NaCl, pH 7.4) at 0.1 g/ml. The homogenate was centrifuged at 9100*g* for 10 min at 4 °C after which the supernatant was filtered through a 0.45 μm filter. The level of viral DNA in the hepatopancreas of each surviving shrimp was monitored by PCR with co-amplification of shrimp actin gene for normalization (Fig. 1b). To quantitate the amount of *Pm*DNV in shrimp, the intensity of the viral PCR product was determined using the Scion Image program and the signal was normalized with the band intensity of shrimp actin. The relative levels of *Pm*DNV/actin were compared and the statistic analyzed by an unpaired t test. The levels of *Pm*DNV in shrimp fed with the formulated diet were significantly lower than that of the control shrimp (87.5%; $p = 0.0001$) (Fig. 1c), indicating that feeding of dsRNAs (ns1 + vp) can effectively inhibit *Pm*DNV replication in shrimp.

To evaluate the potential curative effect of this diet essentially the same experimental conditions were used as previously described, except that shrimp (10 shrimp each, in duplicate) already infected with *Pm*DNV were used in the study, and they were not challenged with *Pm*DNV on days 7 and 8. After feeding for 14 days, semi-quantitative PCR was employed to determine the amount of *Pm*DNV in the surviving shrimp hepatopancreas. After normalization with actin, a significant reduction of *Pm*DNV (64%; $p = 0.01$) was observed in the shrimp fed with dsRNA-ns1 + vp in comparison to the control shrimp (Fig. 2a and b), suggesting that the diet can therapeutically clear existing *Pm*DNV in shrimp after a relatively short time of feeding.

Although the strategy of induction of RNAi via feeding of dsRNA has been applied to viral inhibition by several research groups, the stability of their formulated diets, as well as the potency of viral inhibition vary (Sarathi et al., 2008; Sellars et al., 2011; Saksmerprome et al., 2013; Kumar et al., 2013). For example, control of Laem-singh virus (LSNV) required continuous ingestion of a formulated diet up to 9 weeks for a 20–60% reduction of virus (Saksmerprome et al., 2013), and protection of black tiger shrimp from Gill-associated virus (GAV) was only achieved by injection and not by oral feeding of bacterially expressed dsRNAs (Sellars et al., 2011). To achieve a 68% reduction of shrimp mortality from WSSV infection, 5 days of continuous feeding before and after viral challenge was required. Their diet was coated with inactivated bacteria harboring dsRNA and had to be freshly prepared and kept

in a refrigerator (4 °C) before use (Sarathi et al., 2008; Kumar et al., 2013) whereas our diet can be stored at room temperature for up to 3 months without loss of dsRNA. In this study, *Pm*DNV was clearly diminished in both protective (87.55%) and curative (64%) modes within only 14 days, indicating the high potency of the formulated diet for controlling *Pm*DNV infection in the shrimp. As infection with *Pm*DNV is statistically related to retarded growth in *P. monodon* (Flegel et al., 1999), reduction of *Pm*DNV in infected shrimp should resume the normal shrimp growth. However, whether the growth rate of infected shrimp is restored when *Pm*DNV is reduced by feeding dsRNAs remains to be elucidated.

## Acknowledgments

We thank Professor Duncan Smith for the grammatical corrections. Our appreciation is expressed to Mr. Wichai Boonsai and Mr. Prasong Kasetpittaya for their kindness in providing shrimp, Mrs. Suparp Hongthong for her technical assistance. This work was supported by the Thailand Research Fund (DPG5680001 to S. P. and IRG5780009), the Office of the Higher Education Commission and Mahidol University under the National Research Universities Initiative and a Mahidol University Research grant.

## References

Flegel, T.W., Thamavit, V., Pasharawipas, T., Alday-Sanz, V., 1999. Statistical correlation between severity of hepatopancreatic parvovirus infection and stunting of farmed black tiger shrimp (*Penaeus monodon*). Aquaculture 174, 197–206.

Robalino, J., Bartlett, T., Shepard, E., Prior, S., Jaramillo, G., Scura, E., Chapman, R.W., Gross, P.S., Browdy, C.L., Warr, G.W., 2005. Double-stranded RNA induces sequence-specific antiviral silencing in addition to nonspecific immunity in a marine shrimp: convergence of RNA interference and innate immunity in the invertebrate antiviral response? J. Virol. 79, 13561–13571.

Yodmuang, S., Tirasophon, W., Roshorm, Y., Chinnirunvong, W., Panyim, S., 2006. YHV-protease dsRNA inhibits YHV replication in *Penaeus monodon* and prevents mortality. Biochem. Biophys. Res. Commun. 341, 351–356.

Ongvarrasopone, C., Chanasakulniyom, M., Sritunyalucksana, K., Panyim, S., 2008. Suppression of *Pm*Rab7 by dsRNA inhibits WSSV or YHV infection in shrimp. Mar. Biotechnol. (NY) 10, 374–381.

Lightner, D.V., Redman, R.M., 1985. A provo-like virus disease of penaeid shrimp. J. Invertebr. Pathol. 45, 47–53.

Bonami, J.R., Mari, J., Poulos, B.T., Lightner, D.V., 1995. Characterization of hepatopancreatic parvo-like virus, a second unusual parvovirus pathogenic for penaeid shrimps. J. Gen. Virol. 76, 813–817.

Attasart, P., Kaewkhaw, R., Chimwai, C., Kongphom, U., Namramoon, O., Panyim, S., 2010. Inhibition of *Penaeus monodon* densovirus (*Pm*DNV) replication in shrimp by double-stranded RNA. Arch. Virol. 155, 825–832.

Attasart, P., Kaewkhaw, R., Chimwai, C., Kongphom, U., Panyim, S., 2011. Clearance of *Penaeus monodon* densovirus in naturally pre-infected shrimp by combined ns1 and vp dsRNAs. Virus Res. 159, 79–82.

Attasart, P., Namramoon, O., Kongphom, U., Chimwai, C., Panyim, S., 2013. Ingestion of bacteria expressing dsRNA triggers specific RNA silencing in shrimp. Virus Res. 171, 252–256.

Ongvarrasopone, C., Roshorm, Y., Panyim, S., 2007. A simple and cost effective method to generate dsRNA for RNAi studies in invertebrates. ScienceAsia 33, 35–39.

Sarathi, M., Simon, M.C., Venkatesan, C., Hameed, A.S., 2008. Oral administration of bacterially expressed VP28dsRNA to protect *Penaeus monodon* from white spot syndrome virus. Mar. Biotechnol. (NY) 10, 242–249.

Sellars, M.J., Rao, M., Arnold, S.J., Wade, N.M., Cowley, J.A., 2011. *Penaeus monodon* is protected against gill-associated virus by muscle injection but not oral delivery of bacterially expressed dsRNAs. Dis. Aquat. Organ. 95, 19–30.

Saksmerprome, V., Thammasorn, T., Jitrakorn, S., Wongtripop, S., Borwornpinyo, S., Withyachumnarnkul, B., 2013. Using double-stranded RNA for the control of Laem-Singh Virus (LSNV) in Thai *P. monodon*. J. Biotechnol. 164, 449–453.

Kumar, S.N., Karunasagar, I., Karunasagar, I., 2013. Protection of *Macrobrachium rosenbergii* against white tail disease by oral administration of bacterial expressed and encapsulated double-stranded RNA. Fish Shellfish Immunol. 35, 833–839.

# 12. Cholesterol-based cationic liposome increases dsRNA protection of yellow head virus infection in *Penaeus vannamai*.

Journal of Biotechnology 228 (2016) 95–102

Contents lists available at ScienceDirect

Journal of Biotechnology

journal homepage: www.elsevier.com/locate/jbiotec

# Cholesterol-based cationic liposome increases dsRNA protection of yellow head virus infection in *Penaeus vannamei*

Poohrawind Sanitt[a], Nuttapon Apiratikul[b], Nattisa Niyomtham[c], Boon-ek Yingyongnarongkul[c], Wanchai Assavalapsakul[d], Sakol Panyim[a,e], Apinunt Udomkit[a,*]

[a] *Institute of Molecular Biosciences, Mahidol University, Salaya Campus, Nakhon Pathom 73170, Thailand*
[b] *Department of Chemistry, Faculty of Science, Srinakharinwirot University, Bangkok, 10110, Thailand*
[c] *Department of Chemistry and Center of Excellence for Innovation in Chemistry, Faculty of Science, Ramkhamhaeng University, Bangkok, 10240, Thailand*
[d] *Department of Microbiology, Faculty of Science, Chulalongkorn University, Bangkok, 10330, Thailand*
[e] *Department of Biochemistry, Faculty of Science, Mahidol University, Bangkok, 10400, Thailand*

ARTICLE INFO

*Article history:*
Received 3 February 2016
Received in revised form 13 April 2016
Accepted 28 April 2016
Available online 29 April 2016

*Keywords:*
RNA interference
Shrimp
Cationic liposome
Yellow head virus
Double-stranded RNA delivery

ABSTRACT

Protection of shrimp from yellow head virus (YHV) infection has been demonstrated by injection and oral delivery of dsRNA-YHV protease gene (dsYHV) or shrimp endogenous gene (dsRab7). However, to achieve complete viral suppression and to prolong dsRNA activity, the development of an effective dsRNA delivery system is required. In this study, four cationic liposomes were synthesized and tested for their ability to increase dsRNA efficiency. The results demonstrated that entrapping dsYHV in a cholesterol-based cationic liposome gave the best protection against YHV infection when compared with other cationic lipids. The cholesterol-based cationic liposome-dsYHV (Chol-dsYHV) complex conferred YHV protection in a dose-dependent manner. Injection with Chol-dsYHV at 0.05 μg dsYHV/g shrimp could give comparable level of YHV protection to the injection with 1.25 μg naked dsYHV/g shrimp. The shrimp injected with Chol- dsYHV at 1.25 μg dsRNA/g shrimp showed only 50% mortality at 60 days post injection whereas the naked dsYHV at the same concentration gave 90% mortality. Thus, the liposome-entrapped dsYHV could lower an effective dsRNA concentration in viral protection and prolong dsRNA activity. In addition, encapsulating dsRab7 in the cholesterol-based cationic liposome could protect the dsRab7 from enzymatic digestion, and continuous feeding the shrimp with the diet formulated with the liposome-entrapped dsRab7 for 4 days in the total of 960 μg dsRab7/g shrimp could enhance YHV protection efficiency compared with the naked dsRab7. Our studies reveal that cholesterol-based cationic liposome is a promising dsRNA carrier to enhance dsRNA efficiency in both injection and oral delivery systems.


## 1. Introduction

Yellow head virus (YHV) is a rod shape, positive-sense, single-stranded RNA virus with the genome size of 26,622 nucleotides (Sittidilokratna et al., 2008). The virus was found in Thailand in 1992 and is named for the yellowish cephalothorax and very sallow overall coloration (Flegel, 1997). The virus is a virulent pathogen capable of infecting several penaeid shrimps resulting in huge economic loss in shrimp farm industry (Flegel, 1997; Senapin et al., 2010). Upon YHV infection, severe damage in shrimp lymphoid organ, gill, connective tissues, hemocytes and hematopoietic organ was observed (Wang et al., 1996). YHV binds to a specific receptor (YRP65) at the cell membrane of primary lymphoid cell, which was thought to be the primary target of the virus (Assavalapsakul et al., 2006). YHV was shown to internalize into a target cell *via* the clathrin mediated endocytosis, in which at least clathrin heavy chain and clathrin coat assembly protein 17 were demonstrated to be involved (Jatuyosporn et al., 2014; Posiri et al., 2015). The binding of the virus to its specific receptor YRP65 leads to endocytosis *via* the assembly of clathrin and the formation of a coated pit on the plasma membrane. The coated pit later invaginates and pinches off to form an intracellular clathrin-coated vesicle. Depolymerization of clathrin-coated vesicles results in the formation of early endosome and subsequently late endosome, which is then transported to lysosome. Viruses somehow escaped from the late endosome prior to acidification in the lysosome to cytosol by either membrane fusion or membrane disruption mechanisms (Mousavi et al., 2004). The endosomal trafficking of viruses

* Corresponding author.
*E-mail address:* apinunt.udo@mahidol.ac.th (A. Udomkit).

http://dx.doi.org/10.1016/j.jbiotec.2016.04.049
0168-1656/

from early endosome to late endosome and eventually to lysosome requires several small GTPases in the Rab family (Macovei et al., 2013; Meresse et al., 1995; Liu et al., 2014; Ongvarrasopone et al., 2008; Vanlandingham and Ceresa, 2009).

During the past decade, a small RNA-mediated gene silencing mechanism known as RNA interference (RNAi) has been developed as a tool to prevent YHV infection in shrimp. RNAi is a sequence-specific antiviral mechanism used for an innate antiviral response in invertebrate that is triggered by double-stranded RNA (dsRNA) (Robalino et al., 2004; Tirasophon et al., 2005). Principally, long dsRNA is cleaved into small interfering RNA (siRNA) which is then incorporated into a multi-component complex known as RNA-induced silencing complex (RISC), and unwound into single-stranded RNA. The sense strand of the siRNA guides the RISC to a complementary mRNA target. The cleavage of the mRNA by an RNaseH-like activity of the Argonaute protein, one of protein components in the RISC finally leads to mRNA degradation by cellular nucleases (Wilson and Doudna, 2013).

Delivery system of dsRNA is a crucial tool to convey RNAi to the target cells. Previously, injection of naked dsRNA specific to YHV protease gene could inhibit YHV replication and eventually reduced shrimp mortality (Yodmuang et al., 2006). In addition, suppression of shrimp endogenous gene PmRab7 that is involved in viral transport from late endosome to lysosome could prevent viral replication. This suppression may cause viral accumulation in late endosome and prevent viruses from escaping to the cytosol (Ongvarrasopone et al., 2008). However, delivery of the naked dsRNA to trigger RNAi pathway is limited by dsRNA longevity. It has been shown that inhibition of YHV replication in the shrimp injected with YHV-specific dsRNA (dsYHV) 5 days prior to YHV infection was not as effective as that in the shrimp receiving dsYHV for a shorter period before YHV infection (Yodmuang et al., 2006). In addition, injection of Rab7-specific dsRNA (dsRab7) could not completely suppress *Rab7* mRNA (Ongvarrasopone et al., 2008) and high dose of the dsRab7 injection could be lethal to shrimp (unpublished data). Delivery of naked dsRNA into shrimp may not be an effective way to transfer dsRNA to the target cells, and thus could not prolong sufficient dsRNA activity. To improve dsRNA efficiency, development of a safe and more effective delivery system is required.

Cationic lipids are amphipathic molecules developed for nucleic acid delivery system and usually consist of a hydrophobic head group attached *via* a linker to double hydrocarbon chains or cholesterol derivatives (Wasungu and Hoekstra, 2006). Cationic lipids can adopt various structural phases of cationic liposome when resuspended in an aqueous environment and are biodegradable after administration *in vivo* by endogenous enzymes (Oh and Park, 2009). The lipid composition in liposome surface can interact with negatively charged molecules of nucleic acids providing co-delivery to the target cells (Shim et al., 2013). A number of cationic liposome have been synthesized to develop delivery system for drugs or nucleic acid-based molecule through the circulatory system to target cells *via* oral delivery (Iwanaga et al., 1997), injection (Dong et al., 2012; Misra et al., 2014; Sioud and SØrensen, 2003) or *in vitro* delivery (Serikawa et al., 2000; Apiratikul et al., 2013a). Cationic lipids could also stabilize and prolong DNA complex molecule half-life introduced by an *in vitro* gene delivery system (Hong et al., 1997).

Several kinds of cholesterol based-cationic liposome were synthesized and utilized in siRNA delivery (Kim et al., 2008; Oh and Park, 2009; Tagami et al., 2012). Injection of synthetic cholesterol-based cationic liposome with dsRNA into shrimp was shown to increase dsRNA transfection efficiency (Apiratikul et al., 2013b). However, efficiency and longevity of dsRNA in the liposome complex for viral inhibition were not determined. Here we develop a delivery system using the synthetic cholesterol-based cationic liposome as a dsRNA carrier to enhance the efficiency of viral protection and prolong the activity of dsRNA *in vivo*. Oral delivery of the cationic liposome-dsRNA complex into shrimp is also shown to prevent viral infection.

## 2. Materials and methods

### 2.1. Shrimp culture

Post larvae of *Penaeus vannamei* at 15–20 days old were obtained from a farm in Chonburi, Thailand. The shrimp were reared in sea water at 10 parts per thousand (ppt) salinity (pH 8.0) and fed on commercial tablet food (CP, Thailand) until their body weight were 200–250 mg or 2 g. The shrimp were acclimatized one night before starting an experiment.

### 2.2. Virus stock

The YHV stock for all experiments in this study was prepared as described by Sanitt et al. (2014) with minor adaptation. Briefly, the virus stock were prepared from hemolymph or gills of infected shrimp. The hemolymph of YHV-infected moribund *P. vannamei* was drawn and immediately mixed with anticoagulant(85 mM sodiumcitrate, 62.2 mM citric acid, and 110 mM dextrose, pH 4.9) whereas the gills were ground and resuspended in NTE buffer (0.2 M NaCl, 0.2 M Tris/HCl pH 6.5, 0.02 M EDTA) prior to filter. The solution was centrifuged at 9000*g* for 10 min at 4 °C. The supernatant was collected as crude viral solution and kept in aliquot at −80 °C until use.

### 2.3. Cationic liposome preparation

Four kinds of cationic liposomes were synthesized; cholesterol-based cationic liposome as well as Cy and Dx was prepared as described previously (Apiratikul et al., 2013a,b; Niyomtham et al., 2015) whereas lipid **1** (Fig. 1A and B) was synthesized as follows. Briefly, to a stirred solution of di-*tert*-butyl carbonate (1.2 g, 5.5 mmol) in $CH_2Cl_2$ (20 ml) was added dropwise a solution of (±)-3-amino-1,2-propanediol (**2**) (0.5 g, 5.5 mmol) in $CH_2Cl_2$ (30 ml) and the mixture was stirred for 24 h. The solvent was evaporated under reduced pressure, the residue was suspended in $H_2O$ (100 ml) and extracted with $CH_2Cl_2$ (3 × 50 ml). The combined organic phase was washed with $H_2O$ and dried over anhydrous $Na_2SO_4$. The solvent was concentrated *in vacuo* and the crude product was purified by column chromatography using $CH_2Cl_2$ and $CH_2Cl_2$-MeOH as eluting solvent with gradual increase in concentration of the more polar component to yield compound **3** as a white solid (0.92 g, 88%). Myristic acid (2.4 g, 10.8 mmol), dicyclohexylcarbodiimide (2.2 g, 10.8 mmol) and 4-dimethylaminopyridine (DMAP) were dissolved in dry $CH_2Cl_2$ (15 ml). The reaction mixture was stirred at room temperature for 30 min, a solution of compound **3** (0.5 g, 4.9 mmol) in dry $CH_2Cl_2$ (5 ml) was then added, and the resulting mixture was stirred overnight at the same temperature. The precipitated dicyclohexyl urea was removed by filtration, and the filtrate was evaporated under reduced pressure to give crude product. The product **4** (2.5 g, 92%) was obtained as white solid after usual column chromatographic purification. To a solution of compound **4** (1.1 g, 1.9 mmol) in $CH_2Cl_2$ (5 ml) was added 20% TFA in $CH_2Cl_2$ (20 ml) and the mixture stirred for 1 h. The solvent was removed under stream of nitrogen gas and further dried under vacuum for 2 h to obtain the lipid **1** as white sticky solid (1.8 g, 100% as TFA salt).

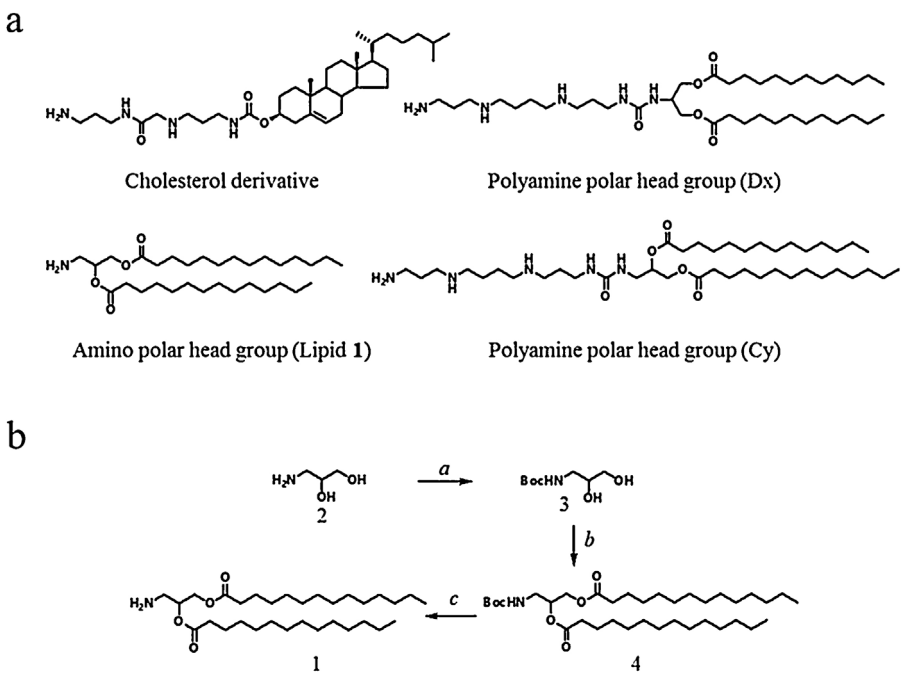


**Fig. 1.** (A) Structures of synthetic cationic lipids used in this study; cholesterol derivative, lipid 1, Cy and Dx. (B) Reagents and Conditions for the Synthesis of lipid **1**: *a*) di-*tert*-butyl dicarbonate, *b*) myristic acid, *c*) TFA.

### 2.4. *dsRNA production in* Escherichia coli

Two recombinant plasmids, pET3a-dsYHV and pET17b-dsRab7, were used to produce dsRNAs targeting *protease* gene of YHV (dsYHV, 400 bp) (Yodmuang et al., 2006) and shrimp *PmRab7* gene (dsRab7, 420 bp) (Ongvarrasopone et al., 2008), respectively. The pET3a-dsYHV and pET17b-dsRab7 were kindly provided by Dr. Witoon Tirasophon and Dr. Chalermporn Ongvarrasopone, Institute of Molecular Biosciences Mahidol University, respectively. Each dsRNA was expressed in *E. coli* HT115 according to the protocol as described previously (Ongvarrasopone et al., 2008). The expression of dsRNA was induced by adding 0.4 mM isopropyl-β-D-thiogalactopyranoside (IPTG) to the bacterial culture, and the culture was further incubated at 37 °C for 4 h. The bacterial cells were then harvested by centrifugation at 6000*g* for 5 min at 4 °C. The cell pellet was used for dsRNA extraction or kept at −30 °C until used for enzymatic digestion assay. The dsRNAs were extracted using Tri Reagent® (Molecular Research Center) according to the manufacturer's protocol.

### 2.5. *Preparation of liposome-dsRNA complex for interaction assay*

Each cationic liposome was prepared in 1 ml of 150 mM NaCl containing 1 mg of cationic lipid and 50 μg of dsYHV (20:1 mass ratio (w/w) of cationic liposome:dsYHV). The mixture was then mixed by vortex mixer for 5 min prior to sonication for 20 min. The liposome complex from each lipid was then centrifuged at 10,000*g* for 3 min. The supernatant was collected while the pellet was then resuspended in 500 μl of 150 mM NaCl. To determine whether the cationic liposome-dsRNA complex was properly formed, both the supernatant and the pellet fractions were re-precipitated with isopropanol separately before analyzed by agarose gel electrophoresis.

For mass ratio assay, the cholesterol-based cationic liposome-dsYHV complex (Chol-dsYHV) was prepared from different ratios of cholesterol-based liposome:dsYHV (w/w) at 5:1, 10:1, 20:1, 40:1 and 80:1 in 1 ml of 150 mM NaCl containing 1 mg of the cholesterol-based liposome. Thereafter, the Chol-dsYHV complex was centrifuged at 10,000*g* for 3 min. The complex formation was determined by analysis of the dsYHV in both the pellet and the supernatant fractions as mentioned above.

### 2.6. *Cationic liposome-dsYHV complex injection assay in shrimp*

Each cationic liposome-dsYHV complex was prepared at the mass ratio 20:1 (w/w) as mentioned above. The mixture was then mixed vigorously until a clump liposome was seen prior to sonication for 20 min to obtain milky suspension. Subsequently, the cationic liposome-dsRNA suspension was diluted in 150 mM NaCl and used for the injection assay. A volume of 50 μl of each cationic liposome-dsYHV complex was injected into the hemolymph of pacific white shrimp, *Penaeus vannamei* (approximately 2 g body weight) to give dsYHV at 0.05 μg/g shrimp, while the control shrimp were injected with 0.05 μg of naked dsYHV/g shrimp. At 24 h following cationic liposome-dsYHV complex injection, the shrimp were injected with 100 μl of $10^{-6}$ dilution of YHV stock solution that caused 100% mortality of shrimp within about 5 days. The second YHV challenge was repeated again on day 7 after the first YHV challenge, and the mortality was recorded daily. For a dose-dependent assay of Chol-dsYHV complex, shrimp were injected with either Chol-dsYHV complex (20:1 mass ratio) or naked dsYHV at 0.05 and 1.25 μg/g shrimp. Twenty-four hours later, the shrimp were challenged with 100 μl of $10^{-6}$ YHV solution, and the shrimp were challenged continuously at every 7 days afterward. The mortality was recorded daily as described above.

### 2.7. *Oral administration of cholesterol-based liposome-dsRab7 complex*

A Chol-dsRab7 was prepared as described above at 20:1 mass ratio and embedded in shrimp diet for feeding as previously described (Sanitt et al., 2014) with minor adaptation. Briefly, 5 ml of the Chol-dsRab7 complex or 6 mg of naked dsRab7 in 150 mM NaCl were mixed with 5 ml of blended ark shell (*Anadara granosa*) in 150 mM NaCl. Subsequently, 10 ml of 2% natural agar (Krungsri Ayudhaya international food industry, Thailand) in 150 mM NaCl (45 °C) was added, and the mixture was solidified in a petri-dish.

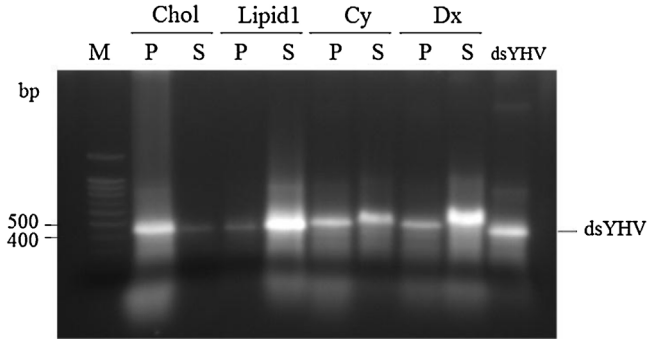


**Fig. 2.** Formation of cationic liposome-dsYHV complexes. One milligram of each cationic lipid (Chol, lipid 1, Cy and Dx) was mixed with 50 μg of dsYHV in 1 ml of 150 mM NaCl. The mixture was then centrifuged at 10,000*g* for 3 min. The supernatant was collected, and the pellet was resuspended in 500 μl of 150 mM NaCl. To determine complex formation between dsRNA and cationic liposome, dsYHV in both the supernatant (S) and the pellet (P) fractions were recovered by isopropanol precipitation and visualized by agarose gel electrophoresis. M is 100 bp DNA ladder marker. The purified dsYHV was loaded as a positive control.

The agar was then cut into pieces of $4 \times 5 \times 5\ mm^3$, each one containing approximately 30 μg of dsRab7. The shrimp (about 250 mg body weight) were divided into three groups, 10 shrimp each, and fed with the diet containing either the Chol-dsRab7 complex, naked dsRab7 or commercial feed for 4 days (twice a day, 2 pieces per meal). Twenty-four hours after feeding for 4 days, the shrimp were submerged in transparent plastic boxes containing 100 ml of $10^{-6}$ YHV dilution in 10 ppt sea water for 8 h. The shrimp were subsequently transferred into an individual basket and continuously fed with commercial feed for 6 days. The mortality of the shrimp in each group was recorded daily.

### 2.8. Enzymatic digestion assay

In order to prove whether the Chol-dsRNA complex would be degraded by shrimp enzymes or not, the enzyme digestion assay was performed. Either hepatopancreas, muscle or hemocyte was collected from 4 shrimp (approximately 1 g in size) and homogenized on ice in 100 μl of 0.1 M Tris, 0.02 M NaCl pH 7.0 buffer for 1 min. The homogenate was then centrifuged at 10,000 rpm at 4 °C for 5 min. The supernatant was used as an enzyme extract in the enzyme digestion reaction. About 100 μg of the enzyme extract from each tissue were mixed with 10 μg of Chol-dsRab7 or naked dsRab7 or $5 \times 10^7$ CFU of *E. coli* expressing dsRab7 and incubated for 6 h at room temperature. The reactions were stopped by keeping at −20 °C, and the dsRab7 from each reaction was extracted using Tri Reagent®. The extracted dsRNA from each enzymatic digestion reaction extract were then analyzed by agarose gel electrophoresis.

## 3. Results

### 3.1. Formation of cationic liposome-dsRNA complex

In order to investigate the complex formation between each cationic lipid and dsYHV, four different types of cationic lipids (Fig. 1A) were used to prepare cationic liposome-dsYHV complex. The analysis of dsYHV distribution in the supernatant or the pellet fractions of the complex mixture by agarose gel electrophoresis showed that the majority of dsYHV were present in the pellet of cholesterol-based liposome-dsYHV complex (Chol-dsYHV), while the dsYHV mixed with other cationic lipids was found mostly in the supernatant (Fig. 2) indicating that the cholesterol-based liposome could entrap dsYHV and form liposome-dsRNA complex better than other cationic liposomes.

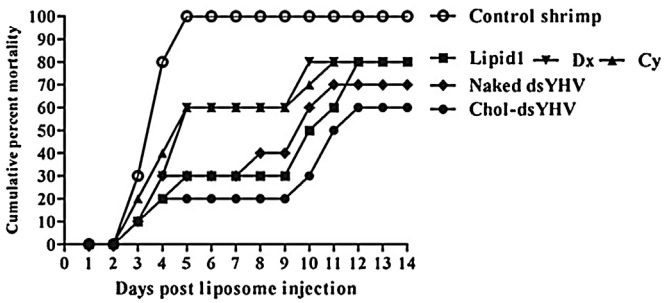


**Fig. 3.** Cationic liposome injection assay. Each cationic liposome-dsYHV complex was injected into 2 g shrimp at 0.05 μg/g shrimp body weight in compared with naked dsYHV (n = 10 in each group). The shrimp were challenged with $10^{-6}$ YHV dilution at 24 h later, and the second YHV challenge was performed on day 7 after the first challenge. The control shrimp received neither the liposome-dsYHV complex nor the naked dsYHV.

To determine whether cationic liposome-dsYHV complexes could enhance the efficiency of dsYHV in silencing the expression of YHV *protease* gene, the cationic liposome-dsYHV from each lipid was injected into shrimp followed by YHV challenge. The result demonstrated that all the shrimp in the control group that received no dsYHV died within 5 days after the first YHV challenge, whereas the shrimp injected with naked dsYHV showed delay mortality that reached only 70% on day 14. All the shrimp injected with any of the four cationic liposome-dsYHV complex also showed delay mortality, but only the shrimp injected with Chol-dsYHV could markedly delay shrimp mortality after the second YHV challenge on day 7, when compared with the shrimp injected with naked dsYHV (Fig. 3). The result suggested that the Chol-dsYHV could enhance dsYHV efficiency and gave better viral protection than naked dsYHV, therefore it was selected for further studies.

In order to further investigate whether the Chol-dsYHV could be used as a dsRNA carrier for YHV protection, the appropriate ratio of cholesterol-based cationic liposome to dsYHV (w/w) that would give the maximal product of liposome-dsYHV complex was first optimized. The efficiency of complex formation was determined by the distribution of dsYHV in the supernatant or in the pellet fraction of the mixture between cholesterol-based cationic liposome and dsYHV. The result in Fig. 4 showed that when mixed at the mass ratios of 5:1 and 10:1 (liposome:dsYHV), the dsYHV band remained in the supernatant fraction indicating that the Chol-dsYHV complex was not generated. By contrast, the ratios of 20:1, 40:1 and 80:1 showed the band of dsYHV in the pellet fraction indicating the formation of liposome-dsYHV complex at these ratios. The ratio 20:1 showed the highest intensity of the dsYHV band in the pellet fraction comparing to other ratios suggesting that the Chol-dsYHV complex was well produced at this ratio, which was the most suitable for liposome-dsYHV preparation.

### 3.2. Cholesterol-based liposome entrapping dsYHV enhances and prolongs dsYHV efficiency

To determine the maximal YHV protection by the Chol-dsYHV complex, different amounts of the complex were used to inject into the shrimp prior to YHV challenge. The result (Fig. 5) demonstrated that control shrimp that received no dsYHV nor Chol-dsYHV reached 100% mortality within 7 days, whereas injection of naked dsYHV at the concentration of 0.05 μg/g shrimp could give protection to YHV at some extent and took 19 days to reach 100% mortality. Injection of Chol-dsYHV containing an equivalent amount of dsYHV could prolong YHV protection up to about 40 days with 90% mortality, which was comparable to the protection by injection of naked dsYHV at 1.25 μg/g shrimp body weight. The Chol-dsYHV complex could reduce the effective concentration of

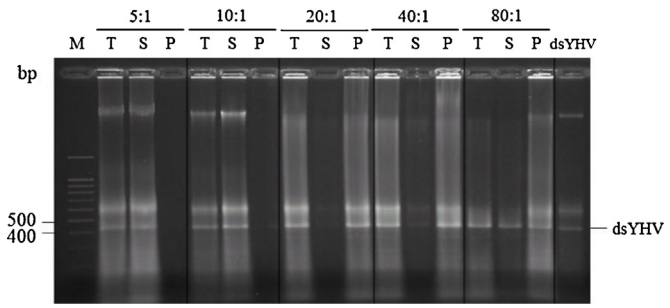


**Fig. 4.** Determination of optimal ratio for liposome complex formation between cholesterol-based lipids and dsYHV. The complex of cholesterol-based lipid-dsYHV (Chol-dsYHV) was prepared in the same volume at different mass ratios of liposome:dsYHV *i.e.* 5:1, 10:1, 20:1, 40:1 and 80:1. The mixture was then centrifuged at 10,000*g* for 3 min to separate free dsYHV from the liposome complex. The dsYHV in the total mixture before centrifugation (T), or in the supernatants (S) and in the pellet (P) after centrifugation from the mixture at each ratio was precipitated, and approximately 2 μg of dsYHV from each ratio were analyzed by agarose gel electrophoresis compared with 1 μg of naked dsYHV (last lane). Lane M is 100 bp DNA ladder marker.

dsYHV to about 25 times when compared to injection of naked dsYHV. In addition, shrimp received the Chol-dsYHV at the concentration of 1.25 μg/g shrimp could also delay shrimp mortality and could prolong dsYHV activity with 80% mortality when compared with the shrimp injected with naked dsYHV at the same concentration confirming that the delivery of dsYHV by the complex liposome could enhance YHV protection.

To investigate the effective period of protection against YHV by the Chol-dsYHV, shrimp were injected with either naked dsYHV or Chol-dsYHV at 1.25 μg/g shrimp body weight, the concentration that gave the best YHV protection, and YHV challenge was performed at 24 h after the injection of naked dsYHV or Chol-dsYHV, and repeated every 7 days. The result of shrimp mortality (Fig. 6) suggested that the control shrimp that received no dsYHV gave 100% mortality within 5 days, whereas the shrimp that were injected with naked dsYHV at 1.25 μg/g shrimp body weight could delay mortality to about five weeks with 90% death. Strikingly, only 50% mortality was observed at the end of the experiment in the shrimp that received the Chol-dsYHV complex suggesting that the activity of dsYHV in the Chol-dsYHV complex could persist with about 50% protection up to two months.

### 3.3. Protection of dsRNA in the cholesterol-based cationic liposome complex from enzymatic digestion

To determine whether the cholesterol-based cationic liposome could be used for oral delivery of dsRNA, shrimp diet containing the liposome complex between cholesterol-based liposome and dsRab7 (Chol-dsRab7) was prepared. Since previous study showed that protection against YHV could be achieved by feeding the shrimp with *E. coli* cells expressing dsRab7 at high concentration (22 mg/g shrimp) (Sanitt et al., 2014) suggesting that the dsRNA could escape from the digestion by shrimp digestive enzymes from hepatopancreas. Thus, in order to ensure that the entrapment of dsRNA within the cholesterol-based cationic liposome could tolerate the digestive enzymes of the shrimp, the *ex vivo* enzymatic digestion assay was performed. Three different forms of dsRab7 *i.e.* naked dsRab7, Chol-dsRab7 and *E. coli*-expressed dsRab7 were digested with total proteins extracted from either hepatopancreas, hemolymph or muscle. The result demonstrated that only the naked dsRab7, but not the Chol-dsRab7 or *E. coli*-expressed dsRab7 could be digested by hepatopancreatic enzymes within 6 h after incubation, whereas the control protein extracts from hemolymph or muscle did not digest dsRab7 in any form (Fig. 7). The result demonstrated that the Chol-dsRab7 complex could protect dsRab7 from degradation similar to the dsRab7 expressed in *E. coli* cells. Therefore the cholesterol-based cationic liposome could be used as a dsRab7 carrier for oral delivery.

### 3.4. Administration of chol-dsRab7 via oral delivery to the shrimp exhibits YHV protection

To investigate whether the cholesterol-based liposome could be employed as a vehicle to deliver dsRNA by oral delivery, shrimp diet containing Chol-dsRab7 complex was prepared and fed to 250 mg shrimp for 4 days in total of approximately 960 μg/g shrimp body weight, and the shrimp were subsequently submerged in $10^{-6}$ YHV solution. The result (Fig. 8) showed that the control shrimp that were fed on comercial feed reached 95% mortality on day 6 whereas shrimp fed with shrimp feed mixed with naked dsRab7 could slightly delay shrimp mortality with the accumulation of 85% death on day 6. Interestingly, shrimp fed with Chol-dsRab7 showed notably delay mortality with 70% on day 6 indicating that the cholesterol-based liposome could be used as a dsRNA carrier for oral delivery.

## 4. Discussion

Although protection of shrimp mortality *via* dsRNA injection or oral delivery was demonstrated for years, the efficient delivery system of dsRNA to target cells still needs to be developed. In this study, the dsRNAs targeting *protease* gene of YHV and shrimp *Rab7* gene were chosen as a model because these dsRNAs were demonstrated to be effective to prevent YHV replication in the shrimp (Ongvarrasopone et al., 2008; Yodmuang et al., 2006).

Cationic liposome has been shown to be one of the most effective agent to deliver negatively charged molecules such as

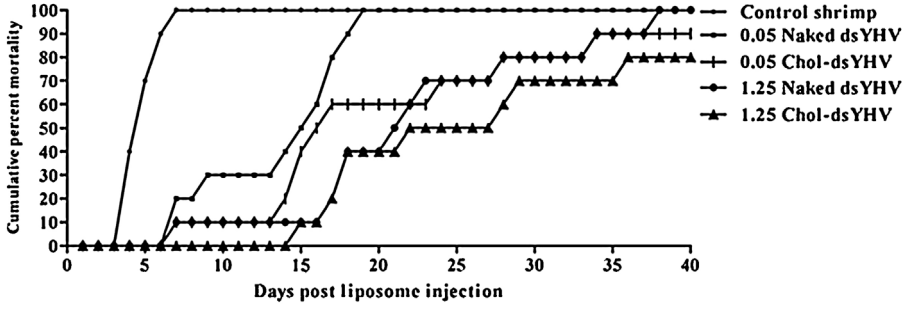


**Fig. 5.** Protection of shrimp against YHV by cholesterol-based lipid-dsRNA complex. Shrimp were injected either with naked dsYHV at 0.05 or 1.25 μg/g shrimp body weight or with the cholesterol-based lipid-dsRNA (Chol-dsYHV) containing equivalent amounts of dsYHV (n = 10 in each group) at 24 h prior to YHV challenge. The YHV challenge was repeated every 7 days until the mortality was steady or 100% mortality was achieved. The control shrimp received neither naked dsYHV nor Chol-dsYHV. The cumulative percent mortality was recorded every day.

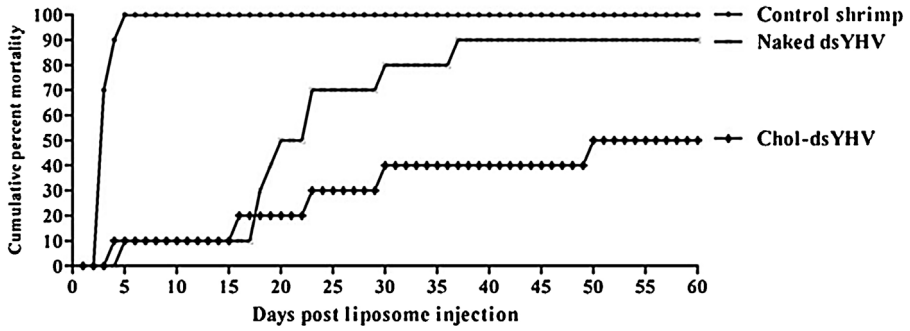


**Fig. 6.** Prolonged YHV-induced shrimp mortality by Chol-dsYHV complex. To investigate the longevity of Chol-dsYHVcomplex in the reduction and delay of shrimp mortality, the shrimp were injected with the naked dsYHV or Chol-dsYHV containing equivalent amount of dsYHV at 1.25 μg/g shrimp body weight followed by YHV challenge at 24 h later, and the YHV challenge was repeated every 7 days. The control shrimp received neither naked dsYHV nor Chol-dsYHV complex. The cumulative percent mortality was recorded daily, and was presented from n = 10.

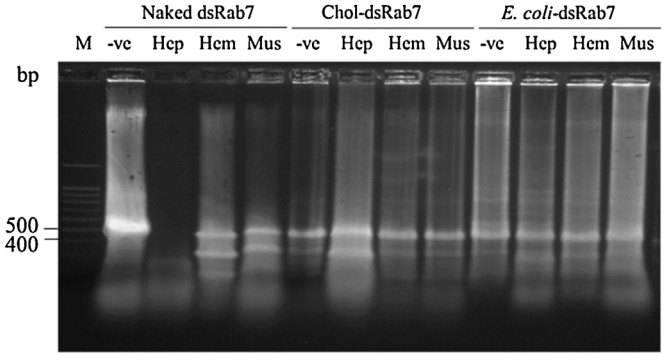


**Fig. 7.** Protection of dsRab7 entrapped in the cholesterol-based liposome from enzymatic digestion. The dsRab7 in different forms which are naked dsRab7, Chol-dsRab7 or *E. coli*-expressed dsRab7 were incubated with total protein extract from hepatopancreas (Hep), hemolymph (Hem) or muscle (Mus) for 6 h. The dsRab7 was then extracted from the reactions by Tri Reagent®, and about 2 μg of dsRab7 from each reaction were visualized on agarose gel electrophoresis. The dsRab7 in 150 mM NaCl solution was used as a negative control for undigested dsRab7 (−ve). M is 100 bp DNA ladder.

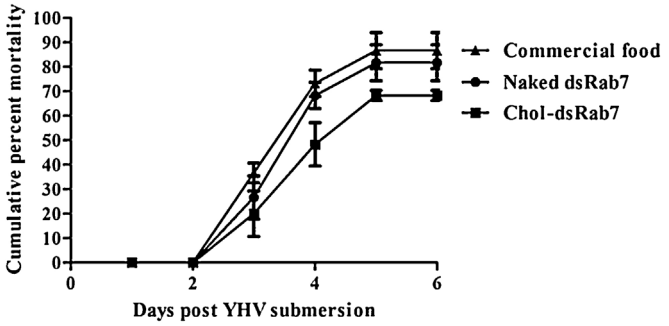


**Fig. 8.** Prevention of shrimp mortality by oral delivery of cationic liposome-dsRab7. Shrimp were fed with diet containing cholesterol-based cationic liposome-dsRab7 (Chol-dsRab7) complex or naked dsRab7 (n = 10 for each group) for 4 days in a total amount of 960 μg/g shrimp followed by YHV challenge at 24 h later. The control shrimp were fed with the commercial feed without either Chol–dsRab7 complex or naked dsRab7. The cumulative percent mortality was recorded every day and presented as mean ± SEM from three independnent experiments.

nucleic acids to target cells (Kim et al., 2008; Misra et al., 2014; Oh and Park, 2009; Serikawa et al., 2000; Sioud and SØrensen, 2003; Tagami et al., 2012), and thus was utilized as a vehicle for dsRNA delivery in this study. We have synthesized four cationic liposomes for dsRNA delivery with the mass ratio of lipid:dsRNA at 20:1 (w/w) to minimize toxicity in the shrimp since some cationic liposomes could cause cytotoxicity in DNA transfection when lipid concentration was higher than 100 μg/ml or the lipid:DNA ratio was lowered at approximately 2:1 (Cortesi et al., 1996; Nguyen et al., 2007; RomØren et al., 2004). Our result also showed that at the ratio of 20:1, the cholesterol-based cationic lipids formed complex well with the dsYHV compared with other ratios, which is similar to previous studies that utilized cholesterol-based cationic liposome for *in vitro* delivery of curcumin (Apiratikul et al., 2013a) and *in vivo* delivery of dsYHV into shrimp (Apiratikul et al., 2013b). Cationic liposome-dsYHV complex formation assay demonstrated that among the four cationic liposomes the cholesterol-based liposome was the most efficient in entrapping dsYHV. The cholesterol- based liposome contains a non polar tetracyclic ring whereas the other three cationic lipids (lipid **1**, Cy and Dx) contain double hydrocarbon chains as a non polar part. The difference between the tetracyclic ring and double hydrocarbon chains may play an important role in the formation of cationic liposomes. It was described that the ratio between hydrophobic to hydrophilic regions determined the competency of liposome formation (Wasungu and Hoekstra, 2006). When the hydrocarbon chain which is a hydrophobic region is larger than that of the cationic head group, the lipids tend to form an inverted hexagonal phase which is a bilayer destabilizing structure (Wasungu and Hoekstra, 2006). Our result also confirmed that the lipid **1** which contains C14, C14 hydrocarbon chains that are much larger than the cationic amino head group had the poorest capabilty to form liposome complex with dsYHV when compared with the other two lipids with double hydrocarbon chains, Cy (C14,C14) and Dx (C12,C12), but contain a polyamine head group (Fig. 1).

In addition, when injected into the shrimp all double hydrocarbon chains cationic liposome-dsYHV complexes showed either similar or poorer YHV protection compared to the naked dsYHV, whereas the Chol-dsYHV gave a better protection against YHV *i.e.* the dalay and lower mortality than the naked dsYHV (Fig. 3). This demonstrated that prevention of shrimp mortality was correlated to the efficiency of complex formation between the cationic liposome and dsYHV that played a key step for successful dsYHV delivery.

The pre-injection of Chol-dsYHV at the concentration of 0.05 μg/g shrimp body weight could give YHV protection at comparable level with the injection of 1.25 μg of naked dsYHV/g shrimp body weight suggesting that the cationic liposome could reduce an effective amount of dsYHV to approximately 25 times. In addition, injection of the Chol-dsYHV at the higher dose (1.25 μg/g shrimp body weight) could prolong dsYHV activity and therefore delay shrimp mortality upto two months. The increase of dsYHV efficiency and prolonging of dsYHV activity might be explained

using a model of the structure formation and cellular internalization of cationic liposme-DNA complex (Tamaddon et al., 2007; Zabner et al., 1995). It has been described that the nagatively charged DNA condenses the positively charged cationic head group, thus leading to the formation of the condense membrane vesicle (Subramanian et al., 2000). The positive charges on the liposome surface could interact with anionic charges of the receptor on the cell surface, and subsequently facilitates the internalization of the liposome complex *via* endocytosis (Tamaddon et al., 2007; Zabner et al., 1995). After entry into the cells, the cationic liposome vesicles aggregate into a large compartment in the cytosol, and was transported to late endosome (Ouahabi et al., 1999; Tamaddon et al., 2007; Zabner et al., 1995). Thereafter, the DNA was gradually released in the acidic pH condition from the late endosome to the cytosol (Tamaddon et al., 2007). It is possible that the injection of cholesterol-based liposome-dsRNA complex may be processed by the same pathway as the liposome-DNA complex, in which a slow release of dsYHV in the acidic condition could maintain viral protection for at least two months. Our results therefore demonstrated for the first time that the long-term protection of shrimp from YHV, at 50% survival rate, could be achieved by Chol-dsYHV injection at the dose of 1.25 μg/g shrimp body weight.

Our work further showed that the Chol-dsRab7 complex could protect dsRab7 from digestion by shrimp digestive enzymes. This is most likely due to the structure of the cationic liposome that entrapped dsRNA inside the vesicle and therefore escaping degradation by the enzymes. Oral delivery of the Chol-dsRab7 containing feed for 4 day that was approximately 960 μg of dsRab7/g shrimp body weight in total could decrease shrimp mortality by about 30% (Fig. 8). Our previous work showed that feeding with *E. coli* expressing dsRab7 about 22 mg/g shrimp could reduce nearly 70% shrimp mortality (Sanitt et al., 2014). Roughly the Chol-dsRab7 could reduce the amuont of dsRab7 for about 10 times comparing with the *E. coli* expressing dsRab7 when delivered by oral feeding. However, the effective dose of dsRab7 *via* oral delivery was about 400 times higher than the dose of 2.5 μg/g shrimp used for injection (Ongvarrasopone et al., 2008). This may be resulted from the limitation of the liposome-dsRab7 internalization from digestive environment or some of the Chol-dsRab7 complex might be destabilized and led to degradation of the dsRab7. As feeding is considered an appropriate dsRNA delivery method in shrimp farm, further improvement on the formulation of Chol-dsRNA-containing shrimp food will provide a new approach for viral protection in shrimp aquaculture.

Taken together, our study demonstrated that cholesterol-based liposome could be a promising dsRNA carrier into the shrimp. It could increase dsRNA efficiency by either reducing an effective amount of dsRNA or prolonging dsRNA activity *via* injection delivery. Interestingly, oral delivery of the cholesterol-based liposome-dsRNA could be a possible strategy for viral protection in shrimp farming. The development of the preparation method to obtain highly stabilized structure of the liposome-dsRNA complex is still required for future investigation. Further study should be also addressed on the formulation of shrimp diet with the cationic liposome-dsRNA complex that would give a better virus protection.

## Acknowledgements

The author would like to thank Dr. Witoon Tirasophon for providing the *E. coli* strain HT115, and the pET3a-dsYHV construct, and Dr. Chalermporn Ongvarasopone for providing the pET17b-dsRab7 construct. We thank Mrs. Orathai Namramoon, Miss Chaweewan Chimwai, Mrs. Suparp Hongthong and Miss Pannee Thongboonsong for their technical assistance. This work is supported by Mahidol University research grant, The Thailand Research Fund (DPG5680001 to SP, RSA5580052 to WA and IRG5780009) and The Office of the Higher Education Commission under the National Research Universities Initiative. Research facility supports from Center of Excellence for Innovation in Chemistry (PERCH-CIC) and The Thailand Research Fund (to BY) are gratefully acknowledged. PS is the recipient of the student fellowship by the Commission on Higher Education, Thailand.

## References

Apiratikul, N., Penglong, T., Suksen, K., Svasti, S., Chairoungdua, A., Yingyongnarongkul, B., 2013a. *In vitro* delivery of curcumin with cholesterol-based cationic liposomes. Russ. J. Bioorg. Chem. 39, 444–450.

Apiratikul, N., Yingyongnarongkul, B., Assavalapsakul, W., 2013b. Highly efficient double-stranded RNA transfection of penaeid shrimp using cationic liposomes. Aquacult. Res. 45, 106–112.

Assavalapsakul, W., Smith, D.R., Panyim, S., 2006. Identification and characterization of a *Penaeus monodon* lymphoid cell-expressed receptor for the yellow head virus. J. Virol. 80, 262–269.

Cortesi, R., Esposito, E., Menegatti, E., Gambari, R., Nastruzzi, C., 1996. Effect of cationic liposome composition on *in vitro* cytotoxicity and protective effect on carried DNA. Int. J. Pharm. 139, 69–78.

Dong, L., Liu, F., Fairman, J., Hong, D.K., Lewis, D.B., Monath, T., et al., 2012. Cationic liposome-DNA complexes (CLDC) adjuvant enhances the immunogenicity and cross-protective efficacy of a pre-pandemic influenza A H5N1 vaccine in mice. Vaccine 30, 254–264.

Flegel, T.W., 1997. Major viral diseases of the black tiger prawn (*Penaeus monodon*) in Thailand. World J. Microbiol. Biotechnol. 13, 433–442.

Hong, K., Zheng, W., Baker, A., Papahadjopoulos, D., 1997. Stabilization of cationic liposome-plasmid DNA complexes by polyamines and poly(ethylene glycol)-phospholipid conjugates for efficient *in vivo* gene delivery. FEBS Lett. 400, 233–237.

Iwanaga, K., Ono, S., Narioka, K., Morimoto, K., Kakemi, M., Yamashita, S., et al., 1997. Oral delivery of insulin by using surface coating liposomes: improvement of stability of insulin in GI tract. Int. J. Pharm. 157, 73–80.

Jatuyosporn, T., Supungul, P., Tassanakajon, A., Krusong, K., 2014. The essential role of clathrin-mediated endocytosis in yellow head virus propagation in the black tiger shrimp *Penaeus monodon*. Dev. Comp. Immunol. 44, 100–110.

Kim, H.R., Kim, I.K., Bae, K.H., Lee, S.H., Lee, Y., Park, T.G., 2008. Cationic solid lipid nanoparticles reconstituted from low density lipoprotein components for delivery of siRNA. Mol. Pharm. 5, 622–631.

Liu, S.L., Wu, Q.M., Zhang, L.J., Wang, Z.G., Sun, E.Z., Zhang, Z.L., et al., 2014. Three-dimensional tracking of Rab5- and Rab7-associated infection process of influenza virus. Small 10, 4746–4753.

Macovei, A., Petrareanu, C., Lazar, C., Florian, P., Branza-Nichita, N., 2013. Regulation of hepatitis B virus infection by Rab5, Rab7, and the endolysosomal compartment. J. Virol. 87, 6415–6427.

Meresse, S., Gorvel, J.P., Chavrier, P., 1995. The rab7 GTPase resides on a vesicular compartment connected to lysosomes. J. Cell Sci. 108, 3349–3358.

Misra, S., Naz, S., Kondaiah, P., Bhattacharya, S., 2014. A cationic cholesterol based nanocarrier for the delivery of p53-EGFP-C3 plasmid to cancer cells. Biomaterials 35, 1334–1346.

Mousavi, S.A., Malerod, L., Berg, T., Kjeken, R., 2004. Clathrin-dependent endocytosis. Biochem. J. 377, 1–16.

Nguyen, L.T., Atobe, K., Barichello, J.M., Ishida, T., Kiwada, H., 2007. Complex formation with plasmid DNA increases the cytotoxicity of cationic liposomes. Biol. Pharm. Bull. 30, 751–757.

Niyomtham, N., Apiratikul, N., Suksen, K., Opanasopit, P., Yingyongnarongkul, B., 2015. Synthesis and *in vitro* transfection efficiency of spermine-based cationic lipids with different central core structures and lipophilic tails. Bioorg. Med. Chem. Lett. 25, 496–503.

Oh, Y.K., Park, T.G., 2009. siRNA delivery systems for cancer treatment. Adv. Drug Deliv. Rev. 61, 850–862.

Ongvarrasopone, C., Chanasakulniyom, M., Sritunyalucksana, K., Panyim, S., 2008. Suppression of PmRab7 by dsRNA inhibits WSSV or YHV infection in shrimp. Mar. Biotechnol. 10, 374–381.

Ouahabi, A.E., Thiry, M., Schiffmann, S., Fuks, R., Nguyen-Tran, H., Ruysschaert, J.M., et al., 1999. Intracellular visualization of BrdU-labeled plasmid DNA/cationic liposome complexes. J. Histochem. Cytochem. 47, 1159–1166.

Posiri, P., Kondo, H., Hirono, I., Panyim, S., Ongvarrasopone, C., 2015. Successful yellow head virus infection of *Penaeus monodon* requires clathrin heavy chain. Aquaculture 435, 480–487.

Robalino, J., Browdy, C.L., Prior, S., Metz, A., Parnell, P., Gross, P., et al., 2004. Induction of antiviral immunity by double-stranded RNA in a marine invertebrate. J. Virol. 78, 10442–10448.

RomØren, K., Thu, B.J., Bols, N.C., Evensen, O., 2004. Transfection efficiency and cytotoxicity of cationic liposomes in salmonid cell lines of hepatocyte and macrophage origin. Biochim. Biophys. Acta 1663, 127–134.

Sanitt, P., Attasart, P., Panyim, S., 2014. Protection of yellow head virus infection in shrimp by feeding of bacteria expressing dsRNAs. J. Biotechnol. 179, 26–31.

Senapin, S., Thaowbut, Y., Gangnonngiw, W., Chuchird, N., Sriurairatana, S., Flegel, T.W., 2010. Impact of yellow head virus outbreaks in the whiteleg shrimp, *Penaeus vannamei* (Boone), in Thailand. J. Fish Dis. 33, 421–430.

Serikawa, T., Suzuki, N., Kikuchi, H., Tanaka, K., Kitagawa, T., 2000. A new cationic liposome for efficient gene delivery with serum into cultured human cells: a quantitative analysis using two independent fluorescent probes. Biochim. Biophys. Acta 1467, 419–430.
Shim, G., Kim, M.G., Park, J.Y., Oh, Y.K., 2013. Application of cationic liposomes for delivery of nucleic acids. Asian J. Pharmacol. 8, 72–80.
Sioud, M., SØrensen, D.R., 2003. Cationic liposome-mediated delivery of siRNAs in adult mice. Biochem. Biophys. Res. Commun. 312, 1220–1225.
Sittidilokratna, N., Dangtip, S., Cowley, J.A., Walker, P.J., 2008. RNA transcription analysis and completion of the genome sequence of yellow head nidovirus. Virus Res. 136, 157–165.
Subramanian, M., Holopainen, J.M., Paukku, T., Eriksson, O., Huhtaniemi, I., Kinnunen, P.K.J., 2000. Characterisation of three novel cationic lipids as liposomal complexes with DNA. Biochim. Biophys. Acta 1466, 289–305.
Tagami, T., Suzuki, T., Matsunaga, M., Nakamura, K., Moriyoshi, N., Ishida, T., et al., 2012. Anti-angiogenic therapy via cationic liposome-mediated systemic siRNA delivery. Int. J. Pharm. 42, 280–289.
Tamaddon, A.M., Shirazi, F.H., Moghimi, H.R., 2007. Modeling cytoplasmic release of encapsulated oligonucleotides from cationic liposomes. Int. J. Pharm. 336, 174–182.
Tirasophon, W., Roshom, Y., Panyim, S., 2005. Silencing of yellow head virus replication in penaeid shrimp cells by dsRNA. Biochem. Biophys. Res. Commun. 334, 102–107.
Vanlandingham, P.A., Ceresa, B.P., 2009. Rab7 regulates late endocytic trafficking downstream of multivesicular body biogenesis and cargo sequestration. J. Biol. Chem. 284, 12110–12124.
Wang, C.S., Tang, K.F.J., Kou, G.H., Chen, S.N., 1996. Yellow head disease-like virus infection in the Kuruma shrimp *Penaeus japonicus* cultured in Taiwan. Fish Pathol. 31, 177–182.
Wasungu, L., Hoekstra, D., 2006. Cationic lipids, lipoplexes and intracellular delivery of genes. J. Controlled Release 116, 255–264.
Wilson, R.C., Doudna, J.A., 2013. Molecular mechanism of RNA interference. Annu. Rev. Biophys. 42, 217–239.
Yodmuang, S., Tirasophon, W., Roshorm, Y., Chinnirunvong, W., Panyim, S., 2006. YHV-protease dsRNA inhibits YHV replication in *Penaeus monodon* and prevents mortality. Biochem. Biophys. Res. Commun 341, 351–356.
Zabner, J., Fasbender, A.J., Moninger, T., Poellinger, K.A., Welsh, M.J., 1995. Cellular and molecular barriers to gene transfer by a cationic lipid. J. Biol. Chem. 270, 18997–19007.

# 13. Rab5, an early endosomal protein required for yellow head virus infection of *Penaeus monodon*.

Aquaculture 459 (2016) 43–53

Contents lists available at ScienceDirect

Aquaculture

journal homepage: www.elsevier.com/locate/aquaculture

# Rab5, an early endosomal protein required for yellow head virus infection of *Penaeus monodon*

Pratsaneeyaporn Posiri [a], Sakol Panyim [a,b], Chalermporn Ongvarrasopone [a,*]

[a] Institute of Molecular Biosciences, Mahidol University (Salaya Campus), Nakhon Pathom 73170, Thailand
[b] Department of Biochemistry, Faculty of Science, Mahidol University, Bangkok 10400, Thailand

ARTICLE INFO

*Article history:*
Received 30 January 2016
Received in revised form 11 March 2016
Accepted 13 March 2016
Available online 15 March 2016

*Keywords:*
Double stranded RNA
RNAi
Black tiger shrimp
Endocytosis
Yellow head disease

ABSTRACT

Yellow head virus (YHV) is a virulent pathogen in black tiger shrimp. It causes high mortality within a few days after infection. In this study, colocalization between YHV and *P. monodon* Rab5 (PmRab5) which is a small GTPase protein was visualized at 10 min to 3 h post-YHV challenge under a confocal microscope. The result indicated that PmRab5 plays a key role in the early stage of endocytosis, and is involved in YHV trafficking process. Molecular cloning showed that the open reading frame of PmRab5 is 633 bp encoding a putative protein of 210 amino acids with an estimated molecular weight of 23 kDa. PmRab5 contained all Rab-specific signature motifs: Rab family motif (RabF), Rab subfamily motif (RabSF), G-boxes and cysteine prenylation signal. Silencing of PmRab5 by specific dsRNA reduced YHV replication inside the cells. Furthermore, lack of PmRab5 expression exhibited a delay of shrimp mortality after YHV infection. The results demonstrated that PmRab5 is involved in YHV early endosomal trafficking, suggesting its role in the early step of infection.
*Statement of relevance:* Silencing of PmRab5 may be applicable for inhibition of YHV.


## 1. Introduction

Enveloped yellow head virus (YHV) belongs to the genus *Okavirus*, family *Roniviridae* in the order *Nidovirales* which is a highly virulent pathogen against *Penaeus monodon* or black tiger shrimp. *P. monodon* is an economically important aquaculture shrimp in Thailand. YHV is a positive-sense ssRNA virus of approximately 27 kb, with poly-(A) tail. Morphology of YHV revealed an envelope bacilliform which has a particle size of about 50–60 × 190–200 nm. Within the YHV particle, it contains the internal helical nucleocapsid which is closely surrounded by an envelope studded with prominent peplomers or spikes (Nadala et al., 1997; Sittidilokratna et al., 2008). YHV contains three structural proteins: two major structural transmembrane glycoproteins (gp116 and gp64) and a nucleoprotein (p20) (Jitrapakdee et al., 2003).

Infection of several enveloped viruses is initiated by the viral glycoprotein binding to its cellular receptor. The conformational change in the virus particle promotes endocytic internalization into the host cell. The virus is delivered from the surface membrane toward early endosomes, maturing endosomes, late endosomes and lysosomes. The acidic condition of the endosomal compartment can trigger the penetration of the viral genome into cytosol. The low pH induces conformational changes of the fusion protein which exists in the viral membrane resulting in host-virus membrane fusion. The virus then uncoats and releases the genome into the cytoplasm (Greber et al., 1994; Marsh and Helenius, 2006; Mercer et al., 2010). Intracellular membrane traffic between these membranous organelles by vesicular transport requires tight regulation to ensure both fidelity and efficiency. The Rab GTPase family which belongs to the Ras superfamily plays a central role in regulating vesicle transports, including vesicle budding, delivery, tethering and fusion with the target membrane (Hutagalung and Novick, 2011; Stenmark, 2009). The intracellular localization and associated vesicle transport of plasma membrane to early endosome and mature endosome requires Rab5 protein. Rab5 associates with plasma membrane-derived clathrin-coated vesicles (Bucci et al., 1992) and mediates tethering with Early Endosome Antigen1 (EEA1), a Rab5 effector protein (Merithew et al., 2003). Then, the trafficking of vesicles from mature endosome to late endosome and lysosome is regulated by Rab7 (Hutagalung and Novick, 2011; Mercer et al., 2010; Stenmark, 2009).

However, molecular mechanisms of the early steps in intracellular trafficking of YHV entry into the shrimp cell are poorly defined. Recently, it has been demonstrated that YHV utilizes clathrin-mediated endocytosis to invade shrimp cells (Jatuyosporn et al., 2014, Posiri et al., 2015). In addition, silencing of *P. monodon* Rab7 (PmRab7), a late endosomal marker resulted in inhibition of YHV replication, suggesting that YHV could not move from the late endosome to the lysosome where its genome was uncoated and released into the cytoplasm for replication (Ongvarrasopone et al., 2008). How YHV is trafficked from the plasma membrane toward late endosomal

* Corresponding author at: Institute of Molecular Biosciences, Mahidol University (Salaya Campus), 25/25 Phutthamonthon 4 Rd. Salaya, Phutthamonthon district, Nakhon Pathom 73170, Thailand.
*E-mail address:* chalermporn.ong@mahidol.ac.th (C. Ongvarrasopone).

http://dx.doi.org/10.1016/j.aquaculture.2016.03.026
0044-8486/

**Table 1**
Primer sequences of the experiments.

| Primers | Sequences (5′–3′) | Experiments |
|---|---|---|
| dRab5-F | AAGGGCCAGTTCCACGAGTACCA(G/A)GA | Amplify PmRab5 partial sequences |
| dRab5-R | AAGATGTCGTTCACGTTCATGGCGGT | |
| PmRab5-R1 | GGTCTGGGCCTCTTCATATTCAACC | 5′ RACE of PmRab5 |
| PRT | CCGGAATTCAAGCTTCTAGAGGATCCTTTTTTTTTTTTTTT | Reverse transcription and RACE assay |
| PmRab5-R2 | CCTTTACCCAGGTCTTAGCACGACC | 5′ RACE of PmRab5 |
| PM1 | CCGGAATTCAAGCTTCTAGAGGATCC | 5′ RACE of PmRab5 |
| FullR5-F2 | GGTTGTGTGGTTGATCCTG | Full-length of PmRab5 cDNA |
| FullR5-R | TTTTTTCTTAAAAATGTCTAACAC | |
| stPmRab5-F1-*Xba*I | *Xba*I<br>GCTCTAGAGTCAACTATTGGAGCTGCA | Amplification of sense-loop region of dsRNA-PmRab5 |
| lpPmRab5-R1-*Kpn*I | *Xba*I<br>GGGGTACCTATTGGACAGGCTGACATC | |
| stPmRab5-F2-*Eco*RI/*Xho*I | *Eco*RI *Xbo*I<br>GGAATTCCTCGAGGTCAACTATTGGAGCTGCA | Amplification of antisense region of dsRNA-PmRab5 |
| stPmRab5-R2-*Kpn*I | *Kpn*I<br>GGGGTACCCTTAGCAGAGGTCTCCATAA | |
| PmRab5-F1 | GGAGCTGCATTTCTGACACAGACAG | 3′ RACE of PmRab5 and detection of PmRab5 mRNA |
| PmRab5-R1 | GGTCTGGGCCTCTTCATATTCAACC | Detection of PmRab5 mRNA |
| PmActin-F | GACTCGTACGTGGGCGACGAGG | Detection of PmActin mRNA |
| PmActin-R | AGCAGCGGTGGTCATCTCCTGCTC | |
| YHV(hel)-F | CAAGGACCACCTGGTACCGGTAAGAC | Detection of YHV mRNA |
| YHV(hel)-R | GCGGAAACGACTGACGGCTACATTCAC | |

compartment has not been investigated. An increasing evidence for the requirement of Rab5 in the early entry step of several viruses including dengue virus, West Nile virus and foot-and-mouth disease virus (Johns et al., 2009; Krishnan et al., 2007) could suggest a possible role of Rab5 for YHV entry into shrimp cells. Therefore, in this study, the molecular mechanism of Rab5 in YHV entry into the shrimp cells was investigated.

## 2. Materials and methods

### 2.1. Primary hemocyte culture

Hemolymph was collected from *P. monodon* using sterile syringe and 18 gauge needle with anticoagulant AC-1 (27 mM Sodium citrate, 34.33 mM NaCl, 104.5 mM Glucose, 198.17 mM EDTA, pH 7.0) in a ratio 1:1. The mixture of hemolymph and anticoagulant was centrifuged at 550 ×*g* for 10 min to separate the hemocyte pellet from the hemolymph. The hemocyte pellet was washed in 1 ml of L-15 culture medium washing solution (2× Leibovitz L-15 medium, 15% (*v*/*v*) fetal bovine serum, 200 IU/ml penicillin and 200 μg/ml streptomycin). Then the washing step was repeated three times. After that, the hemocytes were resuspended in 1 ml of L-15 culture medium working solution (2× Leibovitz L-15 medium, 15% (*v*/*v*) fetal bovine serum, 200 IU/ml penicillin, 200 μg/ml streptomycin, and 15% (*v*/*v*) shrimp meat extract). The hemocyte number was counted under a light microscope by using hemocytometer. The cells ($10^5$ cells per well) were seeded into a 24-well plate.

### 2.2. Yellow head virus (YHV) stock

Viral free shrimp was injected with YHV to propagate the virus. All use of 'shrimp' refers to *P. monodon*. Hemolymph was collected with AC-1 solution from YHV infected moribund shrimp. The hemolymph was centrifuged at 20,000 ×*g* for 20 min at 4 °C to remove hemocyte debris. Then, free YHV particles were collected by ultracentrifugation (100,000 ×*g*) for 1 h. Virus pellets were dissolved with 150 mM NaCl and stored at −80 °C until used. YHV titer was determined by using RT-PCR with YHV helicase gene.

**Table 2**
Percent amino acid sequence identity of PmRab5 compared with each organism. Accession number of organisms used for Rab5 protein domain and phylogenetic analysis are listed.

| Organisms | Accession number | Rab5 isoforms | Percent identity of PmRab5 compared with each organism |
|---|---|---|---|
| *Aedes aegypti* | XP_001658691 | AaRab5 | 77 |
| *Aiptasia pulchella* | AAV34202 | ApRab5 | 85 |
| *Apis mellifera* | XP_003251474 | AmRab5B | 76 |
| *Ascaris suum* | ADY48161 | AsRab5B | 79 |
| *Bombyx mori* | NP_001037614 | BmRab5 | 78 |
| *Canis lupus* | NP_001003317 | ClRab5A | 75 |
| | XP_531627 | ClRab5B | 81 |
| | CAA81626 | ClRab5C | 81 |
| *Danaus plexippus* | EHJ77299 | DpRab5 | 81 |
| *Danio rerio* | NP_957264 | DrRab5A | 75 |
| | AAI65047 | DrRab5C | 77 |
| *Homo sapiens* | CAG38731 | HsRab5A | 75 |
| | CAG46491 | HsRab5B | 81 |
| | CAG46699 | HsRab5C | 81 |
| *Litopenaeus vannamei* | AFK08607 | LvRab5 | 100 |
| *Loa loa* | XP_003136717 | LlRab5 | 77 |
| *Medicago truncatula* | AES68021 | MtRab5C | 48 |
| *Mus musculus* | BAF02855 | MmRab5A | 75 |
| | CAA59016 | MmRab5B | 81 |
| | BAF02857 | MmRab5C | 80 |
| *Oryza sativa* | AAK38149 | OsRab5 | 60 |
| *Penaeus monodon* | KT896540 | PmRab5 | – |
| *Physcomitrella patens* | BAG09234 | PpRab5 | 48 |
| *Suberites domuncula* | ABD65432 | SdRab5 | 76 |
| *Tribolium castaneum* | EFA04701 | TcRab5 | 84 |
| *Xenopus tropicalis* | NP_001008068 | XtRab5A | 76 |
| | AAH75323 | XtRab5B | 80 |
| | CAJ81259 | XtRab5C | 76 |

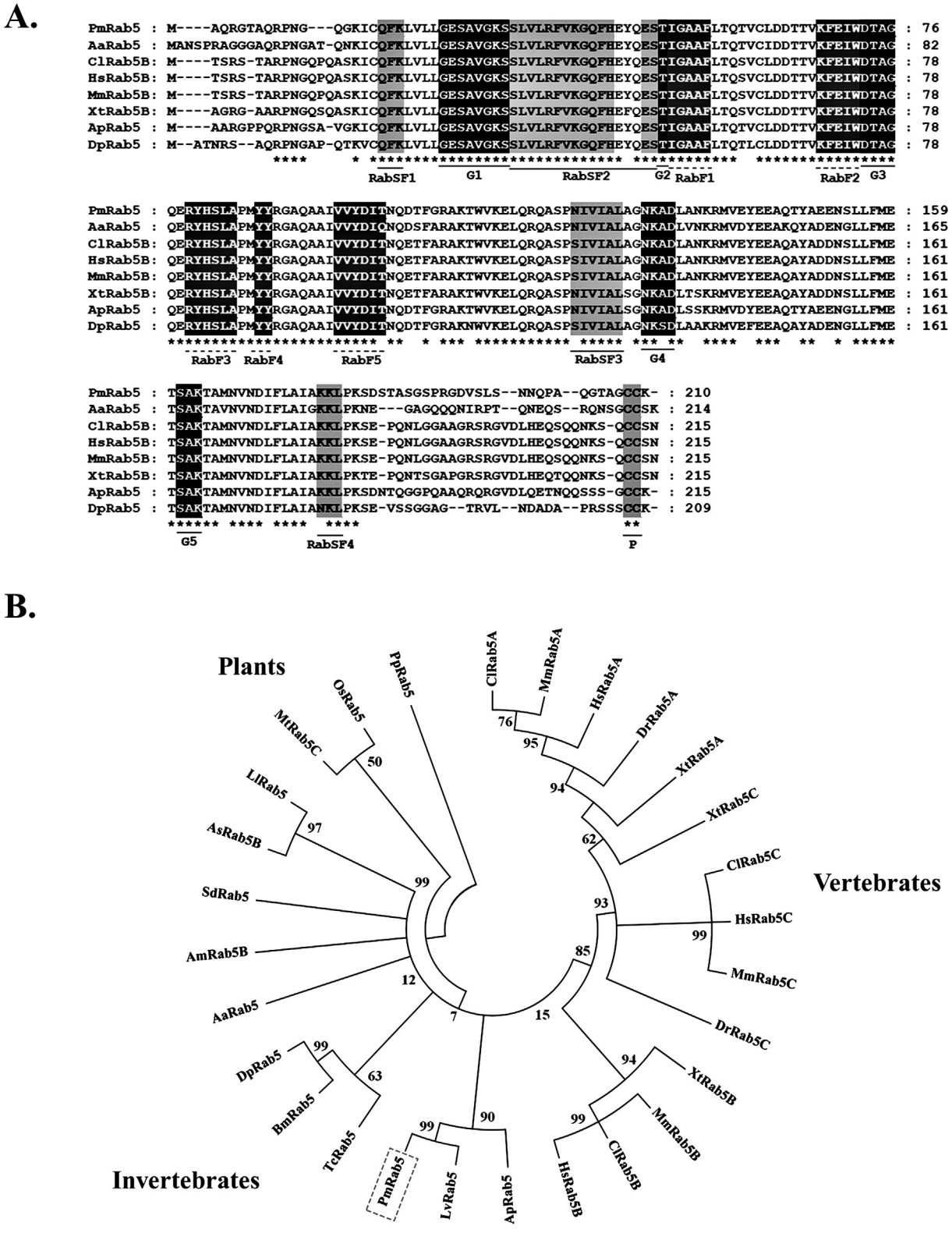


**Fig. 1.** PmRab5 domains and phylogenetic tree analysis. (A) Amino acid sequence alignment of Rab5 proteins from selected organisms demonstrated a signature of five Rab family motifs (RabF1–RabF5) (light gray shade), four Rab subfamily domains (RabSF1–RabSF4) (heavy gray), five G-boxes (G1–G5) (black) and a prenylation site (P). Star (*) represents the consensus amino acid sequence. (B) Phylogenetics tree analysis of Rab5 based on amino acid sequences. Molecular Evolutionary Genetics Analysis (MEGA) 4.1 program was used for phylogenetic tree construction from several species: *Aedes aegypti* (Aa), *Aiptasia pulchella* (Ap), *Apis mellifera* (Am), *Ascaris suum* (As), *Bombyx mori* (Bm), *Canis lupus* (Cl), *Danaus plexippus* (Dp), *Danio rerio* (Dr), *Homo sapiens* (Hs), *Litopenaeus vannamei* (Lv), *Loa loa* (Ll), *Medicago truncatula* (Mt), *Mus musculus* (Mm), *Oryza sativa* (Os), *Penaeus monodon* (Pm), *Physcomitrella patens* (Pp), *Suberites domuncula* (Sd), *Tribolium castaneum* (Tc), and *Xenopus tropicalis* (Xt).

*2.3. Immunofluorescence staining of YHV and P. monodon Rab5 (PmRab5)*

The primary hemocytes ($10^5$ cells) in 24-well plates with cover-slip were incubated at 4 °C. After 30 min, the cells were washed with ice-cold phosphate buffer saline (1× PBS, pH 7.4) and then infected with YHV at a multiplicity of infection (MOI) of 10 for 30 min at 4 °C. The cells were then transferred to 28 °C for 10 min to allow the cells to recover (specified as time 0). Next, the cells were fixed in ice-cold 4% paraformaldehyde at different time points, 0 min, 10 min, 30 min, 1 h, 3 h, 6 h, and 12 h, followed by three washing steps with ice-cold 1× PBS pH 7.4 for 5 min each. The fixed hemocytes were permeabilized with 0.1% Triton X-100 in 1× PBS, pH 7.4, and then blocked with 10% fetal bovine serum. Then, the cells were incubated with rabbit anti-Rab5 primary antibody (ab94690, abcam, USA) at 1:400 dilution at room temperature, overnight. Then the cells were incubated with mouse anti-gp64, a YHV detecting antibody (kindly provided by Professor Paisarn Sithigorngul, Department of Biology, Faculty of Science, Srinakharinwirot University) at 1:200 dilution. After 2 h, the cells were washed 3 times with 0.05% Tween-20 in 1× PBS, pH 7.4, and then incubated with secondary antibody, goat anti-mouse Alexa Fluor® 488 and goat anti-rabbit Alexa Fluor® 594 (Invitrogen), (1:500 dilution) for 1 h in the dark, and washed three times with 0.05% Tween-20 in 1× PBS, pH 7.4. Subsequently, the nuclei of the hemocytes were stained with TO-PRO®-3 iodide at 1:500 dilution (Invitrogen) in 1× PBS, pH 7.4, at room temperature for 1 h in the dark, and washed three times with 0.05% Tween-20 in 1× PBS, pH 7.4. The cover slips were mounted with anti-fade permount (Invitrogen). Fluorescence signals were detected by using a confocal microscope (FluoView FV10i — Olympus).

*2.4. Cloning of the full-length PmRab5 cDNA from P. monodon*

Multiple sequence alignment of Rab5 proteins from several species (Table 2) was aligned and used to design degenerate primers, dRab5-F

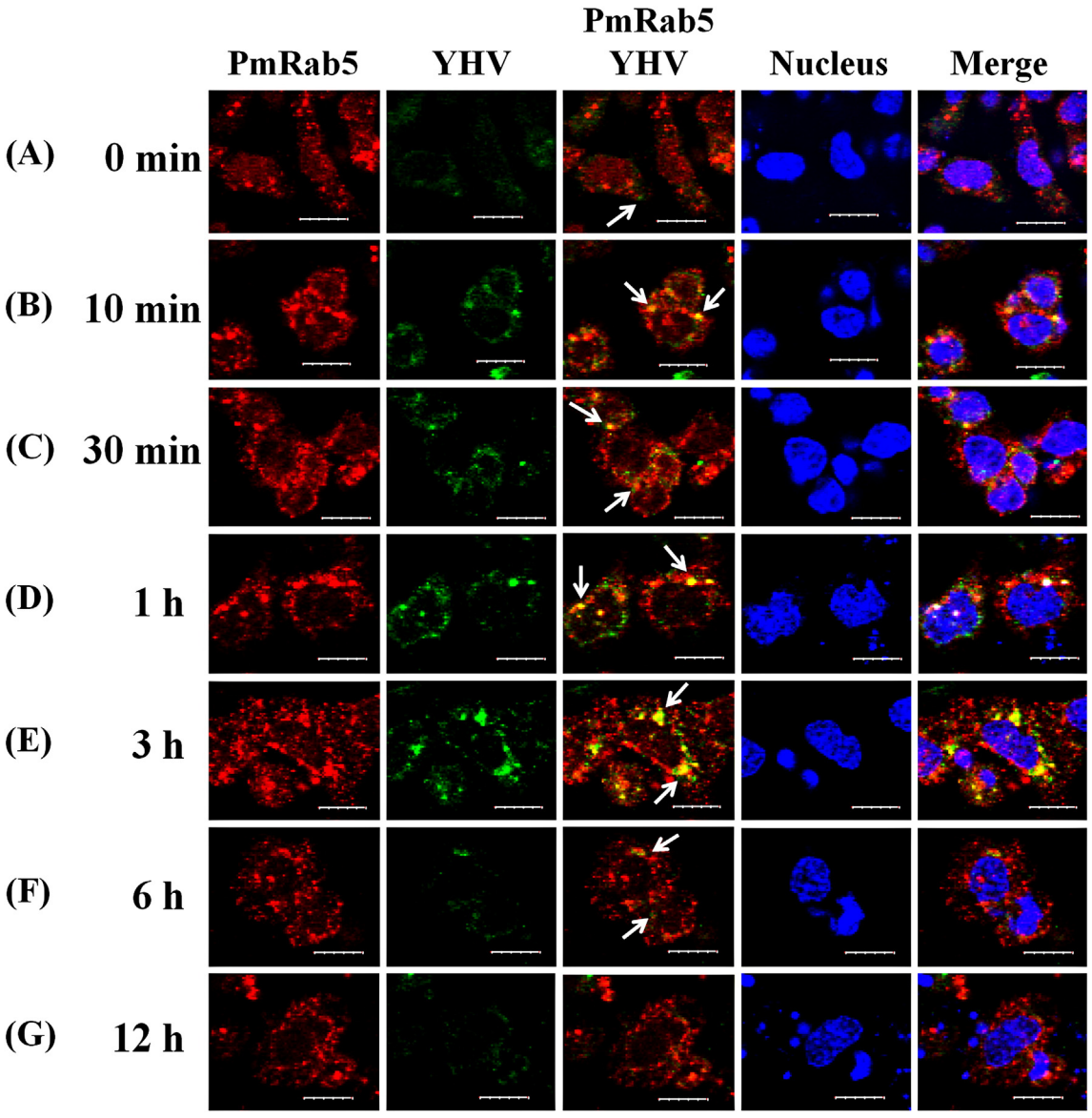


**Fig. 2.** Visualization of the interaction between PmRab5 protein and YHV particles. The primary hemocytes were first incubated with YHV and then the infected cells were fixed at various time points. (A) At time point 0 min post-infection, no colocalization between YHV and PmRab5 was observed. YHV particles could be detected around the cell (arrow). (B and C) YHV particles demonstrated colocalizing with PmRab5 (arrow) at 10 and 30 min post-infection. (D and E) Increased intensity of the colocalization signal (arrow) was observed at 1 to 3 h post-infection. (F) The signal of YHV particles at time 6 hpi showed inside the cells without colocalization with PmRab5 (arrow). (G) At 12 hpi, YHV signal was hardly detected. PmRab5 signal was detected by anti-Rab5 antibody and showed in red. YHV particle was detected by anti-gp64 antibody and showed in green. Colocalization of PmRab5 and YHV was shown as yellow. Cell nuclei were stained blue with TOPRO®-3 iodide. Scale bar is 10 μm.

and dRab5-R (Table 1), to PCR amplify the partial sequence of PmRab5. The PCR condition was: a hot-start at 95 °C for 5 min, then 30 cycles of 95 °C for 30 s, 46 °C for 30 s, and 72 °C for 45 s, followed by 72 °C for 7 min. Next, the expected PmRab5 band was cut and gel purified using Gel/PCR DNA fragments extraction kit (Geneaid). The fragment (346 bp) was cloned into pGEM-T easy vector (Promega) and sequenced (First Base Co, Ltd., Malaysia).

The 5′ and 3′ ends of PmRab5 were amplified by using rapid amplification of cDNA ends (RACE) approach. For 5′-RACE, the cDNA was first generated by using Superscript III® reverse transcriptase (Invitrogen) with a PmRab5-specific primer, PmRab5-R1 (Table 1). Then, the RNA template was removed by RNaseH (Promega) and the first-stranded cDNA was purified by ethanol precipitation, followed by Geneaid spin column (Geneaid). The purified cDNA was performed an polyA-tailing by terminal deoxynucleotidyl transferase (TdT) (Promega). Then, polyA-tailed cDNA was used as template to perform the first PCR with PmRab5-R1 and PRT primers. Next, the obtained PCR product was diluted at 1:100 and used as template for nested PCR with PmRab5-R2 and PM1 nested primer (Table 1). For 3′ RACE, first-strand cDNA was generated by Impromp II™ reverse transcriptase (Promega) with PRT primer (Table 1). Then, cDNA was used as template for the first PCR with PmRab5-F1 (Table 1) and PRT primer. All of RACE products were purified, cloned and sequenced as described above.

The 3 partial sequences obtained from PCR using degenerate primers, 5′ and 3′ RACE products were *in silico* assembled to obtain the full-length PmRab5 cDNA. In order to verify that the assembled sequence is indeed corresponded to the full-length PmRab5 sequence, PCR was performed using primers targeting to the 5′ and 3′ ends, fullR5-F2 and fullR5-R (Table 1), and Vent® DNA polymerase (New England Biolabs). The PCR condition was as follow: denaturation at 95 °C for 5 min, 30 cycles of 95 °C for 30 s, 51 °C for 30 s, and 72 °C for 2 min 30 s, followed by 72 °C for 7 min. PCR products were purified, cloned and sequenced as previously described.

### 2.5. Sequence analysis of PmRab5 cDNA

Sequence analysis was performed with BLASTN (http://blast.ncbi.nlm.nih.gov). The conserved domain of the deduced amino acid sequences were predicted using NCBI database (Zhu et al., 2004). Molecular weight and isoelectric point (pI) of the protein were performed with Expert Protein Analysis System (www.expasy.org). Rab5 protein sequences from several organisms were obtained from GenBank database. Multiple alignments were performed using VectorNTI program

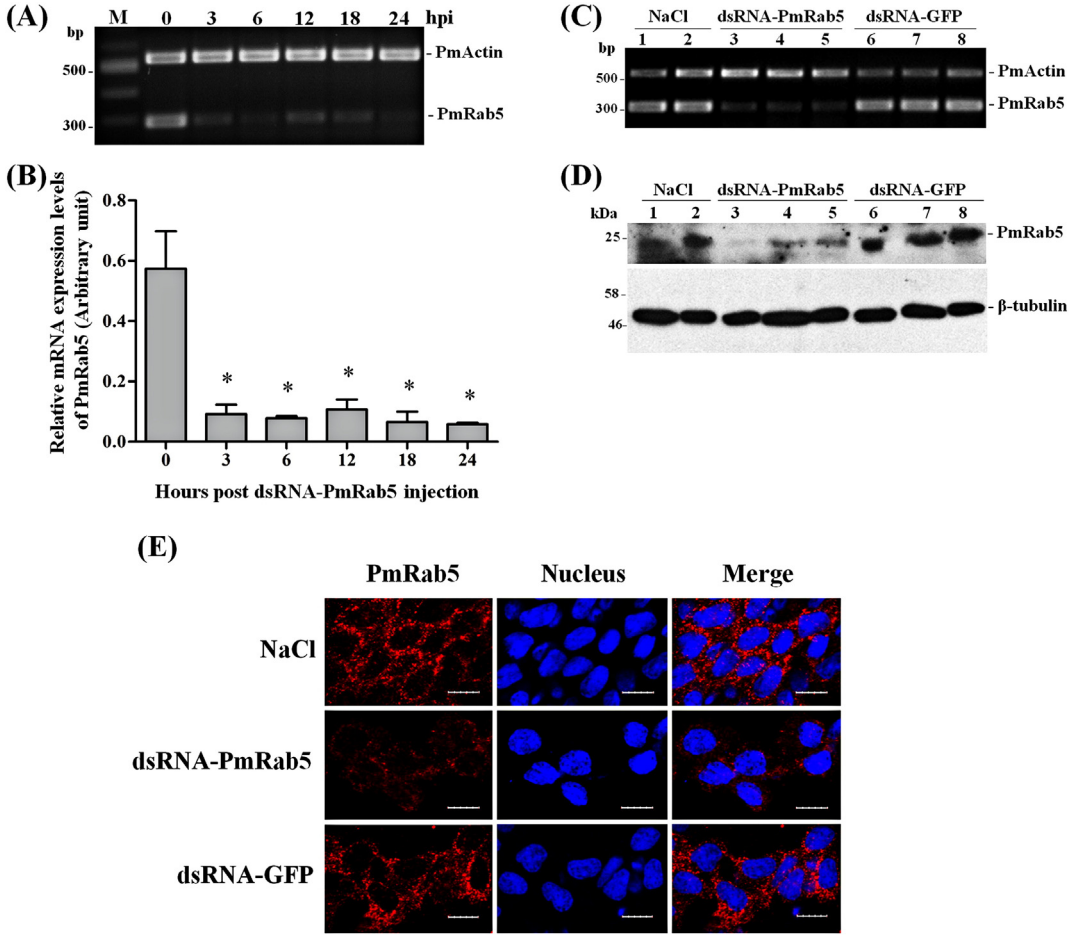


**Fig. 3.** Knockdown effect of PmRab5 by dsRNA-PmRab5. (A) A representative gel of RT-PCR products of PmRab5 and PmActin expression of shrimp injected with dsRNA-PmRab5. The hemolymph was collected at 0, 3, 6, 12, 18 and 24 h post-dsRNA injection. M is 1 kb+ DNA marker. (B) The relative mRNA expression levels (mean ± SEM) of PmRab5 normalized with PmActin and expressed as arbitrary unit (n = 3 for each time course of post-dsRNA injection). (*) represents statistically significant difference between before (time 0) and after dsRNA-PmRab5 injection at various time courses ($p < 0.05$). The mRNA level of PmRab5 and PmActin (C); and, protein level of PmRab5 and β-tubulin (D) of shrimp injected with NaCl (lanes 1–2), dsRNA-PmRab5 (lanes 3–5) and dsRNA-GFP (lanes 6–8) at 24-h post-dsRNAs injection. (E) Confocal immunofluorescence study of the hemocytes collected at 24-h post-dsRNAs injection compared to the NaCl and unrelated dsRNA-GFP control groups. The localization of PmRab5 was represented in red. Cell nuclei were stained blue with TOPRO®-3 iodide. Scale bar is 10 μm.

(Invitrogen). Molecular Evolutionary Genetics Analysis (MEGA) 4.1 program was used for phylogenetic analysis based on the neighbor-joining method (Kumar et al., 2008).

### 2.6. Construction of the recombinant plasmid for production of dsRNA-PmRab5

Recombinant plasmid containing stem-loop of dsRNA-PmRab5 was constructed in pGEM-3Zf+ (Promega) and pET-17b (Novagen) vectors. Sense-loop region of the dsRNA, size 494 bp, was amplified from the first-strand cDNA by stPmRab5-F1-*Xba*I and lpPmRab5-R1-*Kpn*I specific primers (Table 1). Antisense region, size 394 bp, was amplified by stPmRab5-F2-*EcoR*I/*Xho*I and stPmRab5-R2-*Kpn*I primers (Table 1). The PCR fragment of sense-loop was cloned into pGEM-3Zf+ followed by the antisense fragment in the sense and antisense orientation, respectively. Then, this stem-loop fragment of size about 888 bp was subcloned into *Xba*I and *Xho*I sites of pET-17b vector for construction of recombinant plasmid, named pET17b-PmRab5, which was used for *in vivo* bacterial expression of dsRNA-PmRab5. In addition, recombinant plasmid containing stem-loop of dsRNA-GFP (kindly provided by Asst. Prof. Witoon Tirasophon) was used to express dsRNA-GFP which was used as an unrelated dsRNA (Ongvarrasopone et al., 2007).

### 2.7. Production of dsRNA-PmRab5 by in vivo bacterial expression

Recombinant plasmid pET17b-PmRab5 was transformed into a ribonuclease (RNase) III mutant HT115 *Escherichia coli* strain. This strain is modified to express T7 RNA polymerase from an isopropyl-β-D thiogalactopyranoside (IPTG) inducible promoter. Therefore, dsRNAs can be produced in the HT115 bacterial host after induction with 0.1 mM IPTG. Double stranded RNA was extracted and purified as previously described (Ongvarrasopone et al., 2007; Posiri et al., 2013). The quality of dsRNA was characterized by ribonuclease digestion assay using RNase A and RNase III. dsRNA concentration was estimated by agarose gel electrophoresis and compared to the intensity of 100 bp DNA marker.

### 2.8. Black tiger shrimp culture

Juvenile shrimp, sizes about 10 g, were obtained from commercial shrimp farms in Thailand. The shrimp were maintained in large boxes with oxygenated sea water at 20 ppt salinity for 1 day before experiment and fed with commercial diet every day. Half of the water was exchanged every 2 days.

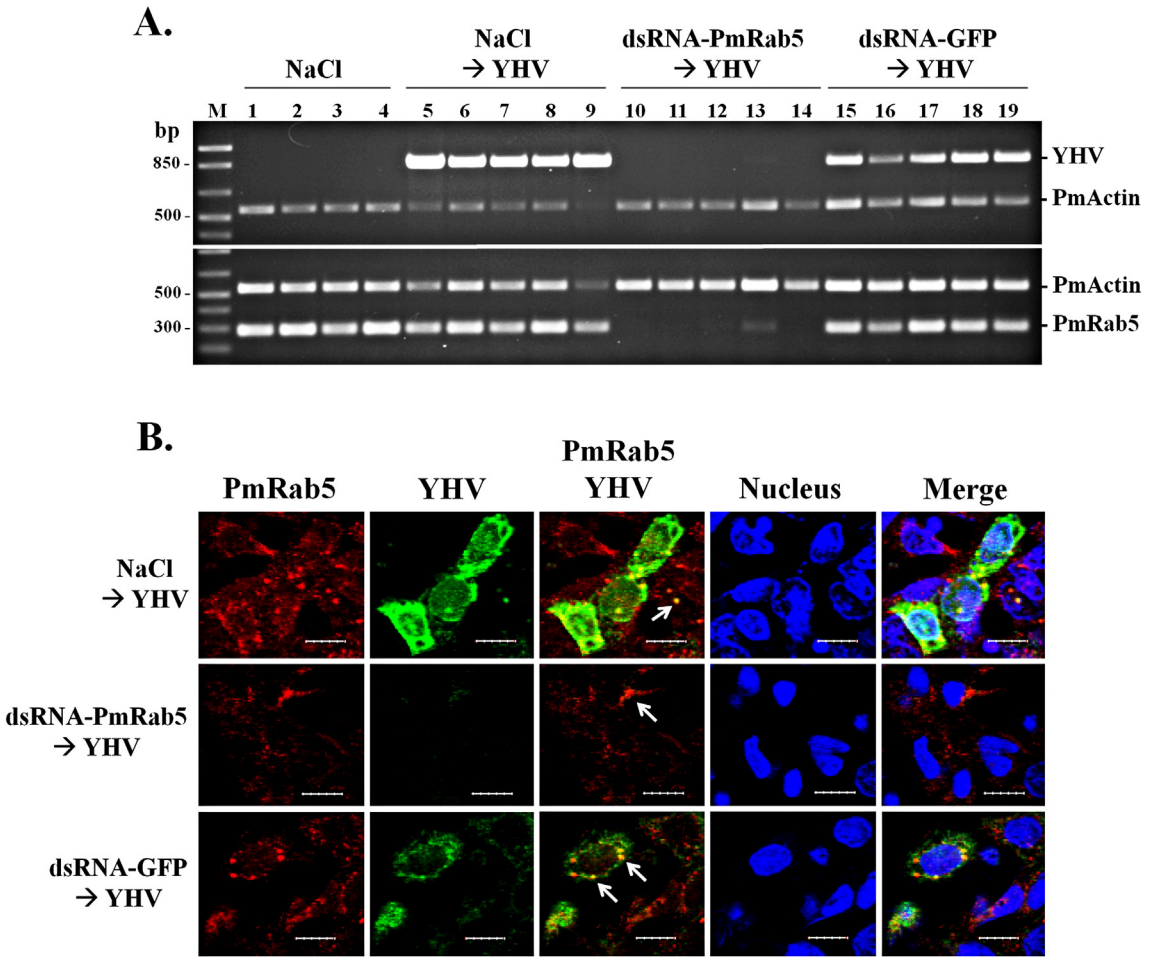


**Fig. 4.** Depletion of PmRab5 during YHV infection. (A) A representative gel of RT-PCR products of YHV (top panel), PmRab5 (bottom panel) and PmActin from gill tissues of shrimp injected with NaCl only (lanes 1–4) and challenged with YHV (lanes 5–9) and shrimp injected with dsRNA-PmRab5 (lanes 10–14) or dsRNA-GFP (lanes 15–19) prior to YHV challenge. M is 1 kb+ DNA marker. (B) Confocal immunofluorescence study demonstrated that knockdown of PmRab5 by dsRNA-PmRab5 disrupted YHV trafficking during the early-stage of YHV infection. The hemocytes were collected at 48 h post-YHV injection from shrimp injected with NaCl, 2.5 $\mu g \cdot g^{-1}$ shrimp of dsRNA-PmRab5 or 2.5 $\mu g \cdot g^{-1}$ shrimp of dsRNA-GFP prior to YHV challenge. The PmRab5 signal is represented in red. YHV is represented in green. The colocalization between YHV particles and PmRab5 are shown by arrows. Cell nuclei were stained blue with TOPRO®-3 iodide. Scale bar is 10 μm.

### 2.9. Suppression of PmRab5 mRNA by dsRNA-PmRab5 in P. monodon

The knockdown effect of PmRab5 mRNA using dsRNA-PmRab5 was tested by injection of dsRNA into hemolymph. Shrimp were injected with 2.5 $\mu g \cdot g^{-1}$ shrimp of dsRNA-PmRab5 dissolved in 150 mM NaCl. Then, hemolymph was collected at time 0, 3, 6, 12, 18 and 24 h post-dsRNA injection to extract total RNA. Suppression effect of the PmRab5 was analyzed by RT-PCR to determine mRNA level.

In addition, hemocytes of shrimp injected with 2.5 $\mu g \cdot g^{-1}$ shrimp of dsRNA-PmRab5, unrelated dsRNA-GFP and NaCl were collected to observe PmRab5 mRNA by using RT-PCR and protein level by western blot analysis and an immunofluorescence assay.

### 2.10. Effect of dsRNA-PmRab5 during YHV infection

To study the function of PmRab5 on YHV infection, shrimp was injected into hemocoel with dsRNA-PmRab5 or dsRNA-GFP at 2.5 $\mu g \cdot g^{-1}$ shrimp. After 24-h post-injection (hpi), YHV was injected. Then, gill was collected at 48 h post-YHV challenge to detect PmRab5 and YHV mRNA expressions. Hemocytes of each group were collected to investigate PmRab5 and YHV protein levels by an immunofluorescence assay. Injection of 150 mM NaCl alone or prior to YHV challenge was used as experimental controls.

### 2.11. Shrimp mortality assay

The mortality of shrimp injected with dsRNA-Rab5 with YHV challenge was observed every 12 h. Shrimp size about 1 g and 15 shrimps per group were tested. Four independent experiments were performed. Shrimps were injected with 150 mM NaCl, 2.5 $\mu g \cdot g^{-1}$ shrimp of dsRNA-PmRab5 or unrelated dsRNA-GFP. After 24-h post-injection, YHV was injected. Dead shrimps were recorded every 12 h.

### 2.12. RNA isolation and RT-PCR

Total RNA from gill tissues or hemolymph was isolated by Trizol® reagent (Molecular Research Center) following the manufacturer's procedure. The RNA concentration was measured by Nanodrop ND-1000

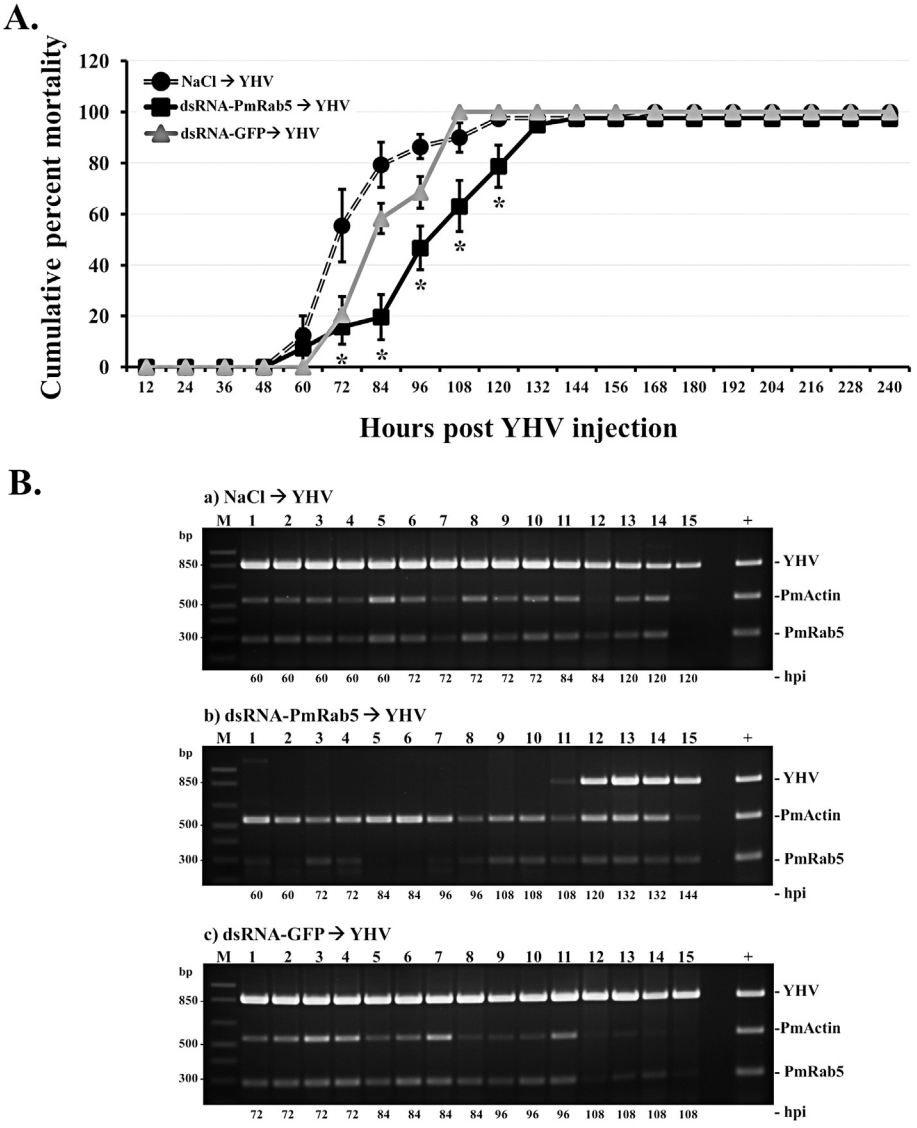


**Fig. 5.** Cumulative mortality assay in the PmRab5 knockdown shrimp upon YHV infection. (A) The cumulative percent mortality of shrimp injected with NaCl, 2.5 $\mu g \cdot g^{-1}$ shrimp of dsRNA-PmRab5, or 2.5 $\mu g \cdot g^{-1}$ shrimp of dsRNA-GFP 24 h before YHV challenge. Dead shrimps were recorded every 12 h post-YHV injection. (*) represents statistically significant difference between NaCl → YHV and dsRNA-PmRab5 → YHV injection ($p < 0.05$). (B) A representative gel of RT-PCR products for YHV and PmRab5 mRNA levels of dead shrimp. PmActin was used as internal control. (a) NaCl → YHV group, (b) dsRNA-PmRab5 → YHV group and (c) dsRNA-GFP → YHV group. The number on the bottom of each lane demonstrated the time (hours of post-YHV challenge, hpi) of dead shrimp. M is 1 kb+ DNA marker.

spectrophotometer (Nanodrop Technologies). RNA (2 μg) was used as template to generate the first-strand cDNA by Improm-II™ reverse transcriptase (Promega) using PRT primer (Table 1). PmRab5 was amplified by PCR using primers PmRab5-F1 and PmRab5-R1. PmActin mRNA expression, used for internal control, was amplified by PmActin-F and PmActin-R1 specific primers (Table 1). Multiplex PCR for PmRab5 and PmActin was amplified according to this condition: 95 °C for 5 min, 25 cycles of 95 °C for 30 s, 60 °C for 30 s, and 72 °C for 45 s, followed by 72 °C for 7 min. YHV expression was amplified by using YHV(hel)-F and YHV(hel)-R primers (Table 1). PCR products were electrophoresed on 1.5% agarose gel. The intensity of each band after subtracting the background was quantified by using ImageJ (version 1.46r) program. The relative expression level of PmRab5 was normalized with PmActin level and expressed as an arbitrary unit.

### 2.13. Western blot analysis

Hemocyte proteins were extracted by using Buffer T (8 M Urea, 2 M Thiourea, 0.4% Triton X-100, 60 mM DTT, 1 mM PMSF, 1× Protease inhibitor cocktail (Sigma)). The protein lysate of each shrimp was electrophoresed in 10% SDS-polyacrylamide gel (SDS-PAGE). The proteins in SDS-PAGE were transferred from gel onto a PVDF membrane (Bio-Rad) by electrophoresis with 1× transfer buffer [0.025 M Tris–HCl pH 8.3, 0.192 M glycine, and 20% (*v*/*v*) methanol]. The membrane was blocked in 5% skimmed milk in 1× PBS containing 0.05% Tween-20 (PBST). PmRab5 and β-tubulin were detected by incubating the membrane with rabbit anti-Rab5 (ab94690, abcam, USA) and anti-β-tubulin (kindly provided by Dr. Phattara-Orn Havanapan) antibody, respectively. Then, the membrane was washed with PBST for 10 min at least 3 times. After that, it was incubated with horseradish peroxidase conjugated to goat anti-rabbit polyclonal antibodies (Sigma), followed by washing as described above. The signal was detected by Luminata™ Forte Western HRP Substrate (Millipore Corporation). PmRab5 and β-tubulin have sizes about 23 and 50 kDa, respectively.

### 2.14. Statistical analysis

The relative mRNA levels of PmRab5 normalized with PmActin were presented as mean ± SEM. Cumulative percent mortality was plotted as mean ± SEM. Moreover, significant differences of each experimental group were tested by analysis of variance (ANOVA). A probability (p) value less than 0.05 was used to define significant difference.

## 3. Results

### 3.1. Full-length cDNA and amino acid sequences of PmRab5

The conserved domains from the alignment of Rab5 proteins from several organisms were used to design primers to amplify the partial sequence of Rab5 from gill tissue of *P. monodon* by PCR. A partial sequence of 346 nucleotides of the putative PmRab5 showed more than 90% sequence identity to Rab5 protein of other species (data not shown). The 5′ and 3′ ends of PmRab5 were obtained by using RACE approach. The full-length cDNA of PmRab5 was confirmed by using specific primers targeting the 5′ and 3′ ends. It comprised of 1293 bp with a 113 bp 5′ untranslated region (UTR), a 633 bp of open reading frame (ORF) (nucleotide 114–746), a 547 bp 3′ UTR with polyadenylation (poly-A) signal. The Kozak's consensus sequence (*AXXATGG*) was present at nucleotide 111–117 (*ATTATGG*). Moreover, a typical poly-A signal (*AATATTA*) was found at nucleotide 1252–1258 (Supplementary Fig. 1). The sequence of PmRab5 cDNA was submitted into the GenBank database under the accession number KT896540.

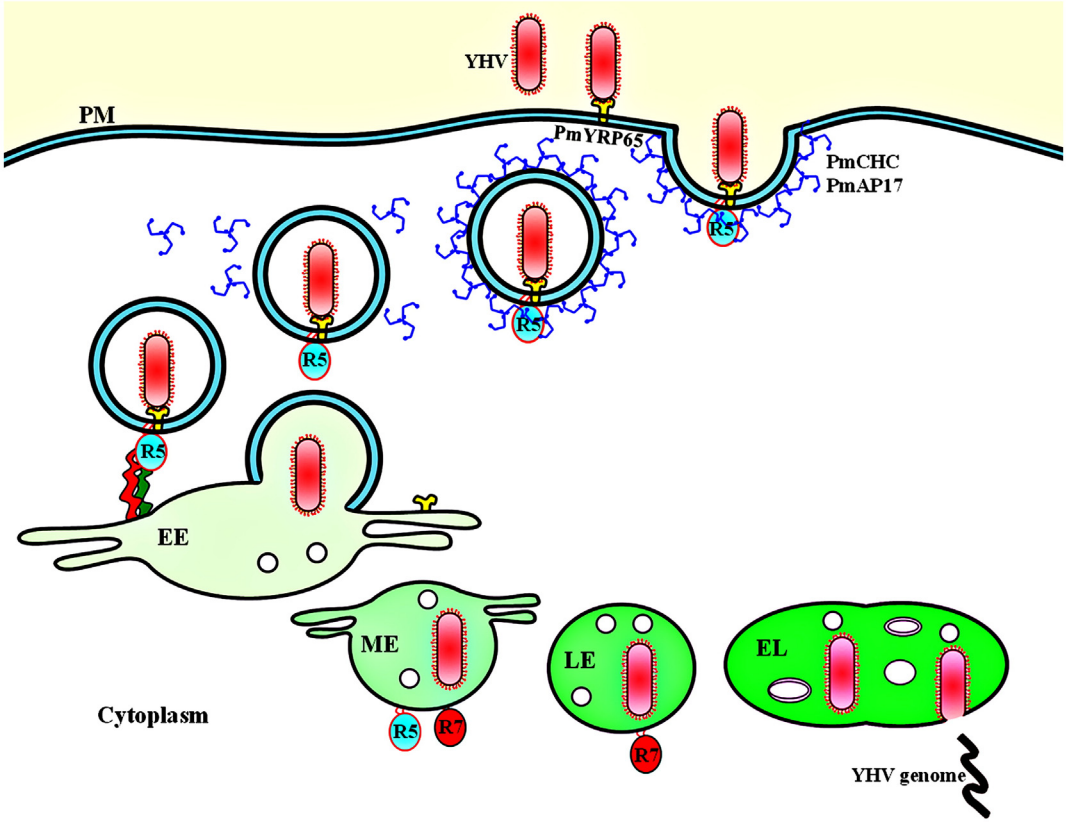


**Fig. 6.** Schematic model of YHV trafficking into shrimp cell. YHV binds with its receptor (PmYRP65) and internalizes into the cells *via* clathrin-mediated endocytosis which required PmCHC and PmAP17 proteins. Vesicle containing the virus is transported from plasma membrane (PM) to early endosome (EE) and then moved toward maturing endosome (ME), late endosome (LE) and endolysosome (EL). These processes, PM to EE and to ME are regulated by PmRab5 (R5) whereas ME to LE and to EL are regulated by PmRab7 (R7) protein. YHV genome may be released by acidic condition in endolysosome into the cytoplasm where the replication process begins.

The deduced amino acid sequence of PmRab5 is 210 amino acids with an estimated molecular weight of 22.97 kDa and a pI of 8.29. Blastp search of NCBI database showed high sequence homology of PmRab5 protein with other known Rab5 proteins in the database (Table 2). Moreover, the alignment of PmRab5 to Rab5 proteins from several organisms such as mosquito (*Aedes aegypti*), dog (*Canis lupus*), human (*Homo sapiens*), mouse (*Mus musculus*), frog (*Xenopus tropicalis*), sea anemone (*Aiptasia pulchella*) and butterfly (*Danaus plexippus*) demonstrated the conserved motifs of Rab protein family, including five Rab family motifs (RabF1–5), four Rab subfamily motifs (RabSF1–4) which defined Rab5 protein, five signature domains for GTP-binding sites (G1–G5) and a putative prenylation signal (*XCCX*) at the C-terminal of the invertebrates sequence (Stenmark and Olkkonen, 2001; Zhu et al., 2004) (Fig. 1A). Phylogenetic tree analysis separated Rab5 protein into 3 clusters, including vertebrate, invertebrate and plant. The tree revealed that PmRab5 is in the invertebrates group (Fig. 1B). The expression of PmRab5 in *P. monodon* was examined by multiplex RT-PCR. The results demonstrated that PmRab5 was expressed at similar levels in several tissues including brain, thoracic ganglia, nerve cord, gill, lymphoid organ, hepatopancreas, ovary and hemocytes (Supplementary Fig. 2).

### 3.2. YHV and PmRab5 are colocalized in the hemocytes during YHV infection

Rab5 protein regulates endocytic vesicle membrane that transports the cargo from plasma membrane to the early endosome (Bucci et al., 1992). This process is an early step for many viruses to enter into the cells (Cheng et al., 2012; Clemente and de la Torre, 2009; Johns et al., 2009; Macovei et al., 2013). To elucidate the function of PmRab5 that is possibly involved in the molecular trafficking process of YHV entry into hemocytes, colocalization of YHV and PmRab5 was investigated. Primary hemocyte culture was infected with YHV. Localization of YHV and PmRab5 were investigated at 0 min, 10 min, 30 min, 1 h, 3 h, 6 h and 12 h post-infection (pi.). The signal of YHV was detected around the cell surface and no colocalization of YHV particles and PmRab5 was observed at 0 min. From 10 to 30 min, strong colocalized signals of YHV and PmRab5 were detected. The signals were strongest at time 1 to 3 hpi. Interestingly, the colocalization signal was faint at 6 hpi and completely absent at 12 hpi (Fig. 2).

### 3.3. PmRab5 was suppressed by specific dsRNA in shrimp

In order to study the function of PmRab5 in shrimp, RNA interference (RNAi) was used as a tool to investigate its role. First, dsRNA targeting PmRab5 (dsRNA-PmRab5) was constructed and tested for its suppression of endogenous PmRab5 transcript. Shrimps received dsRNA-PmRab5 injection showed significant reduction of PmRab5 transcript at more than 85% from 3 hpi to 24 hpi (Fig. 3A and 3B). Moreover, specificity of the knockdown effect by dsRNA-PmRab5 was also tested. Shrimps received dsRNA-PmRab5 demonstrated reduction of PmRab5 at both the mRNA and protein levels. In contrast, the knockdown effect of PmRab5 was not seen in shrimp injected with unrelated dsRNA-GFP or NaCl-injected groups (Fig. 3C and 3D). In addition, immunofluorescence staining of the hemocytes obtained from shrimps injected with dsRNA-PmRab5 demonstrated faint PmRab5 signal when compared to that of the NaCl and dsRNA-GFP groups (Fig. 3E).

### 3.4. YHV requires PmRab5 for entry into shrimp cells

To study the suppression effect of PmRab5 during YHV challenge, shrimps were injected with dsRNA-PmRab5 at 2.5 $\mu g \cdot g^{-1}$ shrimp 24 h prior to YHV challenge. Injection of dsRNA-GFP was used as an unrelated control group. Then, gills were collected for total RNA extraction after 48 h post-YHV challenge. Injection of dsRNA-PmRab5 demonstrated approximately 97% reduction of PmRab5 transcript when compared to the NaCl and dsRNA-GFP groups, resulting in hardly observable YHV mRNA level. On the other hand, injection of NaCl or dsRNA-GFP prior to YHV challenge showed high levels of YHV (Fig. 4A). Moreover, immunofluorescence staining of hemocytes collected 48 h post-YHV challenge in dsRNA-PmRab5 injected group showed faint signal of PmRab5 protein when compared to the hemocytes from NaCl or dsRNA-GFP group. Interestingly, the depleted PmRab5 cells hardly showed any YHV particles inside the cells. Colocalization between YHV particles with PmRab5 could be barely detected in the PmRab5-knockdown cells. However, a clear colocalization signal of PmRab5 and YHV could be clearly observed in the hemocytes from NaCl and dsRNA-GFP injected group (Fig. 4B).

### 3.5. Silencing of PmRab5 levels delayed YHV replication and shrimp mortality in infected shrimp

To further investigate the suppression effect of PmRab5 in YHV infected shrimp, shrimp mortality assay was performed. Shrimp injected with dsRNA-PmRab5 followed by YHV challenge exhibited 97.5% cumulative mortality at 132 hpi. Rate of shrimp death in this group still unchanged after 240 hpi. On the other hand, shrimp challenged with YHV alone or injected with unrelated dsRNA-GFP followed by YHV challenge that used as the control groups demonstrated 100% mortality at 168 and 108 hpi, respectively. A significant decrease of cumulative percent mortality in YHV infected shrimp could be observed at 72–120 hpi in the PmRab5 knockdown group when compared to the control groups (Fig. 5). To check YHV levels, shrimps died at various time points were sampled. YHV mRNA levels could not be detected during 60–108 hpi in dead shrimp that the PmRab5 expression was suppressed. However, YHV mRNA levels could be observed after 120 hpi (Fig. 5B (b)). In contrast, high levels of YHV expression can be detected in all dead shrimps from the control groups (Fig. 5B (a and c)).

## 4. Discussion

Yellow head virus is a serious causative agent that led to high mortality rate in *P. monodon*. Understanding of the virus trafficking pathway especially the mechanism of YHV infection is still poorly understood. Knowledge of the virus life cycles needs to be examined to shed light on providing useful information and to develop approaches for prevention and cure of shrimp from YHV infection. The endocytosis pathway of YHV has been characterized. Specifically, YHV utilized clathrin-mediated endocytosis which required clathrin coated vesicle protein including *P. monodon* clathrin heavy chain (PmCHC) and clathrin coat assembly protein 17 (AP17) to invade shrimp cells (Jatuyosporn et al., 2014; Posiri et al., 2015). Moreover, Rab5, a small GTPase protein formed complex with guanine-nucleotide dissociation inhibitor (GDI) and then associated into clathrin-coated vesicle membrane. After the association, GDI is released and Rab5 is converted into GTP-bound form to regulate downstream processing (Horiuchi et al., 1995; McLauchlan et al., 1997). Rab5 protein regulates the transportation of the vesicle from plasma membrane to early endosome of the endocytic pathway (Bucci et al., 1992). Therefore, YHV possibly utilizes the Rab5 protein to invade the host cells. In addition, previous study in *P. monodon* has identified a small GTPase Rab7 protein as a WSSV-VP28 binding protein in shrimp (Sritunyalucksana et al., 2006). The protein plays a crucial role in regulation of vesicle formation and membrane trafficking from late endosome to lysosome which is a sequential process from early endosome (Hutagalung and Novick, 2011; Stenmark, 2009). Interestingly, the *P. monodon* Rab7 (PmRab7) was involved in YHV replication in shrimp (Ongvarrasopone et al., 2008). However, this is the first report demonstrating that Rab5 protein is involved in YHV infection in *P. monodon*.

In this study, PmRab5 demonstrated conserved regions of Rab family and Rab5 subfamily which were similar to other organisms including *Aiptasia pulchella* (Chen et al., 2004) and many other vertebrates

(Fig. 2). In shrimp, its amino acid sequence identity is highly conserved to human Rab5B (81.1%). Differences in the three isoforms of Rab5 proteins (Rab5A, 5B, and 5C) have no effect in the regulation of trafficking pathway from plasma membrane to early endosome but they are differentially recognized by different specific kinases (Bucci et al., 1995; Chiariello et al., 1999). In addition, colocalization between YHV and PmRab5 was observed in the hemocytes from 10 min to 3 h and rarely observed from 6 to 12 hpi. These results suggested that YHV and PmRab5 were transported together until 3 hpi. Then, YHV may be uncoated and released into the cytoplasm for replication process. Previously, Semliki Forest virus (SFV) and dengue virus (DENV) demonstrated colocalization with early endosome antigen 1 (EEA1), an effector protein of Rab5, at early time of infection and then later associated with Rab7. After that the viruses which were in hybrid organelles would separate from Rab5 and colocalize with only Rab7 (van der Schaar et al., 2008; Vonderheit and Helenius, 2005). The colocalization of YHV and Rab7 has not been reported but this event may be similar to SFV and DENV.

The function of PmRab5 on YHV replication was also investigated by using RNA interference technique. Levels of PmRab5 mRNA were suppressed at more than 85% by specific dsRNA after 3 hpi and showed partial recovery after 3 dpi (data not shown). Depletion of Rab5 protein causes accumulation of small vesicles around the cytoplasm due to the vesicles could not be fused with early endosome (Bucci et al., 1992). The fusion of the vesicles from plasma membrane with early endosome occurred from specific interaction of Rab5 and EEA1 protein. Rab5 protein could bind to both $C_2H_2Zn^{2+}$ finger and FYVE domain of EEA1 protein (Lawe et al., 2000; Merithew et al., 2003). Inhibition of the membrane fusion might block the transportation of many essential cargo proteins and might lead to cell death. Moreover, Rab5 protein is involved in the internalization of integrin which is critical for caspase-8 functions to regulate cell motility, metastasis and survival (Torres et al., 2010). Therefore, silencing of PmRab5 may cause a loss of cell equilibrium and induces death in shrimps. Furthermore, depletion of PmRab5 by using dsRNA could silence YHV mRNA levels and suppressed YHV infection in shrimp cells. These results suggested that YHV required PmRab5 for transportation into the cell similar to other envelope positive-sense single-stranded RNA viruses such as dengue virus (DENV), West Nile virus (WNV) or hepatitis C virus (HCV). Knockdown of Rab5 by siRNA showed the reduction of both DENV and WNV (Krishnan et al., 2007) while a dominant negative mutant of Rab5 could be used to decrease RNA progeny of HCV (Stone et al., 2007). Moreover, Rab5 protein is required for many viruses such as Borna disease virus (BDV), bovine ephemeral fever virus (BEFV), hepatitis B virus, and foot and mouth disease virus (FMDV) to transport within the host cell (Cheng et al., 2012; Clemente and de la Torre, 2009; Johns et al., 2009; Macovei et al., 2013). Taken together, the model of YHV entry into shrimp cell is proposed (Fig. 6). First, YHV glycoprotein 116 binds with PmYRP65, a shrimp cell receptor. Then, it utilizes clathrin dependent endocytosis to enter into the cells. The virus requires PmRab5 and PmRab7 to regulate the transportation from plasma membrane to early endosome and from early endosome to late endosome, respectively (Assavalapsakul et al., 2006; Jatuyosporn et al., 2014; Ongvarrasopone et al., 2008; Posiri et al., 2015). When the pH was lowered, YHV genome may be released into the cytoplasm for replication process which is similar to other enveloped RNA viruses, such as SFV and Sindbis virus (Glomb-Reinmund and Kielian, 1998; Helenius et al., 1980). In conclusion, YHV requires PmRab5 transport within the shrimp cell.

Supplementary data to this article can be found online at http://dx.doi.org/10.1016/j.aquaculture.2016.03.026.

## Acknowledgments

We would like to thank Asst. Prof. Dr. Kusol Pootanakit for critically reading the manuscript, Prof. Dr. Paisarn Sithigorngul and Dr. Phattara-Orn Havanapan for providing anti-YHV gp64 antibody and anti-β-tubulin antibody, respectively and Ms. Chaweewan Chimawei, Mrs. Suparb Hongthong and Ms. Punnee Tongboonsong for technical assistance on culturing shrimp. We also would like to thank Mr. Wichai Boonsai from Choochai farm in Chonburi province and shrimp genetic improvement center in Surat Thani province, Thailand for providing shrimp samples. This work was supported by grants from Mahidol University under the National Research University Initiative (NRU) and Thailand Research Fund (BRG5780006 to C.O., DPG5680001 to S.P. and IRG 5780009). PP is supported by the grant DPG5680001.

## References

Assavalapsakul, W., Smith, D.R., Panyim, S., 2006. Identification and characterization of a *Penaeus monodon* lymphoid cell-expressed receptor for the yellow head virus. J. Virol. 80 (1), 262–269.

Bucci, C., Lütcke, A., Steele-Mortimer, O., Olkkonen, V.M., Dupree, P., Chiariello, M., Bruni, C.B., Simons, K., Zerial, M., 1995. Co-operative regulation of endocytosis by three Rab5 isoforms. FEBS Lett. 366, 65–71.

Bucci, C., Parton, R.G., Mather, I.H., Stunnenberg, H., Simons, K., Hoflack, B., Zerial, M., 1992. The small GTPase Rab5 functions as a regulatory factor in the early endocytic pathway. Cell 70, 715–728.

Chen, M.C., Cheng, Y.M., Hong, M.C., Fang, L.S., 2004. Molecular cloning of Rab5 (ApRab5) in *Aiptasia pulchella* and its retention in phagosomes harboring live zooxanthellae. Biochem. Biophys. Res. Commun. 324, 1024–1033.

Cheng, C.Y., Shih, W.L., Huang, W.R., Chi, P.I., Wu, M.H., Liu, H.J., 2012. Bovine ephemeral fever virus uses a clathrin-mediated and dynamin 2-dependent endocytosis pathway that requires Rab5 and Rab7 as well as microtubules. J. Virol. 86, 13653–13661.

Chiariello, M., Bruni, C.B., Bucci, C., 1999. The small GTPases Rab5a, Rab5b and Rab5c are differentially phosphorylated *in vitro*. FEBS Lett. 453, 20–24.

Clemente, R., de la Torre, J.C., 2009. Cell entry of Borna disease virus follows a clathrin-mediated endocytosis pathway that requires Rab5 and microtubules. J. Virol. 83, 10406–10416.

Glomb-Reinmund, S., Kielian, M., 1998. The role of low pH and disulfide shuffling in the entry and fusion of semliki forest virus and sindbis virus. Virology 248, 372–381.

Greber, U.F., Singh, I., Helenius, A., 1994. Mechanisms of virus uncoating. Trends Microbiol. 2, 52–56.

Helenius, A., Kartenbeck, J., Simons, K., Fries, E., 1980. On the entry of Semliki Forest virus into BHK-21 cells. J. Cell Biol. 84, 404–420.

Horiuchi, H., Giner, A., Hoflack, B., Zerial, M., 1995. A GDP/GTP exchange-stimulatory activity for the Rab5-RabGDI complex on clathrin-coated vesicles from bovine brain. J. Biol. Chem. 270, 11257–11262.

Hutagalung, A.H., Novick, P.J., 2011. Role of Rab GTPases in membrane traffic and cell physiology. Physiol. Rev. 91, 119–149.

Jatuyosporn, T., Supungul, P., Tassanakajon, A., Krusong, K., 2014. The essential role of clathrin-mediated endocytosis in yellow head virus propagation in the black tiger shrimp *Penaeus monodon*. Dev. Comp. Immunol. 44, 100–110.

Jitrapakdee, S., Unajak, S., Sittidilokratna, N., Hodgson, R.A., Cowley, J.A., Walker, P.J., Panyim, S., Boonsaeng, V., 2003. Identification and analysis of gp116 and gp64 structural glycoproteins of yellow head nidovirus of *Penaeus monodon* shrimp. J. Gen. Virol. 84, 863–873.

Johns, H.L., Berryman, S., Monaghan, P., Belsham, G.J., Jackson, T., 2009. A dominant-negative mutant of Rab5 inhibits infection of cells by foot-and-mouth disease virus: implications for virus entry. J. Virol. 83, 6247–6256.

Krishnan, M.N., Sukumaran, B., Pal, U., Agaisse, H., Murray, J.L., Hodge, T.W., Fikrig, E., 2007. Rab 5 is required for the cellular entry of dengue and West Nile viruses. J. Virol. 81, 4881–4885.

Kumar, S., Nei, M., Dudley, J., Tamura, K., 2008. MEGA: a biologist-centric software for evolutionary analysis of DNA and protein sequences. Brief. Bioinform. 9, 299–306.

Lawe, D.C., Patki, V., Heller-Harrison, R., Lambright, D., Corvera, S., 2000. The FYVE domain of early endosome antigen 1 is required for both phosphatidylinositol 3-phosphate and Rab5 binding. J. Biol. Chem. 275, 3699–3705.

Macovei, A., Petrareanu, C., Lazar, C., Florian, P., Branza-Nichita, N., 2013. Regulation of hepatitis B virus infection by Rab5, Rab7, and the endolysosomal compartment. J. Virol. 87, 6415–6427.

Marsh, M., Helenius, A., 2006. Virus entry: open sesame. Cell 124, 729–740.

McLauchlan, H., Newell, J., Morrice, N., Osborne, A., West, M., Smythe, E., 1997. A novel role for Rab5-GDI in ligand sequestration into clathrin-coated pits. Curr. Biol. 8, 34–45.

Mercer, J., Schelhaas, M., Helenius, A., 2010. Virus entry by endocytosis. Annu. Rev. Biochem. 79, 803–833.

Merithew, E., Stone, C., Eathiraj, S., Lambright, D.G., 2003. Determinants of Rab5 interaction with the N terminus of early endosome antigen 1. J. Biol. Chem. 278, 8494–8500.

Nadala, E.C.B., Tapay, L.M., Loh, P.C., 1997. Yellow-head virus: a rhabdovirus-like pathogen of penaeid shrimp. Dis. Aquat. Org. 31, 141–146.

Ongvarrasopone, C., Chanasakulniyom, M., Sritunyalucksana, K., Panyim, S., 2008. Suppression of PmRab7 by dsRNA inhibits WSSV or YHV infection in shrimp. Mar. Biotechnol. 10, 374–381.

Ongvarrasopone, C., Roshorm, Y., Panyim, S., 2007. A simple and cost effective method to generate dsRNA for RNAi studies in invertebrates. Sci. Asia 33, 35–39.

Posiri, P., Kondo, H., Hirono, I., Panyim, S., Ongvarrasopone, C., 2015. Successful yellow head virus infection of *Penaeus monodon* requires clathrin heavy chain. Aquaculture 435, 480–487.

Posiri, P., Ongvarrasopone, C., Panyim, S., 2013. A simple one-step method for producing dsRNA from *E. coli* to inhibit shrimp virus replication. J. Virol. Methods 188, 64–69.
Sittidilokratna, N., Dangtip, S., Cowley, J.A., Walker, P.J., 2008. RNA transcription analysis and completion of the genome sequence of yellow head nidovirus. Virus Res. 136, 157–165.
Sritunyalucksana, K., Wannapapho, W., Lo, C.F., Flegel, T.W., 2006. PmRab7 is a VP28-binding protein involved in white spot syndrome virus infection in shrimp. J. Virol. 80, 10734–10742.
Stenmark, H., 2009. Rab GTPases as coordinators of vesicle traffic. Nat. Rev. Mol. Cell Biol. 10, 513–525.
Stenmark, H., Olkkonen, V.M., 2001. The Rab GTPase family. Genome Biol. 2, 3007.1–3007.7.
Stone, M., Jia, S., Heo, W.D., Meyer, T., Konan, K.V., 2007. Participation of Rab5, an early endosome protein, in hepatitis C virus RNA replication machinery. J. Virol. 81, 4551–4563.
Torres, V.A., Mielgo, A., Barbero, S., Hsiao, R., Wilkins, J.A., Stupack, D.G., 2010. Rab5 mediates caspase-8-promoted cell motility and metastasis. Mol. Biol. Cell 21, 369–376.
van der Schaar, H.M., Rust, M.J., Chen, C., van der Ende-Metselaar, H., Wilschut, J., Zhuang, X., Smit, J.M., 2008. Dissecting the cell entry pathway of dengue virus by single-particle tracking in living cells. PLoS Pathog. 4, e1000244.
Vonderheit, A., Helenius, A., 2005. Rab7 associates with early endosomes to mediate sorting and transport of semliki forest virus to late endosomes. PLoS Biol. 3, 1225–1238.
Zhu, G., Zhai, P., Liu, J., Terzyan, S., Li, G., Zhang, X.C., 2004. Structural basis of Rab5-Rabaptin5 interaction in endocytosis. Nat. Struct. Mol. Biol. 11, 975–983.